Title
The structure/function relationship of the lipooligosaccharides from Haemophilus ducreyi

Author
Melaugh, William,

Publication Date
1994

Peer reviewed|Thesis/dissertation

The Structure/Function Relationship of the Lipooligosaccharides from *Haemophilus ducreyi*

by

William Melaugh

DISSERTATION

Submitted in partial satisfaction of the requirements for the degree of

DOCTOR OF PHILOSOPHY

in

Pharmaceutical Chemistry

in the

GRADUATE DIVISION

of the

UNIVERSITY OF CALIFORNIA

San Francisco

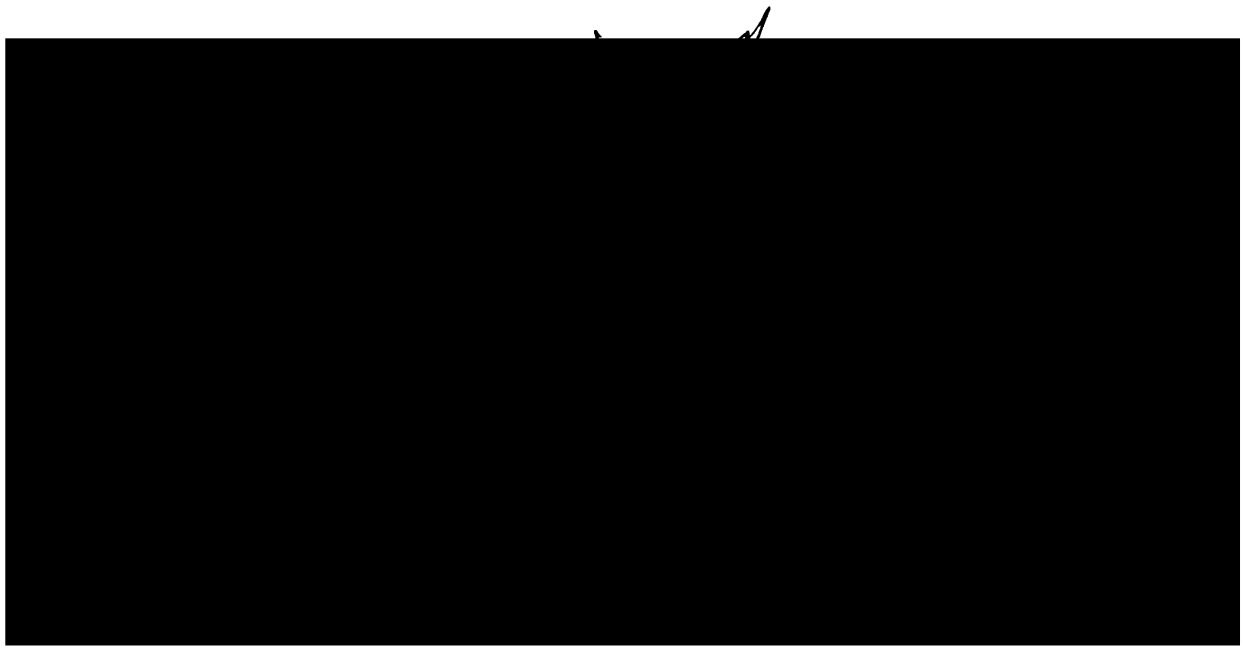

Acknowledgements

I would like to thank my advisor and mentor Professor Brad Gibson for all the advice and support he gave me in this research. Brad always tempered the rigors of scientific investigation with a sense of humor that made working in his laboratory a delightful experience. I will forever be indebted to Dr. Nancy Phillips for the unflagging support she gave me and for the saintly patience she showed in answering my non-stop barrage of questions. I learned from Nancy that if something is worth doing, it is worth doing well.

I would like to thank others in my research group who were always willing to help when it was needed: Dr. Connie John who paved the way, Lorri Reinders and Denes Medzihradszky who were generous with their advice, my good friend and comrade Jeff Engstrom, my fellow graduate students Wade Hines and Michael Tullius and a special word of thanks to the wandering Finnish philosopher Seppo Auriola who spent several months as a visiting scientist working in our laboratory.

I am indebted to the people in the Mass Spectrometry Facility at U.C.S.F. especially Professor Al Burlingame who directs the facility and Professor Arnie Falick who was always around to solve the day to day crises I seemed to encounter when working there. Without the help and expertise of Fred Walls and Dave Maltby in maintaining the instruments, this work would not have been possible.

I also acknowledge my great debt to our collaborators at S.U.N.Y. at Buffalo, in particular, Dr. Tony Campagnari and Dr. Mike Apicella who furnished the LOS samples and conducted the immunochemical studies.

I would like to mention several people without whose guidance and encouragement I would not have attained this goal: Professors George Kenyon, Les Brooks and Gene Schaumberg.

Lastly, I owe much to my friend and teacher Brian O' Brien who taught me how to think about science.

Collaborations

I would like to acknowledge the work carried out by several co-workers and collaborators which made this research possible. Chapters 2, 3 and 4 of this dissertation are based on published papers. At the time of writing, Chapter 5 is about to be submitted as a journal article.

Chapter 2 is based largely on the following paper: Melaugh, W., Phillips, N. J., Campagnari, A. A., Karalus, R. & Gibson, B. W. (1992), "Partial characterization of the major lipooligosaccharide from a strain of *Haemophilus ducreyi*, the causative agent of chancroid, a genital ulcer disease", *J. Biol. Chem. 267*, 13434-13439. The mass spectrometric analyses and structural work were done at U.C.S.F. primarily by myself. The isolation of LOS and immunochemical work were performed in Dr. Campagnari's laboratory at S.U.N.Y. at Buffalo.

Chapter 3 is based on the following paper: Melaugh, W., Phillips, N. J., Campagnari, A. A., Tullius, M. V. & Gibson, B. W. "Structure of the major oligosaccharide from the lipooligosaccharide of *Haemophilus ducreyi* strain 35000 and evidence for additional glycoforms", (Accepted for publication in Biochemistry August 1994). The structural determination work by mass spectrometry and NMR was done at U.C.S.F. I carried out the mass spectrometry component and Dr. Nancy Phillips in my research group was responsible for the NMR work. A fellow graduate student Michael Tullius performed the sialic acid linkage determination. Isolation of LOS and immunochemical analyses were done by Dr. Campagnari at S.U.N.Y. at Buffalo.

Chapter 4 is based on the following paper: Campagnari, A. A., Karalus, R., Apicella, M. A., Melaugh, W., Lesse, A. J. & Gibson, B. W. (1994), "Use of pyocin to select a *Haemophilus ducreyi* variant defective in lipooligosaccharide biosynthesis". *Infect. Immun. 62*, 2379-2386. I carried out the structural determination work which was completed at U.C.S.F. Isolation of the LOS, production of pyocin-variants and

immunological and immunochemical studies were done in Dr. Campagnari's laboratory at S.U.N.Y. at Buffalo.

Chapter 5 is based largely on the following paper which is about to be sent for publication: Melaugh. W., Campagnari, A. A. & Gibson, B. W. "The lipooligosaccharides of *Haemophilus ducreyi* are highly sialylated". Structural determinations of LOS and oligosaccharides were done by myself at U.C.S.F. Isolation of LOS and immunochemical and immunological work were performed at S.U.N.Y. at Buffalo by Dr. Campagnari.

The mass spectrometric electrospray experiments described in Chapter 6 were performed by myself at U.C.S.F. Seppo Auriola, a visiting scientist from Finland, did the MALDI experiment. LOS was isolated from bacteria by Dr. Campagnari at S.U.N.Y. at Buffalo.

The Structure/Function Relationship of the Lipooligosaccharides from *Haemophilus Ducreyi*

by
William Melaugh

ABSTRACT

Haemophilus ducreyi is a sexually transmitted pathogen that colonizes the genital epithelium in humans, causing genital ulcers or chancroid. Its surface lipooligosaccharides (or LOS) have recently been shown to play a crucial role in ulcer formation and preliminary data indicate that LOS are also important for cell adhesion and invasion. The aim of the research has been to determine the structures of *H. ducreyi* LOS and to relate them, if possible, to their biological functions. In order to achieve this goal, the LOS from *H. ducreyi* strain 35000 was analysed in depth. The structure of the major oligosaccharide, released by mild acid hydrolysis and analyzed by liquid secondary ion mass spectrometry, tandem mass spectrometry and NMR is shown below and has several interesting features, including an unusual branch heptose and an epitope, terminating in lactosamine, that mimics structures found in human blood group antigens.

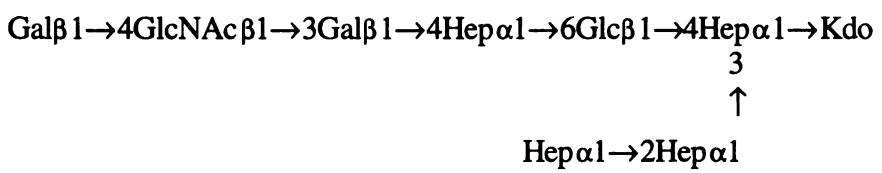

To determine if these structural features were common to other strains of *H. ducreyi*, the structure of the oligosaccharide from the LOS of strain 188 was investigated and turned out to be similar to the structure determined for strain 35000. A variant of the 188 wild-type strain, isolated after treatment with pyocin, produced LOS which lacked terminal lactosamine and this strain showed greatly diminished adherence and cytotoxicity in cultured human keratinocyte assays. Other wild-type strains studied contained a major LOS species with the same oligosaccharide structure shown above

except for the Kenyan strain 33921 which had a much smaller oligosaccharide branch lacking terminal lactosamine. Assays conducted on this strain also showed reduced adherence and cytotoxicity pointing to the potential significant role of terminal lactosamine in the pathogenic process.

Lastly, electrospray mass spectrometry showed that the oligosaccharide region of all the strains studied except strains 188-2 and 33921 contained sialic acid. It appeared that terminal lactosamine must be the acceptor for sialic acid and immunochemical studies indicated that sialyllactosamine was important both in adherence and in allowing the organism to evade the host defenses.

List of Abbreviations

BPH	butyl phenylhydrazine
CI	chemical ionization
CID	collision induced dissociation
1D	one-dimensional
2D	two-dimensional
COSY	2D *J*-correlated spectroscopy
Da	daltons
DQF-COSY	double-quantum filtered COSY
EI	electron impact ionization
ESI/MS	electrospray ionization mass spectrometry
Gal	galactose
GalNAc	*N*-acetylgalactosamine
GC/MS	gas chromatography/mass spectrometry
Glc	glucose
GlcNAc	*N*-acetylglucosamine
Hep	L-*glycero*-D-*manno*-heptose or D-*glycero*-D-*manno*-heptose
Hex	hexose
HexNAc	*N*-acetylhexosamine
HOHAHA	2D homonuclear Hartmann-Hahn spectroscopy
HPAEC	high performance anion exchange chromatography
HPLC	high performance liquid chromatography
Kdo	3-deoxy-D-*manno*-octulosonic acid
keV	kilo electron volts
LOS	lipooligosaccharide
LSIMS	liquid secondary ion mass spectrometry
M	molar
$(M-nH)^{n-}$	multiply charged depronated molecular ion
$(M+nH)^{n+}$	multiply charged protonated molecular ion
MAb	monoclonal antibody
MALDI	matrix assisted laser desorption/ionization mass spectrometry
M_r	molar mass
MS/MS	tandem mass spectrometry
m/z	mass to charge ratio
Neu5Ac	sialic acid
NMR	nuclear magnetic resonance spectroscopy
NOE	nuclear Overhauser effect
NOESY	2D nuclear Overhauser effect spectroscopy
PEA	phosphoethanolamine
PPEA	pyrophosphoethanolamine
PMAA	partially methylated alditol acetate
SDS-PAGE	sodium dodecyl sulfate polyacrylamide gel electrophoresis
TLC	thin layer chromatography
TIC	total ion chromatogram
UV	ultraviolet light

Table of Contents

List of Tables

List of Figures

CHAPTER 1.

INTRODUCTION

1. Biology of Haemophilus ducreyi *Haemophilus ducreyi* is a Gram-negative bacterium that colonizes the genital epithelium and causes the sexually transmitted disease chancroid also known as genital ulcer disease (Johnson et al., 1988; Albritton, 1989; Morse, 1989). Ducrey first established the cause of the disease in 1889 by inoculating the skin of the forearm of patients with secretions from their own genital ulcers (Ducreyi, 1889). At weekly intervals he inoculated a new site with material from the most recent ulcer. He continued the infections through fifteen generations and was able to locate the microorganism, since named after him, both inside and outside neutrophils (Morse, 1989). Around the turn of the century Bezancon isolated the causative agent of chancroid on blood agar and succeeded in demonstrating that it fulfilled Koch's postulates (Bezancon et al., 1900).

It is generally believed that *H. ducreyi* enters through a break in the epithelium. At first it causes local inflammation followed by an accumulation of polymorphonuclear leukocytes (Sullivan, 1940; Albritton, 1989). Within 2 or 3 days a pustule forms that soon ruptures resulting in a genital ulcer with ragged edges (Morse, 1989). The base of a well-established chancroid ulcer has a granular appearance and may be covered by a gray or yellow necrotic purulent exudate (Sullivan, 1940). The ulcer contains many newly formed blood vessels and bleeds easily on scraping. There is little inflammation of the surrounding skin (Morse, 1989). Ulcers are generally quite painful in males, but most females with the disease are unaware of their condition and systemic infection is rare (Albritton, 1989).

The prevalence of chancroid in developing countries of Asia and Africa is high (Kibukamusoke, 1965; Weisner et al., 1983). In the United States the number of incidences of the disease peaked in 1947 when over 9,000 cases were reported. Since

then, until the late seventies, an average of about 900 cases was reported annually. The eighties witnessed a sharp resurgence in occurrences of the disease. In 1987 over 5,000 cases were logged (Morse, 1989) and the situation has deteriorated since that time. In recent years there have been minor epidemics in New York, Los Angeles, San Francisco and Florida, mainly among poor minority heterosexuals (Greenblatt, 1990).

Before the advent of antimicrobial therapy chancroid often proved to be a prolonged illness lasting anywhere between 30 and 40 days and recurrence was common. Nowadays most cases can be treated adequately with antibiotics (Albritton, 1989) but the growing prevalence of antibiotic-resistant strains is creating an alarming medical problem. *H. ducreyi* has been shown to contain plasmids that confer resistance to many classes of drugs, such as sulfonamides, aminoglycosides, tetracyclines, ampicillin and penicillin (Morse, 1989). The immediate cause for concern is evidence that genital ulcers break down the normal skin barrier and consequently increase exposure to HIV. Recent data from Kenya show that up to 80% of HIV transmissions in East Africa are related to synergism between HIV and STDs that cause genital ulcers, such as chancroid, herpes and syphilis (Check, 1992), and in Africa, as well as in many other developing parts of the world, most genital ulcers are due to chancroid (Johnson et al., 1988). The pathogenicity of *H. ducreyi* is at present not well understood at the molecular level. It is important therefore that we obtain information concerning the molecular basis of *H. ducreyi* pathogenesis so that we can combat the disease in this country as well as in other parts of the world.

2. Outer membrane components Studies with other pathogenic bacteria indicate that surface components such as capsular polysaccharides and constituents of the outer membrane are often important virulence factors (Smith, 1977). The outer membrane surface of Gram-negative bacteria is composed of lipids, outer membrane proteins (OMP)

and lipopolysaccharides (LPS). These surface components interact with mucous, host-cell membranes and circulating glycoproteins that initiate the host immune response.

2.1 OMP, Pili and Cytotoxins Characterization of the OMPs of different strains of *H. ducreyi* by sodium dodecyl sulfate polyacrylamide gel electrophoresis (SDS-PAGE) shows that at least seven different subtypes exist in the molecular weight range of 24-50 kDa (Odumeru et al., 1983; Taylor et al., 1985). To determine which of these proteins are exposed on the cell surface, whole cells were treated with radioactive reagents to label their surface-exposed proteins. SDS-PAGE of whole cell lysates from six strains tested and subsequent autoradiography of the gels showed that two proteins of molecular weight 39 and 27-30.5 kDa were highly labeled, indicating substantial surface presentation (Abeck & Johnson, 1987). Although the 39 kDa protein appears to be common to all the strains tested, it is not clear what role this protein plays in the pathogenesis of *H. ducreyi.* This may be the same protein later identified by Spinola as the most abundant protein in the outer membrane of *H. ducreyi* (Spinola et al., 1993). Based on amino acid sequence homology the protein was determined not to be a classical porin but rather belonged to the OmpA family of proteins. Spinola also described the binding of MAb 3B9 raised against nontypable *Haemophilus influenzae* to a non-heat-modifiable 18 kDa OMP found on the surface of 35/35 strains of *H. ducreyi* from different parts of the world (Spinola et al., 1992). The possible role of this protein was not reported.

Some strains of bacteria express on their outer membranes fine hair-like appendages called pili which are made up of a large number of protein monomers called pilin. It has been found that 10 of 12 *H. ducreyi* strains examined expressed pili and that the molecular weight of the pilin monomer was 24 kDa. Preliminary conclusions from binding studies indicated that the pili of *H. ducreyi* may bind to different receptors than the pili of other non-enteric pathogens (Spinola et al., 1990). A more recent study suggests that many strains of *H. ducreyi* are able to bind to extracellular matrix proteins such as fibrinogen, fibronectin, collagen, gelatin and laminin through specific interactions with their pili (Abeck

et al., 1992). To date, the evidence that pili or OMP of *H. ducreyi* play a role in cell adherence or evasion of the host defense system has not been forthcoming. Indeed, an evaluation of the humoral immune response to OMP of *H. ducreyi* disclosed that the response was cross-reactive with other *Haemophilus* species and elevated levels of antibody were detected in patients who did not have chancroid (Alfa et al., 1993). On the other hand, LPS elicited a specific response that was detected only in patients with chancroid.

There are conflicting reports on the ability of *H. ducreyi* to elaborate toxins which are responsible for its cytotoxic activity. A recent report identifies a hemolysin produced by *H. ducreyi* (Palmer & Munson Jr., 1993). Lagergård has reported that 6 of 10 *H. ducreyi* strains tested produced a cytotoxin which was active mainly on human cell lines. The cytotoxin was thought to be a protein based on its inhibition by heat and pronase treatment (Purven & Lagergård, 1992; Lagergård et al., 1993). The same researchers also showed that antibodies produced by immunization of rabbits with *H. ducreyi* bacterial sonicates could neutralize this cytotoxic activity (Lagergård & Purven, 1993). On the other hand, Abeck tested 10 strains of *H. ducreyi* for their ability to produce extracellular enzymes which might contribute to their pathogenicity and did not detect protease, elastase, lecithinase, lipase or collagenase activity in any of the culture filtrates. Moreover, he did not detect cytotoxic activity in cell-free culture filtrates when tested *in vitro* using either an established tissue culture cell line or a primary cell culture of human keratinocytes. He concluded that extracellular products do not play a role in host invasion or production of tissue damage by *H. ducreyi* and that the damage to tissue is more likely to be caused by interactions of *H. ducreyi* LPS with host inflammatory mediators (Abeck et al., 1991; Abeck & Korting, 1991). There is no consensus for the existence of one or more soluble protein exotoxins but the possibility cannot be ruled out.

2.2 LPS The outer-cell membrane glycolipids have been shown to be important determinants in the pathogenicity of many strains of bacteria (Smith, 1977), and must be considered as potentially important in the pathogenicity and virulence of *H. ducreyi*. The outer-membrane glycolipids of bacteria that colonize mucosal surfaces of the genital and respiratory tracts such as *Neisseria gonorrhoeae*, *Haemophilus influenzae* and *Neisseria meningitidis* lack the repeating O-antigens (long polysaccharides comprised of a variable number of repeated oligosaccharide units) of enteric LPS (Griffiss et al., 1988; Gibson et al., 1989; Phillips et al., 1990). They tend to have short glycans with various degrees of branching. These structures consist of core-like oligosaccharide regions attached to lipid A which anchors the structure to the outer membrane. In some ways these lipooligosaccharides (LOS) resemble glycosphingolipids of mammalian cell membranes.

2.2.1 Evidence for LOS Role in Pathogenesis Although other outer membrane components may play a role in the pathogenesis of chancroid, in our laboratory we have focused on LOS for several reasons. For one, our recent structural studies of the LOS from the mucosal pathogens *N. gonorrhoeae* and *H. influenzae* suggest that they contain a common structural epitope, which can also be found in the glycose moiety of the human erythrocyte glycosphingolipid lactoneotetraglycosylceramide (Phillips et al., 1990). Recently it has been shown that the monoclonal antibody (MAb) 3F11 generated against *N. gonorrhoeae* also binds to many strains of *H. ducreyi* (Campagnari et al., 1990). Such findings imply that the oligosaccharide portions of the LOS surface antigens of *H. ducreyi* contain epitopes (some of which are shared by *N. gonorrhoeae*) that mimic human antigens, enabling the organism to evade the host immune system. Two, there is growing evidence in recent years for the role of carbohydrates, especially those containing sialic acid, in cell adhesion processes (Springer & Lasky, 1991). Consequently, the elucidation of LOS structure should provide important clues to the part it plays in enabling the organism to establish itself on genital mucosal surfaces. Three, both Tuffrey and our

collaborators at SUNY Buffalo have presented data from experiments using intradermal injection of live and heat-killed *H. ducreyi* in mice and rabbits that have shown that LOS by itself can cause lesions (Tuffrey et al., 1990; Campagnari et al., 1991). There is also ample evidence from studies on other bacteria that the lipid A portion of the LPS molecule is responsible for a bewildering array of endotoxic activities (Brade et al., 1988). For example, lipid A is known to cause the production of many endogenous mediators such as interleukin 1 and tumor necrosis factor (TNF). When one considers that the endogenous mediator platelet-activating factor (PAF) is involved in stomach ulcers (Rosam et al., 1986) and that injections of LPS in rats cause the release of PAF (Doebber et al., 1985), it is easy to theorize that lipid A may well be involved in the mechanism of ulcer formation in chancroid.

The primary problem in sorting out the details of the pathogenic process is the lack of suitable biological assays for assessing the virulence of *H. ducreyi*. The traditional approach involves the production of cutaneous skin lesions in rabbits and mice after intradermal inoculation. It has been reported that both rabbit (Feiner et al., 1945; Dienst, 1948; Purcell et al., 1991) and mouse (Tuffrey et al., 1990) succumb to skin lesions after intradermal injections of live or heat-killed *H. ducreyi*. Campagnari and Tuffrey have also demonstrated that LOS by itself caused ulceration and necrosis in the rabbit model (Tuffrey et al., 1990; Campagnari et al., 1991). These data implicate LOS as the causative agent. As can be seen from Table 1.1 the LOS from other bacteria besides *H. ducreyi* can cause skin lesions in the rabbit model. However, at doses of less than 10 ng the LOS of *H. ducreyi* is capable of causing lesions and extensive necrosis, whereas doses greater than 1 μg of LOS are required from other organisms and the lesions in these cases are considerably smaller.

Table 1.1 Effects of intradermal inoculation of 20 μg LOS (abscess size (mm), day 4)[a]

Species	Strain	Mean Abscess Size (+/- SE)[b]
H. ducreyi	33921	14.7 (+/- 0.25)
H. ducreyi	CIP542	10.2 (+/- 0.25)
H. ducreyi	35000	8.5 (+/- 0.28)
N. gonorrhoeae	1291	9.0 (+/- 0.0)
H. influenzae	2019	3.0 (+/- 0.0)
E. coli	LE392	2.5 (+/- 0.28)

[a]Represents values from four animals (rabbits)

[b]SE (Standard error of the mean)

Purcell has argued that experience with *Treponema pallidum*, which also causes genital ulcers, emphasizes the importance of reduced ambient temperature in enhancing lesion formation in the animal model. Since the rabbit normal temperature is higher than human skin, he proposed that lowering the temperature better approximated the human situation. Consequently he used a temperature dependent (15-17°C) rabbit model where lower inocula were sufficient to consistently produce necrotic lesions (Purcell et al., 1991). It appears that *H. ducreyi* achieve close to optimal growth conditions under these lower temperatures and consequently more LOS is available at the site of injection. A more elaborate study in which *H. ducreyi* were grown in subcutaneous chambers implanted in mice demonstrated that infection could be maintained for months at a time compared to at most one week for the previously described models (Trees et al., 1991). Such a model may prove extremely useful for studying the effects of *in vivo* growth on the antigenic composition of *H. ducreyi*.

Nevertheless, the validity of using animal models to determine virulence in humans must be called into question by the fact that a strain previously considered avirulent

(CIP542) in the rabbit skin lesion assays has been found to cause infection in humans. Preliminary data from a very recent report on using primates for the study of chancroid indicate that the advantage of employing an animal model closely related to the target host may circumvent the problem that virulence factors important in causing disease display host specificity (Totten et al., 1994). An even more recent and daring experiment, in the true tradition of Ducreyi himself, concludes that human experimental infection with *H. ducreyi* is well tolerated and safe and may in the long run be the ideal way to study the disease (Spinola et al., 1994).

Meanwhile our collaborator Dr. Campagnari has recently been successful in using cultured human keratinocytes isolated from freshly removed human neonatal foreskins to both assess LOS cytotoxicity and to measure adhesion and invasion of *H. ducreyi.* Since keratinocytes are probably the first cells encountered by *H. ducreyi* in the early stages of infection these assays promise to be more relevant than those previously described for animal models. Data from cultured human keratinocyte adherence assays conducted in Campagnari's laboratory revealed that the four *H. ducreyi* strains tested bound with approximately 15-25% adherence. Maximum % adherence was achieved after 2 hours. The *E. coli* strain and the three *Moraxella catarrhalis* strains tested showed no significant adherence at any of the time points (Brentjens et al., 1994). Preliminary data from an invasion assay of keratinocytes using *H. ducreyi* strain 35000 and its isogenic transposon mutant defective in LOS biosynthesis indicated that around 10% of the parent strain was able to invade after 4 hours, whereas virtually none of the mutant entered the cells (Campagnari, unpublished results). Campagnari has also demonstrated the cytotoxic effects of the LOS from four strains of *H. ducreyi* on human cultured human keratinocytes (unpublished results). These assays allow a much better assessment of the virulence of different strains of *H. ducreyi* than those previously described for animal models and they facilitate the determination of how the structures of the LOS of these strains relate to their pathogenicity.

2.2.2 Model for LOS Role in Infection We have proposed a preliminary model for the roles of LOS in the initial stages of *H. ducreyi* infectivity (Fig. 1.1). Skin with its stratified epithelium presents a much more formidable mechanical barrier to penetration by bacteria than do mucose membrane epithelial surfaces (Smith, 1977). Consequently, a breach of the outermost layers, the stratum corneum and the stratum granulosum, is required for successful entry. LOS is probably involved in attachment of the microorganism to lectins on host keratinocytes located in the superficial layers. Since the LOS of other mucosal pathogens such as *N. gonorrhoeae* and *H. influenzae* resemble host glycosphingolipids and probably serve to evade the host immune response (Phillips et al., 1990), it seems reasonable to suppose that a similar mechanism is operating in *H. ducreyi.* Those organisms that gain entry into the stratum spinosum may bind to receptors on skin macrophages called Langerhan (L) cells or keratinocytes through some portion of their LOS. This triggers the Langerhan cells or keratinocytes to release cytokines such as inerleukin-2, α-interferon and tumor necrosis factor (TNF), which mediate the host immune response.

3. H. ducreyi LOS Structure Based on Biological and Immunochemical Data

A generalized model for the structure of the LOS from *Haemophilus* is shown (Fig. 1.2). It is based in part on its similarity to the LOS determined for *H. influenzae* strain 2019 (Phillips et al., 1992). The LOS molecule is composed of an oligosaccharide linked by a ketosidic bond through one or more 3-deoxy-D-*manno*-octulosonic acid (Kdo) residues to a membrane-associated lipid A. The oligosaccharide consists of core and branch regions. The core is composed of two unusual sugars, L-*glycero*-D-*manno*-heptose (Hep) and Kdo. In addition, charged residues such as phosphate and phosphoethanolamine (PEA) are frequent constituents of the core region. This core is relatively constant, but the branch region can vary to a large extent, its most commonly found sugars being glucose (Glc),

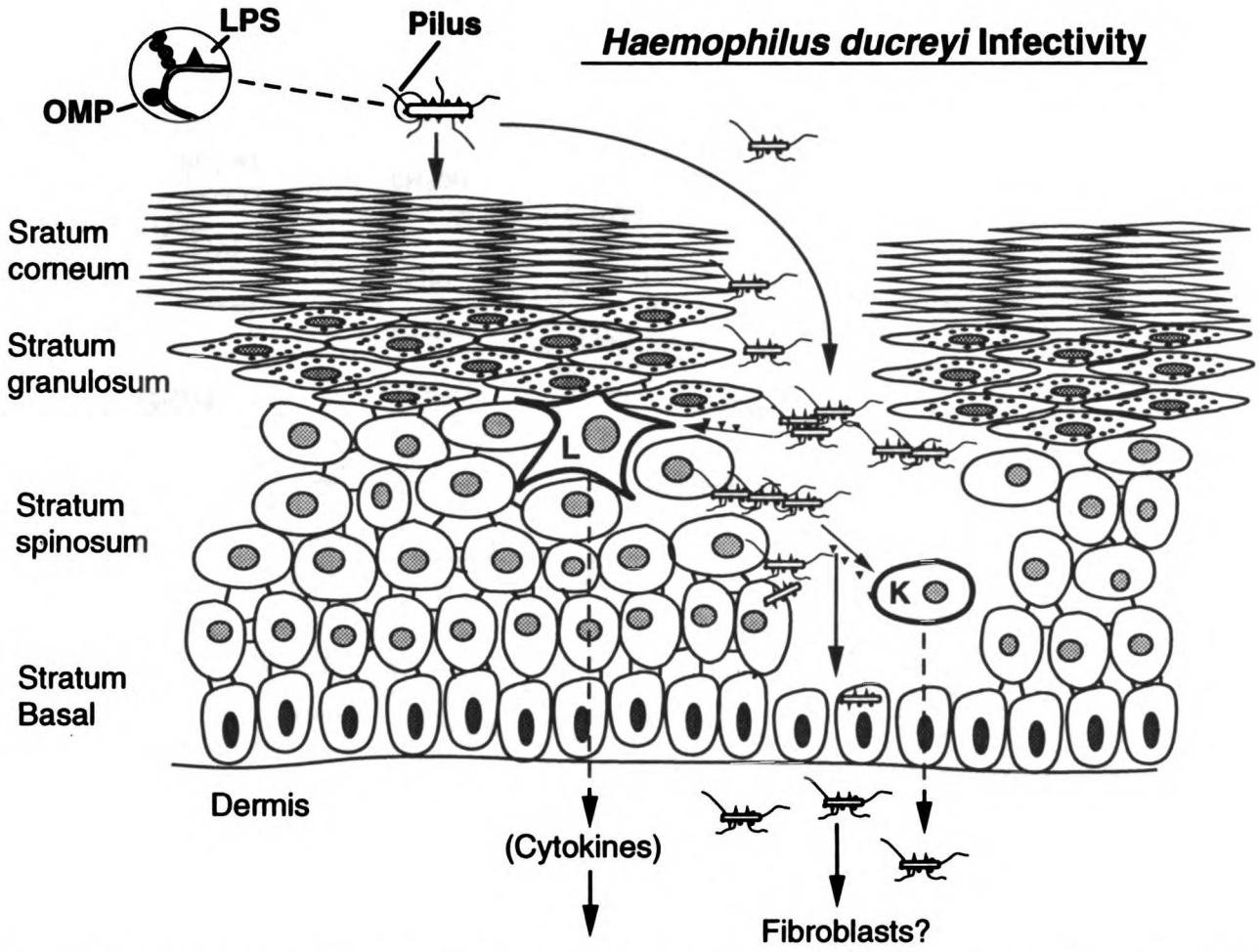

Figure 1.1. Potential roles of *H. ducreyi* LOS in the initial stages of infection and invasion. LOS may bind to receptors on keratinocytes (K) or Langerhan (L) cells and mediate the host pathogenic response through the release of cytokines such as IL-2 and TNF. *H. ducreyi* may further affect fibroblasts in the dermal layer, causing de-nucleation either by direct invasion or through the release of cytokines or exotoxins.

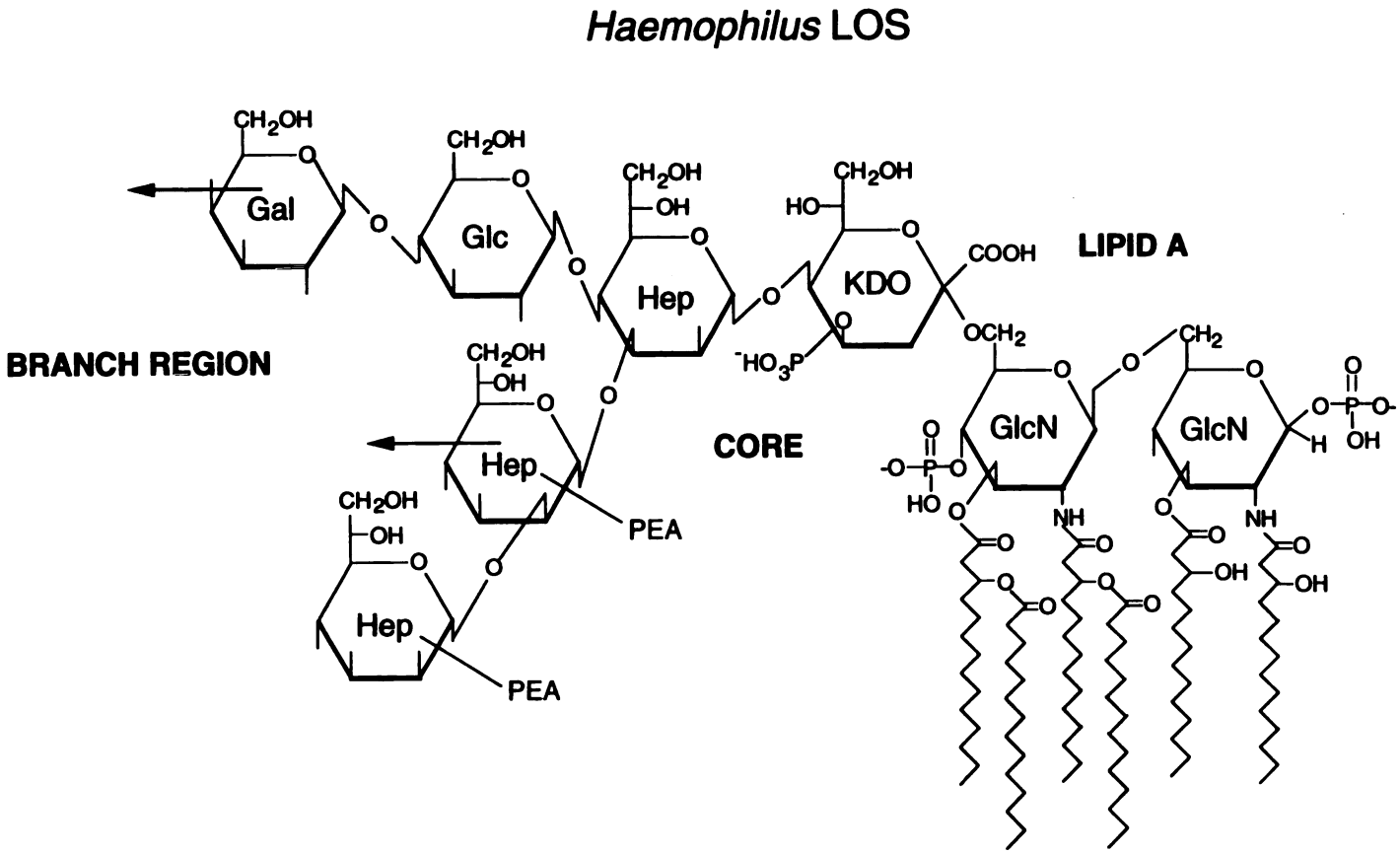

Figure 1.2. Generalized model of *Haemophilus* LOS based in part on the structure published for *H. influenzae* strain 2019. The arrows indicate some LOS contain extended branches off the first and second core heptoses.

galactose (Gal), *N*-acetylglucosamine (GlcNAc) and *N*-acetylgalactosamine (GalNAc) (see Appendix Fig. 1).

The lipid A molecule is composed of a β1,6-linked D-glucosamine disaccharide which bears an α-glycosidically linked phosphate on position 1 of the reducing end and an ester-linked phosphate on the 4' position of the non-reducing terminus. The phosphorylated glucosamine disaccharide is substituted with various fatty acids in amide and ester linkages.

Until this project was initiated, no detailed structural analysis of *H. ducreyi* LOS had been undertaken. Two groups had shown, using SDS-PAGE analysis and silver-staining of gels, that the outer-membrane glycolipids of *H. ducreyi* lacked the O-antigenic side chains found in the LPS of enteric bacteria (Abeck et al., 1987; Odumeru et al., 1987) and resembled more the LOS of *N. gonorrhoeae* and *H. influenzae*. All other available structural information was deduced from biological and immunochemical studies.

It was demonstrated that LOS from avirulent strains of *H. ducreyi* were capable of removing from human serum bactericidal activity against serum-sensitive strains (Odumeru et al., 1985). On the other hand, LOS from virulent strains did not possess this capability. This seemed to suggest that the structure of LOS is crucial in determining whether or not a strain exhibits sensitivity or resistance to inactivation by serum. In a later report it was shown that the LOS SDS-PAGE profiles of avirulent strains were similar, but differed from those of virulent strains and that the total glycose:Kdo ratio of the LOS of virulent strains was greater than that of avirulent strains (Odumeru et al., 1987). Taken together these data indicated that the composition of the oligosaccharide region of the LOS of *H. ducreyi* may be the determining factor in serum-sensitivity or serum-resistance of different strains.

Corroboration for this emerged from antibody binding studies. Recent structural studies conducted in our laboratory of the LOS from the mucosal pathogens *N. gonorrhoeae* and *H. influenzae* suggested that they contain a common structural epitope that

is also found in the carbohydrate part of human erythrocyte glycosphingolipids. We theorized therefore that the LOS surface antigens of *H. ducreyi* may contain epitopes that mimic human antigens allowing the organism to evade the host immune response. A set of monoclonal antibodies raised against *N. gonorrhoeae* was tested for cross-reactivity with epitopes expressed by *H. ducreyi* LOS (Campagnari et al., 1990). MAb 3F11, which was made in response to gonococcal LOS, reacted to a 4.8 kDa LOS band in 98% of gonococcal strains (Mandrell et al., 1988) and also bound to a similar 4.8 kDa band on the LOS of 16/17 *H. ducreyi* strains tested. This 3F11 epitope has been characterized as immunochemically similar to the terminal region of paragloboside, a precursor to a major human blood group antigen (Mandrell et al., 1988). The presence of this epitope in the carbohydrate region of *H. ducreyi* LOS may represent a form of host mimicry, possibly allowing the organism to evade the host immune response.

Confirmation of the structure of the 3F11 epitope came from studies of the oligosaccharide region of the LOS from *N. gonorrhoeae* strain F62 (Yamasaki et al., 1991) and five pyocin variants of *N. gonorrhoeae* strain 1291 (John et al., 1991). The wild type strain was found to display the lacto-*N*-neotetraose antigen (Galβ1→4GlcNAcβ1→3Galβ1→4Glcβ1) which is recognised by the MAb 3F11 (Fig. 1.3). The oligosaccharide structures of 1291a and 1291c-e represent consecutive sugar deletions from the major wild type structure. MAb 3F11 did not bind to these variant strains presumably because of the absence of the terminal lactosamine i.e. Galβ1→4GlcNAc. The 1291b oligosaccharide configuration reveals an alternative biosynthetic pathway in which a terminal Gal is added to the lactose moiety. Antibody binding studies suggest that this structure is similar or identical to the P^k antigen of human glycosphingolipids (Fig. 1.4). All this implies that these organisms, in their LOS biosynthesis, are imitating the biosynthesis of human glycosphingolipids which diverge after forming a lactose disaccharide to generate the P^k and the paragloboside blood group antigens (Clausen & Hakomori, 1989) (Fig. 1.4).

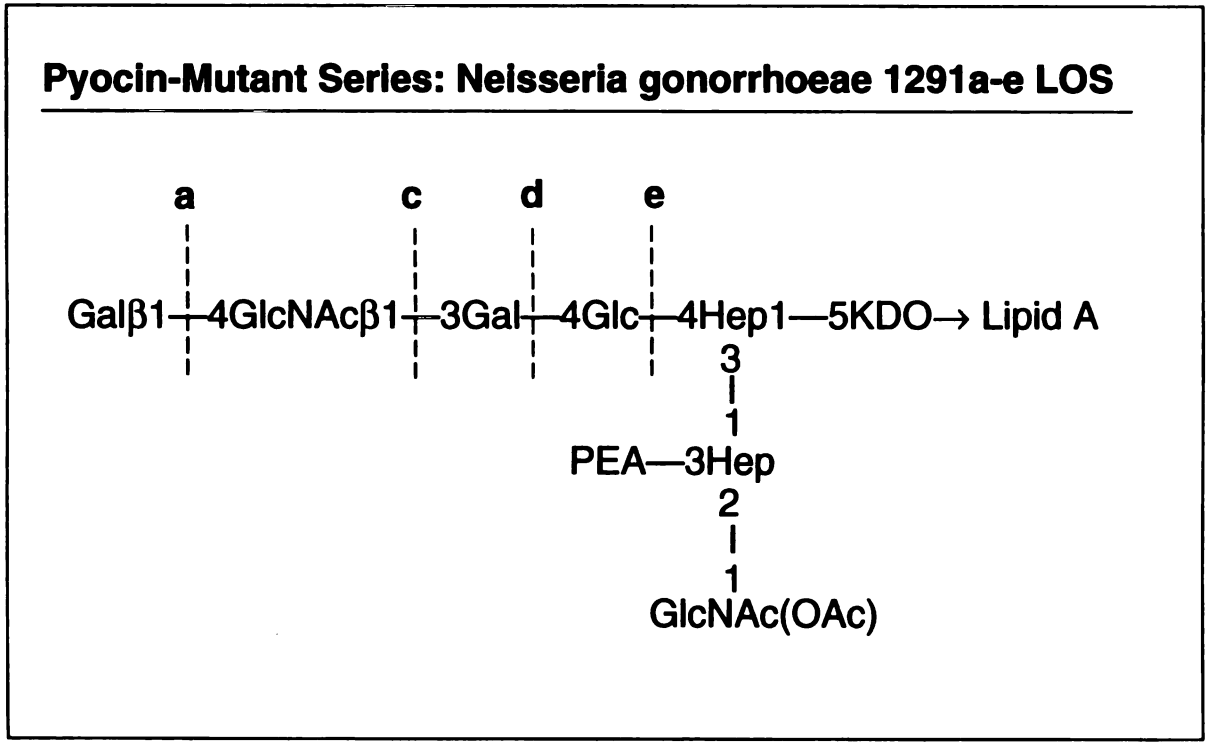

Figure 1.3. Structures of the oligosaccharides from the 1291a-e pyocin variants of *N. gonorrhoeae*. The oligosaccharide from the wild type strain contains the lacto-*N*-neotetraose antigen. The oligosaccharide from 1291b has a terminal Gal linked to the lactose disaccharide of the oligosaccharide from 1291c.

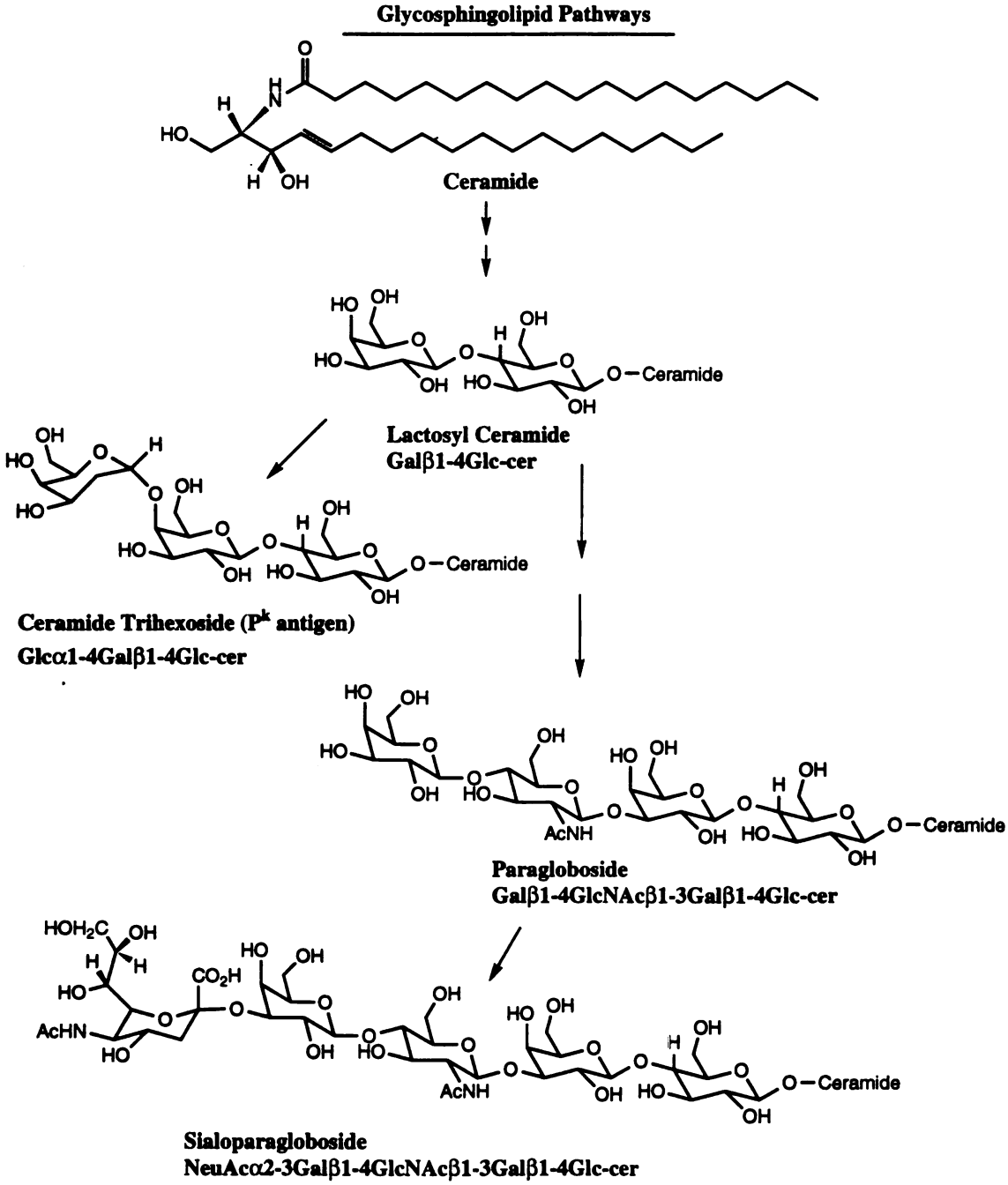

Figure 1.4. Glycosphingolipid biosynthetic pathways showing the formation of blood group antigens.

The host mimicry theory was further supported by analysis of the LOS from *H. influenzae* nontypable strain 2019 (Phillips et al., 1992). The major dephosphorylated oligosaccharide from this strain was shown to have the following structure:

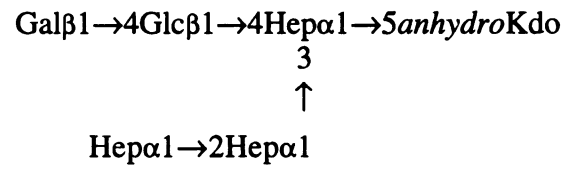

The terminal lactose portion represents an epitope found on lactosylceramide, a human glycosphingolipid which is also a precursor to human blood group antigens (Fig. 1.4).

Earlier in a collaborative effort our laboratory had identified the presence of sialic acid in the LOS from a prototype meningococcal strain (Mandrell et al., 1991). Sialylation of LOS in *Neisseria* is proving to be an important biological event. It has been shown to endow bacteria with the ability to evade lysis by human serum (Tan et al., 1986; Parsons et al., 1989) and/or killing by human neutrophils (Tan et al., 1986; Kim et al., 1992; Wetzler et al., 1992). The fact that treatment of various *H. ducreyi* strains with neuraminidase increased binding to the MAb 3F11 suggests that at least some components of their LOS are sialyated.

Despite the dearth of structural detail, it was clear that there was ample evidence that the LOS from *H. ducreyi* displayed many intriguing features which might produce clues to how the organism causes disease. It was with this rationale that LOS structure/function studies were undertaken.

4. Review of Strategies for LOS Structural Analysis LOS are amphipathic molecules which are composed of a hydrophilic carbohydrate region and a hydrophobic lipid A. This has the disadvantage of making it difficult to purify the intact molecule which tends to aggregate in solution. The traditional approach has been to selectively hydrolyze the bond that links Kdo to lipid A under mild acid conditions. The oligosaccharide and lipid A moieties are then purified and characterized separately as outlined in Fig. 1.5.

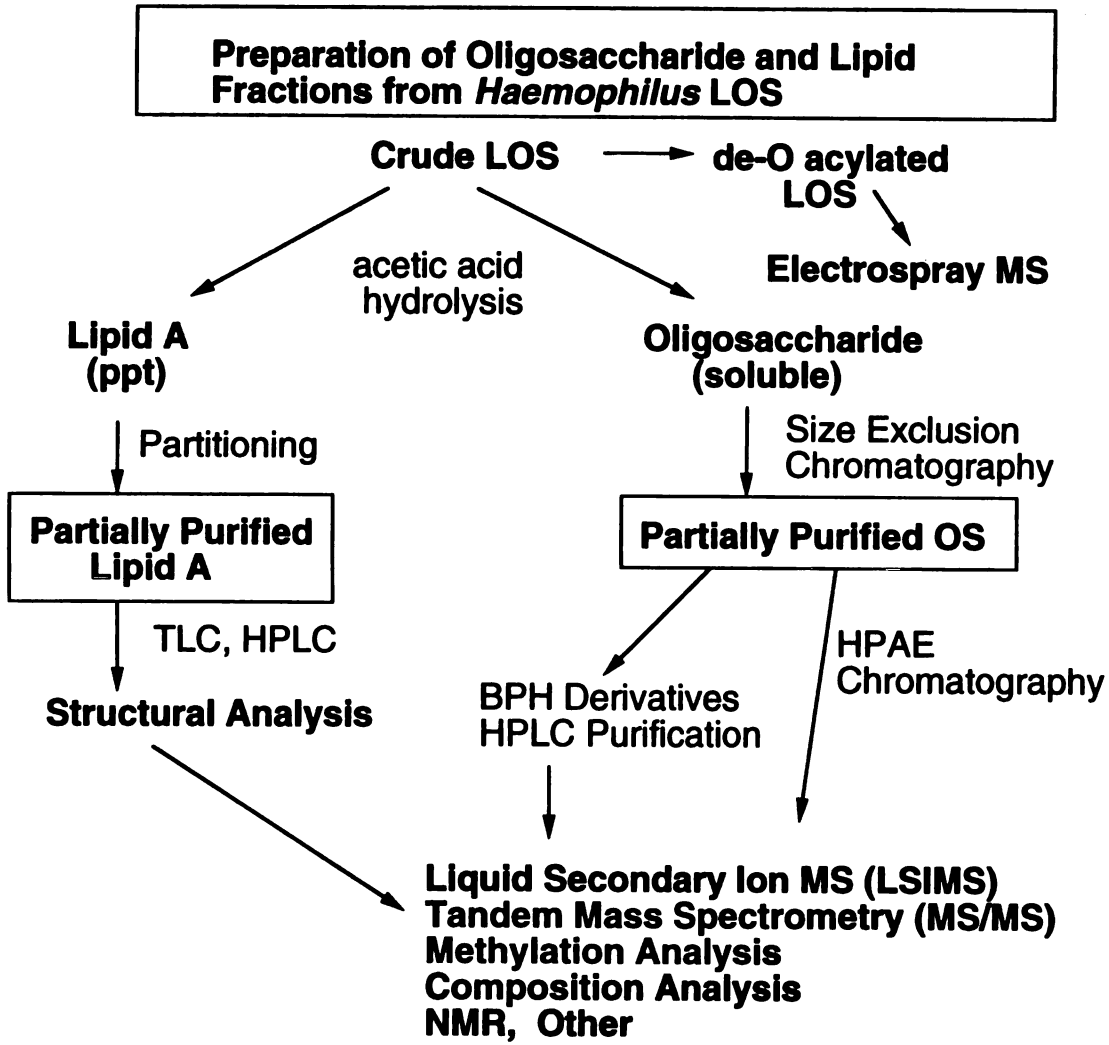

Figure 1.5. Scheme outlining the steps involved in purifying and analysing *Haemophilus* LOS.

To determine the complete structure of an oligosaccharide four types of analyses are performed (Hellerquist & Sweetman, 1990). Compositional analysis discloses which sugars are present and their molar ratios. Linkage analysis determines how the sugars are attached to one another. Anomeric configuration analysis reveals the stereochemistry of the glycosidic bonds and sequence analysis tells the order in which the sugars are linked.

Before embarking on these analyses the oligosaccharide pool generated by mild acid hydrolysis of LOS must be separated and desalted. To accomplish this many different types of chromatographic purification schemes have been attempted over the years. Most of the earlier methods such as thin layer chromatography (TLC), gas chromatography (GC) and supercritical fluid chromatograhpy (SFC) suffer from the disadvantage that they require pre-chromatographic derivatization of the sample. Liquid chromatography (LC) techniques are much more useful for carbohydrate analysis. Some of these such as reverse phase chromatography also require that the sample be first derivatized. Others such as metal-loaded cation exchange chromatography are less than ideal for biological samples since other compounds present in the sample such as organic acids are efficient metal chelators and can pull the metals from the cation exchange sites of the stationary phase. The method which has generally found the greatest utility for oligosaccharide separation and purification is gel filtration chromatography (GFC), also called size exclusion or gel permeation chromatography. As the name suggests molecules are separated on the basis of size, or more precisely, hydrodynamic volumes. Very large molecules are completely excluded from the pores of the stationary phase and are eluted in the void volume. The smallest molecules spend the most time in the stationary phase so that the order of elution is inversely related to molecular weight. This is the technique that we routinely employ in our laboratory.

Because carbohydrates do not have a strong chromophore, detection by ultra violet absorbance is extremely poor. Likewise most sugars do not fluoresce; consequently fluorescence detection, like detection by UV absorbance requires sample derivatization with

all the drawbacks involved. One solution is to radioactively label the sample by reduction to the alditol form with sodium borotritiide. Probably the most widely used method for carbohydrate detection, and the one we routinely use in our laboratory, is refractive index. It is based on the principle that any solute in the eluant will change its refractive index. Finally electrochemical detection, in particular pulsed amperometric detection (PAD), is becoming widely used for the monitoring of carbohydrates in LC systems (Townsend et al., 1988). As in other electrochemical methods detection is based on the oxidation of the sample. Only a small percentage of the sample is oxidized at the working electrode and the problem of electrode fouling which plagued previous electochemical methods is overcome by the introduction of a cleaning cycle.

4.1 Compositional analysis Compositional analysis of oligosaccharides has been revolutionized by the advent of high-performance anion exchange chromatography with pulsed amperometric detection (HPAEC-PAD) (Townsend et al., 1988). Before its introduction the determination of sugar composition was an extremely tedious and time-consuming task involving a great deal of chemical manipulation of the sample (Hardy et al., 1988). Methods in common use included GC analysis of monosaccharides as volatile derivatives and LC analysis of chemically derivatized monosaccharides (Honda, 1984). Although anion exchange chromatography had been used for many years to analyse acidic sugars it was not considered feasible for neutral carbohydrates. Carbohydrates are, however, weak acids whose pKa's fall in the range of 12-14. This means that at high pH they are partially or completely ionized and can therefore be separated by anion exchange chromatography. Such an approach of course requires that the column material be stable at high pH. This became possible with the introduction by Dionex of polymeric non-porous pellicular resins. It is fortunate that the types of reactions that carbohydrates are known to undergo at high pH, such as 'peeling' of 3-*O*-substituents on reducing sugars, are slow at room termperature and do not occur to any extent over the time required to perform the chromatography. The upshot is that with the use of the appropriate hydrolysis and gradient

conditions monosaccharides such as Glc, Gal, GlcNAc and GalNAc can be easily resolved and more readily quantified.

4.2 Linkage analysis The daunting task of solving a complete carbohydrate structure can be readily appreciated if one considers analysis of a pentasaccharide. Let us assume that compositional analysis of this pentasaccharide revealed the presence of Glc, Gal, GlcNAc and GalNAc in the molar ratios of 2:1:1:1. Let us also assume for the sake of simplicity that these sugars exist only in the D-pyranose form. This means that Glc and Gal can be linked through one of four different carbons to their neighbours and each linkage can be in the α or β arrangement. GlcNAc and GalNAc can be attached to their neighbours through one of three different carbons. Already there are $8^3 \times 6^2 = 18{,}432$ potential structures for this simple pentasaccharide and we have not even considered the fact that the sugars can be arranged randomly in any order. With 5 sugars, one of which appears twice, there are 5!/2! or 60 arrangements possible. This brings the total to over one million distinct structures. It is easy to see why chemists until fairly recently shunned the study of complex carbohydrate structures. In the past twenty years, however, technological breakthroughs have made it possible to solve the structures of many complex carbohydrates. For example, the application of new technology (discussed below) to the problem of linkage analysis has enabled the rapid determination of attachment positions and ring forms on oligosaccharide samples as low as 0.1 μmol (Hellerquist & Sweetman, 1990). The power of this method is immediately obvious if we consider the drastic reduction it affords in the number of possible structures for our pentasaccharide. After determination of linkage positions the number of structures falls from over a million to less than two thousand.

The most widely used method for determinatin of linkage in carbohydrates involves separation of the partially methylated alditol acetates (PMAAs) by GC and identification of the linkage positions by electron impact (EI) and chemical ionization (CI) mass spectrometry (Lindberg, 1981). There are variations on this theme such as the reductive

cleavage method which produces partially methylated anhydroalditols that are subsequently characterized by GC/MS of their acetates (Gray, 1990). There is also the method of periodate oxidation followed by fast atom bombardment mass spectrometry (FAB/MS) (Angel & Nilsson, 1990). Periodate will cleave sugars with vicinal hydroxyl groups between the carbons to form aldehydes. When the products of this reaction are reduced, permethylated and analysed by LSIMS, the linkage positions between the sugars can be deduced from the ions present in the mass spectrum. Both of these techniques can be extremely useful especially to clarify ambiguities that may arise in the methylation analysis method.

About thirty years ago Hakomori showed that Cory's methylsulfinyl carbanion reagent could be used to completely methylate sugars (Hakomori, 1964). The method has more recently been adapted to microscale analysis of carbohydrates (Levery & Hakomori, 1987). To make the PMAAs from an oligosaccharide four steps are required. First, the oligosaccharide is dissolved in DMSO and the carbohydrate OH groups are ionized by the addition of powdered NaOH (Larson et al., 1987). Methyl iodide is added and an SN_2 type reaction occurs in which O^- is the nucleophile and I^- is the leaving group. This effectively replaces all the hydrogens on hydroxyl groups with methyl moieties. Second, the sample is now hydrolysed to produce the monosaccharides. Only those positions which were previously linked in the oligosaccharide will not be methylated. In the third step, the monosaccharides are reduced to their alditols using sodium borodeuteride which isotopically labels one end of the sugar. This eliminates structural ambiguities that may exist in the interpretation of the mass spectra. The sugars are finally acetylated with acetic anhydride and the locations of the acetyl groups reveal the linkage positions in the oligosaccharide. The PMAAs are then analysed by GC/MS in both the EI and CI modes and the spectra compared to standards to determine the identities of the sugars present, their ring forms and linkage positions. EI alone does not usually furnish all the information sought. Ionization with electrons is a highly energetic process that gives extensive

fragmentation but very often leaves no trace of the molecular ion. CI on the other hand produces ions by the relatively soft process of proton transfer from a reagent gas such as ammonia and intense protonated molecular ions are generally visible.

4.3 Anomeric Configurations There are three ways to determine anomeric configurations. The most reliable method, if enough sample is available, is by nuclear magnetic resonance (NMR). The chemical shifts of most oligosaccharide protons fall in the range 3.5-4.3 ppm. In a one-dimensional (1D) spectrum this is an extremely congested region. Fortuitously, anomeric protons have chemical shifts between 4 and 6 ppm where there are few other resonances. Consequently one can readily differentiate between the α configuration and the β configuration by chemical shifts and coupling constants. With the exception of mannose, α protons tend to have smaller coupling constants and greater chemical shifts than β protons. Generally speaking, protons in the α-anomeric configuration have *J* vicinal coupling constants in the 1-3 Hz range and chemical shifts greater than 5 ppm. The vicinal coupling constants of protons in the β-anomeric configuration are in the 7-8 Hz range and their chemical shifts are usually less than 5 ppm (Michon et al., 1990). If milligram quantities of pure material are available, the complete oligosaccharide structure can often be determined almost entirely from two-dimensional (2D) NMR techniques.

Khoo et al. have reported the assignment of anomeric configurations in oligosaccharides by a combination of chemical and mass spectrometric methods (Khoo & Dell, 1990). Chromium trioxide oxidizes β-pyranosides to keto-esters while leaving α-pyranosides largely intact. The method is based on analysis by mass spectrometry of the deuteroacetylated derivatives of the oligosaccharides before and after oxidation with chromium trioxide. The ions observed in the mass spectra reveal the places in the sequence where oxidation occured. Deuterated derivatives help to ensure that mass increments representing oxidation are not confused with under- or over-acetylated products. Nevertheless, the approach is fraught with problems. The study was conducted on simple

oligosaccharides whose structures were known beforehand. Many fragment ions appear in the spectra whose identities would be difficult to predict had the samples not been previously characterized. It remains to be seen if the method can be adapted to more complex unknown carbohydrates.

The third approach to stereochemical assignment of glycosidic linkages is through the use of specific enzymes (Maley et al., 1989). There are enzymes called glycosidases which will cleave only glycosidic bonds with a particular stereochemistry. For example α-glycosidases recognize only α-anomers and will not touch β-anomers. Consequently it is possible, by treating the oligosaccharide sequentially with these enzymes and monitoring the products by mass spectrometry or some chromatographic method such as HPAEC-PAD, to determine the anomeric linkages. One needs to be absolutely sure of the purity of the enzymes before embarking on this method. Other probes such as lectins and monoclonal antibodies are generally employed to confirm prior determination of anomeric configurations.

4.4 Sequence Analysis of Oligosaccharides Sequence analysis of oligosaccharides was accelerated by the arrival of fast atom bombardment or liquid secondary ion mass spectrometry (LSIMS) around 1980 (Dell, 1987). Until that time workers depended heavily on standard chemical methods, which were extremely tedious, for composition and sequence information (Lindberg, 1981). In the LSIMS experiment a thin layer of viscous material such as glycerol or a mixture of glycerol/thioglycerol is applied to the metal tip of the probe. A solution of the sample (usually 1 μl) is added to the probe tip which is bombarded with a beam of accelerated ions such as cesium (Falick et al., 1986). The transfer of kinetic energy converts those molecules near the surface to positive and negative ions which are sputtered into the gas phase, extracted, and mass analysed according to the particular mass spectrometer being used (Hellerquist & Sweetman, 1990). The advantages of LSIMS over previous mass spectrometric methods such as field desorption mass spectrometry (FDMS) and electron impact mass spectrometry (EIMS) became immediately

apparent. For the first time it was possible to consistently obtain high quality spectra of relatively large (up to 3,000 Da) polar biological molecules (Dell, 1987).

The molecular weights of oligosaccharides can be determined, typically to within 0.2 daltons, by LSIMS analysis (see Appendix Table 1). As we have already seen, relatively few sugars constitute the molecular building blocks that make up bacterial oligosaccharides (see Appendix Fig. 1). Consequently, one can severely restrict possible sugar compositions by using a computer program that searches for combinations of building blocks that add up to a target mass. This allows one to apply a preliminary composition to the oligosaccharide consisting of generic sugars. LSIMS also gives a rough measure of sample heterogeneity. Generally speaking, even after chromatographic purification, the oligosaccharides consist of complex mixtures which vary both in phosphorylation states and sugar compositions. Treatment of the sample with aqueous HF, which cleaves phosphate ester bonds, and reanalysis by LSIMS establishes the number of phosphoesters present by mass difference.

Although it is possible to obtain limited fragmentation of glycosidic bonds from LSIMS of underivatized oligosaccharides, generally some type of derivatization of the sample is required to produce more extensive sequence information. One of the most common derivatization procedures is permethylation. However, the classic method of permethylation is not particularly suited to oligosaccharides with Kdo on the reducing terminus because of destructive side reactions that complicate the LSIMS spectra (Gibson et al., 1989; Dell et al., 1990). As an alternative to permethylation, various alkyl *p*-amino-benzoates were found to be much more useful derivatizing reagents for LSIMS analysis of carbohydrates which lack Kdo on the reducing terminus (Webb et al., 1988; Poulter & Burlingame, 1990). In this reaction the amino group of the derivatizing reagent forms a Schiff base with the carbonyl of the reducing end of the carbohydrate. The resulting imine is then reduced to the secondary amine with sodium cyanoborohydride. These types of derivatizations increase the hydrophobicity of the oligosaccharide, promoting surface

activity within the glycerol/thioglycerol matrix in LSIMS. Because only molecules near the surface of the matrix are sputtered into the gas phase during the desorption process, this greatly increases the sensitivity of the mass spectral analysis. These derivatives also add a sensitive UV chromophore to the carbohydrate allowing for good HPLC separations and ideal for further purification of the oligosaccharide pool remaining after GFC. Unfortunately, low yields were obtained when these reagents were used on bacterial oligosaccharides which contained Kdo at the reducing terminus (John, 1990).

The best reagents we have found to derivatize Kdo-containing oligosaccharides which still retain the advantages of the *p*-amino-benzoates are the alkylphenylhydrazines (John & Gibson, 1990). The hydrazones formed by reaction of these reagents with Kdo are more stable to hydrolysis than the imines formed by the alkyl *p*-amino-benzoates and consequently no reduction step is required. It turns out that it is actually advantageous to have Kdo at the reducing terminus because with an α-hydroxy aldose or ketose there is a tendency to form the ozazone. Since Kdo is deoxy at the 3 position one does not find reaction products containing more than one molecule of the hydrazino-compound. LSIMS spectra of alkylphenylhydrazine derivatives generally show fragment ions arising from cleavage of branch glycosidic bonds with charge retention on the reducing terminus (John & Gibson, 1990; Phillips et al., 1992; Phillips et al., 1993).

Even with sample derivatization, fragment ion data from LSIMS spectra of oligosaccharides are rarely enough to make a complete sequence assignment. Furthermore, other oligosaccharides present in the sample can be confused with fragment ions, particularly those resulting from glycosidic bond cleavage. Under the conditions of the LSIMS experiment the core heptoses are resistant to cleavage so that it is not possible to assign branch points. This becomes possible under the high-energy collision-induced-dissociation (CID) conditions used in tandem mass spectrometry (MS/MS) (John, 1990; Phillips et al., 1990; Phillips et al., 1992). In an MS/MS experiment ions are initially generated in the LSIMS ion source of the first mass spectrometer (MS-1) (Gillece-Castro &

Burlingame, 1990). Using the double-focusing analyzer of MS-1, a particular ion of interest is selected and focused into a collision cell where a collision gas such as helium serves to increase its internal energy causing unimolecular dissociation reactions. The fragment ions obtained from the collision cell are refocused and mass-analysed in a second double-focusing analyser (MS-2). The beauty of this method is that a daughter-ion spectrum showing extensive fragmentation (see Appendix Figs. 2, 3 and 4) of the parent ion can be obtained from one specific species in a mixture. This limits the number of chromatographic steps required in sample preparation as well as furnishes abundant reducing and non-reducing terminal fragment ions which allow complete oligosaccharide sequence assignment in terms of the generic monosaccharides i.e. Hex, Hep, HexNAc etc.

4.5 Complete Structure Determination of oligosaccharides by NMR

Following preliminary ^{1}H and ^{13}C-NMR studies which can be used to determine the monosaccharide components, linkage positions and anomeric configurations (Yamasaki et al., 1991; Phillips et al., 1992), the complete oligosaccharide structure can be determined using 2-D NMR methods (Dabrowski, 1987). Protons belonging to isolated monosaccharide spin systems can be assigned by establishing spin-spin coupling networks. 2-D *J*-correlated spectroscopy (COSY) (Dabrowski et al., 1983; Ingaki et al., 1987; Romanowska et al., 1988) and phase-sensitive double-quantum filtered COSY (DQF-COSY) spectroscopy (Rance et al., 1983) can be used to establish direct coupling connectivities, and homonuclear Hartmann-Hahn (HOHAHA) spectroscopy (Rance et al., 1983; Ingaki et al., 1987) can show relayed connectivities. The identities of monosaccharide residues may be established by determining vicinal coupling constants for ring protons, which indicate sugar configuration. Coupling constant values are readily obtained by analysis of the fine structure of the cross-peaks in DQF-COSY spectra (Rance et al., 1983).

Once the isolated sugar spin systems have been assigned, oligosaccharide sequence assignments can be determined using 1-D and 2-D nuclear Overhauser effect (nOe) spectroscopy (Hall & Saunders, 1980; Kumar et al., 1980; Rance et al., 1983). In these experiments, connectivity is established by observing inter-residue nOes between anomeric protons and aglyconic protons. For simultaneous determination of dipolar couplings throughout the oligosaccharide, 2-D NOESY spectroscopy (Lerner & Bax, 1987) can be performed at a number of different mixing times. If sufficient sample is available, ^{13}C-^{1}H correlation spectroscopy (Lerner & Bax, 1987; Abeygunawardana et al., 1990) can also be used to establish inter-residue connectivities. A combination of DQF-COSY, HOHAHA, and NOESY experiments, similar to those used in the sequencing of the *H. influenzae* 2019 hexasaccharide (Phillips et al., 1992), is generally sufficient to unambiguously establish the complete oligosaccharide structure.

4.6 Analysis of Lipid A Previous work on *Neisseria* and *Haemophilus* strains suggests that most of the variability in LOS lies in the oligosaccharide portion and that lipid A is the more conserved part of the molecule. Nevertheless, within the lipid A moiety variations may take the form of different numbers of carbon atoms in the fatty acid chains, and deviations in the kind and extent of acyloxyacyl groups and phosphoryl residues. Considering the long list of biological activities ascribed to lipid A in other species of bacteria, it appeared that structural studies on the purified lipid A from *H. ducreyi* might help to explain the highly cytotoxic effect of its LOS.

Many of the techniques discussed above for the structural analysis of oligosaccharides are also applicable to the determination of lipid A structure. For example most of the structural details can be obtained by NMR and the various mass spectrometry methods mentioned previously. Nevertheless there are unique features to the analysis of lipid A that need to be addressed. After the initial acetic acid hydrolysis, the precipitated lipid A can be purified by partitioning in chloroform/methanol/water and subjected

immediately to LSIMS analysis. However at this stage the sample may be fairly heterogeneous and usually some chromatographic step is required. Many types of chromatography have been successful in partitioning the crude lipid A but the one most widely used is TLC (Takayama et al., 1986; Johnson et al., 1990). The spots are visualized by fluorescence or partial dichromate-sulfuric acid charring, scraped from the plate, redissolved in chloroform/methanol and centrifuge-filtered. They are now ready to be characterized by mass spectrometry.

Under LSIMS conditions one observes the molecular ion and fragment ions which represent losses of fatty acid groups, particularly the more labile *O*-acyl groups. Also evident are ions corresponding to fragments arising from cleavage of the glycosidic bond between the two glucosamines (Takayama et al., 1986; Cotter et al., 1987). It is, however, even with the help of MS/MS, impossible to obtain the definitive structure of lipid A by mass spectrometric means alone. Usually a combination of chemical and enzymatic modifications followed by mass spectrometric analysis is necessary to achieve that goal (Johnson et al., 1990; Johnson et al., 1990; Masoud et al., 1991). An alternative approach is to convert lipid A to its dimethyl or dimethylpentasilylated derivatives and analyse by NMR (Takayama et al., 1988; Johnson et al., 1990; Johnson et al., 1990).

For fatty acid analysis and quantitation, lipid A is first hydrolysed to release the hydrocarbon chains which are then methylated with diazomethane (Batley et al., 1985). An alternative method uses boron trifluoride to simultaneously hydrolyse and esterify the fatty acids. The stereochemistry of the **R** or **S** substituted fatty acids can be determined by making the D-phenylethylamide derivatives (Reitschel, 1976). The fatty acids are then analysed by GC/MS and compared to external standards.

4.7 Analysis of Intact LOS The aspiration of every LOS chemist is to discover a way to analyse LOS directly without any chemical degradation of the sample. With a few exceptions, it has not been generally possible to solubilize LOS to the extent necessary to make it amenable to mass spectrometric analysis. Indeed, it is highly fortuitous that the

ketosidic linkage between Kdo and lipid A is selectively cleavable by mild acid hydrolysis. Otherwise structural analysis of LOS would have progressed at a painfully slow rate. The problem of course is that the use of chemical methods such as acid hydrolysis may degrade the molecule in some manner. For example it is conceivabe that some of the heterogeneity seen in the mass spectra of both oligosaccharide and lipid A comes from breaking of glycosidic bonds during acid hydrolysis. The point is that there are considerable advantages from a biological point of view to looking at the intact species.

John et al. had glimpsed a largely 'intact' molecule of LOS by pushing the limits of LSIMS (Mandrell et al., 1991). The technology available at the time did not permit a more sensitive analysis. The 'intact' LOS in question had, before LSIMS analysis, been dephosphorylated with aqueous HF and treated with hydrazine to selectively cleave *O*-linked fatty acids on lipid A. This LSIMS spectrum showed, in addition to the expected molecular ion, an LOS component that was 291 Da higher in mass. This was consistent with the addition of a sialic acid residue. Since sialic acid would be lost during the traditional acetic acid hydrolysis required to separate the oligosaccharide from lipid A, this was an exciting experimental observation at the time, although the quality of the spectrum was poor. The signal abundances of both the sialylated and non-sialylated species were low and there was the distinct possibility that even the moderate HF-treatment used in the experiment might be expected to cleave at least some of the sialic acid glycosidic bonds. The breakthrough however, was that *O*-deacylation rendered the LOS molecule water-soluble and, even though still phosphorylated (Fig. 1.6), the LOS was now amenable to analysis by a new technique called electrospray ionization mass spectrometry (ESI-MS) (Edmonds & Smith, 1990). In fact when the same *O*-deacylated LOS was run by ESI-MS the spectrum showed intense well-defined peaks for both sialylated and asialo LOS species. Moreover, the ESI-MS spectrum indicated a much greater level of sialylation than was first suspected from the LSIMS data. These data provided the first clues that electrospray mass spectrometry would revolutionize LOS structural analysis.

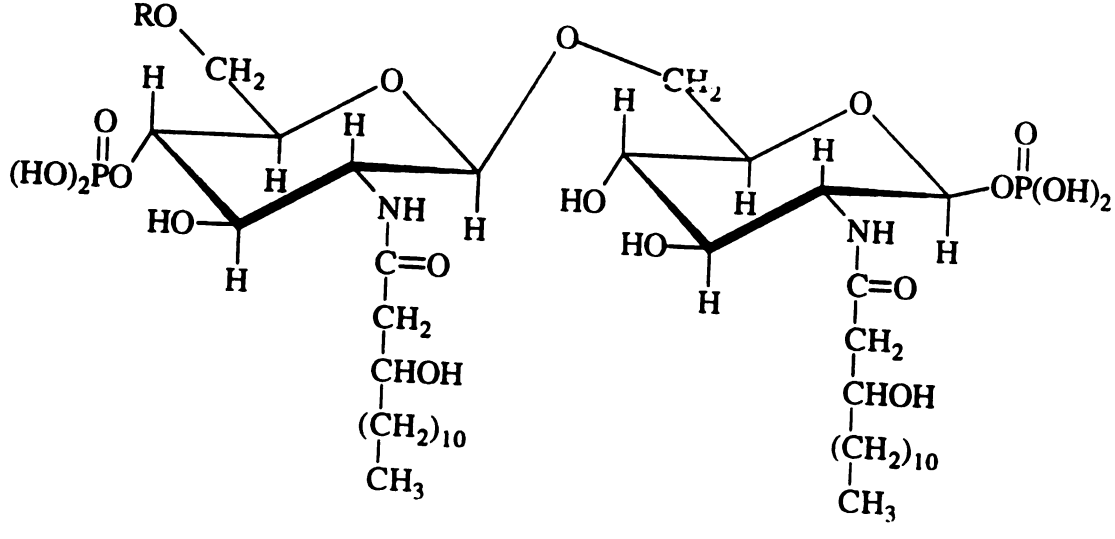

Figure 1.6. Structure of *O*-deacylated lipid A from *Haemophilus*. R represents the oligosaccharide portion of the LOS.

Electrospray ionization allows the transfer of large polar biomolecules (greater than 100,000 daltons) from the liquid to the gas phase for direct mass determination (Edmonds & Smith, 1990). Solvent containing the biomolecules emerges through a hollow needle and is dispersed as a fine spray by a high voltage electric field. Ions of one polarity are preferentially drawn into the drops by the electric field as they are separated from the bulk liquid. The separation is not complete so that each charged droplet contains solvent and both positive and negative ions. Ions in the droplets are freed of solvent by a current of warm gas. As the solvent evaporates and the radius of the droplet gets smaller, the electric field at the surface increases and ions migrate towards the surface. At some critical field value ions are emitted from the droplets directly into the gas phase and drawn into the high vacuum of a quadrupole mass analyser (Fenn et al., 1990).

ESI-MS produces abundant multiply charged ions, usually protonated in the positive mode or deprotonated in the negative mode, although other adducts such as sodium are common. These ions are registered on the basis of their mass-to-charge ratio, *m/z*. Fortuitously many of theses ions fall in the 500-2000 *m/z* range of normal instruments, even when the parent mass is greater than 2000. The *m/z* value for each peak has three unknown elements, the mass of the parent molecule, the number of charges on the ion, and the mass of each species (e.g. H, Na, K, etc. which tend to form adducts with sample ions) contributing one of the charges (Fenn et al., 1990). Fortunately ions of adjacent peaks generally differ by one charge so that any pair of ions can be used to calculate the charge state and molecular weight (Appendix Fig. 5). Each additional ion can be used as an independent measurement of the molecular weight so that algorithms which signal-average over all the ions in a single spectrum can provide very accurate molecular weights.

In a typical ESI-MS experiment run in the negative-ion mode, *O*-deacylated LOS produces multiply deprotonated molecular ions whose charge state generally reflects the number of phosphates present in the molecule. For example, most lipid A moieties contain

two phosphate groups and if there are no other phosphates or other residues capable of stabilizing negative charge on the oligosaccharide portion, the most abundant charge state will be the doubly charged ion. The presence of one or more phosphates on the oligosaccharide will shift the deprotonated molecular ions to the triply charged state or higher. Calculation of the molecular weight of the LOS from two peaks in the spectrum is facile (Appendix Fig. 5). When one considers that the only previously available method for LOS molecular weight determination was SDS-PAGE, one sees immediately that as far as mass accuracy and resolution are concerned ESI-MS is a vast improvement. The molecular weights obtained from ESI-MS are typically accurate to within one or two daltons and are sufficient to predict preliminary monosaccharide compositions from a relatively 'intact' LOS form.

ESI-MS is also extremely useful for assessing overall LOS heterogeneity. We have seen time and again in our laboratory major discrepancies in the degree of heterogeneity observed in the oligosaccharide region by LSIMS compared to ESI-MS. Often truncated or extended analogs representing saccharide deletions from or additions to the major species, which are prominent in ESI-MS of LOS, are not observed in LSIMS of oligosaccharides. This heterogeneity may have important biological implications and it may also serve as a guide towards improving oligosaccharide separation and purification.

Lastly ESI-MS allows one to identify acid-labile moieties such as sialic acid which are lost from the LOS during mild acid hydrolysis. We had earlier observed that there was a tendency for the LOS from certain *Haemophilus* species to lose some component linked to Kdo during acetic acid hydrolysis (Phillips et al., 1992). ESI-MS showed that the component was actually a phosphate group. It is difficult to underestimate how important these structural details may be in understanding the structure/function relationship of the LOS from *H. ducreyi*. Consequently a major focus of this present work was to analyse 'intact' LOS by ESI-MS to guarantee that no acid labile residues are lost in the initial acetic acid hydrolysis step, to determine the exact number of Kdos present in the LOS and to help

in elucidating the structural features of native LOS that are responsible for ulcer formation. For example it was important to identify the presence of sialic acid on particular oligosaccharide epitopes in order to understand the influence of this residue on biological activity. Variations in other parts of the LOS molecule such as phosphorylation of oligosaccharide or lipid A and differences in *N*- and *O*-linked fatty acids, any of which may have profound biological consequences, are likewise more easily observed by analysis of 'intact' LOS. Therefore the capabilities of ESI-MS in the determination of LOS structure were emphasized in the course of this work.

CHAPTER 2.

PRELIMINARY CHARACTERIZATION OF THE MAJOR LIPOOLIGOSACCHARIDE FROM *HAEMOPHILUS DUCREYI* STRAIN 35000

INTRODUCTION

As mentioned in the introduction, although there is ample evidence to support the importance of *H. ducreyi* LOS in the pathogenesis of chancroid, limited structural data is currently available. Elucidation of the molecular structure of *H. ducreyi* LOS is likely to provide critical information pertaining to the roles these glycolipids play in the pathogenic and immunologic processes. We began our investigation of LOS structure with studies of the major LOS from *H. ducreyi* strain 35000. This strain was first isolated in Winnepeg in 1975 (Odumeru et al., 1987). It was chosen because it had been the subject of previous biological and immunochemical studies. It has a type A outer membrane protein and was reported to be virulent in both the temperature dependent rabbit model (Purcell et al., 1991) and in the earlier rabbit model (Feiner et al., 1945; Dienst, 1948). Western blot studies using MAb 3F11, originally directed to the LOS of *N. gonorrhoeae*, had identified an epitope immunochemically similar to the terminal tetrasaccharide of paragloboside, a precursor to a major blood group antigen, on the LOS of the majority of *H. ducreyi* strains, including strain 35000 (Campagnari et al., 1990). The expression of a human antigen on the surface of this organism might offer some indication as to how it is able to evade the host immune defenses and/or establish disease. For these reasons we considered strain 35000 an excellent choice to begin our structural analysis of *H. ducreyi* LOS.

EXPERIMENTAL

Materials LPS from *Salmonella typhimurium* TV119 Ra mutant, glucose, galactose, glucosamine, galactosamine, Kdo and anhydrous hydrazine were all obtained from Sigma (St. Louis, MO). An alditol acetate mixture prepared from the LPS of *Aermonas liqefaciens* serotype SJ19 was kindly provided by G. Aspinall (University of York, Canada) and butyl phenylhydrazine by J. Webb (Illinois State University). Aqueous HF (48%) was purchased from Mallinckrodt (Muskegon, MI) and sodium borodeuteride (98% D) from Aldrich. Acetonitrile, water and methanol were obtained from Burdick and Jackson (Muskegon, MI). Acetic anhydride was purchased from Supelco (Bellefonte, PA), methyliodide from Fluka (Switzerland) and the standard test mixture of partially methylated alditol acetates from Biocarb (Lund, Sweden). All other reagents and solvents used were of reagent grade.

Isolation and purification of LOS The LOS from *H. ducreyi* strain 35000 was isolated using a modified phenol water extraction procedure of Westphal and Jahn (Westphal & Jahn, 1965). Briefly the dried organisms were suspended in a mixture of hot water/phenol which was kept at 65°C for 10-15 min. The mixture was then cooled to 10°C and centrifuged at 80,000 x *g* for 45 min and the top aqueous layer saved. The bottom phenol layer was heated to 65°C, hot water added and the mixture shaken vigorously at 65°C for 15 min. The mixture was centrifuged as before and the aqueous layers combined and dialyzed against running water for 72 h. The LOS sample was then centrifuged for 8 h at 80,000 x *g*. The pellet was re-suspended in water, centrifuged at 105,000 x *g* for 3 h and lyophilized. A two liter growth of overnight culture gave ≈ 0.8 g of dried organisms which yielded ≈ 10-12 mg of LOS.

For mass spectrometric analysis, a small amount of LOS was *O*-deacylated according to the procedure of Helander *et al.* (Helander et al., 1988). The original procedure used ≈ 100 mg of LOS, therefore we scaled down this method to be appropriate

for much smaller amounts of LOS. Briefly, 1 mg of LOS was incubated with 200 µl of anhydrous hydrazine for 20 min at 37°C. The sample was then cooled to -20°C and chilled acetone added dropwise to precipitate the *O*-deacylated LOS which was then centrifuged at 12,000 x *g* for 20 min. The supernatant was removed and the pellet washed again with cold acetone and centrifuged. The precipitated *O*-deacylated LOS was then resuspended in 500 µl of water and lyophilized. In one experiment, the *O*-deacylated LOS was further treated with 48% aqueous HF to remove phosphate. Since hydrazine and HF are both extremely toxic these reactions must be performed in a hood. Excess HF was removed as described in the next section.

Isolation and purification of oligosaccharide fraction Twenty mg of LOS from *H. ducreyi* strain 35000 was hydrolysed in 10 ml 1% acetic acid for 2 h at 100 °C. The hydrolysate was centrifuged at 5000 x *g* for 20 min at 4 °C and the supernatant removed. The pellet was washed twice with 5 ml of H_2O followed by centrifugation at 5000 x *g* for 20 min at 4 °C. The supernatant and washings were pooled and lyophilized.

Approximately 10 mg of the dried oligosaccharide was dissolved in 300 µl of 0.05 M pyridinium acetate (pH 5.2), centrifuge-filtered and loaded onto two Bio-Gel P-4 columns connected in series (1.6 x 80 cm, <400 mesh, 30 °C). Samples were eluted in the pyridinium acetate buffer at a flow rate of 10-12 ml/h. Fractions were collected every 10 min and dried down on a Speed-Vac concentrator.

For composition analysis, small aliquots of the oligosaccharide fractions were hydrolyzed in 2 M trifluoroacetic acid for 3 h at 100°C. The hydrolysate was evaporated to dryness in a Speed-Vac concentrator, redissolved in 20 µl H_2O and dried. Monosaccharide separation and quantitation was carried out by high pH anion exchange chromatography (HPAEC) with pulsed amperometric detection as previously described (Phillips et al., 1990).

To remove phosphoester moieties, approximately 100 µg of oligosaccharide was placed in a 1.5 ml polypropylene tube and cold 48% aqueous HF was added to make a 10

μg/μl solution. The reaction mixture was incubated for 16 h at 4 °C. Excess HF was removed under a stream of nitrogen in a polypropylene desiccator *in vacuo*. Solid NaOH was used as a desiccant and an in-line NaOH trap was connected to a water aspirator.

Preparation of butyl phenylhydrazone-oligosaccharides Bio-Gel purified oligosaccharide (≈100 μg) was dissolved in water, transferred to 1 ml glass Reacti-Vials (Pierce) and dried. To each sample approximately 3 molar equivalents of butyl phenylhydrazine (BPH) in 40 μl of methanol (John & Gibson, 1990) was added followed by the addition of 10 μl of water and 0.5 μl of glacial acetic acid for every 100 μg of butyl phenylhydrazine. The reaction mixture was placed in a heating block at 80° C for 30 min, cooled and dried under a stream of nitrogen. The BPH-oligosaccharide mixtures were redissolved in water and separated by high performance liquid chromatography (HPLC) with a Vydac C-18 column (25 cm x 4.6 mm i.d.). The oligosaccharides were eluted with a linear gradient of 0 to 60% acetonitrile at a flow rate of 1 ml/min on a Rainin gradient HPLC system. Both water (solvent A) and acetonitrile (solvent B) contained 0.05% trifluoroacetic acid. The derivatized BPH-oligosaccharides were detected at 335 nm with a Kratos 783 variable wavelength detector, and dried prior to mass spectrometric analysis.

Fractionation and characterization of lipid A Crude lipid A preparations from *H. ducreyi* strain 35000 and *S. typhimurium* Ra mutant (≈10 mg) were suspended in 0.1 N HCl at a concentration of 2.5 mg/ml and sonicated for 10 min. The mixture was heated at 100 °C for 20 min and cooled. Five volumes of chloroform/methanol (2:1, v/v) were added to two volumes of the hydrolysis mixture and vortexed. This mixture was centrifuged at 5,000 x g for 15 min and the lower organic layer plus the middle emulsion layer were recovered and evaporated to dryness. A small aliquot of this fractionated lipid A was hydrolyzed in 6 N HCl at 100 °C for 4 h and analyzed by HPAEC for monosaccharide composition as described above. Fatty acids analysis was carried out by hydrolyzing the lipid A in 14% BF_3/methanol at 100 °C for 6 h followed by GC/MS analysis of the methyl

esters as previously described (Batley et al., 1985). Thin layer chromatography (TLC) of the resulting lipid A fraction was performed using 250 μm silica-gel LK5 plates (Whatman) as described by Johnson *et al.* (Johnson et al., 1990). Spots were visualized at 366 nm, scraped off and eluted with $CHCl_3$/methanol/water (10/5/1,v/v/v).

Methylation analysis Linkage analysis was performed on purified oligosaccharide using the microscale method of Levery and Hakamori (Levery & Hakomori, 1987), which was modified by replacing NaH with NaOH as previously described (Phillips et al., 1990). Final analysis of the partially methylated alditol acetates were carried out using a VG70SE mass spectrometer equipped with a Hewlett Packard 5890 gas chromatograph and an on-column injector (J&W Scientific). Samples were separated on a 30 m DB-1 column with a 1-μm film thickness (J&W Scientific). For comparison, a purified HF-treated *Salmonella typhimurim* Ra oligosaccahride containing equimolar amounts of the follwing sugars; terminal Gal, terminal Hep, 1,2-linked Gal, 1,2-linked Glc, 1,3,6-linked Glc, 1,3-linked Hep and 1,3,7-linked Hep.

Mass spectrometric analysis Both underivatized and derivatized oligosaccharides were directly analyzed by liquid secondary ion mass spectrometry (LSIMS). The oligosaccharides and their corresponding BPH derivatives were dissolved in water, dried on the probe under vacuum and redissolved in thioglycerol/glycerol (1/2, v/v). Lipid samples were dissolved in chloroform and 1 μl of nitrobenzyl alcohol/triethanolamine (1/1, v/v) was applied as the liquid matrix. Samples were then analyzed on a Kratos MS 50S mass spectrometer retrofitted with a cesium ion source (Falick et al., 1986) and operating at a resolution of 1500-2000 (m/Δ m, 10% valley). A primary ion beam of 10 keV was used to ionize the samples and secondary ions were accelerated at 6 kV. Scans were acquired at 300 s/decade and recorded on a Gould electrostatic recorder. Ultramark® 1206 was used for manual calibration to an accuracy better than ± 0.2 Da.

Tandem mass spectra (MS/MS) were obtained on a four-sector Kratos Concept II HH mass spectrometer fitted with an optically-coupled 4% diode array detector on MS II as previously described (Walls et al., 1990). A cesium ion beam energy of 18 keV produced molecular ions which were selected in MS-I and passed to the helium collision cell floated at a potential of 2 kV where the gas pressure was adjusted to attenuate the parent ion beam by two-thirds of its initial value. The daughter ions were detected and analyzed in MS-II with successive 4% frames and a constant B/E ratio.

A VG Bio-Q mass spectrometer with an electrospray ion source operating in the negative ion mode was used to mass analyze the *O*-deacylated LOS. The LOS samples were dissolved in triethylamine/water (1:1) and 3 µl were injected via a Rheodyne injector into a constant stream of 10 mM ammonium acetate/acetonitrile (1/1, v/v) running at 2 µl/min. Mass calibration was carried out with an external horse heart myoglobin reference using the supplied VG Bio-Q software.

RESULTS

Oligosaccharide Composition and Structure Size-exclusion chromatography of the oligosaccharide fraction from *H. ducreyi* 35000 LOS gave the elution profile shown in Figure 2.1. Analysis of the most abundant fractions (#57 and #58) by LSIMS identified a single major oligosaccharide with a deprotonated molecular ion, $(M-H)^-$, at m/z 1676.6[a] (M_r 1677). Aqueous HF treatment of this oligosaccharide and subsequent LSIMS analysis did not change its mass, indicating the lack of phosphate or phosphoethanolamine. Composition analysis of the major fraction using HPAE chromatography identified glucose (Glc), galactose (Gal), glucosamine (GlcN) and L-*glycero*-D-*manno*-heptose (Hep) in a molar ratio of 1/2.5/1.1/2.7, but no Kdo was observed. In addition to these components, a

[a] Nominal masses are given throughout the text for both ions and molecular weights unless otherwise noted. Both values are based on the isotopically pure ^{12}C-component of the natural isotopic distribution.

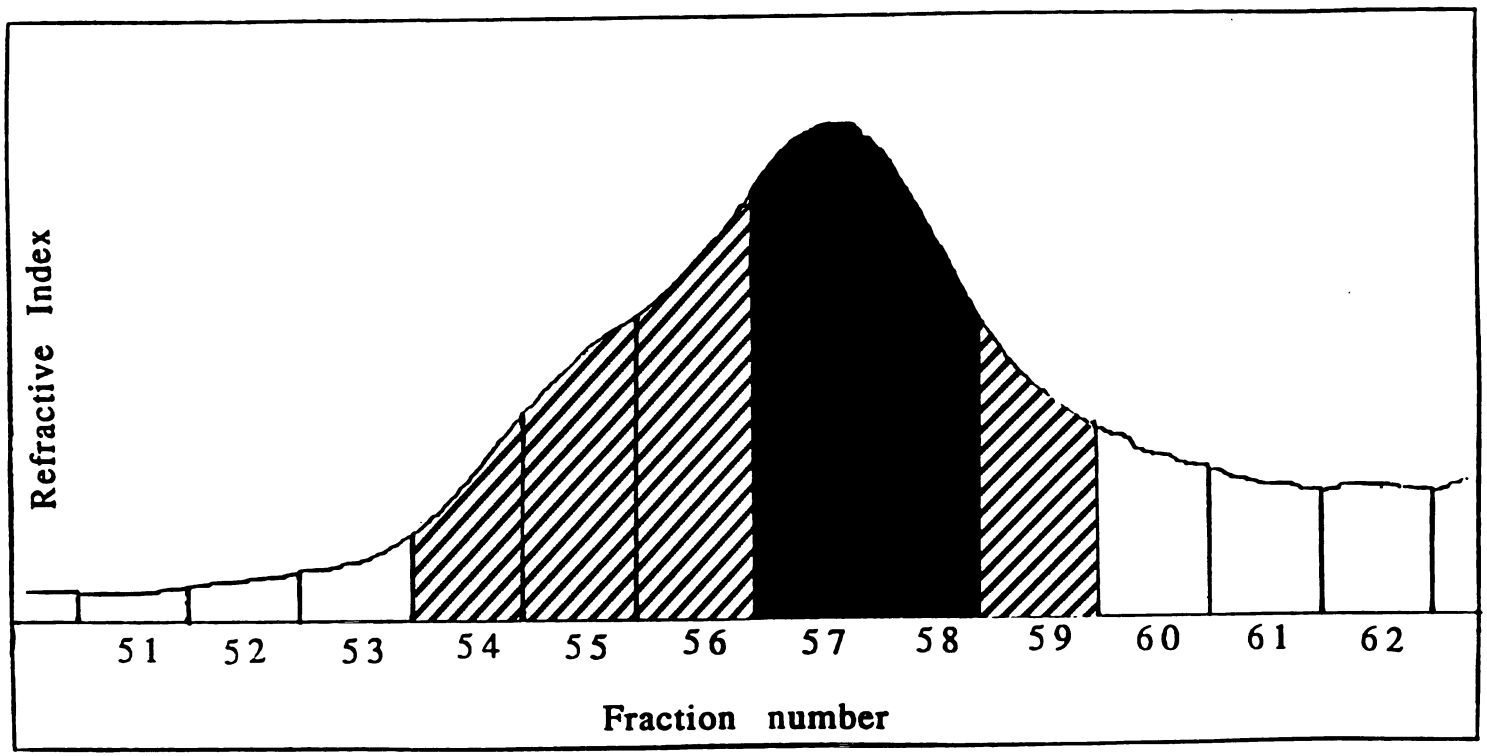

Figure 2.1. Elution profile of *H. ducreyi* oligosaccharides on a Bio-Gel P-4 column. Fractions 57 and 58 were used for the preparation of BPH derivatives and in the tandem mass spectrometry experiments. In all fractions analyzed (54-59), the oligosaccharide with M_r 1677, was the base peak. In fractions 54, 55, 56 and 57, a much less abundant ion was also seen at m/z 1884, but its identity has not yet been established. The elution volume of fraction 58 was 150 mL, and V_0 and V_t for the column were ≈ 80 and 280 mL, respectively. The elution volumes of maltoheptose and maltotetraose were 230 and 260 mL, respectively.

peak was observed eluting just prior to the peak for heptose of ≈30% the relative area. Consistent with this information, a computer calculation[b] yielded a single overall composition of Hex_3 $HexNAc_1$ Hep_4 $(Kdo\text{-}H_2O)_1$, with this last Kdo species representing an anhydro form that would not be readily identified in the composition analysis (see Appendix Table 2A).

The presence of a modified Kdo in the LOS of *H. ducreyi* was not unexpected as we had previously encountered an anhydro Kdo in our studies of the LOS from the related bacteria *Haemophilus influenzae*, strain 2019 (Phillips et al., 1990). In *H. influenzae* 2019 LOS, the formation of the anhydro Kdo form was linked to the presence of a phosphate group on the C-4 position that undergoes β-elimination during mild acid hydrolysis (Phillips et al., 1990). A proposed mechanism for the elimination reaction is shown in Figure 2.2. The phosphate on the C-4 position of Kdo is β to the C-2 carbonyl carbon and can readily undergo elimination under the conditions of mild acid hydrolysis. The reaction most likely produces alkene derivatives of Kdo which can subsequently undergo rearrangement to form anhydro ring structures (Auzanneau et al., 1991). To confirm the presence of a similar labile phosphate on the Kdo of *H. ducreyi* LOS, the intact LOS was de-*O*-acylated in mild hydrazine and treated with aqueous HF to remove any phosphoester moieties prior to mild acid hydrolysis. LSIMS analysis of the released oligosaccharide yielded a $(M\text{-}H)^-$ ion at m/z 1694, 18 Da higher in mass than that previously observed.

In order to obtain sequence information of this major oligosaccharide, the corresponding BPH derivative of the M_r 1677 oligosaccharide was prepared and separated by HPLC. The derivatization scheme for the formation of BPH-OS is shown in Figure 2.3. Butyl phenylhydrazine reacts under acidic conditions with the open chain form of Kdo to form phenylhydrazones which are fairly stable to hydrolysis. The HPLC elution

---

[b] A computer algorithm (Gretta Carbos) developed by W. Hines was used to search all possible compositions for a specific observed mass. In practice, minimum and maximum values for each monomer are assigned to the search along with an overall mass precision.

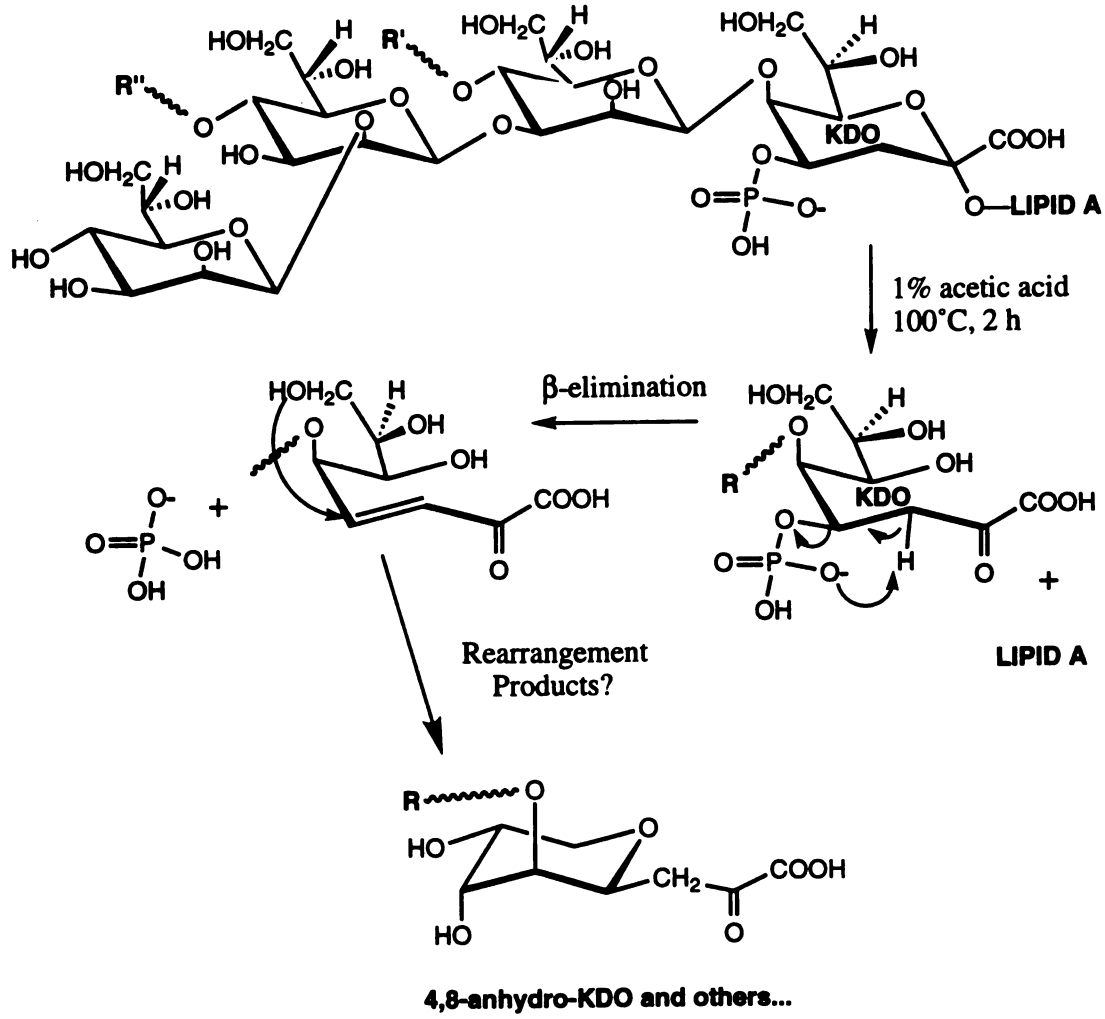

Figure 2.2. β-elimination of phosphate during acetic acid hydrolysis of *Haemophilus* LOS. The α,β-unsaturated ketone intermediate that is initially formed rearranges to yield various anhydro-Kdo structures, one of which is shown.

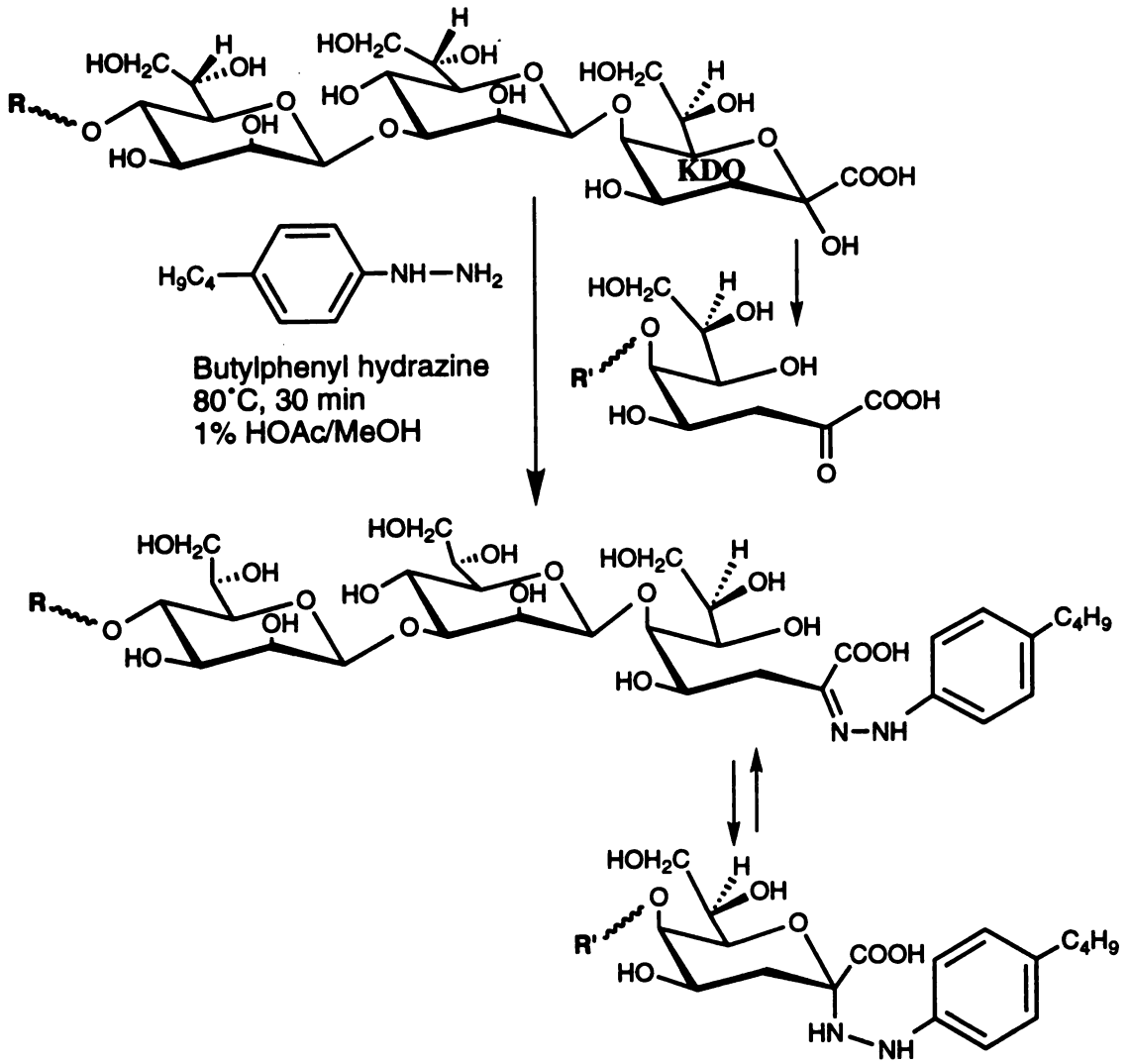

Figure 2.3. Derivatization scheme for the production of butyl phenylhydrazine oligosaccharide derivatives.

profile of the corresponding BPH derivative(s) of this major oligosaccharide showed seven peaks of near equal abundance. LSIMS analysis yielded the expected molecular ion for the hydrazine derivative at m/z 1822 for all seven peaks, and each peak produced a more or less identical spectrum to that shown in Figure 2.4. This result was consistent with the presence of anhydro Kdo at the reducing terminus which has previously been shown to produce a series of diastereomers upon reaction with substituted hydrazines [N. Phillips, unpublished data]. Analysis of the accompanying fragment ions in these LSIMS spectra identified at least two branches; a Hex→HexNAc→Hex→Hep→Hex branch defined by an abundant reducing terminal Y-type ion series (*m/z* 1660, 1457, 1295, 1103 and 941) and a non-reducing terminal Hep (m/z 1630). Y-type ions are formed by cleavage of the glycosidic oxygens with charge retention on the reducing terminal fragment (Domon & Costello, 1988) (see Appendix Figs. 2 and 3). These data allowed us to construct the following partial structure; Hex→HexNAc→Hex→Hep→Hex→(Hep→)Hep_2→Kdo, where the inner core heptose arrangement was still undefined.

To both confirm and complete this preliminary structure, tandem mass spectrometry was performed on both the underivatized oligosaccharide and the corresponding BPH-derivative(s). After collision induced dissociation in the intermediary collision cell, an array of ion fragments is generated from a single isotopic molecular ion that provides more detailed structural information than that typically seen in a conventional LSIMS experiment. One such MS/MS spectrum is shown in Figure 2.5 for the underivatized oligosaccharide at m/z 1676. In this spectrum, Y-ions at m/z 795, 1292 and 1484 now define the inner-core region as a heptose trisaccharide attached to *anhydro*Kdo. The remaining fragment ions are consistent with the structure determined from the BPH-oligosaccharide detailed in Figure 2.4. Given that this structure contains an unusual branch heptose that is not part of the core region, MS/MS analysis was also carried out on the two Y-ions (see Appendix Fig. 2) representing cleavage on either side of this heptose in the underivatized oligosaccharide, i.e. m/z 1149 ($Y_{4\alpha}$) and 957 ($Y_{3\alpha}$), to make sure that no other interpretation exists. These

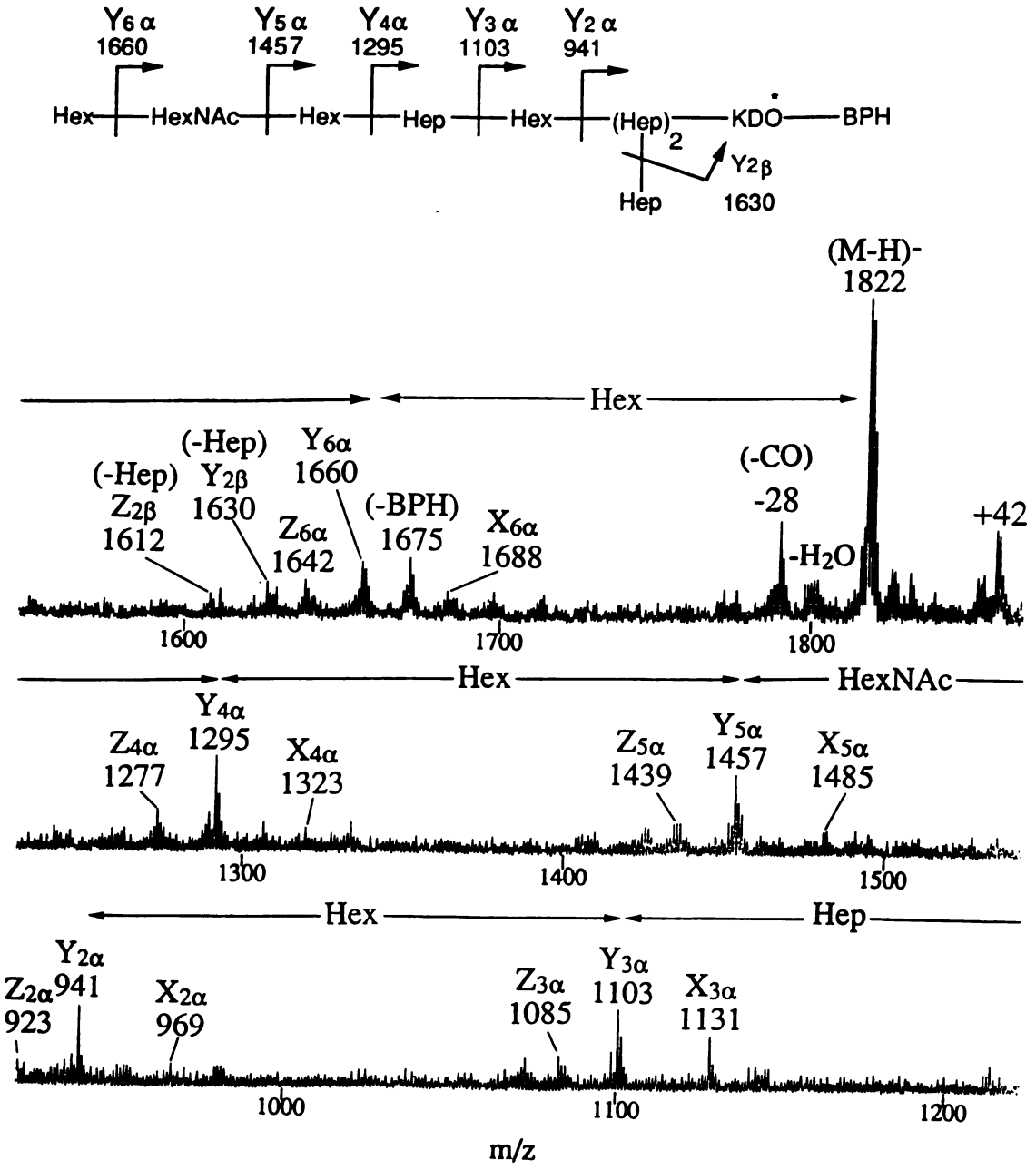

Figure 2.4. Partial negative-ion LSIMS spectrum of BPH-derivatized oligosaccharide from *H. ducreyi* strain 35000. The fragmentation nomenclature used is that proposed by Domon and Costello (1988). The α and β subscripts refer to the major and minor oligosaccharide branches, respectively.

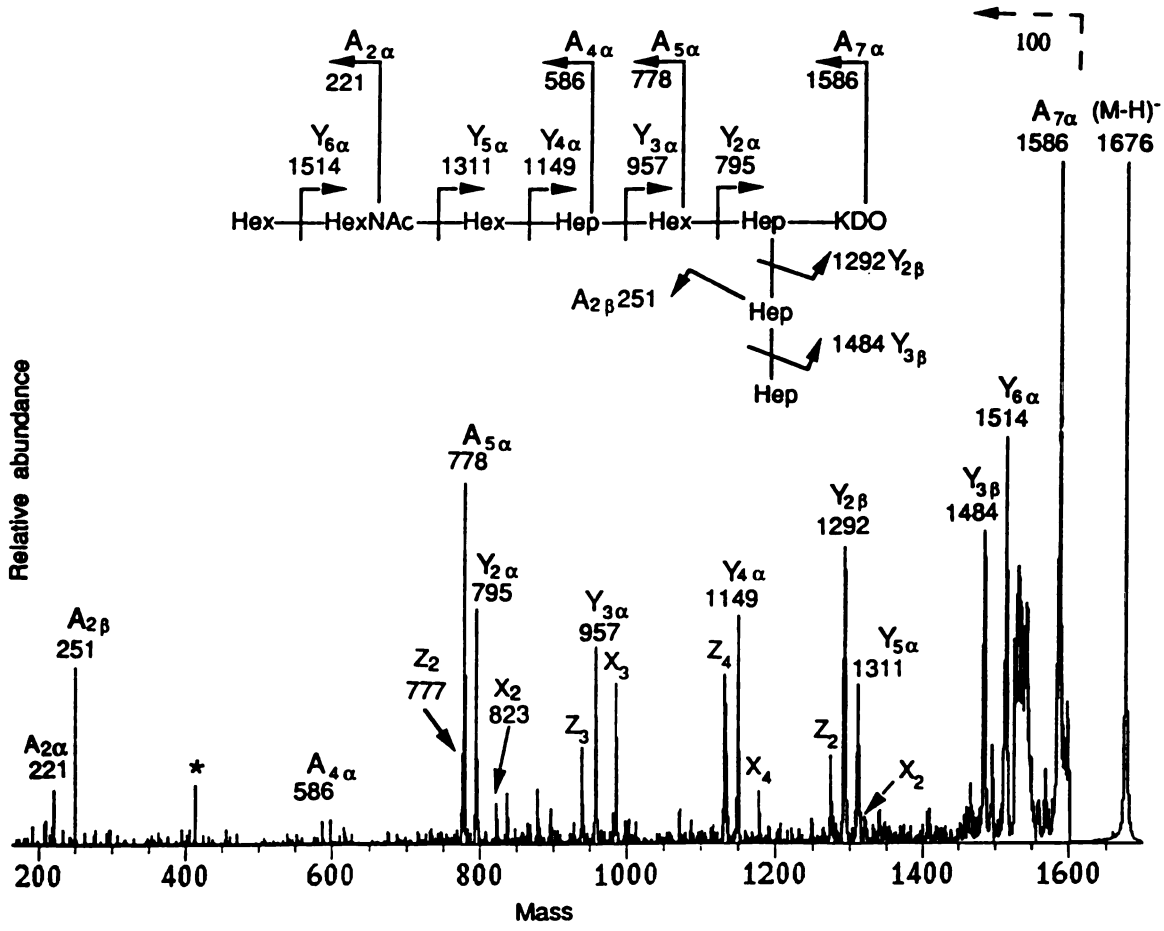

Figure 2.5. MS/MS spectrum of underivatized oligosaccharide from *H. ducreyi* strain 35000. The peak at m/z 413 which is marked by an asterisk is unassigned.

two MS/MS spectra (data not shown) yielded fragment ions that were consistent with the structure as presented in Figure 2.5. Specifically, the MS/MS spectrum of m/z 1149 showed only a loss of heptose from the non-reducing terminus at m/z 957 (Δm 192 Da) while the MS/MS spectrum of m/z 957 gave losses for both hexose at m/z 795 (Δm 162 Da) and heptose at m/z 765 (Δm 192 Da). Taken together, a complete biantennary structure containing nine sugars can now be proposed as Hex→HexNAc→Hex→Hep→Hex→(Hep→ Hep→)Hep→Kdo.

To identify the monosaccharides and their linkages, methylation analysis of the major oligosaccharide fraction was performed. The partially methylated alditol acetates (PMAAs) were analyzed by GC/MS in both electron impact and chemical ionization modes. As shown in Figure 2.6, this oligosaccharide is comprised of terminal galactose (1,5-di-*O*-acetyl-2,3,4,6-tetra-*O*-methyl-galactitol), 1,3-linked galactose (1,3,5-tri-*O*-acetyl-2,4,6-tri-*O*-methyl-galactitol), 1,6-linked glucose (1,5,6-tri-*O*-acetyl-2,3,4-tri-*O*-methyl-glucitol), terminal heptose (1,5-di-*O*-acetyl-2,3,4,6,7-penta-*O*-methyl-heptitol),1,4-linked heptose (1,4,5-tri-*O*-acetyl-2,3,6,7-tetra-*O*-methyl-heptitol), 1,2-linked heptose(1,2,5-tri-*O*-acetyl-3,4,6,7-tetra-*O*-methyl heptitol), 1,3,4-linked heptose (1,3,4,5-tetra-*O*-acetyl-2,6,7-tri-*O*-methyl-heptitol), and 1,4-linked N-acetyl-glucosamine (2-acetamido-2-deoxy-1,4,5-tri-*O*-acetyl-3,6-di-*O*-methyl-glucitol). With the exception of Kdo, which would not be expected to form a stable PMAA under these conditions, eight monosaccharides were identified in roughly equimolar amounts and are consistent with those expected from our preliminary structure. When this data is combined with the previous mass spectrometric data, the oligosaccharide structure can now be narrowed down to only a few possibilities:

I Gal1→4GlcNAc1→3Gal1→4Hep1→6Glc1→3,4Hep1→Kdo
↑
Hep1→2Hep1

II Gal1→4GlcNAc1→6Glc1→4Hep1→3Gal1→3,4Hep1→Kdo
↑
Hep1→2Hep1

III Gal1→4GlcNAc1→3Gal1→2Hep1→6Glc1→3,4Hep1→Kdo
↑
Hep1→ 4Hep1

IV Gal1→4GlcNAc1→6Glc1→2Hep1→3Gal1→3,4Hep1→Kdo
↑
Hep1→4Hep1

Although the precise placement of the two monosubsitituted hexoses (1,3-Gal and 1,6-Glc) and heptoses (1,2-Hep and 1,4-Hep) in this oligosaccharide cannot be made at this point, several lines of evidence point to the structure containing the assignments shown in **I**. First, the terminal Gal1→4GlcNAc1→3Gal1→ sequence is consistent with Galβ1→4GlcNAcβ1→3Galβ1→, the terminal trisaccharide region of paragloboside. As previously reported, the monoclonal antibody 3F11, which recognizes the terminal saccharide region of paragloboside, binds strongly to the LOS of *H. ducreyi* strain 35000 (Campagnari et al., 1990). This high binding suggests that this paragloboside structure is contained, at least in part, in the non-reducing terminal region of this LOS. Second, the PMAAs for terminal heptose, 1,2-linked heptose, and 1,3,4-linked heptose eluted at the exact positions as the corresponding heptoses of *H. influenzae* 2019, suggesting that the core of *H. ducreyi* 35000 is analogous to that of *H. influenzae* 2019 which contains a Hepα1→2Hepα1→3(4)αHep1→ core, all consisting of L-*glycero*-D-*manno*-heptose (Phillips et al., 1992). If so, the heptose on the non-reducing terminal branch is 1,4-linked. Furthermore, compositional analysis revealed the presence of a heptose that is not L-*glycero*-D-*manno*-heptose. To verify this, the oligosaccharide was hydrolysed to its

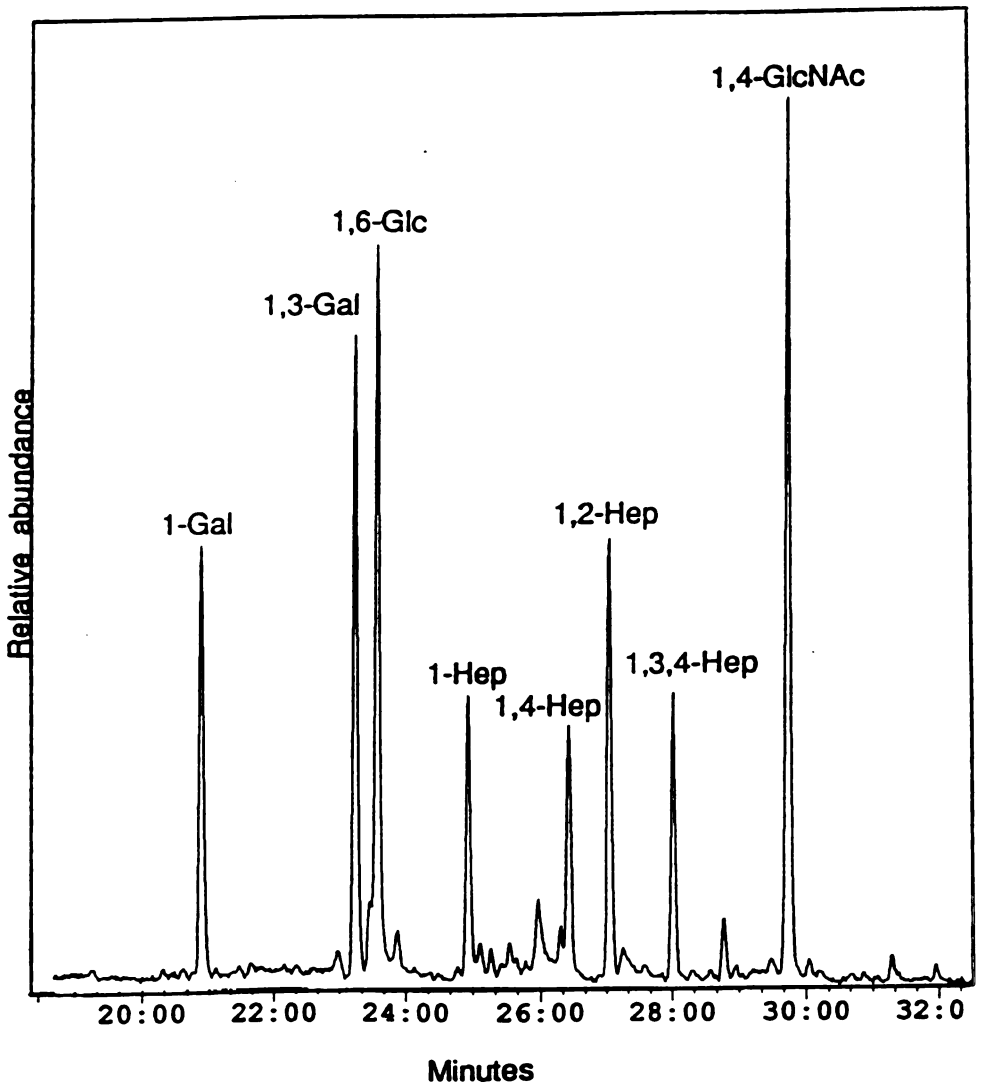

Figure 2.6. Total GC/MS ion chromatogram in the electron impact mode of PMAAs from *H. ducreyi* strain 35000. Peak areas relative to terminal galactose are follows: 1-linked Gal (1.0), 1,3-linked Gal (1.5), 1,6-linked Glc (1.7), 1-linked Hep (0.65), 1,4-linked Hep (0.57), 1,2-linked Hep (0.94), 1,3,4-linked Hep (0.70), and 1,4-linked GlcNAc (1.8). By determining the relative molar response factors for the PMAAs that were also present in the oligosaccharide isolated from *S. typhimurium* Ra LPS (i.e. terminal Gal and terminal Hep), the *molar* ratio of these same two sugars in the *H. ducreyi* oligosaccharide was found to be 0.96, close to the predicted *molar* ratio of 1.0.

monosaccharides, which were then reduced to their alditols and peracetylated. When these peracetylated monosaccharides were analyzed by GC/MS a second earlier eluting heptose was observed with a characteristic $(M+NH_4)^+$ ion at m/z 525 of approximately one-third the abundance of the peracetylated L-*glycero*-D-*manno*-heptose (data not shown). Comparative GC/MS analysis of the alditol acetates from *H. ducreyi* and from *Aeromonas liqefaciens* serotype SJ19, whose oligosaccharide contains both L-*glycero*-D-*manno*-heptose and D-*glycero*-D-*manno*-heptose, clearly identified D-*glycero*-D-*manno*-heptose as this less abundant heptose component. Therefore, we made the tentative assignment that this D-*glycero*-D-*manno*-heptose is the 1,4-linked heptose on the branch region.

Partial Structure of Lipid A The lipid A fraction from *H. ducreyi* LOS was analyzed by LSIMS after first partitioning in $CHCl_3$/methanol/0.1N HCl (2/1/2, v/v/v) (see Figure 2.7a). The molecular ions for both a diphosphorylated (*m/z* 1823.9) and monophosphorylated (*m/z* 1743.9) species are clearly prominent. Also evident in the spectrum are ions corresponding to loss of myristoyl groups (m/z 1613) and the elimination of an ester-linked hydroxymyristoyl (m/z 1597) and myristoxymyristoyl (m/z 1387) group as their corresponding ketenes. The X, Y, Z-type ions, indicative of glycosidic bond cleavage between the two glucosamines (which were independently identified in the HPAEC composition analysis) are also evident at m/z 738, 710 and 692, respectively. Losses of phosphates from many of these ions were also observed, but it is not clear whether this represents heterogeneity in the lipid or part of the LSIMS fragmentation process.

To further explore details of the lipid A structure, tandem mass spectrometry was performed on the major lipid A fragment ions at m/z 1823, 1597, 1387 and 710. The MS/MS spectrum of the m/z 710 ion is shown in Figure 2.7b. In this spectrum, the peak at m/z 466 represents the elimination of the *O*-linked hydroxymyristoyl group as the free acid. The peak at m/z 240 probably indicates a two bond cleavage of the *O*-linked hydroxymyristoyl group as an acid and loss of the N-linked hydroxymyristoyl group, this

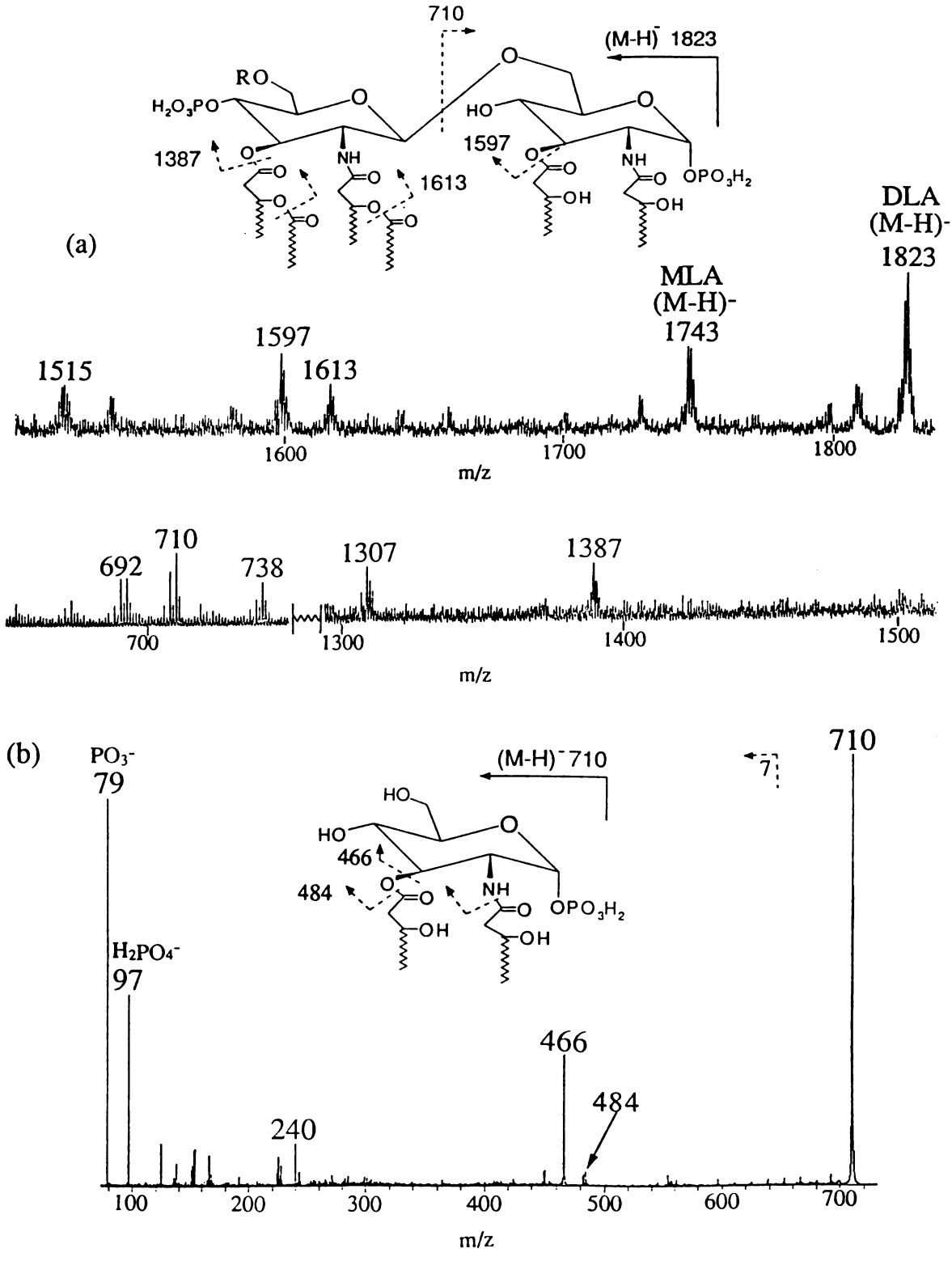

Figure 2.7. (a) Negative-ion LSIMS spectrum of the lipid A from *H. ducreyi* strain 35000 and (b) the corresponding MS/MS spectrum of one of the major fragment ions at m/z 710.

time as a ketene. At low mass, abundant ions at m/z 97 ($H_2PO_4^-$) and 79 (PO_3^-) are seen that arise from elimination of phosphate. This spectrum and the others (data not shown) are all consistent with the lipid A structure as detailed in Figure 2.7 above.

To better assay for heterogeneity in the lipid preparation, the crude sample was then partially separated by TLC. Three minor spots appeared at R_f values of approximately 0.35, 0.5 and 0.6 with a major (multiple) band at $R_f \approx 0.8$. The LSIMS spectrum of the major band gave the same $(M-H)^-$ ion at m/z 1823 seen previously in the crude fraction, as well as a less abundant ion at m/z 1991. This latter ion could not be readily accounted for, but by mass difference might correspond to further substitution of the M_r 1824 lipid with an unusual C_{11} fatty acid (ΔM, 168 Da). Fatty acid analysis of the intact LOS, however, revealed the presence of only myristic and β–hydroxymyristic acids. Fatty acid analysis was carried out by hydrolyzing the LOS in 14% BF_3/methanol at 100° C for 6 h followed by GC/MS analysis of the methyl esters (Batley et al., 1985). While more structural information is needed to definitively place the fatty acids and phosphates on the glucosamine disaccharide, this preliminary analysis shows that lipid A from *H. ducreyi* is similar to the lipid A of *H. influenzae* strain I-69 Rd^-/b^+ (Helander et al., 1988).

Analysis of Intact LOS At this point, the precise nature of the linkage between the oligosaccharide and lipid A moieties had not been established, nor the identity of the acid labile group attached to Kdo. Mass spectrometric analysis of the intact LOS would provide this information, but the aggregated state and low solubility of LOS has generally precluded such a measurement. However, removal of the base labile O-acyl fatty acids on the lipid A moiety greatly reduces these problems and enables a largely "intact" LOS to be analyzed (Phillips et al., 1990). Therefore, *O*-deacylated HF-treated LOS of *H. ducreyi* 35000 was prepared and analyzed by LSIMS. A molecular ion was observed at m/z 2469.3 (average M_r 2470) which corresponds to a species containing the previously determined

nonasaccharide:

Gal1→4GlcNAc1→3Gal1→4Hep1→6Glc1→(Hep1→2Hep1→)3,4Hep1→Kdo,

directly linked to the lipid moiety consisting of a glucosamine disaccharide containing the two (hydrazine resistant) *N*-linked β-OH myristoyl groups. When *O*-deacylated (non-HF treated) LOS was analyzed, the electrospray mass spectrum produced two abundant multiply charged ions, $(M-4H)^{4-}$ at m/z 676.7 and $(M-3H)^{3-}$ at m/z 902.2, yielding an *average* M_r of 2710. This mass is 240 Da larger than the *average* mass of the *O*-deacylated HF-treated LOS, and signifies the presence of three phosphate groups, two of which have been previously assigned to the lipid A moiety. This third phosphate group must therefore be the acid labile moiety on the Kdo.

DISCUSSION

In this chapter we have presented a partial structure of the LOS of *H. ducreyi* strain 35000. Previous reports have analyzed the chemical composition of the LOS from various strains of *H. ducreyi*, but no structural data was presented (Odumeru et al., 1987). Elucidation of the molecular structure of *H. ducreyi* LOS may provide critical information pertaining to the role these components play in the pathology and host immunochemical response of *H. ducreyi* infection.

The proposed structure of the major *H. ducreyi* LOS form (see Figure 2.8) contains some unusual features. The lack of phosphate or phosphoethanolamine in the core heptose region is in direct contrast to virtually all other LOS of related mucosal bacteria (Galanos et al., 1977). However, the presence of phosphate on the Kdo may in some way compensate for the lack of other phosphoester moieties in this core region, although the significance of these phosphate moieties is unknown. The presence of a 1,4-linked heptose, most likely D-*glycero*-D-*manno*-heptose, in the branch region is also atypical of both enteric and non-enteric bacterial LOS (Galanos et al., 1977), although a terminal D-*glycero*-D-*manno*-

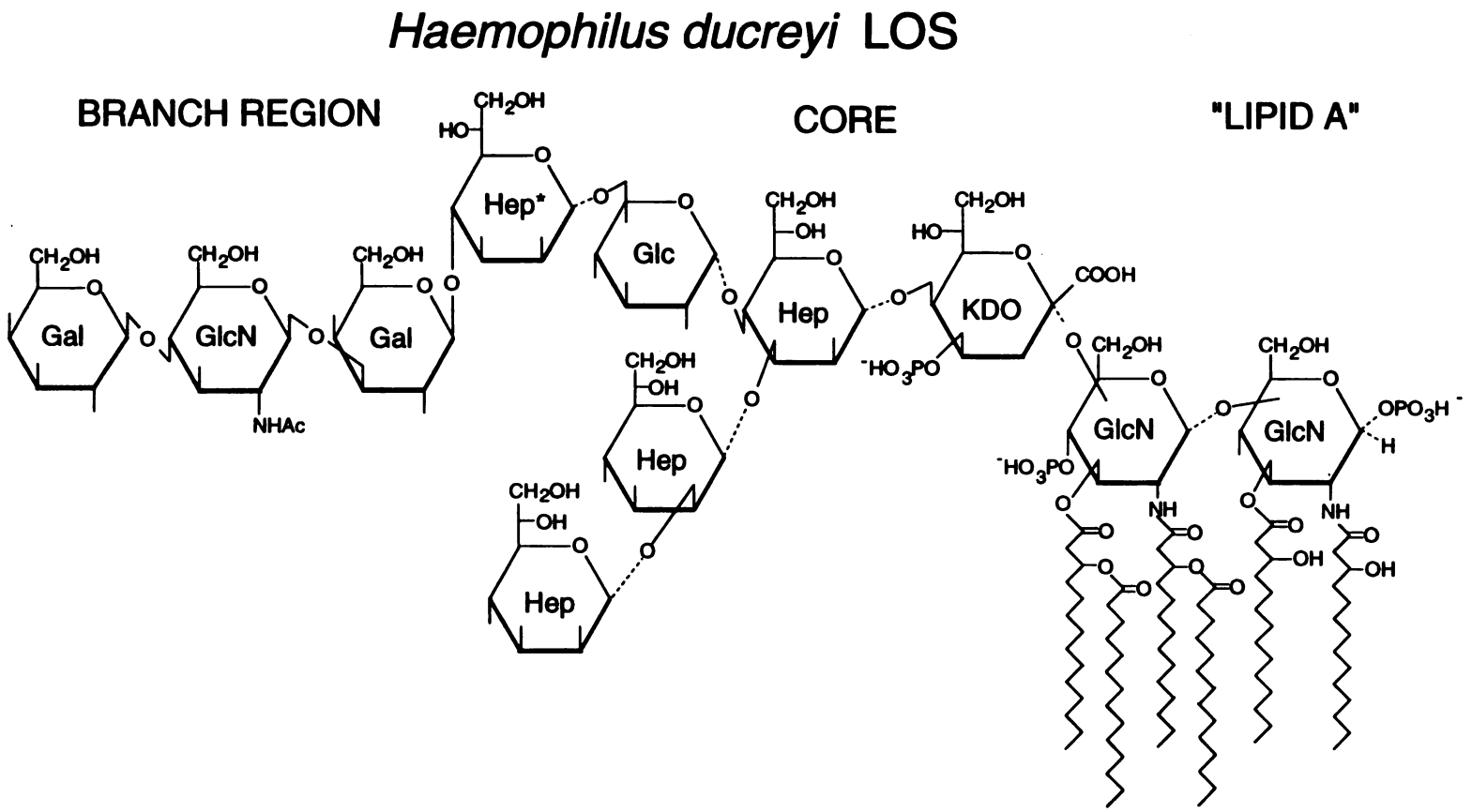

Figure 2.8. Proposed partial structure of *H. ducreyi* strain 35000 LOS. The anomeric configurations of the terminal trisaccharide region are based on the binding of the monoclonal antibodies 3F11 and O6B4, which recognize the lacto-*N*-neotetraose moiety of paragoloboside, Galβ1→4GlcNAcβ1→3Galβ1→4Glcβ1→Ceramide. The heptose trisaccharide core region is presumed to be similar to *H. influenzae* 2019 LOS, but the anomeric configurations are not indicated. The asterisk next to the branch 1,4-linked heptose refers to the likelihood of a D-*glycero*-D-*manno*-heptose form at this position. The lipid A structure is based in part on the LOS reported for the deep-rough mutant of *H. influenzae* I-69 Rd^{-}/b^{+} (Helander et al., 1988).

heptose has been reported in the outer core LOS region of a strain of *Proteus mirabilis* (Radziejewska-Lebrecht & Mayer, 1989). If this sugar proves to be a common structural feature in the LOS of other strains of *H. ducreyi*, this heptose may provide a unique target for therapeutic intervention, or possibly as part of a more specific diagnostic indicator. We needed to examine LOS from several other strains of *H. ducreyi* to determine if this is a common feature shared among these organisms.

Immunochemical studies have previously shown that the LOS of most *H. ducreyi* strains express an epitope which is also present on the LOS of many *N. gonorrhoeae* and *N. meningitidis* strains (Campagnari et al., 1990). This epitope is immunochemically similar to the terminal tetrasaccharide of paragloboside (Galβ1→4GlcNAcβ1→3Galβ1→4Glc1→Ceramide), a precursor to a major human blood group antigen (Mandrell et al., 1988). Our structural studies suggest that an epitope similar to this tetrasaccharide exists in the terminal trisaccharide of the LOS from *H. ducreyi* 35000. Monoclonal antibody 3F11 reacts with this terminal saccharide and also binds to the terminal region of paragloboside (Mandrell et al., 1988). The significance of this epitope on the LOS of these mucosal pathogens is unclear, but the presence of this structure on microbial surfaces could mask the pathogen on the mucosal surface and blunt the host immune response. Previous studies involving humans recovering from gonococcal infection suggest that this is the case since the human response is limited primarily to serotypic LOS determinants rather than the conserved antigenic sites (Galanos et al., 1977). It has also been suggested that this region may function as an adherence factor or as a receptor which could bind to membrane lectin-like structures (Mandrell et al., 1988).

The similarity between the LOS of *H. ducreyi* and *Neisseria* is also evident in their biological activities. Recent animal studies involving the intradermal injection of LOS from *H. ducreyi* and *N. gonorrhoeae* show that these organisms express LOS with similar toxic activity (Tuffrey et al., 1990; Campagnari et al., 1991). Since the lipid A moiety of *N. gonorrhoeae* LOS mediates damage to fallopian tube mucosa *in vitro* (Gregg et al., 1981),

it is likely that the lipid A of *H. ducreyi* plays an analogous role in the pathology found in a typical skin lesion (or ulcer).

Our next immediate goal was to unambiguously define the major oligosaccharide structure including anomeric configurations and to identify by ESI-MS other glycoforms present in the LOS and their relationship to the major structure. These experiments are described in Chapter 3.

CHAPTER 3.

COMPLETE STRUCTURE OF THE MAJOR OLIGOSACCHARIDE FROM THE LOS OF *HAEMOPHILUS DUCREYI* STRAIN 35000 AND EVIDENCE FOR ADDITIONAL GLYCOFORMS

INTRODUCTION

In the last chapter we reported a preliminary structure for the major LOS from *H. ducreyi* strain 35000 that contained several unusual features, including the likely presence of terminal lactosamine. In this chapter, we present the complete structure of this major oligosaccharide as determined by NMR studies which now confirms the presence of lactosamine on the non-reducing terminus and other aspects of the preliminary structure. Furthermore, chemical and mass spectrometric data are presented that verify the presence of sialic acid in the LOS from strain 35000, as well as additional glycoforms of lower abundances. We considered it important to determine the complete oligosaccharide structure of this strain so that a framework could be established in which to compare the oligosaccharide structures of strains we would subsequently analyse. In this way we could more quickly determine if there were common structural features among different strains. Furthermore, it would allow us to recognize an oligosaccharide structure that deviated in even some small detail from the oligosaccharide structure determined for this LOS. Indeed, subtle changes in oligosaccharide structure might have profound biological consequences.

In addition to the complete assignment or this major oligosaccharide structure, we were interested in exploring the heterogeneity of LOS structures within strains. For example, when we had originally run the *O*-deacylated LOS of strain 35000 by ESI-MS to identify the acid labile group attached to Kdo, the LOS in the ESI-MS spectrum appeared to be much more complex (heterogeneous) than we had previously observed from the LSIMS

analysis of the oligosaccharide (see Chapter 2). This was due in part to the fact that ESI-MS is a much more sensitive technique and is able to detect species present even in low abundances, i.e. the signal has a larger dynamic range.

Therefore to pursue these two objectives, we embarked on more detailed ESI-MS studies of *O*-deacylated LOS from strain 35000 in the expectation that the identity of these glycoforms might present some insights into the LOS biosynthetic process as well as the phenomenon of phase variation.

EXPERIMENTAL

Isolation, purification and SDS-PAGE analysis of LOS. LOS from *H. ducreyi* strain 35000 was isolated and purified using a modified phenol/water extraction procedure (Westphal & Jahn, 1965) as described in Chapter 2. The LOS was analyzed by SDS-PAGE on a 14% polyacrylamide gel as we have previously described (Campagnari et al., 1990). The gels were silver stained according to the method of Tsai and Frasch (Tsai & Frasch, 1982). The apparent molecular weights of the major LOS bands were estimated by comparison with the relative migration of the LOS from *Neisseria gonorrhoeae* strain PID_2 (data not shown).

Preparation of chemically modified LOS. To prepare water soluble LOS that was more amenable to mass spectrometric analysis, ≈1 mg of LOS was *O*-deacylated under mild hydrazine conditions as previously described in Chapter 2. To distinguish the presence of HexNAc (203 Da) from the isobaric mass of phosphate plus phosphoethanolamine (80 + 123 Da, respectively), a portion of the *O*-deacylated LOS was further treated with 48% aqueous HF to remove phosphate esters. Briefly, 100 µg of *O*-deacylated LOS was dissolved in 10 µL of 48 % aqueous HF for 16 hours at 4°C. The

resulting *O*-deacylated, dephosphorylated LOS was used as is after removing excess HF in a vacuum desiccator.

Isolation and purification of oligosaccharide fraction. OS from *H. ducreyi* strain 35000 was isolated and purified for NMR analysis as described in detail in Chapter 2. For determination of oligosaccharide heterogeneity an alternate gel filtration high performance liquid chromatography (HPLC) system was employed consisting of a Waters 6000A HPLC pump and two 600 x 7.5 mm Bio-Sil TSK-125 columns (BioRad) connected in series. Samples were eluted in 50 mM pyridinium acetate (pH 5.2) at a flow rate of 1 ml min^{-1}. Detection was as described above. Fractions were collected in 0.5-1 ml volumes.

Mass spectrometric analysis. Fractions from the gel filtration column were first analyzed by liquid secondary ion mass spectrometry (LSIMS) as described in detail elsewhere (Phillips et al., 1990). *O*-deacylated LOS and the unfractionated oligosaccharide pool were also analyzed by electrospray ionization mass spectrometry (ESI-MS) on a VG/Fisons Platform quadrupole mass spectrometer in the negative-ion and/or positive-ion mode (Gibson et al., 1993). The total oligosaccharide pool obtained after mild acid hydrolysis of LOS was first dissolved in water to make a 10 µg/µl solution. Approx. 1 µl of this solution was then mixed with 4 µl of the electrospray running solvent and injected via a Rheodyne injector into a running solvent of H_2O/acetonitrile (1/1, v/v) containing 1% acetic acid at a flow rate of 10 µl/min. *O*-deacylated LOS was analyzed in a similar fashion. Mass calibration was carried out with either an external carbohydrate or LOS reference standard using the supplied VG/Fisons software.

Nuclear Magnetic Resonance Spectroscopy. All 1D and 2D ^1H NMR spectra were recorded on a GE GN-500 spectrometer at 25°C. The major oligosaccharide (M_r 1677, approx. 0.5 mg) was lyophilized several times from 99.96% D_2O (Aldrich) and then

dissolved in 0.3 ml of 99.996% D_2O (Cambridge Isotope Laboratories). A trace of acetone was added to the sample as an internal reference (δ 2.225). The phase sensitive double-quantum filtered COSY (DQF-COSY) spectrum (Rance et al., 1983) was acquired with time-proportional phase incrementation of the first pulse (Redfield & Kuntz, 1975; Marion & Wüthrich, 1983). The data matrix consisted of 800 x 1024 data points, acquired with 16 scans per t_1 value and a spectral width of ± 2000 Hz. The matrix was apodized with a 45°-shifted sine-bell window function in both dimensions and zero-filled to produce a 2K x 2K real data matrix. The 2D homonuclear Hartmann-Hahn (HOHAHA) spectra were obtained using the MLEV-17 sequence (Bax & Davis, 1985) and quadrature detection (States et al., 1982). A spectral width of ± 2000 Hz was used with 90-ms and 120-ms relay mixing times. Data matrices of 560 x 2048 and 512 x 1024 data points were acquired for the 90-ms and 120-ms spectra, respectively. Both spectra were recorded with 16 scans per t_1 increment, and the matrices were zero-filled and apodized with gaussian window functions in both dimensions to give 2K x 2K real points. The 2D nuclear Overhauser effect (NOESY) spectrum was acquired in the phase-sensitive mode (States et al., 1982), using a 350-ms mixing time and 3.0-s interscan delay. The spectral width was ± 2000 Hz and the data matrix contained 512 x 1024 data points, with 16 scans per t_1 value. Zero-filling and gaussian apodization functions were used in both dimensions to give a final 2K x 2K matrix. All data processing was done on a VAX computer with a UNIX operating system using programs developed and modified at the UCSF NMR facility as previously described (Basus et al., 1988), including some recent improvements (M. Day and D. Kneller, unpublished data).

Sialic Acid Linkage Determination. LOS was dissolved in 0.1% (v/v) Triton X-100 to give a 10 mg/ml solution. A 200 µg (20 µl) aliquot of LOS was then added to 70 µl of 50 mM NaOAc buffer (pH 5.5) followed by the addition of 10 mU of Newcastle Disease Virus sialidase dissolved in 10 µl of 50 mM NaOAc at pH 5.5. This final reaction mixture

was incubated at 37 °C for 10 h and small aliquots of the reaction mixture (5 µl) were removed at various time points (t = 4, 6, 7 and 10 h) for the determination of the released sialic acid (Neu5Ac) as described elsewhere (Mandrell et al., 1992). After 7 h, a larger 10 µl aliquot was removed and 100 mU *Clostridium perfringens* sialidase dissolved in 10 µl of 50 mM NaOAc (pH 5.5) was added and the reaction mixture again incubated at 37°C.

RESULTS

Our preliminary structure for the major oligosaccharide from *H. ducreyi* strain 35000 LOS was based on tandem mass spectrometric and methylation analyses, which yielded several possible structures (Melaugh et al., 1992):

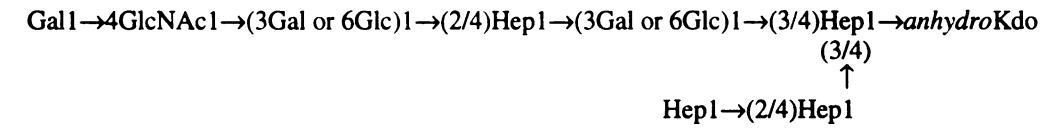

These proposed structures contain *anhydro*Kdo on their reducing termini which is formed by β-elimination of a phosphate group from the 4-position of intact Kdo during the acetic acid hydrolysis step (Auzanneau et al., 1991). The uncertainties in the sequence involve the placement of the di-linked hexoses and heptoses and the arrangement of the two oligosaccharide branches.

On the basis of its strong binding to monoclonal antibody 3F11, which recognizes the terminal region of the lacto-*N*-neotetraose epitope of paragloboside, Galβ1→4GlcNAcβ1→3Galβ1→4Glcβ1→ceramide (Mandrell et al., 1988; Campagnari et al., 1990), we originally suggested that the terminal trisaccharide of *H. ducreyi* 35000 LOS was Galβ1→4GlcNAcβ1→3Gal. This tentative assignment dictated that the remaining monosubstituted hexose, 1,6-Glc, be linked to the 1,3,4-Hep. From GC/MS analyses of alditol acetates and partially methylated alditol acetates, it was established that the 1-Hep, 1,2-Hep, and 1,3,4-Hep were L-*glycero*-D-*manno*-heptoses and the 1,4-Hep was a D-

glycero-D-*manno*-heptose (Melaugh et al., 1992). Three L-*glycero*-D-*manno*-heptoses were previously identified in the Hepα1→2Hepα1→3(4)Hepα1→5Kdo core of the LOS from a related bacterium, *H. influenzae* nontypable strain 2019 (Phillips et al., 1992), suggesting that this core structure may be conserved in *Haemophilus* LOS. This argued for assigning the 1,4-linked D-*glycero*-D-*manno*-heptose as the unusual heptose in the longer branch. From these data a most likely preliminary oligosaccharide structure was proposed, although no further structural data was available to confirm or complete the assignment (Melaugh et al., 1992):

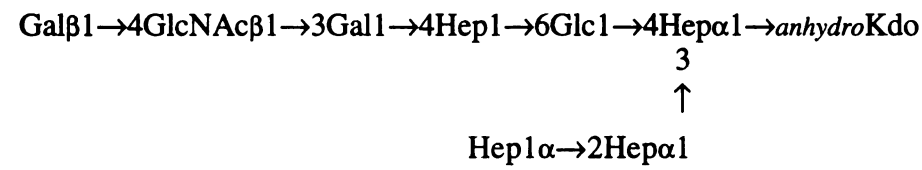

NMR Analysis of the Major Oligosaccharide from Strain 35000. To define the precise linkages and anomeric configurations of the major oligosaccharide from *H. ducreyi* 35000, a series of NMR experiments was carried out. The 1D ^{1}H NMR spectrum of the major oligosaccharide (M_r 1677) showed multiple anomeric resonances, consistent with an oligosaccharide sample containing several diastereomeric forms of *anhydro*Kdo at the reducing terminus (Figure 3.1). As was previously observed in the hexasaccharide released from the LOS of *H. influenzae* strain 2019 (Phillips et al., 1992), this reducing terminal microheterogeneity causes the proton resonances from saccharides closest to the reducing terminus to appear as multiple signals, whereas the more distant residues are not noticeably affected. Integration of the anomeric resonances permitted a total of eight anomeric protons to be accounted for as follows: I (δ 5.103, 5.083, 5.037; *J* = sm), II (δ 5.786, 5.764, 5.752; *J* = sm), III (δ 5.115; *J* = sm), IV (δ ≈4.50; *J* ≈ 8 Hz), V (δ 4.925; *J* = sm), VI (δ 4.497; *J* = 8.0 Hz), VII (δ 4.723; *J* = 8.0 Hz), and VIII (δ 4.481; *J* = 8.0 Hz). The four highfield-shifted anomeric signals with large coupling constants (*J* = 8.0 Hz) suggested β-linked residues, most likely including the three hexoses (1-Gal, 1,3-Gal,

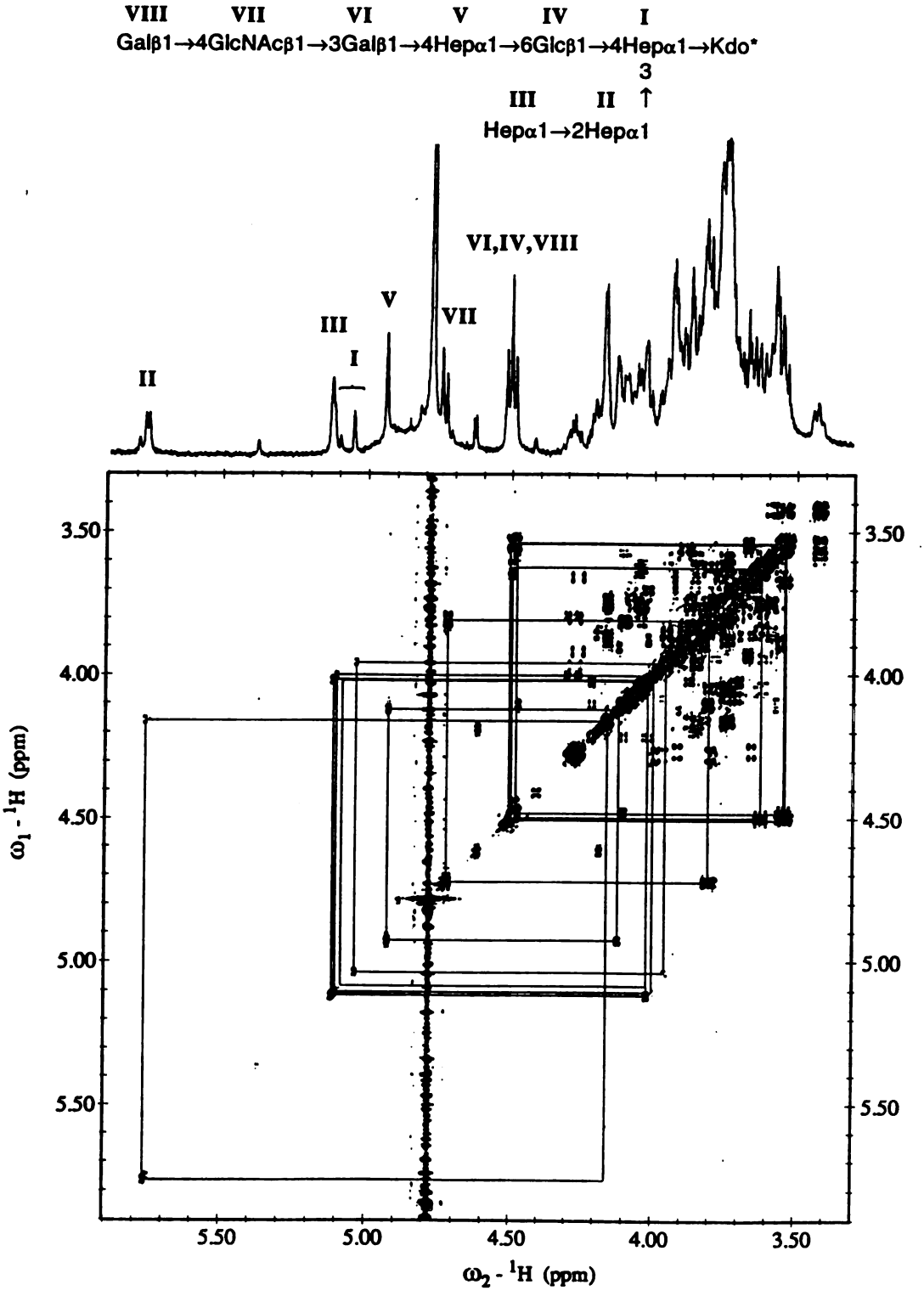

Figure 3.1. Section of the 500-MHz phase-sensitive DQF-COSY spectrum of the major oligosaccharide from *H. ducreyi* strain 35000 (M_r 1677) and the corresponding region of the 1D ^{1}H NMR spectrum. Anomeric protons are labeled as shown in Table 3.1, and H-1/H-2 cross-peaks are connected with lines on the 2D spectrum. The peak at δ 4.78 is HOD, and the peaks at δ 4.617, 4.475, and 4.409 are from *anhydro*Kdo.

and 1,6-Glc) and one 1,4-GlcNAc present in the oligosaccharide. The remaining four lowfield-shifted anomeric resonances were tentatively assigned to the four Hep residues, all of which were expected to have the *manno* configuration, including three L-*glycero*-D-*manno*-heptoses and one D-*glycero*-D-*manno*-heptose.

To assign most of the ring protons in sugar residues I through VIII, DQF-COSY (Figure 3.1) and 2D HOHAHA (Figure 3.2A) spectra were obtained and analyzed in combination. Where possible, apparent vicinal coupling constants were measured from DQF-COSY cross-peaks and used to establish monosaccharide identities. Working from the lowfield to the highfield anomeric proton resonances, the monosaccharide spin systems were analyzed as outlined below.

The most lowfield-shifted anomeric proton resonance, II, consisted of three broad singlets which were all coupled to H-2 protons at $\delta \approx 4.16$. For this residue, H-3, H-4, and H-5 were assigned from cross-peaks to H-1 in the HOHAHA spectrum (Figure 3.2A). The small $J_{1,2}$ and $J_{2,3}$ coupling constants measured from DQF-COSY cross-peaks (Table 3.1) were consistent with the *manno* configuration. Protons H-1 to H-3 of residue III could be assigned from DQF-COSY connectivities, with the assignment of H-4 coming from the H-1/H-4 HOHAHA cross-peak. Again, the $J_{1,2}$ and $J_{2,3}$ values measured for this residue were appropriate for a *manno*-heptose. The anomeric proton of residue I consisted of three broad singlets, one of which was partially overlapping with H-1 of III. This pattern of three resolved anomeric resonances was seen for the 1,3,4-linked heptose from the *H. influenzae* 2019 hexasaccharide (Phillips et al., 1992). As was the case with that residue, this spin system was difficult to follow. The HOHAHA spectrum suggested that the H-2 and H-3 protons of I were strongly coupled in each case, with only the most intense anomeric signal (δ 5.037) showing a barely resolved H-1/H-3 cross-peak. However, this information was sufficient to follow coupling connectivities to H-4 and H-5 in the DQF-COSY spectrum, as was done in the assignment of the *H. influenzae* 2019 hexasaccharide. The remaining lowfield-shifted anomeric proton resonance, V, was

Table 3.1. Partial Proton NMR Assignment of the Major Oligosaccharide (M_r 1677) from *H. ducreyi* strain 35000 (D_2O, 25°C)[a]

VIII VII VI V IV I
Galβ1→ 4GlcNAcβ1→3Galβ1→ 4Hepα1→ 6Glcβ1----------→4Hepα1→Kdo*
3
↑
Hepα1--→2Hepα1------
III II

proton	VIII	VII	VI	V	IV	III	II	I
H-1	4.481	4.723	4.497	4.925	≈4.50[b]	5.115	5.786	5.103
							5.764	5.083
							5.752	5.037
H-2	3.542	3.806	3.623	4.120	≈3.54[b]	4.020	4.163	4.002
							4.158	4.019
							4.164	3.958
H-3	3.672	≈3.74	3.749	3.900	3.420	3.876	3.830	3.990
								4.000
								3.917
H-4	3.928	3.743	4.161	3.922	3.576	3.818	3.555	4.275
								4.288
								4.264
H-5	≈ 3.74[c]	3.587			3.559		4.051	3.797
								3.791
								3.656
H-6		3.851			3.809			4.081[c]
H-6'		3.957			4.102			
NAc		2.041						
$J_{1,2}$	8.0[d]	8.0[d]	8.0[d]	<3	≈8	<3	<3	<3
$J_{2,3}$	10	10	10	4	≈9	4	4	
$J_{3,4}$	4		4		≈9	8	10	10
$J_{4,5}$		10						10

[a] Chemical shifts are reported in ppm and *J* values are apparent coupling constants (Hz) obtained from DQF-COSY cross peaks, unless otherwise noted. Kdo* = *anhydro*Kdo.

[b] Average of three overlapping signals arising from reducing-terminal microheterogeneity.

[c] Tentative assignments made from NOESY data.

[d] *J* values measured from the 1D spectrum.

associated with the fourth *manno*-heptose spin system. Coupling connectivity from H-1 to H-3 of V could be followed in the DQF-COSY spectrum and the HOHAHA spectrum suggested that H-4 of this spin system was downfield-shifted and strongly coupled to the H-3 resonance.

Of the highfield-shifted anomeric resonances, VII was the farthest downfield. Spin system VII was mapped from H-1 to H-2 and H-4 to H-6/6' using the HOHAHA cross-peaks to follow DQF-COSY connectivities from both ends of the spin system. While the chemical shift of H-3 could not be established from the DQF-COSY data, the intense cross-peak at $\delta \approx 3.74$ in the HOHAHA spectrum suggested that H-3 was strongly coupled to H-4. This and the measured J values suggested a monosaccharide with the *gluco* configuration, which in this case could be either the 1,4-GlcNAc or the 1,6-Glc residue. Since its anomeric proton was not affected by reducing terminal microheterogeneity, this residue was presumably not proximal to the inner core area. At 500 MHz, the remaining three anomeric protons, IV, VI, and VIII, overlapped to give what looks like a large broad triplet, evidently arising from two sharp doublets and one complex set of closely occurring doublets. Spin system VI, whose H-1 proton was the lowfield-shifted sharp doublet, could only be mapped from H-1 to H-4 in the DQF-COSY and HOHAHA spectra, suggesting a sugar with the *galacto* configuration. This was supported by the small $J_{3,4}$ value measured. The same was true for spin system VIII, whose anomeric proton was the highfield-shifted sharp doublet. Thus, these spin systems represent the two galactose residues present in the oligosaccharide. The final spin system, IV, was mapped from H-1 to H-4 and H-5 to H-6/6' in the DQF-COSY spectrum after the H-6 and H-6' resonances were clearly located from cross-peaks to H-2 in the HOHAHA spectrum. In this case, the H-6 and H-6' protons gave very weak HOHAHA cross-peaks to H-1. Nonetheless, combined data suggested the *gluco* configuration for this residue.

The oligosaccharide sequence was established by analysis of interresidue NOEs observed in the 2D NOESY spectrum (Figure 3.2B). Starting with the core region, the

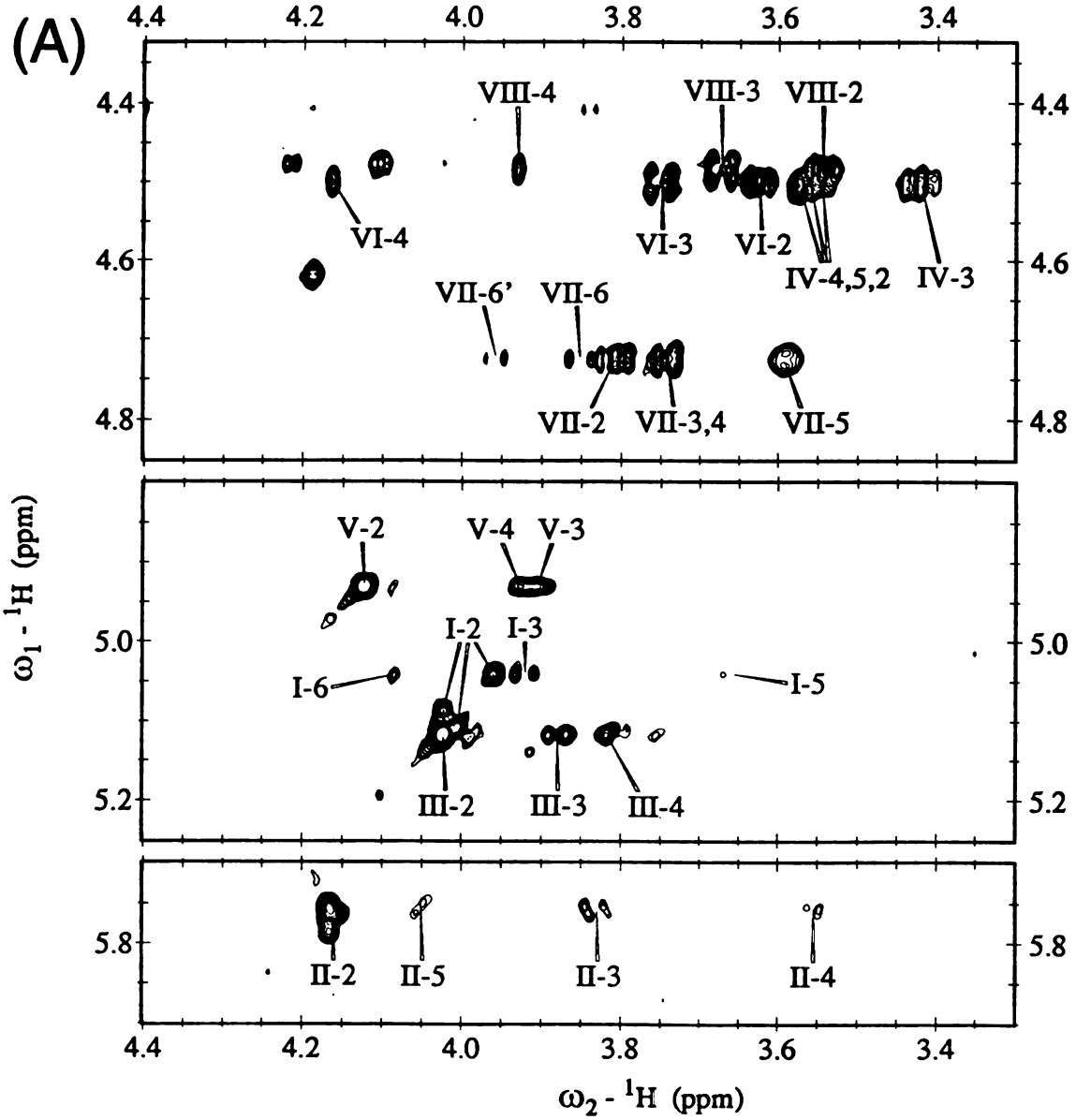

Figure 3.2. (A) Selected regions of the 2D HOHAHA spectra of the major oligosaccharide from *H. ducreyi* strain 35000 acquired with 90-ms (top) and 120-ms (middle and bottom) mixing times.

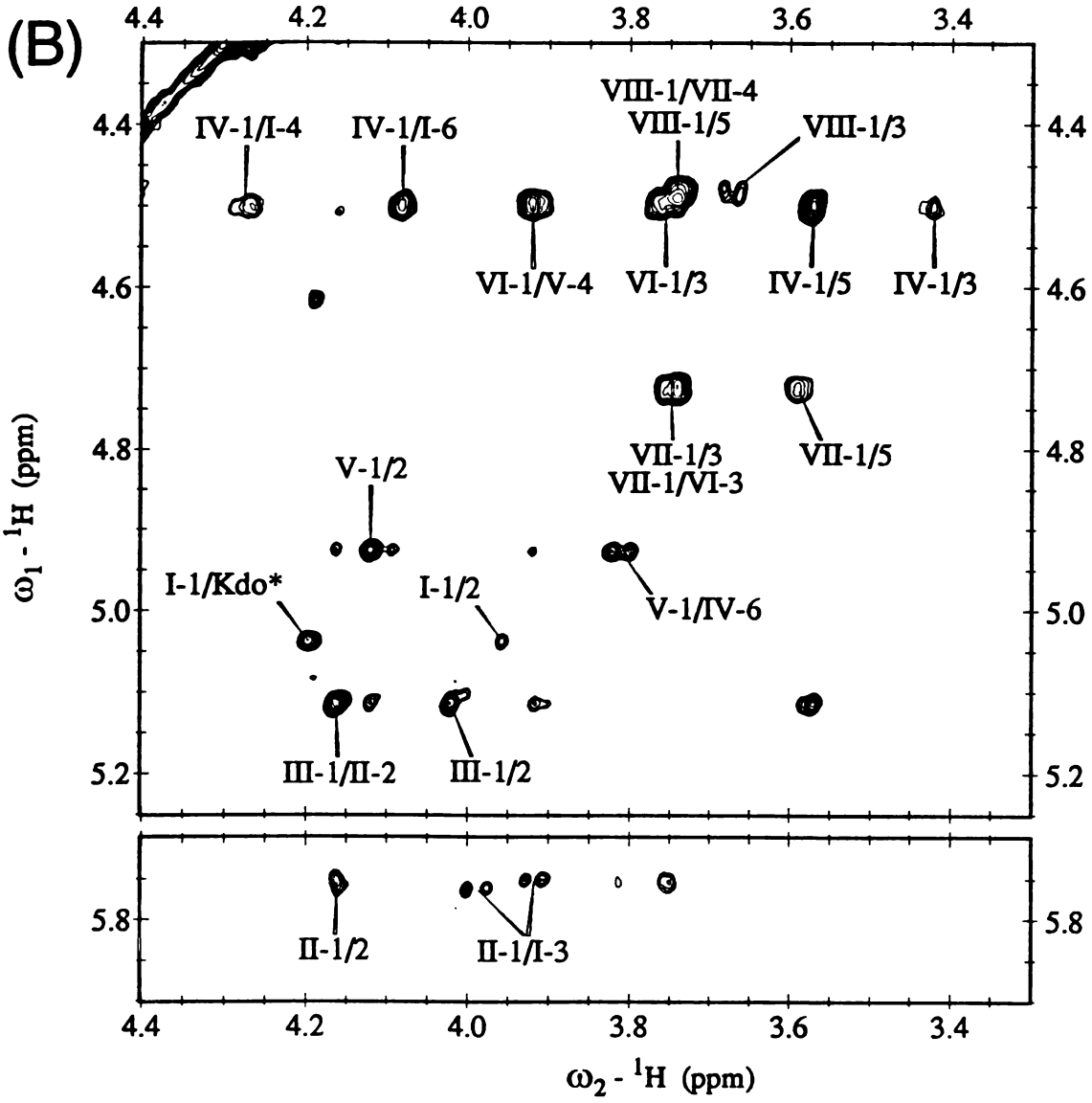

Figure 3.2. (B) Corresponding regions of the 2D NOESY spectrum run with a 350-ms mixing time. A NOE cross-peak between III-1 and II-1 is present in the full spectrum. The assignment of VIII-5 is tentative. Additional unassigned NOESY cross-peaks to the anomeric protons of III (δ 4.120, 3.916, and 3.570) and II (δ 3.750) are present in the spectrum.

anomeric resonances of the three core heptoses (residues I, II, and III) all showed intraresidue NOEs to their respective H-2 protons, consistent with α-linked heptoses in the *manno* configuration. The anomeric proton of heptose III showed strong interresidue NOEs to H-1 and H-2 of residue II, indicating that Hep III was the terminal heptose linked to the 2-position of Hep II. An interresidue NOE between two anomeric protons is characteristic of 1,2-linkages in the α-configuration (Romanowska et al., 1988) and was also observed for the Hepα1→2Hepα1→ disaccharide branch in the *H. influenzae* 2019 hexasaccharide (Phillips et al., 1992). The anomeric proton of Hep II also showed an interresidue NOE to H-3 of Hep I, establishing that Hep II was linked to the 3-position of Hep I. Thus, the linkages of this *H. ducreyi* Hep_3 core appear to be identical to the Hep_3 core of *H. influenzae* 2019 LOS.

The anomeric proton of β-galactose residue VIII showed an intraresidue H-1/H-3 NOE cross-peak, and an interresidue cross-peak to H-4 of VII, which may be overlapping with the expected intraresidue H-1/H-5 cross-peak. The absence of additional interresidue NOE cross-peaks to VIII indicated that VIII was the non-reducing terminal β-Gal linked to the 4-position of VII, which established VII as the 1,4-GlcNAc moiety. Residue VII showed an intraresidue H-1/H-5 NOE cross-peak, in addition to an interresidue cross-peak to H-3 of β-Gal VI, which is presumably overlapping with an intraresidue H-1/H-3 cross-peak. Thus, the linkage of β-GlcNAc residue VII to β-Gal residue VI established the *H. ducreyi* 35000 terminal trisaccharide as Galβ1→4GlcNAcβ1→3Galβ1→.

H-1 of VI showed an intraresidue NOE cross-peak to H-3, and an interresidue cross-peak to H-4 of V, which linked β-Gal VI to the 4-position of Hep V. The expected H-1/H-5 intraresidue cross-peak for VI probably overlaps with another signal and could not be located with certainty. Consistent with the other α-linked *manno*-heptoses, Hep V showed an intraresidue H-1/H-2 NOE cross-peak. An interresidue cross-peak between H-1 of V and H-6 of IV established the linkage of Hep V to the 6-position of β-Glc IV. Residue IV showed intraresidue H-1/H-3 and H-1/H-5 cross-peaks, and interresidue cross-

peaks to H-4 and a resonance tentatively assigned to H-6 of Hep I. These same interresidue cross-peaks were observed in the NOESY spectrum of the *H. influenzae* 2019 hexasaccharide, again supporting the similarities of the two *Haemophilus* species core structures. Thus, the NOESY data support a complete carbohydrate structure for the *H. ducreyi* 35000 oligosaccharide as shown in Table 3.1, where the core heptoses are L-*glycero*-D-*manno*-heptoses and the 1,4-linked heptose is a D-*glycero*-D-*manno*-heptose.

Analysis of Oligosaccharide Heterogeneity. SDS-PAGE and mass spectrometric analyses of *O*-deacylated LOS from strain 35000 reveal the presence of several other LOS besides the major species as determined by the current NMR studies and previously published LSIMS data (Melaugh et al., 1992) (see also Chapter 2). For example, SDS-PAGE analysis clearly shows the presence of three major LOS glycoforms and several minor forms of lower molecular weight (see Figure 3.3). The major LOS band at 4.5 kDa had previously been shown to react with the monoclonal antibody 3F11 (Campagnari et al., 1991) and likely corresponds to the LOS containing the terminal lactosamine group. The band just above with an estimated mass of 5.1 kDa is sensitive to neuraminidase and is likely the sialylated analog of this major component.

Electrospray ionization mass spectrometry of the total *O*-deacylated LOS initially indicated the presence of five separate glycoforms (Gibson et al., 1993). Based on their molecular weights, these additional LOS species were interpreted as representing both extended and truncated analogs of the major lactosamine-containing oligosaccharide now confirmed by NMR. Further ESI-MS analysis of this LOS preparation has now revealed a sixth LOS component (LOS-**F**) at *m/z* 1041.4 (M_r 3127.2) as can be seen from Figure 3.4 and the composition assignments listed in Table 3.2.

In contrast to the SDS-PAGE and ESI-MS data of LOS and *O*-deacylated LOS, the original LSIMS and tandem mass spectrometric data of the individual oligosaccharide fractions clearly defined only one major oligosaccharide structure at M_r 1677 correponding

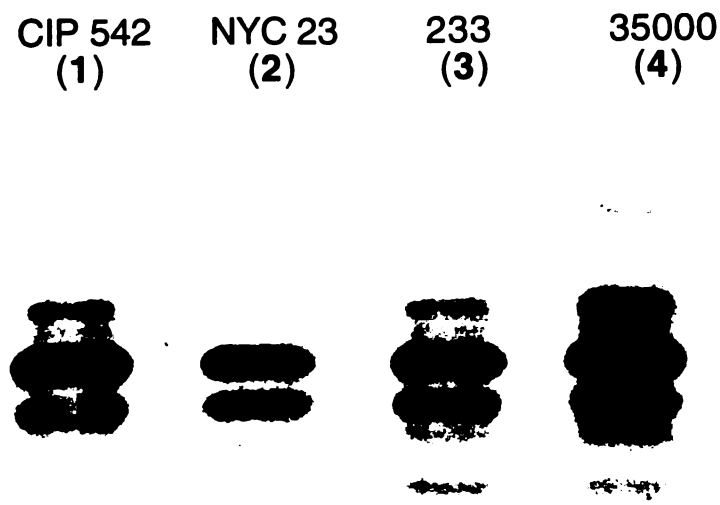

Figure 3.3. SDS-PAGE of the LOS from *H. ducreyi* strains CIP 542 (lane 1), NYC 23 (lane 2), 233 (lane 3), and 35000 (lane 4). The two bands present in NYC 23 correspond to LOS with M_r's of ≈ 5.1 and 4.5 kDa. These two bands also appear as the major two bands in strain 35000, the smaller of which at M_r ≈ 4.5 kDa binds the monoclonal antibody 3F11.

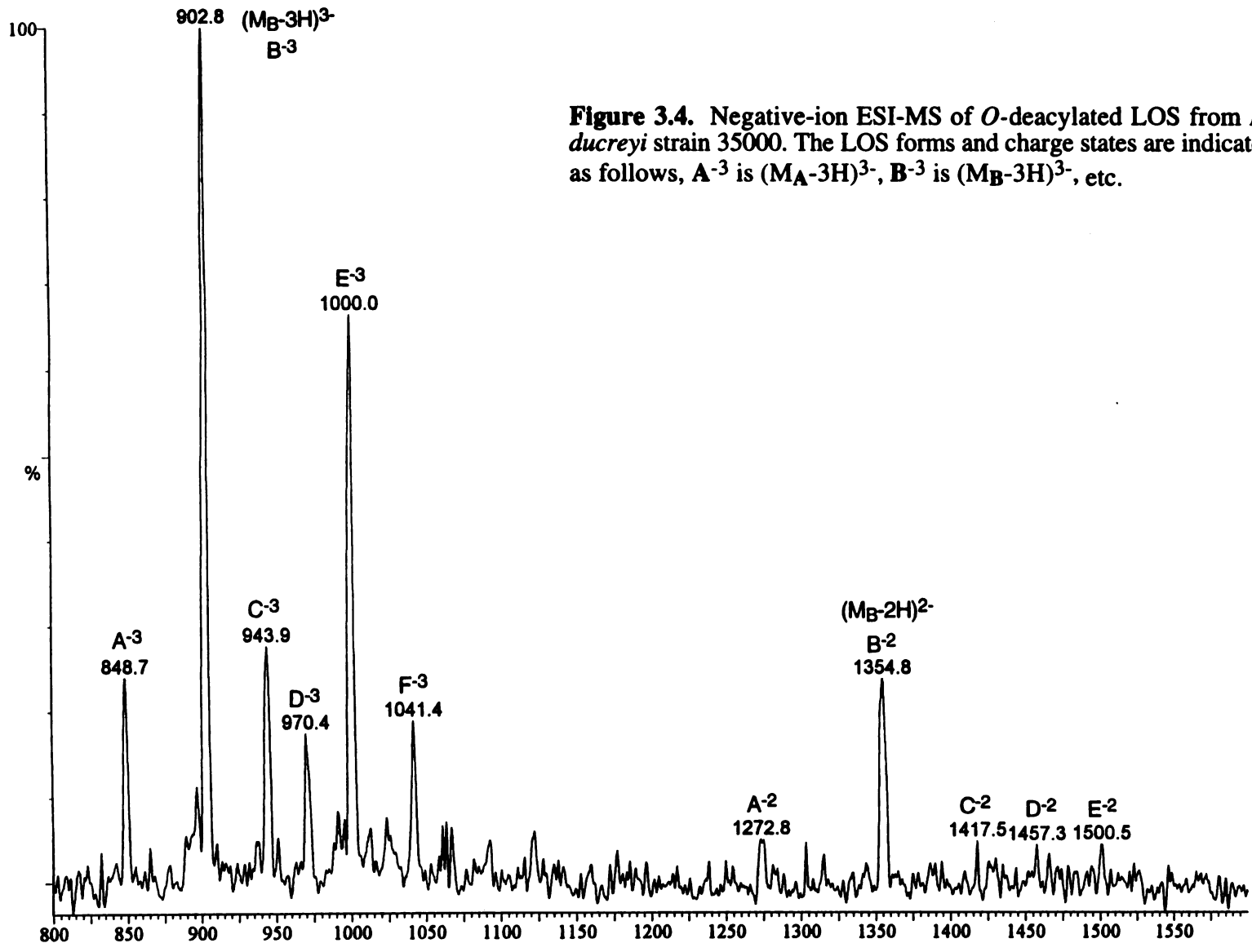

Figure 3.4. Negative-ion ESI-MS of *O*-deacylated LOS from *H. ducreyi* strain 35000. The LOS forms and charge states are indicated as follows, $\mathbf{A}^{-3}$ is $(M_A\text{-}3H)^{3-}$, $\mathbf{B}^{-3}$ is $(M_B\text{-}3H)^{3-}$, etc.

Table 3.2. ESI-MS Analyses of *O*-deacylated LOS from *H. ducreyi* strain 35000

Molecular Weight (M_r) Observed[a]	Calculated	Relative Ion Abundance	Proposed Composition
A = 2549.1	2549.3	24	Hex_2 HexNAc Hep_4 Kdo(P) lipid A[b]
B = 2711.4	2711.5	100	Hex_3 HexNAc Hep_4 Kdo(P) lipid A
C = 2834.7	2834.5	28	Hex_3 HexNAc Hep_4 PEA Kdo(P) lipid A
D = 2914.2	2914.7	17	Hex_3 $HexNAc_2$ Hep_4 Kdo(P) lipid A
E = 3003.0	3002.7	67	Neu5Ac Hex_3 HexNAc Hep_4 Kdo(P) lipid A
F = 3127.2	3125.7	20	Neu5Ac Hex_3 HexNAc Hep_4 PEA Kdo(P) lipid A

[a] All molecular weights are reported as their average mass values.

[b] After *O*-deacylation, the lipid A moiety is converted into diphosphoryl diacyl lipid A containing two N-linked β-hydroxymyristic acid chains with an average M_r of 953.0089.

to LOS-**B** glycoform (Melaugh et al., 1992). However, LSIMS is frequently not sensitive enough to detect weak ions at higher masses. Indeed, re-examination of later eluting fractions provided only indirect evidence for an additional oligosaccharide at M_r 1514, corresponding to the loss of one hexose unit (162 Da). However, the assignment of even this second oligosaccharide is in some doubt due to the fact that LSIMS spectra of even pure oligosaccharides produce small fragment ions at lower mass formed by cleavage at glycosidic oxygens (Y-type ions) (Domon & Costello, 1988). These ions have nominal masses that are identical to molecular weights of truncated species. Furthermore, unless these "truncated oligosaccharides" are chromatographically separated or judged to be too large to originate from gas phase fragmentation of the higher mass oligosaccharide species, it is very difficult to assign their origin as fragment ions or chemically distinct oligosaccharides.

Since it was not possible to unambiguously verify the additional glycoforms by LSIMS, a more thorough investigation of the oligosaccharide fraction was carried out by ESI-MS. ESI-MS is generally considered to be a much more sensitive analytical method which, under the conditions used here, does not produce fragment ions. Analysis of the total oligosaccharide fraction from *H. ducreyi* strain 35000 (see Figure 3.5) yielded a number of peaks that were consistent with the LOS heterogeneity assessed from the ESI-MS and SDS-PAGE gel data (see Figures 3.3 and 3.4, and Table 3.2). Furthermore, the precise masses obtained are mostly in agreement with the proposed compositions suggested from the *O*-deacylated LOS data (see Table 3.2). For example, the base peak at *m/z* 838.2 can be assigned as the doubly charged peak for the previously identified major oligosaccharide terminating in lactosamine with M_r = 1677. The peak at *m/z* 757.1 contains one less hexose and the higher mass peak at *m/z* 939.7 contains an additional *N*-acetylhexosamine (or phosphate and PEA). The peak at *m/z* 898.3 has been tentatively assigned as the addition of PEA to the major oligosaccharide (M_r = 1677+123), but its measured mass is somewhat lower than expected (see Table 3.3). Lastly, another extended

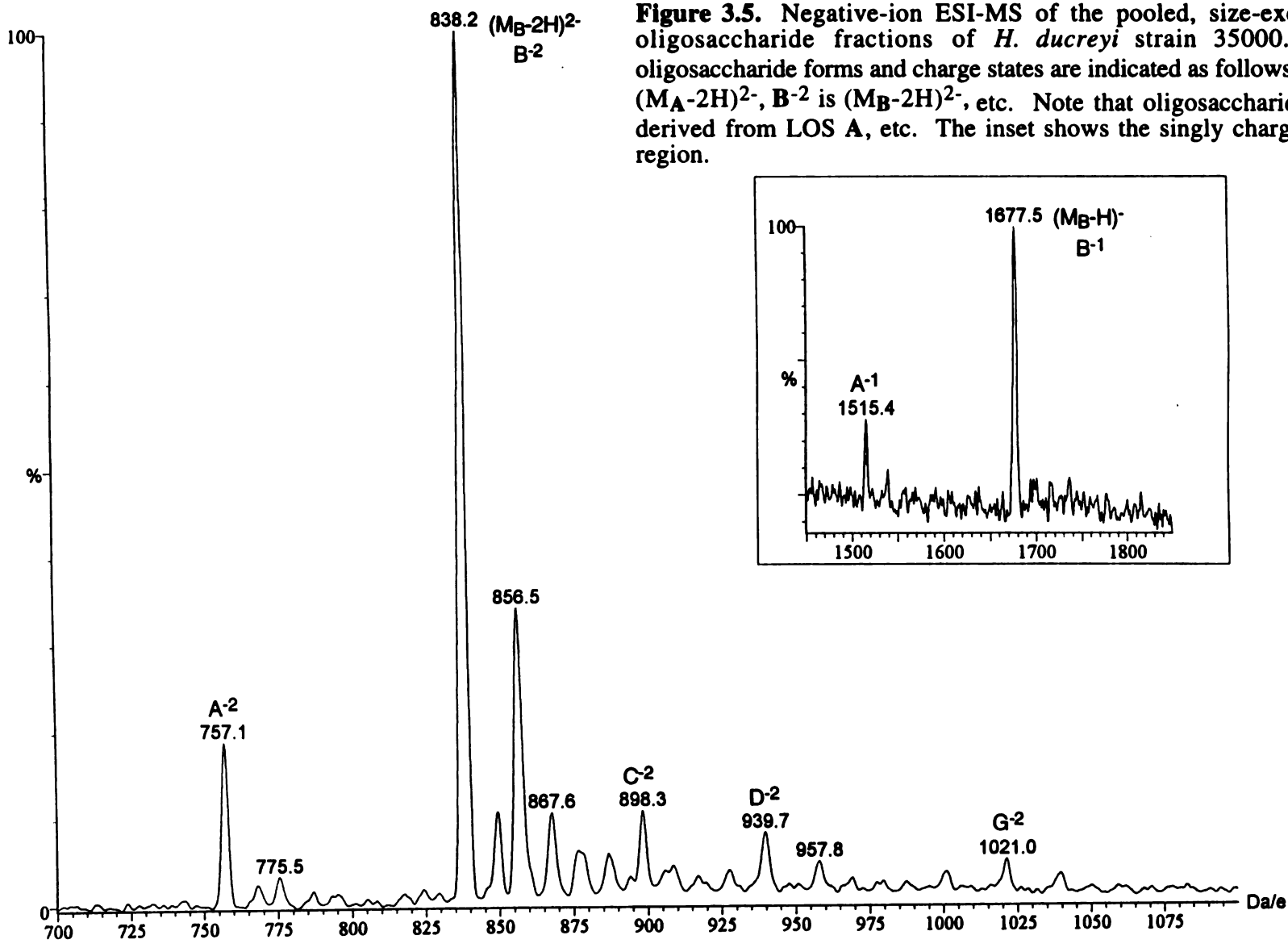

Figure 3.5. Negative-ion ESI-MS of the pooled, size-exclusion oligosaccharide fractions of *H. ducreyi* strain 35000. The oligosaccharide forms and charge states are indicated as follows, $\mathbf{A}^{-2}$ is $(M_{\mathbf{A}}\text{-}2H)^{2-}$, $\mathbf{B}^{-2}$ is $(M_{\mathbf{B}}\text{-}2H)^{2-}$, etc. Note that oligosaccharide **A** is derived from LOS **A**, etc. The inset shows the singly charged m/z region.

Table 3.3. ESI-MS Analyses of oligosaccharides from LOS of *H. ducreyi* strain 35000

Molecular Weight (M_r)		Relative Ion Abundance	Proposed Composition
Observed[a]	Calculated		
A = 1516.2	1516.3	19	Hex_2 HexNAc Hep_4 *anhydro*Kdo
B = 1678.4	1678.5	100	Hex_3 HexNAc Hep_4 *anhydro*Kdo
C = 1798.6	1801.5	11	Hex_3 HexNAc Hep_4 PEA *anhydro*Kdo
D = 1881.4	1881.7	9	Hex_3 $HexNAc_2$ Hep_4 *anhydro*Kdo
G = 2044.0	2043.8	5	Hex_4 $HexNAc_2$ Hep_4 *anhydro*Kdo

[a] All molecular weights are reported as their average mass values. Additional peaks were seen that corresponded to the addition of sodium, potassium and HCl, i.e., $(M - 2H + Na)^-$, $(M - 2H + K)^-$, $(M - H + HCl)^-$.

analog not observed in the ESI-MS spectrum of the *O*-deacylated LOS is seen at *m/z* 1021.0. This latter peak is consistent with the addition of *N*-acetylhexosamine (or phosphate and PEA) and hexose to the major oligosaccharide (M_r = 1677+ 203 + 162). The remaining peaks in this spectrum correspond to various molecular ion adducts of these oligosaccharides, such as the peak at *m/z* 856.5 which arises from the addition of HCl to the doubly charged deprotonated molecular ion, i.e., $(M - 2H + HCl)^{2-}$. As expected, the sialylated oligosaccharides are absent from this spectrum since they are converted to their asialo analogs during acetic acid hydrolysis.

Analysis of O-deacylated and HF-treated O-deacylated LOS. Since there was still some uncertainty regarding the identification of HexNAc (203 Da) versus an alternative assignment of phosphate and phosphoethanolamine (80 + 123 = 203 Da) for the LOS glycoforms **D** and **G**, the *O*-deacylated LOS preparation was further treated with aqueous HF to remove phosphate and PEA groups. A comparison of the before and after spectra (data not shown) of these two LOS preparations clearly shows that the molecular weights of all LOS components except for LOS-**C** shifted by the loss of 240 Da, the mass difference expected for removal of the three phosphates which are known to reside on Kdo and lipid A, i.e., diphosphoryl lipid A and 4-phosphoKdo (Melaugh et al., 1992). LOS-**C**, however, was no longer present as a distinct peak as one would have predicted once its single PEA group was removed, making it identical to the LOS-**B** glycoform. Therefore, the mass spectral data of the *O*-deacylated, dephosphorylated LOS support the presence of an additional HexNAc on the LOS-**D** and -**G** glycoforms, as well as the assignment of a PEA moiety to LOS-**C** as listed in Table 3.3.

Sialic Acid Linkage Analysis. Lastly, to determine how the sialic acid is linked to the terminal lactosamine acceptor, Galβ1→4GlcNAc, the LOS was treated with sialidase. First, Newcastle Disease Virus sialidase was used, an enzyme specific for Neu5Acα2→3

linkages, followed by treatment with *Clostridium perfringens* sialidase, a enzyme with broader specificities, i.e., Neu5Acα2→3,6, or 8. The amount of sialic acid released by the NDV sialidase digestion was 6 pmol Neu5Ac/μg LOS, as measured by high pH anion exchange chromatography of the enzyme digests. The amount released by adding extra *C. perfringens* sialidase was 8.7 pmol Neu5Ac/μg LOS.

DISCUSSION

In this chapter, we have completed the structure determination of the major oligosaccharide from the LOS of *H. ducreyi* strain 35000 and have confirmed several features proposed in our preliminary characterization (see Figure 3.6). The core Hep_3Kdo region of this oligosaccharide is identical to that in *H. influenzae* nontypable strain 2019 (Phillips et al., 1992), and consists of three α-linked L-*glycero*-D-*manno*-heptoses and reducing terminal Kdo, which is phosphorylated in the intact LOS structure. Two strains of *H. influenzae* type b have also been found to produce LOS with this common core structure, although additional branching from the Hep_3 core was observed in these strains (Phillips et al., 1993; Schweda et al., 1993). Furthermore, the major *H. influenzae* oligosaccharide structures contain one or two PEAs on the Hep_3 core, whereas the major *H. ducreyi* 35000 oligosaccharide is only partially substituted with PEA.

The 1,4-linked D-*glycero*-D-*manno*-heptose present in the *H. ducreyi* 35000 LOS was confirmed by 2D NMR studies to exist on the oligosaccharide branch, separated from the core heptoses by a 1,6-linked β-glucose residue. The oligosaccharide branch terminates in a lactosamine disaccharide, which most likely is the recognition site for monoclonal antibody 3F11, which recognizes the terminal region of paragloboside (Mandrell et al., 1988). Indeed, the branch heptose breaks up what would otherwise have been a tetrasaccharide very similar to the lacto-*N*-neotetraose antigen, a structure seen in both *N. meningitidis* (Jennings et al., 1983; Michon et al., 1990; Gamian et al., 1992) and *N.*

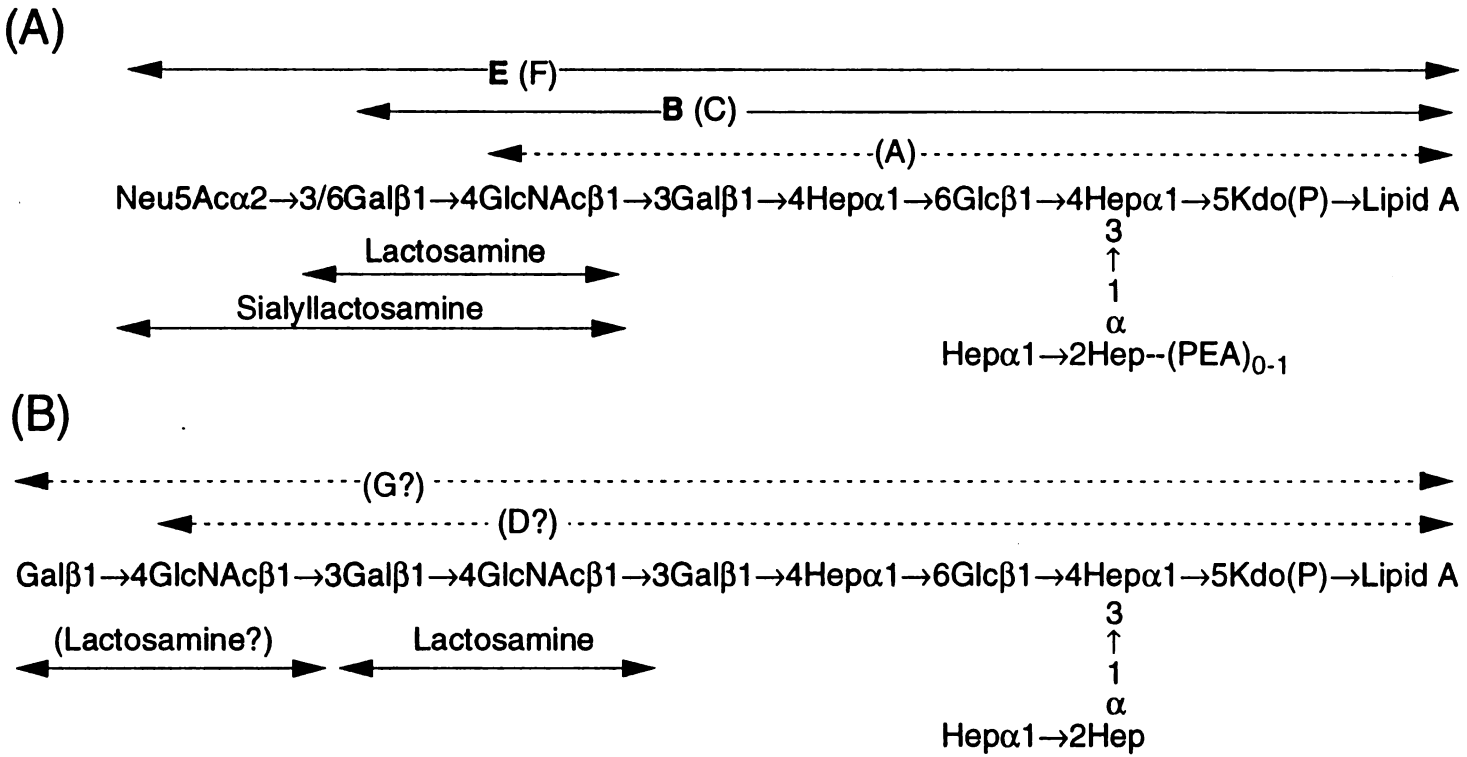

Figure 3.6. Proposed total structures of *H. ducreyi* 35000 LOS glycoforms. LOS structures listed in (A) are based on the lactosamine and sialyllactosamine glycans (LOS-**A**, **B**, **C**, **E** and **F**). LOS structures in part (B) are more speculative (LOS-**D** and **G**), and may consist of the addition of a second lactosamine disaccharide as a biosynthetic alternative to sialic acid.

gonorrhoeae LOS (John et al., 1991; Yamasaki et al., 1991). Enzymatic susceptibility of the LOS to the Newcastle Disease Virus sialidase shows that this lactosamine is largely sialylated via an α2→3 linkage to lactosamine, although a small amount may also be present in an α2→6 or α2→8 linkage due to the incomplete release of sialic acid. Complete release of sialic acid was accomplished with the non-specific sialidase from *C. perfringens*. It should be noted that sialic acid linked α2→3 to lactosamine has been recently reported in an LOS from *N. meningitidis* (Yamasaki et al., 1993).

We have also investigated the source of the heterogeneity in the terminal glycan regions of these LOS and have concluded that besides the major oligosaccharide as determined from NMR and mass spectrometric data (LOS-**B**), several other glycoforms are present which in the most part can be explained as biosynthetic intermediates of this major LOS structure (see Figure 3.6). In addition to these intermediates, three additional glycoforms apparently arise through an alternative biosynthetic pathway leading to the addition of sialic acid (sialyllactosamine) or HexNAc and Hex as a biosynthetic alternative to sialic acid. The addition of a second lactosamine disaccharide suggests the formation of a polylactosamine-like structure). It should be noted that a similar divergent biosynthetic pathway has been reported for *N. gonorrhoeae* LOS (Yamasaki et al., 1991).

The significance of such a diverse set of LOS glycoforms in one strain is not clear, but evidence to date suggests that *H. ducreyi* does not undergo significant phase variation of surface antigens, including LOS, and therefore may require different LOS structures to perform specific and distinct biological functions. Recent structure studies on the oligosaccharide regions of lipooligosaccharides from pathogenic *Neisseria* and *Haemophilus* provide convincing evidence that the LOS are mimicking human glycoconjugates (Mandrell et al., 1988; Gibson et al., 1993; Phillips et al., 1993; Yamasaki et al., 1993). These structural similarities to host antigens may represent the key to understanding the roles LOS play in the pathology of the diseases these bacteria cause. For example, LOS species that terminate in lactosamine may be necessary for adhesion and

invasion of host cells. In contrast, the LOS terminating in sialyllactosamine might better be explained as necessary for providing an evasion mechanism against host immune and defense response. In support of this latter interpretation, recent studies of pathogenic *Neisseria* have suggested that sialylation of LOS confers serum-resistance to strains that are otherwise serum-sensitive (Parsons et al., 1989; Frangipane & Rest, 1993), as well as reducing opsonized phagocytosis and/or killing by human neutrophils (Estabrook et al., 1992; Kim et al., 1992; Rest & Frangipane, 1992). The development of mutant strains that express only a single or small subset of this LOS repertoire should allow us the means to better unravel the functions of these different LOS. Towards this latter goal, we will analyse in the next chapter, the LOS from the wild-type strain 188 and a variant strain of this wild-type designated 188-2 which by SDS-PAGE analysis appears to biosynthesize a truncated form of LOS. The hope is that by comparing the LOS structures of these two strains and then examining their respective abilities to cause lesion formation in the cultured human keratinocyte model, we will gain information about which features of LOS may be crucial to the pathogenic process.

CHAPTER 4.

THE USE OF PYOCIN TO SELECT A *HAEMOPHILUS DUCREYI* VARIANT DEFECTIVE IN LIPOOLIGOSACCHARIDE BIOSYNTHESIS

INTRODUCTION

In the last two chapters we described the structural characterization of the major oligosaccharide from the LOS of *H. ducreyi* strain 35000 which defined a terminal lactosamine that is partially sialylated. We theorized that lactosamine may be necessary for adhesion and invasion of host cells, whereas sialyllactosamine may serve as an evasion mechanism against the immune response. One approach to examining this theory is to make variants which are defective in LOS biosynthesis. If, for example, one could make a variant which lacked terminal lactosamine, it would then be possible to assay its adherence and cytotoxic properties in the cultured human keratinocyte model.

Earlier researchers had made a series of mutants from *Salmonella* and *Escherichia* by exposing them to bacteriophages. These mutants were in some manner deficient in their LPS structures. Some lacked the *O*-antigen polysaccharide while others showed truncations in the branch and core regions of their oligosaccharides. These mutants were extremely useful in elucidating oligosaccharide biosynthetic pathways and solving structure problems (Luderitz et al., 1966; Galanos et al., 1977).

More recently our collaborators have used pyocins, bacteriocins isolated from *Pseudomonas aeruginosa*, to select LOS variants from *N. gonorrhoeae* which had sequential deletions in their oligosaccharides (Dudas & Apicella, 1988; John et al., 1991). They have shown that the probable LOS binding site for pyocin corresponds to the presence of the epitope reactive with MAb 3F11. Structural analyses have recently been completed on the LOS of the pyocin survivors and this information will be critical in

relating LOS structure to biologic function involving the pathogenesis of *Neisseria* (John et al., 1991).

Based on the similarities between the LOS of *H. ducreyi* and *N. gonorrhoeae*, we sought to determine if *H. ducreyi* were pyocin susceptible and if pyocin selection could be used to generate stable, LOS oligosaccharide variants from these organisms. Such LOS variants would be useful in comparative experiments aimed at understanding the role of *H. ducreyi* LOS in the pathogenesis of chancroid. The exact mechanism for the generation of pyocin variants is unknown. Earlier, pyocin was thought to be a proteinaceous toxin, but more recently it is believed to be a bacteriophage containing single-stranded DNA. A schematic of the proposed mechanism for the production of pyocin-resistant variants is shown in Figure 4.1. Pyocin, represented as the shaded hexagon, binds to LOS receptors on the surface of the bacterial cell. Most cells are lysed but those variants which survive now have altered LOS which can no longer function as pyocin receptors.

EXPERIMENTAL

Bacteria. *H. ducreyi* strains 35000, 27722, 023233, 188 and CIP542 were obtained from our collection. The bacteria were cultured on chocolate agar plates at 34°C and 5% CO_2 as previously described (Campagnari et al., 1991). Any colonies resistant to pyocin lysis were confirmed by colony morphology, Gram stain, requirement for X but not V factor, oxidase positivity, catalase negativity, and the inability to ferment glucose, lactose and sucrose (Campagnari et al., 1991). The *P. aeruginosa* strains used for the production of pyocins were obtained from our own collection and grown on supplemented GC medium base as described in the gonococcal studies (Dudas & Apicella, 1988).

Pyocin Isolation. Pyocins were isolated from *P. aeruginosa* strains by the method described by Morse et al. (Morse et al., 1976).

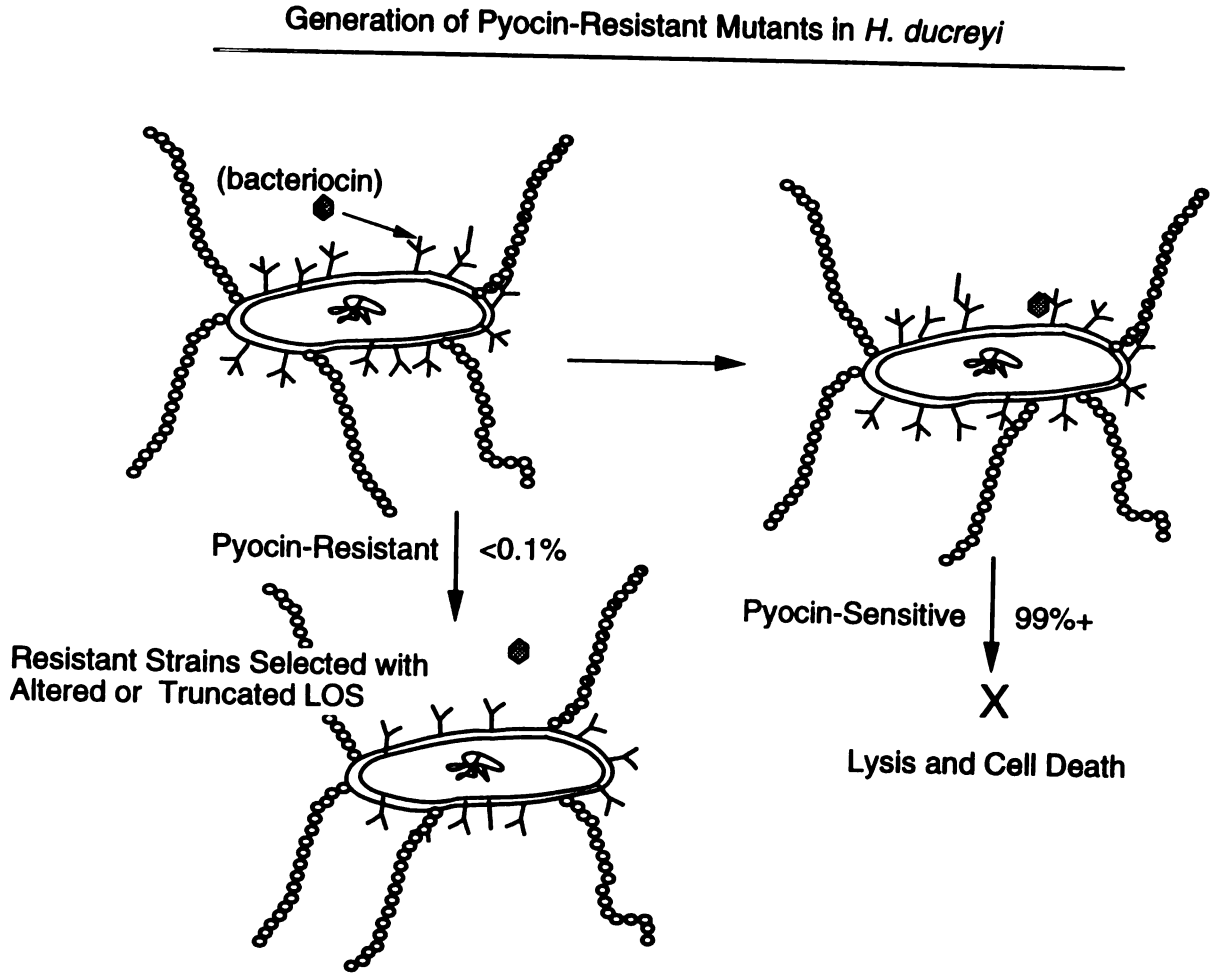

Figure 4.1. Proposed scheme for the production of pyocin-resistant variants in *H. ducreyi.*

Pyocin Selection. The pyocin assay was performed on a lawn of *H. ducreyi* using the procedure described previously (Dudas & Apicella, 1988). Briefly, the organisms were harvested from an overnight growth on chocolate agar and suspended in brain heart infusion broth and hemin, supplemented with isovitalex and fetal bovine serum. The final concentration of bacteria was 10^7 colony forming units per ml. Approximately 100 µl of each bacterial suspension was plated onto the surface of a chocolate agar plate and 10 µl of each purified pyocin preparation was spotted in a defined area on each lawn. The plates were incubated at 35°C overnight in a 5% CO_2 incubator. After 18-24 hours the plates were observed for a zone of lysis where each pyocin was placed. In the initial screening for pyocin sensitivity, each strain was scored as sensitive (S), resistant (R) or partially sensitive (T). Colonies that were present in a zone of lysis were individually picked and expanded for analyses.

Lipooligosaccharide preparations. The LOS from parental and selected pyocin survivors were purified using a modification of the method described by Inzana (Inzana, 1983). LOS analyzed by mass spectrometry were isolated using the phenol-water method described by Westphal and Jann (Westphal & Jahn, 1965).

SDS-PAGE. The LOS preparations were initially analyzed by sodium-dodecyl sulfate-polyacrylamide electrophoresis on 14% acrylamide gels with 2.5% urea (Laemmli, 1970). Subsequent analyses were performed using the tricine gel method which provided better resolution of the LOS banding patterns (Lesse et al., 1990).

Colony blot assays. Pyocin survivors were analyzed for the expression of the MAb 3F11 oligosaccharide epitope using colony blots as previously described (Campagnari et al., 1990).

Composition and Linkage Analysis. Prior to compositional analysis, oligosaccharide fractions from strain 188 and its pyocin variant, 188-2, were prepared by acetic acid hydrolysis of the LOS (≈2 mg/ml) for 2 hours at 100°C. Monosaccharide compositions of the released oligosaccharide fractions from the LOS of both strains were

obtained after partial purification on two tandem Bio-Sil TSK-125 columns (60 x 0.75 cm) running with 50 mM pyridinium-acetate (pH 5.2) at a flow rate of 1 ml/min. Detection was carried out by on-line refractive index (Knauer). The partially purified oligosaccharide fractions were hydrolyzed in 2 M trifluoroacetic acid for 3 h at 100°C. The resulting monosaccharides were separated and quantified by HPAEC-PAD (Phillips et al., 1990). To determine linkages of the various sugars, partially methylated alditol acetates were prepared from the oligosaccharide fraction as described in Chapter 2. Briefly, NaOH was used with dimethylsulfoxide to prepare the corresponding alkoxide oligosaccharides, which were then methylated with CH_3I, hydrolyzed, reduced with $NaBD_4$, and acetylated (Levery & Hakomori, 1987). The resulting PMAAs were analyzed by GC/MS using a VG-70 mass spectrometer coupled to a 30 meter DB-1 capillary column (J&W Scientific). A temperature program of 120°C to 250°C at 4°C/min was used with electron impact detection (70 eV, 500 μA trap current, 2 mA emission current, and 180°C source temperature). A partially methylated alditol acetate mixture obtained from the purified major oligosaccharide of *Salmonella typhimurium* Ra LPS (Sigma) was used as a standard for correlating retention times.

Mass Spectrometry. To determine the molecular weights of the LOS species and assess the heterogeneity of LOS glycoforms from both the wild-type strain and pyocin variant, LOS were analysed by negative-ion ESI-MS after *O*-deacylation with mild hydrazine (Helander et al., 1988). We have found that *O*-deacylation of LOS greatly increases its water solubility and reduces its tendency to aggregate, making it more amenable to analysis by ESI-MS techniques. Approximately 1 mg of *O*-deacylated LOS from strains 188 and 188-2 was prepared as described in Chapter 2. For ESI-MS analysis, the lyophilized *O*-deacylated LOS samples were dissolved in water and injected into a stream of H_2O/CH_3CN (3:1) containing 1% acetic acid (Gibson et al., 1993). Mass spectra were taken in the negative-ion mode on a VG/Fison BioQ triple quadrupole mass spectrometer operating in the negative-ion mode with a constant flow rate of 3 μl/min.

Mass spectra were then averaged and mass assigned via the VG/Fisons data system using an external calibrant. Average LOS molecular weights were calculated using the molecular weight of the conserved diphosphoryl diacyl lipid A moiety, M_r 953.0089, added to the interval average mass values of the monosaccharide and phosphate constituents: hexose (Hex), 162.1424; heptose (Hep), 192.1687; *N*-acetylhexosamine (HexNAc), 203.1950, 3-deoxy-D-*manno*-octulosonic acid (Kdo, 220.1791); 5-*N*-acetylneuraminic acid (sialic acid or Neu5Ac), 291.2579; phosphoethanolamine (PEA), 123.0483, and phosphate (P), 79.9799.

To confirm the composition assignments of the oligosaccharide portions of these LOS as suggested from monosaccharide and ESI-MS data, the oligosaccharide fractions from 188 and 188-2 LOS were separately analyzed by LSIMS on a Kratos MS50S mass spectrometer (Phillips et al., 1990). LSIMS analysis of oligosaccharides affords a higher degree of mass accuracy (± 0.3 Da) than the ESI-MS experiments and can also provide limited sequence information through the presence of fragment ions. Oligosaccharides were dissolved in water and small aliquots (≈ 2-5 μg) were transferred to the LSIMS probe along with 1 μl of thioglycerol/glycerol (1:2, v:v). A Cs^+ beam of 10 keV was used and the resulting ions were accelerated at 8 keV. Spectra were taken at 300 s/decade and manually calibrated to an accuracy of better than ± 0.2 Da using an external Ultramark calibrant. Since the MS50S mass spectrometer is run under conditions that resolve the isotopic distribution of the various ions ($M/\Delta M \approx 2000$), masses are reported as their most abundant isotopically pure component. To calculate the ^{12}C-containing molecular ions, the following exact interval mass values were used; Hex, 162.0528; Hep, 192.0634; HexNAc, 203.0794, Kdo, 220.0583; *anhydro*Kdo, 202.0477; Neu5Ac, 291.0954; PEA, 123.0085; and H_2O, 18.0106.

RESULTS

After initial determinations of pyocin sensitivity (Table 4.1) pyocin N was selected to use in these studies. Pyocin N was used on *H. ducreyi* strains 35000, 27722, 023233, CIP542 and 188. Of these strains, 12 colonies were isolated from the zones of lysis. Three from *H. ducreyi* strain 35000, 2 from strain 023233 and 7 from strain 188. These colonies were expanded in culture and the identity of the strains were confirmed as described in the methods. The LOS preparations from each colony were compared to the parental LOS profile by SDS-PAGE and silver stain as described (Tsai & Frasch, 1982; Inzana, 1983). The results indicated that 1 isolated colony, from *H. ducreyi* strain 188, appeared to assemble an LOS with a different SDS-PAGE banding pattern. Figure 4.2 is a silver stain of a tricine gel illustrating that the LOS from pyocin survivor isolate number 2 (lane 2) had a more rapidly migrating electrophoretic banding pattern as compared to the parental strain 188 (lane 1). It appears that the LOS from this pyocin N survivor, termed 188-2, is a truncated version of the major LOS species assembled by *H. ducreyi* strain 188.

Previous studies by Campagnari et al. have shown that MAb 3F11 reacts with a 4.8 kDa LOS band present on 97% of the *H. ducreyi* strains in their collection (Campagnari et al., 1990). Based on the LOS SDS-PAGE profile of the pyocin survivor 188-2, colony lifts were performed and probed with MAb 3F11. Figure 4.3 is an example of a colony lift showing that MAb 3F11 reacted to *H. ducreyi* strain 188 (panel A) but not to the pyocin selected strain 188-2 (panel B). These data suggest that the *H. ducreyi* strain 188-2 has lost all or part of the terminal trisaccharide present on the native LOS. Repeated passage and selection of *H. ducreyi* strain 188-2 has shown that this LOS variant appears to be stable.

The ESI-MS spectra of the *O*-deacylated LOS from strain 188 and 188-2 shown in Figure 4.4 indicated a substantial change had occurred in the pyocin survivor to a much simpler and less heterogeneous LOS mixture. In contrast, the spectrum of the parent strain

Table 4.1.

Susceptibility of *H. ducreyi* strains to lysis by pyocins[a]

H. ducreyi strains	Pyocins											
	C	D	E	F	G	H	I	J	K	L	M	N
CIP542	S	R	R	T	S	R	T	R	R	S	S	S
27722	S	R	R	T	S	R	R	R	R	R	S	S
188	S	R	R	R	S	R	S	S	S	S	S	S
35000	S	R	R	T	S	R	T	R	T	S	S	S
023233	S	R	R	T	S	T	R	R	T	T	S	S

[a]Abbreviations: R, resistant; S, sensitive; T, turbid (partially sensitive)

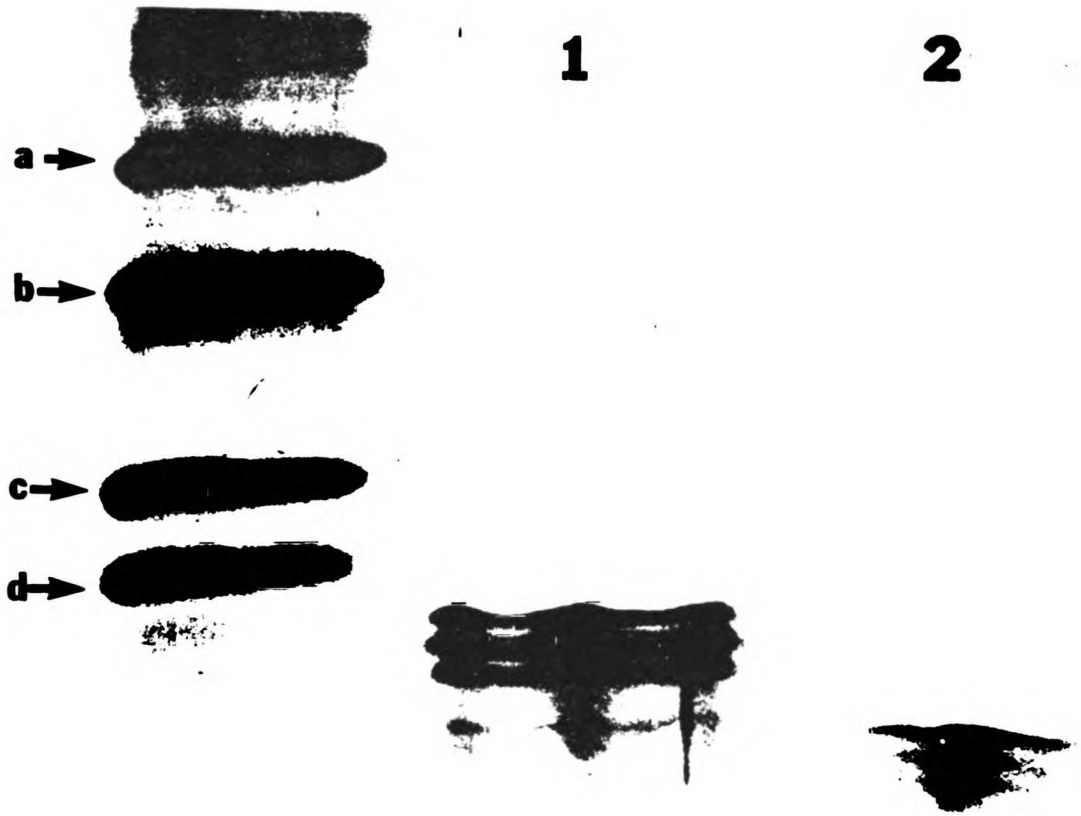

Figure 4.2. SDS-PAGE on a 14% tricine gel. Lane 1 contains purified LOS from *H. ducreyi* strain 188. Lane 2 contains LOS from the pyocin selected *H. ducreyi* strain 188-2. The molecular weight markers are: a, 16.9 kDa; b, 14.4 kDa; c, 6.2 kDa; d, 2.5 kDa.

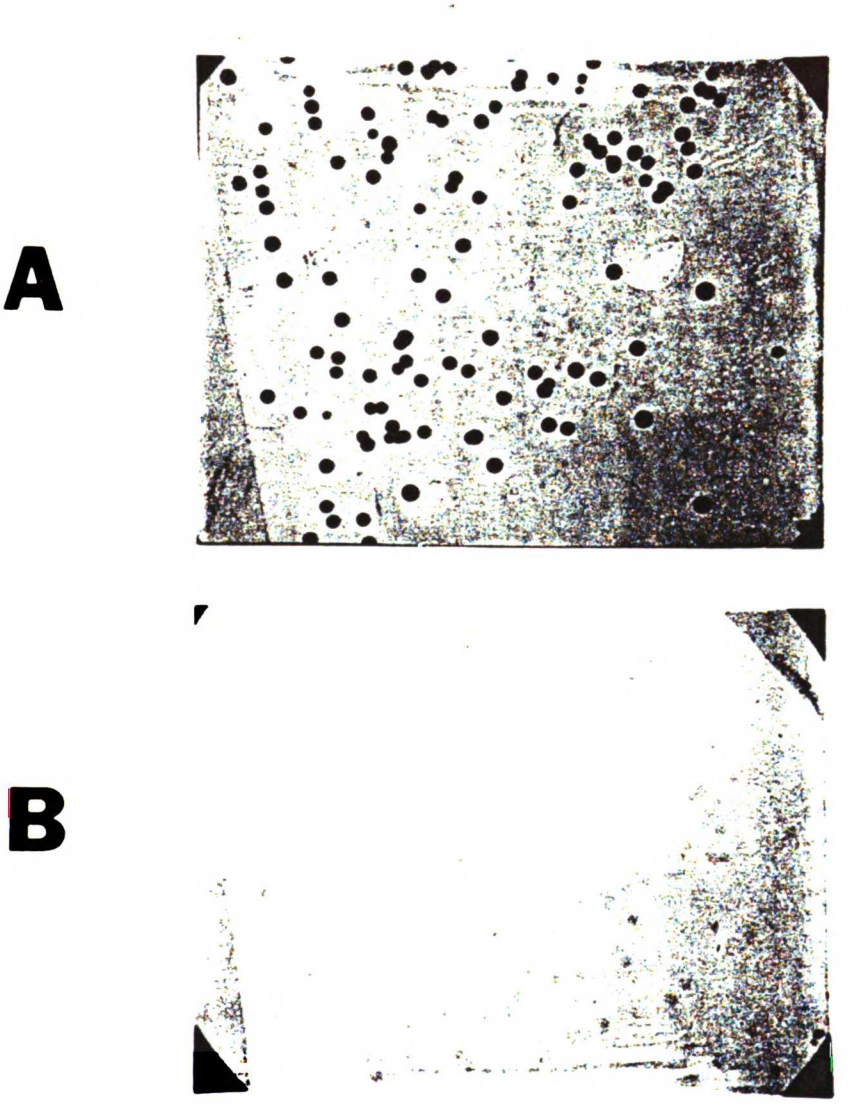

Figure 4.3. Colony lift assay of *H. ducreyi* strain 188 (panel A) and *H. ducreyi* strain 188-2 (panel B) probed with MAb 3F11.

188 contained many of the same peaks previously reported for *H. ducreyi* strain 35000 (Gibson et al., 1993), but was considerably more heterogeneous. For example, the ESI-MS spectrum of *O*-deacylated LOS from parental *H. ducreyi* strain (Fig. 4.4A) clearly shows two dominant triply charges peaks at *m/z* 943.6 and 1041.6, as well as their anhydro counterparts at *m/z* 938.2 and 1034.7, corresponding to the average molecular weights of 2833.4 (LOS L) and 3127.8 (LOS N), respectively (see Table 4.2). These are similar to the two major components observed earlier for strain 35000 (Gibson et al., 1993), which were found to differ by the presence or absence of sialic acid ($\Delta m \approx 291$ Da). However, a multitude of less abundant secondary peaks, the bulk of which appear also to be triply charged ions, were also present. These peaks can mosty be assigned as LOS components containing an additional phosphoethanolamine (PEA) moiety, and/or sequential saccharide deletions down to a conserved $Hep_3Kdo(P)$-*O*-deacyl lipid A core, i.e., LOS A, M_r 1830.3 (see Table 4.2).

The ESI-MS spectrum of the *O*-deacylated LOS from *H. ducreyi* strain 188-2 (Fig. 4.4B) contained peaks which correspond to a relatively simple series of related LOS components with mostly smaller molecular weights. The most abundant LOS form is clearly evident as a triply charged ion, $(M-3H)^{3-}$ at *m/z* 822.3, and a much less abundant doubly charged ion, $(M-2H)^{2-}$ at *m/z* 1233.6. Taken together these pair of ions yield an average M_r of 2469.5 for this major component, LOS C. Curiously, this spectrum is essentially devoid of peaks originating from loss of water, i.e., anhydro LOS forms, which mostly dominatated the spectrum of the parental LOS mixture. In addition to the dominant LOS C from 188-2, there are two other LOS species at lower mass whose molecular weights are consistent with the loss of a single heptose (LOS A, M_r 2276.8) or hexose (LOS B, M_r 2307.3), and two species at higher masses consistent with the addition of PEA (LOS D, M_r 2592.0), or Hex and HexNAc (LOS E, M_r 2712.7) (see Appendix Table 2B). This latter component may represent a very small amount of full length parental LOS (<3%) in the total LOS preparation. Despite the complexity and heterogeneity observed in the

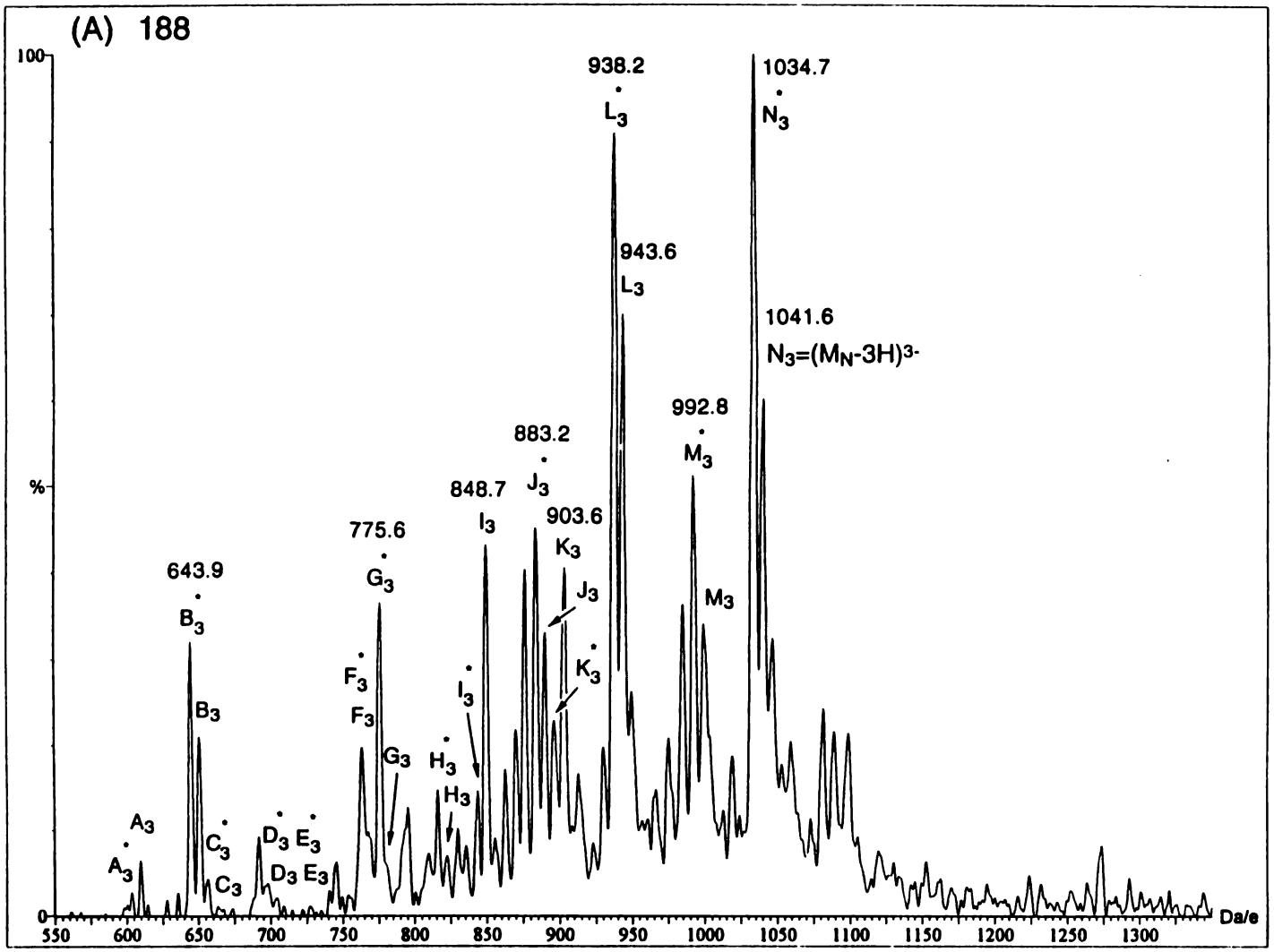

Figure 4.4. (A) Negative-ion electrospray ionization mass spectrum of the *O*-deacylated *H. ducreyi* LOS from the parental strain 188. See Table 4.2 for the assignments of these ions to specific LOS compositions. Due to the complexity observed in the ESI-MS spectrum of 188, only triply charged ions are labeled, e.g., A3 = $(M_A\text{-}3H)^{3-}$, A*3 = $(M_A\text{-}H_2O\text{-}3H)^{3-}$, B3 = $(M_B\text{-}3H)^{3-}$, etc. Other doubly and possibly quadruply charged species also exist, but are of much lower abundance and often overlap with the triply charged components.

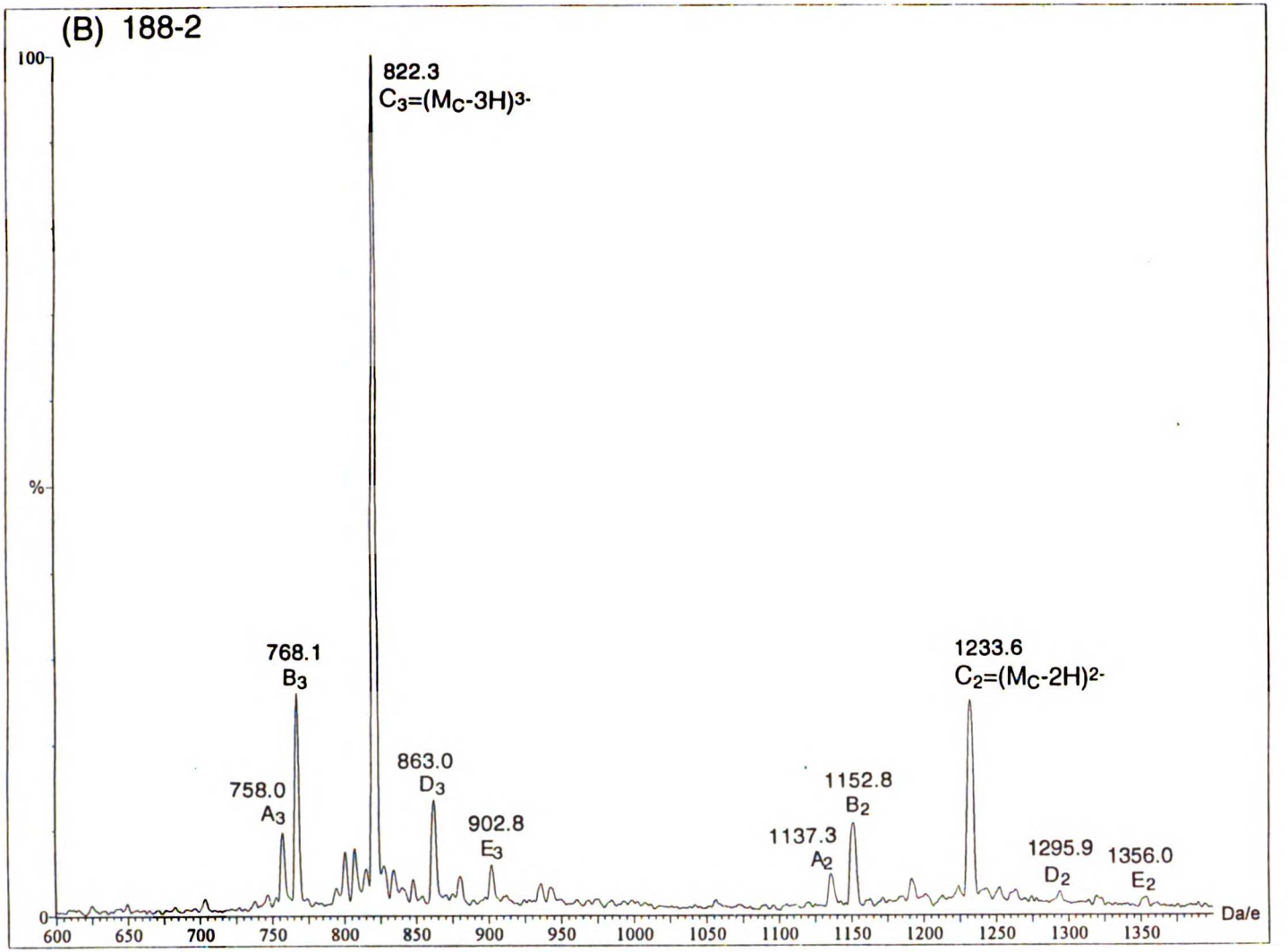

Figure 4.4. (B) Negative-ion electrospray ionization mass spectrum of the *O*-deacylated *H. ducreyi* LOS from the pyocin-variant strain 188-2. See Table 4.2 for the assignments of these ions to specific LOS composition.

Table 4.2. ***ESI-MS Analyses of O-deacylated LOS***

Haemophilus ducreyi Parent Strain 188			
M_r Observed[a]	M_r Calculated	Relative Ion Abundance[b]	Proposed Composition
A / A* = 1830.3 / 1811.0	1829.7 / 1811.6	13	Hep_3 Kdo(P) lipid A[c]
B / B* = 1953.6 /1934.7	1952.7 / 1934.7	37	Hep_3 PEA Kdo(P) lipid A
C / C* = 1991.1 / 1970.7	1991.8 /1973.8	(5)	Hex Hep_3 Kdo(P) lipid A
D / D* = 2115.0 /(2097.3)	2114.8 / 2096.8	(4)	Hex Hep_3 PEA Kdo(P) lipid A
E / E* = 2181.6 /(2166.0)	2184.0 / 2166.0	(2)	Hex Hep_4 Kdo(P) lipid A
F / F* = (2305.8)/ 2291.4	2307.0 / 2289.0	18	Hex Hep_4 PEA Kdo(P) lipid A
G / G* = (2346.0)/ 2329.8	2346.1 / 2328.1	26	Hex_2 Hep_4 Kdo(P) lipid A
H / H* =2469.0 / 2449.2	2469.2 / 2451.1	13	Hex_2 Hep_4 PEA Kdo(P) lipid A
I / I* = 2549.1 / 2533.2	2549.3 / 2531.3	41	HexNAc Hex_2 Hep_4Kdo(P) lipid A
J / J*= 2673.0 /2652.6	2672.4 / 2654.3	49	HexNAc Hex_2 Hep_4 PEA Kdo(P) lipid A
K / K*= 2713.8 / 2691.6	2711.4 / 2693.4	46	HexNAc Hex_3 Hep_4 Kdo(P) lipid A
L / L*= 2833.8 / 2817.6	**2834.5 / 2816.5**	**98**	**HexNAc Hex_3 Hep_4 PEA Kdo(P) lipid A**
M / M* = 3002.4 / 2981.4	3002.7 / 2984.7	46	NeuAc HexNAc Hex_3 Hep_4 Kdo(P) lipid A
N / N* = 3127.8 /3107.1	**3125.8 / 3107.7**	**100**	**NeuAc HexNAc Hex_3 Hep_4 PEA Kdo(P) lipid A**

(Table 4.2 continued)

***Haemophilus ducreyi* Pyocin Variant Strain 188-2**			
A = 2276.8	2277.0	10	Hex_2 Hep_3 PEA Kdo(P) lipid A
B = 2307.3	2307.0	29	Hex Hep_4 PEA Kdo(P) lipid A
C = 2469.5	**2469.2**	**100**	**Hex_2 Hep_4 PEA Kdo(P) lipid A**
D = 2592.0	2592.2	10	Hex_2 Hep_4 PEA_2 Kdo(P) lipid A
E = 2712.7	2711.4	(4)	HexNAc Hex_3 Hep_4 Kdo(P) lipid A

[a] All molecular weights are reported as their average mass values based on the triply charged ions.

[b] Relative abundance are based only triply charged ion species for strain 188 due to difficulties in assigning doubly and quadruply charged ions because of spectral overlap. Numbers in parethesis are considered near the limits of background.

[c] After *O*-deacylation, the lipid A moiety is converted into diphosphoryl diacyl lipid A containing two N-linked β-hydroxymyristic acid chains with an average M_r of 953.0089.

wild-type strain, if one considers only the difference between the most abundant LOS forms in each preparation, i.e., parental LOS N and the pyocin variant LOS C, it is clearly evident that the pyocin variant has undergone a trisaccharide deletion consisting of hexose, *N*-acetylhexosamine and sialic acid, but has picked up an additional PEA moiety.

To obtain additional structure information to support this tentative interpretation, the oligosaccharide fractions from the LOS of both the parental and the pyocin N survivor were subjected to LSIMS analysis. As shown in Fig. 4.5A for the parental *H. ducreyi* strain, the base peak appears as the singly deprotonated molecular ion peak, $(M-H)^-$ at *m/z* 1676.5[a]. A second molecular ion peak of less abundance is also observed at *m/z* 1514.5, which is consistent with the loss of a (terminal?) hexose from the more abundant molecular ion at *m/z* 1676. These masses are in excellent agreement with the expected compositions of Hex3HexNAcHep4*anhydro*Kdo and Hex2HexNAcHep4*anhydro*Kdo (see Appendix Table 2A). These generic composition assignments are also supported by monosaccharide composition analyses as listed in Table 4.3. For the parent strain 188, relative compositions of *approx.* 2:1:1 for Gal/Glc/$GlcNH_2$ were found, in addition to an estimated relative composition of approximately 2:1 for L-*glycero*-D-*manno*-heptose and D-*glycero*-D-*manno*-heptose. As previously observed, Kdo was not seen in the composition analysis due to its conversion to *anhydro*Kdo from phosphorylated Kdo (Melaugh et al., 1992; Phillips et al., 1992). The assignment of phosphorylated Kdo is also supported by the molecular weight data and the triply charge states observed under negative-ion ESI-MS (see Table 4.2). These data can be best explained through the presence of three unsubstituted phosphates ($z = -3$), two of which can be accounted for in the conserved diphosphoryl lipid A, and the remaining phosphate on the oligosaccharide portion. Since neither phosphate nor Kdo was found in the hydrolyzed oligosaccharides, and the mass of the oligosaccharide was 18 Da lower than expected if unmodified Kdo was present, we can

---

[a] Masses for LSIMS are reported as their nominal mass equivalents unless otherwise noted, i.e., m/z 1676 is 1676.5.

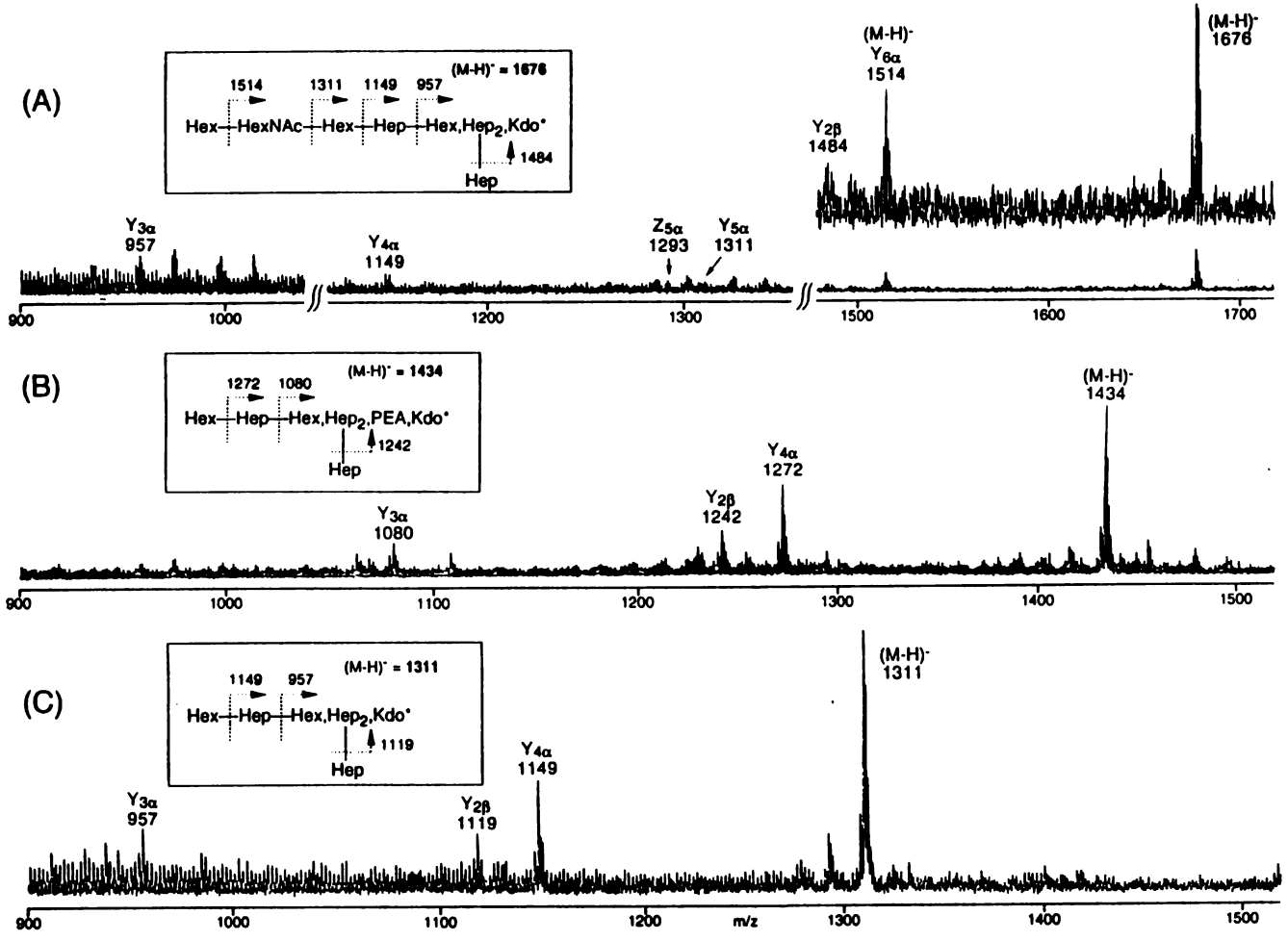

Figure 4.5. Negative-ion LSIMS spectra of the oligosaccharide fractions obtained by acetic acid hydrolysis of the LOS: (A) wild type parental strain 188, $(M-H)^-$ at *m/z* 1676 and 1514; (B) pyocin-variant strain 188-2, $(M-H)^-$ at *m/z* 1434 and 1272; and (C) dephosphorylated pyocin-variant strain 188-2, $(M-H)^-$ at *m/z* 1311 and 1149. Kdo refers to *anhydro*Kdo.

Table 4.3. ***Oligosaccharide Composition and Methylation Analysis***

Composition Analysis[a](mole ratio relative to Glucose)					
Strain	Galactose	Glucose	Heptose	Heptose[b]	$GlcNH_2$
188	1.5	1.0	2.0	1.1	0.8
188-2	0.8	1.0	2.8	0.1	---

Methylation Analysis[c] (relative peak area)								
Strain	t-Gal	3-Gal	6-Glc	t-Hep	2-Hep	3,4-Hep	4-Hep	4-GlcNAc
188	1.0	0.6	1.8	0.5	0.7	0.3	0.6	1.1
188-2	1.0	-----	1.5	0.3/1.3[d]	1.3	.4	---	---

[a] Kdo was not detected in the hydrolyzed oligosaccharide fraction due to its conversion to *anhydro*Kdo forms during acetic acid hydrolysis of LOS.

[b] This second heptose has been tentatively identified as D-glycero-D-*manno*-heptose based on earlier data [Melaugh, 1992], as opposed to the major core heptoses which are L-*glycero*-D-*manno*-heptoses.

[c] Partially methylated alditol acetates are abbreviated according to their substitution pattern as follows: t-Gal is 1,5-di-*O*-acetyl-2,3,4,6-tetra-*O*-methylgalactitol, 3-Gal is 1,3,5-tri-*O*-acetyl-2,4,6-tri-*O*-methylgalactitol, etc.

[d] Two terminal heptoses were found, the ratio stated is the unusual D-glycero-D-*manno*-heptose to the expected terminal core L-*glycero*-D-*manno*-heptose.

conclude that Kdo was initially present in its phosphorylated form. The conversion of phosphorylated Kdo to *anhydro*Kdo during acetic acid hydrolysis has been previously noted by ourselves and others in the LOS from several *Haemophilus* strains (Melaugh et al., 1992; Phillips et al., 1992).

In addition to the two molecular ions identified in the LSIMS spectrum of *H. ducreyi* strain 188, some limited fragmentation is present in the form of the glycosidic Y- and Z-type fragment ions (Domon & Costello, 1988). For instance, fragment ions arising from cleavage at either side of the glycosidic oxygen with charge retention at the reducing terminus are seen at *m/z* 1311 and 1293 (loss of HexNAc,Hex), *m/z* 1149 and 1131 (loss of HexNAc,Hex_2), and *m/z* 957 and 939 (loss of HexNAc,Hex_2,Hep). These fragment ions allowed the partial sequence of the main non-reducing branch to be assigned as Hex→HexNAc→Hex→Hep. Overall, this leaves Hex, Hep_3 and *anhydro*Kdo as the remaining undetermined core oligosaccharide in the parent strain. Tandem mass spectrometry of the most abundant parent ion at *m/z* 1676 yielded a spectrum (Fig. 4.6) that was similar to the one previously reported for the major oligosaccharide from strain 35000 (Melaugh et al., 1992). However, the two peaks in the spectrum marked with asterisks were not seen in the 35000 spectrum and may arise from matrix adducts to sample ions. These data, therefore, allowed a more complete structural assignment for this oligosaccharide:

Hex→HexNAc→Hex→Hep→Hex→Hep→*anhydro*Kdo
↑
Hep→Hep

Linkage analysis of strain 188 revealed eight major sugars eluting in the following order; terminal Gal, 3-Gal, 6-Glc, terminal Hep, 4-Hep, 2-Hep, 3,4-Hep, and 4-GlcNAc (see Table 4.3). These sugars were the same as those previously found in the major oligosaccharide from *H. ducreyi* strain 35000 (Melaugh et al., 1992) (see also Chapter 2). Moreover, the presence of a terminal galactose and a 4-linked *N*-acetylglucosamine can be

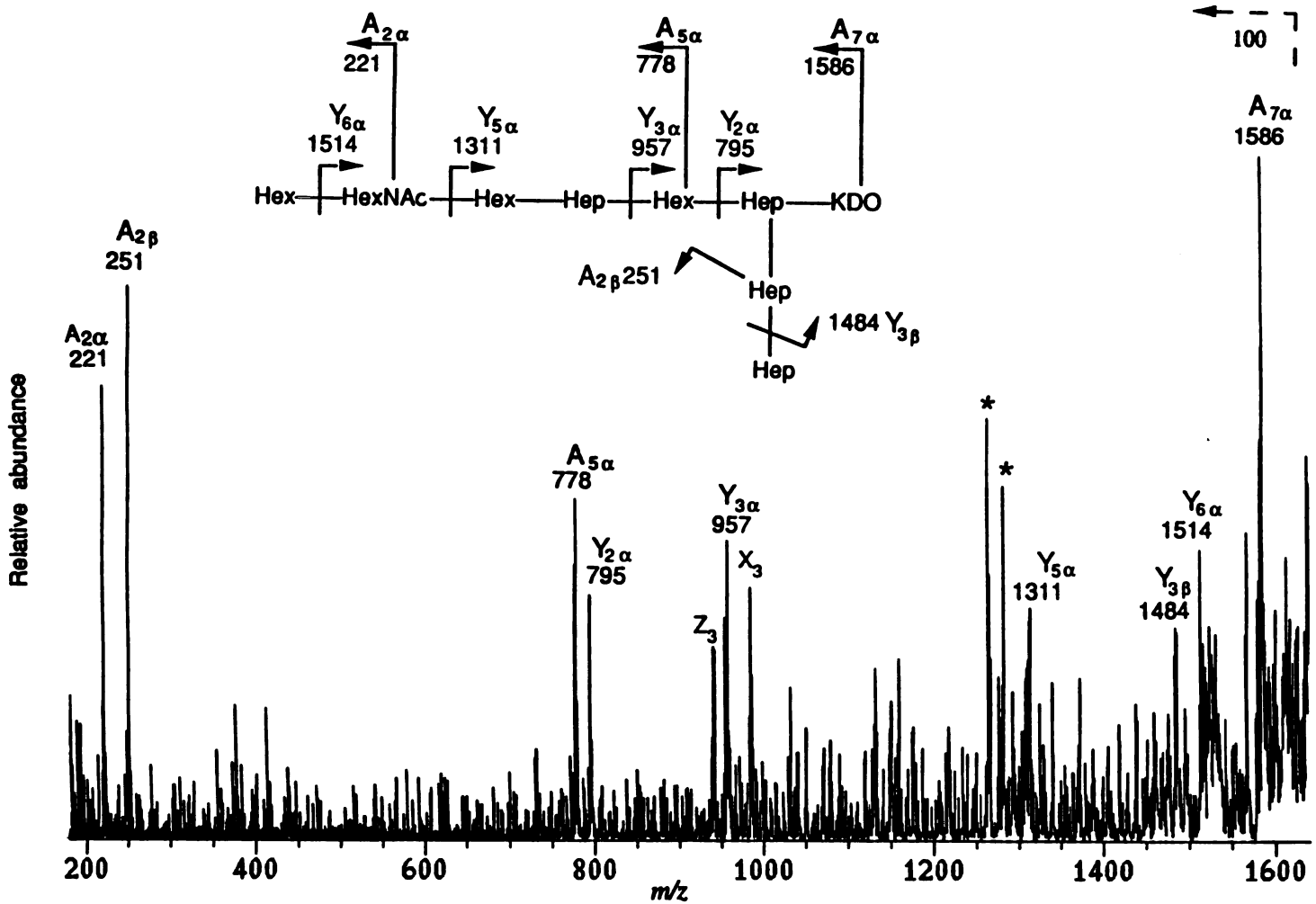

Figure 4.6. MS/MS spectrum of underivatized oligosaccharide from *H. ducreyi* strain 188. The molecular ion at *m/z* 1676 is not shown. Only the major peaks have been assigned. The peaks at *m/z* 1264 and 1282 which are marked with asterisks are unassigned and may arise from matrix adducts to sample ions.

unambiguously assigned to the terminal branch, based on the LSIMS oligosaccharide fragmentation data, as Gal1→4GlcNAc. Given the previously reported high binding of MAb 3F11 to the LOS of this parent strain (Campagnari et al., 1990), this terminal structure is likely to be Galβ1→4GlcNAc, or terminal lactosamine. If *H. ducreyi* strain 188 LOS were to contain the same oligosaccharide as that previously proposed for *H. ducreyi* strain 35000 (Melaugh et al., 1992), the full structure would be:

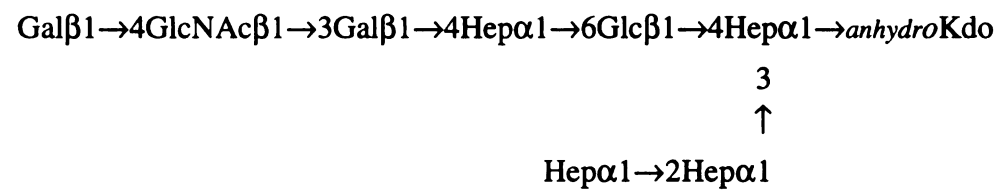

The LSIMS spectrum of the oligosaccharide from the pyocin-survivor, strain 188-2, contains a much smaller oligosaccharide of M_r 1434, as shown in Fig. 4.5B. This mass is in agreement with an oligosaccharide composition of Hex_2,Hep_4,PEA,*anhydro*Kdo. Phosphoethanolamine had previously been assigned to the composition of this LOS based on the ESI-MS molecular weight data (see Table 4.2). Treatment of the oligosaccharide with HF to remove phosphoester moieties and analysis by LSIMS gave the spectrum shown in Fig. 4.5C. Fragment ions in the LSIMS spectrum at *m/z* 1119, and *m/z* 1149 and 957, can be interpreted as arising from glycosidic bond cleavages originating from two separate non-reducing terminal branches; Hep and Hex→Hep, respectively. Therefore, the LOS of the *H. ducreyi* pyocin variant 188-2 clearly lacks the terminal lactosamine structure that endows the parent strain with the acceptor for sialylation as well as the epitope for MAb 3F11 binding (see Fig. 4.7). The tandem MS spectrum of this oligosaccharide is very weak and did not contain any additional information (Fig. 4.8). The peak at *m/z* 1390 may represent the loss of CO_2 from the molecular ion and the peak at *m/z* 1372 may represent an additional loss of H_2O. These structural data strongly suggests that the *H. ducreyi* strain 188-2 synthesizes an LOS with a truncated oligosaccharide branch terminating prior to the formation of the lactosamine disaccharide. However, the LOS of

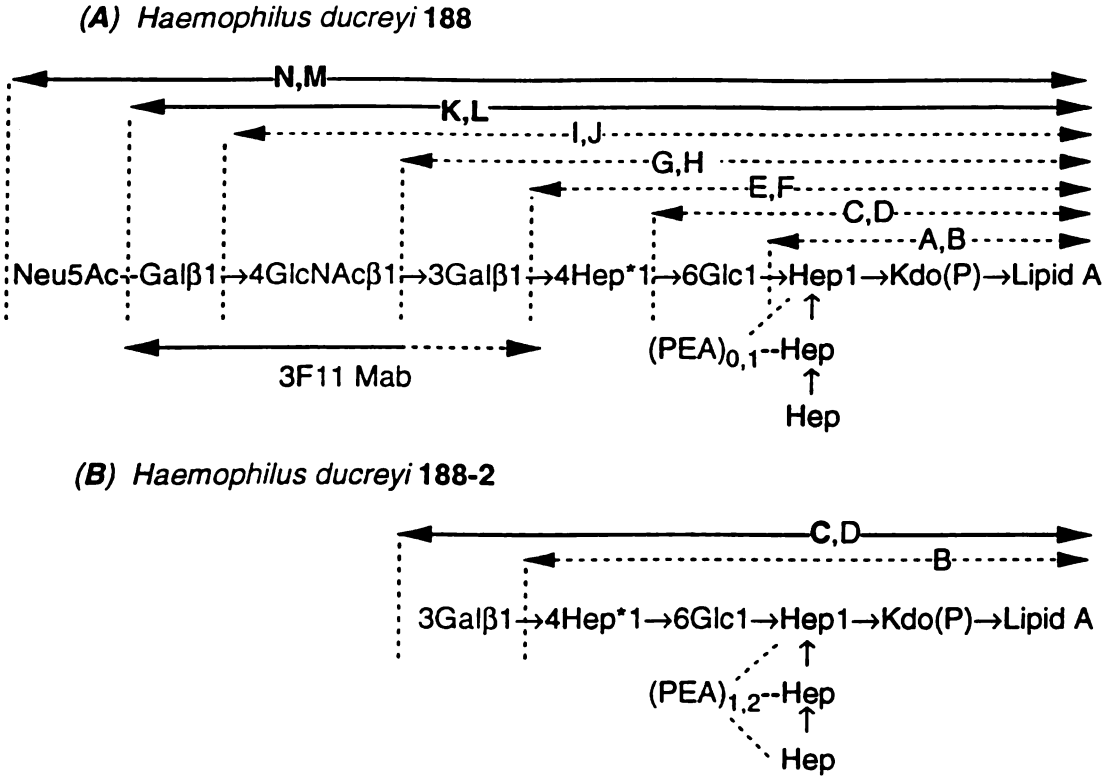

Figure 4.7. Proposed structural differences between the LOS expressed by *H. ducreyi* strain 188 and pyocin-variant, 188-2. Bold lines represent the major LOS species present in each strain. The terminal lactosamine (Galβ1→4GlcNAc) moiety is also indicated for the minimal epitope required for MAb 3F11 binding, which may extend to the 3-linked galactose (Galβ1→4GlcNAcβ1→3Gal) as a further mimicry of the human paragloboside structure, Galβ1→4GlcNAcβ1→3Galβ1→4Glc. In addition to the termination sites in the 188-2 structure shown above, a third LOS variant exists as indicated by ESI-MS data that differs from the major 188-2 LOS C by having three heptose instead of four, suggesting that this variant is capable of synthesizing a Hex_2 branch off the core Hep_3 region which bypasses the branch D-*glycero*-D-*manno*-heptose (Hep*, see above), i.e., Hex-Hex-Hep_3-Kdo-lipid A.

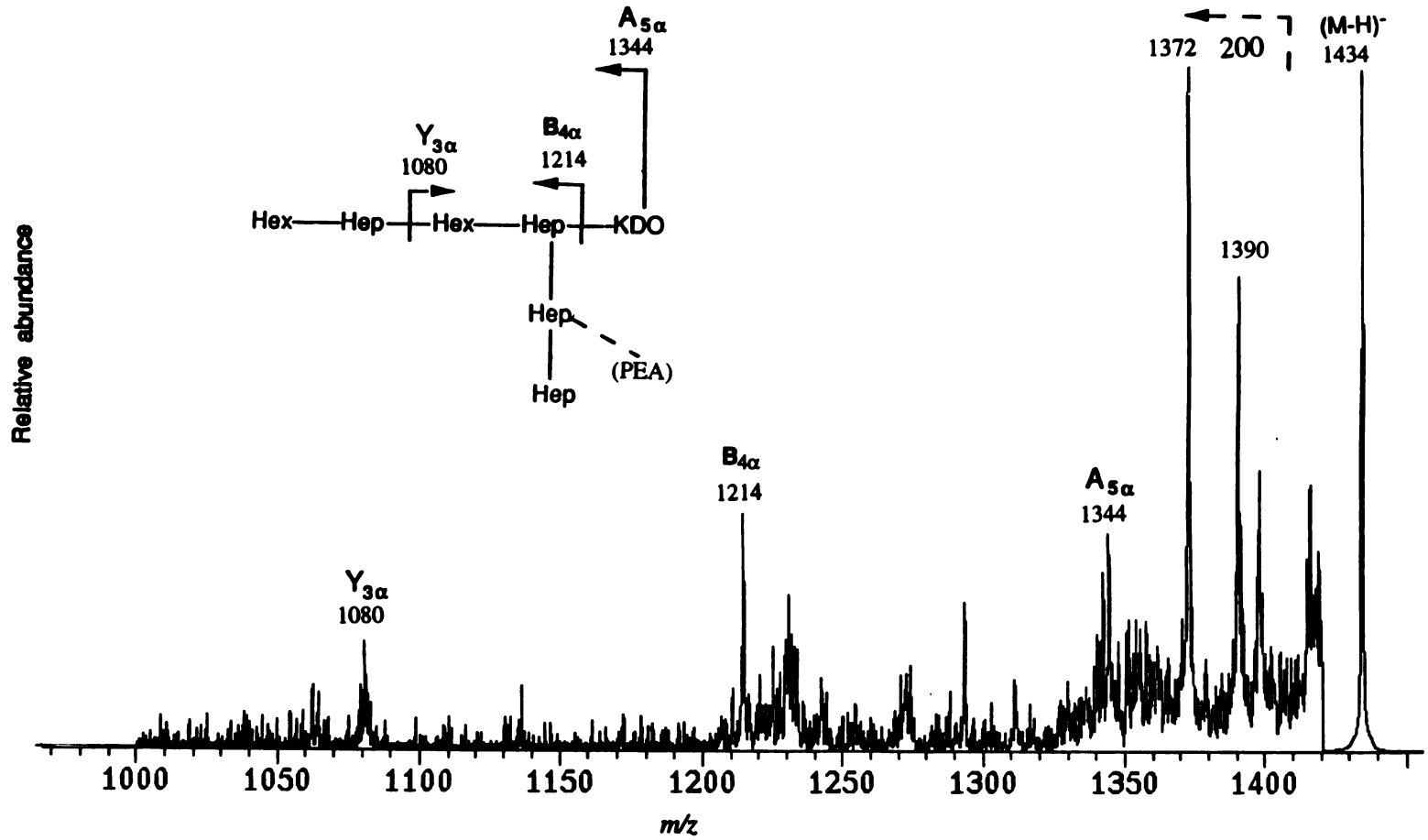

Figure 4.8. MS/MS spectrum of underivatized oligosaccharide from *H. ducreyi* strain 188-2. Only the major peaks have been assigned. The peak at *m/z* 1390 may represent the loss of CO_2 from the molecular ion and the peak at *m/z* 1372 may represent a further loss of H_2O.

the pyocin N survivor also contains at least one PEA group in the core heptose region, and therefore further differs from the parent strain which contains either one or none at all. Composition and methylation analysis of the *H. ducreyi* strain 188-2 also support these interpretations (see Table 4.3). Further structural studies will be needed, however, to fully establish the complete LOS structures present in both the parent and pyocin variant strain.

DISCUSSION

Although the exact mechanism by which pyocin acts remains undefined, previous studies with *N. gonorrhoeae* have suggested that pyocin binds to LOS on the surface of the outer membrane (Morse et al., 1976; Dudas & Apicella, 1988). Moreover, the electrospray mass spectral analysis of the pyocin derived gonococcal LOS variants $1291_{a\text{-}e}$ has shown that pyocins can select for organisms which express a truncated LOS structure (John et al., 1991). In this chapter we have used the same strategy to isolate *H. ducreyi* strain 188-2, a pyocin N survivor, from the parental strain 188. Moreover, repeated passage of strain 188-2 on chocolate agar has not demonstrated any reversion back to the parental LOS phenotype, suggesting that *H. ducreyi* strain 188-2 is stable.

Although there were 11 other colonies which appeared to be resistant to pyocin N, expansion and reselection with pyocin did not produce any survivors (data not shown). The exact explanation for this phenomenon remains obscure, but one possible explanation would be the fastidious clumping nature of *H. ducreyi* (Morse, 1989). The limitations of this technique are such that the ratio of pyocin to bacteria necessary for complete lysis is unknown. It is conceivable that the pyocin may be physically obstructed from attaching to bacteria in the innermost core of a clump and consequently unable to lyse these organisms, however further studies are necessary to support this hypothesis.

Biochemical and mass spectral analyses demonstrated that *H. ducreyi* strain 188-2 assembles a set of truncated LOS structures as compared to the parental strain 188. Mass

spectrometric, composition and linkage studies of this structure revealed that the variant LOS no longer expresses the terminal lactosamine present on the LOS of *H. ducreyi* strain 188. These data were confirmed by the immunologic studies which show that colonies of *H. ducreyi* strain 188-2 have lost reactivity with the MAb 3F11 (Figure 4.3).

The epitope recognized by MAb 3F11 has important pathogenic implications for the success of *N. gonorrhoeae*. Previous studies by Mandrell and colleagues have shown that the epitope recognized by this antibody is identical to that found on the terminal tetrasaccharide of paragloboside, a glycosphingolipid precursor of the major human blood group antigen which terminates in the disaccharide, *N*-acetyllactosamine (Mandrell et al., 1988). Parsons and co-workers have shown that gonococci grown in the presence of cytidine monophosphate-*N*-acetyl neuraminic acid, modify their LOS structure by the addition of *N*-acetyl neuraminic acid (or sialic acid) and consequently become more serum resistant (Parsons et al., 1988). Subsequent studies have demonstrated that the terminal galactose residue of the gonococcal LOS epitopes serve as the acceptor for sialic acid (Mandrell et al., 1992). Immunoelectron microscopic studies of infected urethral exudates have shown the presence of sialylated and non-sialylated LOS moieties during natural gonococcal infection (Apicella et al., 1990).

The LOS assembled by *H. ducreyi* strain 188-2 lacks the terminal trisaccharide present in strain 188. The absence of sialic acid in the LOS preparations of strain 188-2, as compared to the presence of sialic acid detected on *H. ducreyi* strain 188, suggests that the terminal lactosamine structure may serve as the acceptor site for sialylation in this organism. It has been suggested that an important function of the glycosphingolipid-like structures may be in short range attachment to and uptake by human cells (Deal & Krivan, 1990). Indeed, an increasing body of evidence is gathering which indicates that *H. ducreyi* can adhere to and possibly invade human epithelial cells (Lagergård et al., 1993; Lammel et al., 1993). However, we needed to conduct more studies to determine whether the presence of sialic acid on LOS plays a role in this phenomenon.

In summary, we have demonstrated that *H. ducreyi* strains are susceptible to pyocin lysis. We have used pyocin selection to generate a stable *H. ducreyi* variant which assembles a truncated LOS structure when compared to the larger LOS synthesized by the parent strain 188, although the wild-type may also synthesize these shorter LOS as well. We have also seen that the LOS of both wild-type strains examined to date, i.e. strains 188 and 35000 contain sialic acid. The presence of sialic acid in both wild-type strains suggested that we embark on an indepth study of other strains to discover if sialylation is a common theme. If sialylation is found to be conserved among strains, then comparative biological studies could be carried out of the virulence of these strains relative to the variant strain 188-2. Such studies should provide insight into the importance of the role of sialylation in the pathogenesis of genital ulcer disease. These experiments are described in Chapter 5.

CHAPTER 5.

THE LIPOOLIGOSACCHARIDES OF *HAEMOPHILUS DUCREYI* ARE HIGHLY SIALYLATED

INTRODUCTION

As discussed in Chapter 3, one of most distinguishing features of the major oligosaccharide of the LOS from *H. ducreyi* strain 35000 is the presence of non-reducing terminal lactosamine, i.e., Galβ1→4GlcNAc:

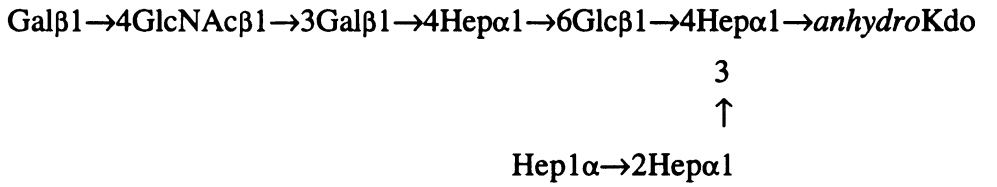

In addition to this major structure, several other glycoforms, whose molecular masses were consistent with the presence of sialic acid, were identified by mass spectrometry. In this chapter, results of our investigation of these potentially sialylated LOS glycoforms are described, as well as studies of several other wild-type strains including 188, NYC23, 233 and 33921. In addition, the pyocin-variant strain 188-2 which was discussed in Chapter 4 will also be considered (Campagnari et al., 1994). Strain NYC 23 is a recent clinical isolate with a low passage history (six passages) and is virulent in both the mouse and rabbit models. It has a type H outer membrane protein (OMP) pattern. Strain 233 was first isolated in New York City in 1985 and has a type D OMP. It has been described in the literature as virulent and preliminary data from our collaborators show its LOS to contain sialic acid. Strain 33921 is a Kenyan strain that does not bind the MAbs 3F11 or 06B4, but binds strongly to MAb 4C8. It is from a geographical region where chancroid is

currently endemic. It has a type F OMP pattern and its LOS banding pattern as observed by SDS-PAGE is much simpler than those of the other strains tested (Campagnari et al., 1990).

It is clear from electrophoretic studies that the LOS from many *H. ducreyi* strains exhibit considerable heterogeneity (Campagnari et al., 1990). To understand pathogenic processes such as phase variation and molecular mimicry it was necessary to assess the exact chemical nature of this heterogenity. To accomplish this, the LOS were first *O*-deacylated under mild hydrazine conditions to remove *O*-linked esters from the lipid A portion. The *O*-deacylated LOS were then analysed by electrospray ionization-mass spectrometry (ESI-MS). The advantage to this method is that we are able to examine a relatively intact LOS form. The traditional method for analysing LOS structure involves acid hydrolysis to separate the oligosaccharide from the lipid A. Such an approach causes chemical degradation of the molecule and chemically labile moieties such as sialic acid are lost in the process. ESI-MS allows us to assess overall LOS heterogeneity and to identify the different glycoforms present (Gibson et al., 1993). One potential disadvantage to this technique is that *O*-acetyl groups, if present on the oligosaccharide, will also be removed. However, to date we have not observed *O*-acetyl groups in the LOS from *H. ducreyi*, unlike their common occurrence in *N. gonorrhoeae* and *N. meningitidis* LOS.

In general, the glycoforms are truncated or elongated analogs (some of which contain sialic acid) of the major oligosaccharide species. In this chapter, I will discuss our results of the analyses of the LOS from six different strains of *H. ducreyi*, four of which are suspected from immunochemical data to contain sialic acid and terminal lactosamine (Campagnari unpublished results). Since lactosamine is thought to be the acceptor for sialic acid, one intriguing question we wished to examine was whether those strains whose LOS possess lactosamine also contain sialic acid and whether those strains whose LOS do not contain lactosamine lack sialic acid.

Of considerable biological interest are the possible roles sialic acid present on LOS play in the pathology of chancroid. Lipooligosaccharides consist of a lipid region which is embedded in the outer membrane of the bacterium, and an oligosaccharide region which projects out into the environment of the bacterial cell. The fact that sialic acid appears on exposed parts of the cell and has a negative charge at physiological pH (pKa of sialic acid is ≈ 2) suggests that it may play a crucial role in cellular functions. Indeed, it has been shown that removal of sialic acid either enzymatically or chemically results in dramatic differences in the behaviour of cells and molecules (Schauer, 1985). Recent results reveal that LOS sialylation decreases the adhesion of meningococci and gonococci to human neutrophils and their subsequent phagocytosis by these immune cells (Estabrook et al., 1992; Rest & Frangipane, 1992). It has also been shown that when gonococci are grown in the presence of CMP-*N*-acetylneuraminic acid (CMP-NANA), they incorporate sialic acid in a 4.5 kDa LOS component which is the same component recognized by the 3F11 monoclonal antibody raised against the LOS of gonococci (Parsons et al., 1988). The 3F11 monoclonal antibody no longer binds the sialylated component, but the binding can be restored by treating the LOS with neuraminidase (Mandrell et al., 1990). These results suggest that sialic acid may play a role in allowing gonococci to evade the host defenses. The aim of this current study is to analyse the LOS of various strains of *H. ducreyi* in order to quantify the extent of sialylation. These data should allow us to plan future studies whose purpose would be to seek to relate the presence of sialic acid on LOS of *H. ducreyi* to specific biological functions.

EXPERIMENTAL

Materials. Glucose, galactose, glucosamine, galactosamine, Kdo, neuraminidase (from *Clostridium perfrigens*) and anhydrous hydrazine were all obtained from Sigma (St. Louis, MO). Aqueous HF (48%) was purchased from Mallinckrodt (Muskegon, MI) and sodium

borodeuteride (98% D) from Aldrich. Acetonitrile, water and methanol were obtained from Burdick and Jackson (Muskegon, MI). Acetic anhydride was purchased from Supelco (Bellefonte, PA), methyliodide from Fluka (Switzerland) and the standard test mixture of partially methylated alditol acetates from Biocarb (Lund, Sweden). All other reagents and solvents used were of reagent grade.

Isolation and purification of LOS. The LOS from *H. ducreyi* strains 35000, 188, 233, NYC23, 188-2 and 33921 were isolated using a modified phenol/water extraction procedure (Westphal & Jahn, 1965) as previously described in Chapter 2.

O-deacylation of LOS. For mass spectrometric analysis, ≈ 1-2 mg of LOS from strains 35000, 188, 233, NYC23, 188-2 and 33921 were *O*-deacylated by treatment with 200 µl anhydrous hydrazine for 20 min at 37°C as described in Chapter 2.

Neuraminidase Treatment of O-deacylated LOS. Portions of the *O*-deacylated LOS samples (≈50 µg) were treated with 50 milliunits of neuraminidase (Sigma Type VI) in 50 µL of PBS, pH 6.0, for 2 h at 37°C. The enzyme digests were desalted by microdialysis against H_2O (Pierce, microdialyser system 500) using a 1000 MW cutoff membrane (Spectra/Por). The retentates were lyophilized and later redissolved in H_2O for mass spectral analyses

Isolation and purification of oligosaccharide fraction. LOS from *H. ducreyi* strains 35000, 188, NYC23, 233, 188-2 and 33921 were isolated and purified as described in Chapter 2. Most of the resulting oligosaccharide fractions were purified on two Bio-Gel P-4 columns but in some cases an alternate gel filtration high performance liquid chromatography (HPLC) system was employed consisting of a Waters 6000A HPLC pump and two 600 x 7.5 mm Bio-Sil TSK-125 columns (BioRad) connected in series. Samples were eluted in 50 mM pyridinium acetate (pH 5.2) at a flow rate of 1 ml min^{-1}. Fractions were collected in 0.5-1 ml volumes.

Composition Analysis. Saccharide composition analysis was performed using small aliquots of the oligosaccharide fractions (≈10-20 μg) and standard conditions; 2 M trifluoroacetic acid for 3 h at 100°C as described earlier (Phillips et al., 1990). Phosphate and phosphoesters were removed using 48% aqueous HF as described in Chapter 2.

Sialylation Analysis. The molar amount of sialic acid was determined by treatment with *Clostridium perfrigens* neuraminidase. First, the weight purity of the LOS samples was determined by assaying for glucosamine content (assuming 3 moles of glucosamine per mole of LOS for strains 35000, 233, NYC23, 188 and 33921 and 2 moles of glucosamine per mole of LOS for the pyocin-variant strain 188-2). To accomplish this, weighed quantities of LOS (≈300 μg) were hydrolyzed in 400 μl of 6N HCl for 4 h, and the resulting glucosamine was analyzed by HPAEC as previously described (Phillips et al., 1990). For sialic acid quantitation similar weighed amounts of LOS (≈300 μg) were treated with *C. perfrigens* neuraminidase (2 mU) or heat inactivated neuraminidase (inactivated by heating at 100°C for 30 min) in a buffer containing 25 mM sodium acetate (pH 6.8) at 37 °C. A second 2 mU aliquot of neuraminidase was added after 2 h and again incubated for an additional 2 h, after which the sample was dried, dissolved in water and passed through a Sep-Pak C18 cartridge (Waters Assoc.) to remove neuraminidase and LOS. Sialic acid was then quantified by HPAEC followed by pulsed amperometric detection using an isocratic elution buffer (380 mM NaOH) at a flow rate of 1 ml/min. Sialic acid eluted after ≈7.8 min.

Methylation analysis. Linkage analysis was performed on purified oligosaccharide using a modification of the microscale method of Levery and Hakomori (Levery & Hakomori, 1987). The resulting PMAAs were analyzed by GC/MS using a VG70SE mass spectrometer as described in Chapter 2.

Mass spectrometric analysis. Underivatized oligosaccharides were directly analyzed by liquid secondary ion mass spectrometry (LSIMS) as described in detail in Chapter 2. For the analysis of *O*-deacylated LOS, either a Platform instrument or a VG/Fison Bio-Q

triple quadrupole mass spectrometer was used in the negative-ion electrospray sampling mode. The LOS samples were analysed as described elsewhere (Gibson et al., 1993).

Cultured human keratinocytes cytotoxicity assay. Briefly, after circumcision, foreskins obtained from the neonatal nursery at Children's Hospital, Buffalo, N.Y. were placed in keratinocyte-serum free medium (K-SFM) with 5 mg/ml of gentamycin (GIBCO). The foreskins were then rinsed in a solution of PBS containing 20 mg/ml of gentamycin, without calcium or magnesium. The tissue specimens were then placed in the caseinolytic agent Dispase (Collaborative Research), mixed 1:1 with Hank's Balanced Salt Solution (GIBCO) and 5 mg/ml of gentamycin at 4°C for 18 hours. After this incubation, the epidermal layer was lifted off and placed in a sterile test tube with 2 ml of trypsin-EDTA (GIBCO). The tissue was incubated for 20-30 minutes at 37°C during which time it was aspirated every 5-7 minutes to dissociate the cells. The action of trypsin was stopped using soybean trypsin inhibitor (GIBCO) at a final concentration of 10 mg/ml. The cells were spun at 500 rpm for 10 min, gently resuspended in keratinocyte-serum free medium containing bovine pituitary extract and recombinant epidermal growth factor and viability was determined using trypan blue exclusion. These were then seeded into 24 well tissue culture plates at a density of $2x10^5$ cells/ml.

The cytotoxicity assay is a modification of the method described by Purven (Purven & Lagergård, 1992). Briefly, 24 well plates were seeded with $2x10^5$ keratinocytes/well in K-SFM as described above. The cells were allowed to form confluent monolayers for 4-5 days and the media was changed every 2 days. LOS was suspended in the K-SFM and sonicated. The media was aspirated from the wells of the keratinocytes, and LOS was added to triplicate wells in final concentrations of 0.2 ng, 2 ng, 20 ng, 200 ng, 2 μg, 20 μg, and 200 μg. The wells were monitored by an inverted microscope at 1-2 h for morphologic changes and detachment. After 4 h the cells were removed from the wells and centrifuged. Both trypan blue and 3-(4,5-dimethylthiazol-2-yl)-2,5-diphenyl-2H-tetrazolium bromide were used to determine viability as previously described by Mossman

(Mossman, 1983). The cells exposed to trypan blue were counted on a hemocytometer and viability was calculated by comparing live to dead cells. Control cells were treated exactly the same, without exposure to LOS.

Cultured human keratinocytes adhesion assay. To characterize the attachment of *H. ducreyi* to human keratinocytes, a modification of a previously described procedure by Shaw and Falkow (Shaw & Falkow, 1988) was used. Briefly, the keratinocyte monolayers became confluent in ≈ 4-5 days. Prior to the introduction of bacteria, the media was changed 6-8 times with keratinocyte-serum free medium without antibiotics. During these washing steps, the bacteria were prepared as follows: dual broth cultures were inoculated with *H. ducreyi* strain and the flasks were placed in a shaker water bath at 35°C. The optical density at 660 nm was measured until the organisms reach mid-log phase. Past studies have determined that this takes approximately 2 h (Campagnari et al., 1991). Once the organisms were at the proper growth phase, the cultures were centrifuged and the bacterial pellets were washed in K-SFM without antibiotics. Based on previous adherence studies, the *H. ducreyi* were suspended to an optical density of 0.2 at 660 nm which should yield $\approx 10^8$ cfu/ml. Serial dilutions used in the adherence assays were plated out to confirm the colony counts.

The plates containing the washed monolayers were then removed from the incubator and any remaining media was discarded. The bacterial suspensions were inoculated into the monolayers in a total volume of 200 ml, or 2-5 x 10^6 cfu/well of keratinocytes. Each bacterial suspension was inoculated in triplicate wells. The plates were incubated at 35°C in 5% CO_2 for 2 h. Aliquots of the *H. ducreyi* suspensions used to infect the monolayers were serially diluted and plated on chocolate agar to provide an accurate count of the actual inoculation. After the incubation period, all the wells were washed and 2 mM EDTA added to half of the wells to remove the keratinocytes. The cells were washed and an aliquot was fixed in 2% glutaraldehyde and 0.1 mM cacodylic buffer for Nomarksy and electron microscopic studies. The remainder of the keratinocytes were

plated out in serial 10x dilutions on chocolate agar plates in triplicate. The plates were incubated at 35°C in 5% CO_2 and counts were determined after 48 h.

RESULTS

In Chapter 3 we determined the complete structure of the major oligosaccharide from strain 35000. In Chapter 4 we presented structural information on the oligosaccharides from the wild-type strain 188 and its pyocin variant 188-2. LSIMS, compositional and methylation analyses data on these strains are included here for comparison purposes.

Analysis of Oligosaccharide Fractions. Gel permeation chromatography of the oligosaccharide fractions from all of the wild-type strains (except strain 33921), followed by LSIMS analysis revealed a single major species with a deprotonated molecular ion, $(M-H)^-$, at *m/z* 1676.5 (M_r 1677.5). When the oligosaccharides were treated with aqueous HF and reanalysed by LSIMS their masses did not change, demonstrating that phosphate and phosphoethanolamine were not present. The LSIMS spectrum of the oligosaccharide from the pyocin variant, strain 188-2, showed a smaller oligosaccharide with a deprotonated molecular ion at *m/z* 1434.5. Treatment of this oligosaccharide with HF to remove phosphoesters shifted the molecular ion to *m/z* 1311, indicating that phosphoethanolamine had been lost (Campagnari et al., 1994) (see also Chapter 4). The LSIMS spectrum of the oligosaccharide of strain 33921 had a molecular ion at *m/z* 1322.4 which corresponds to a much smaller oligosaccharide than those of the other wild-type strains. In the LSIMS spectrum of the oligosaccharide from strain 33921 there are also ions present corresponding to loss of HexNAc, loss of HexNAc-Hex and loss of HexNAc-Hex-Hex. Limited sequence information is also available from fragmentation evident in the LSIMS spectra of each of the other strains (data not shown).

Composition analysis of the major oligosaccharide from each strain using HPAEC-PAD identified glucose, galactose, glucosamine and L-*glycero*-D-*manno*-heptose in the

molar ratios shown in Table 5.1. In the HPAEC profile of strains 35000, NYC23, 188 and 188-2 a peak was observed eluting just before the peak for heptose. This peak has been identified as D-*glycero*-D-*manno*-heptose based on earlier data (Melaugh et al., 1992). During the mild acid hydrolysis required to separate the oligosaccharide moiety from lipid A a phosphate on the C-4 position of Kdo undergoes β-elimination resulting in an *anhydro*Kdo form that is not seen in the composition analysis.

To identify the monosaccharides and their linkages, methylation analysis of the major oligosaccharide from each strain was performed. The PMAAs were analysed by GC/MS in both electron impact and chemical ionization modes. As can be seen from Table 5.2 linkage analyses of strains 35000, NYC23, 233 and 188 gave eight major sugars which eluted in the following order: terminal Gal, 3-Gal, 6-Glc, terminal Hep, 4-Hep, 2-Hep, 3,4-Hep and 4-GlcNAc. Methylation analysis of strain 188-2 shows that this pyocin variant lacks the 3-Gal and 4-GlcNAc seen in the wild-type strains. Strain 33921 has the same core sugars as the other strains and a branch consisting of 4-Glc, 3-Gal and a terminal GlcNAc (Table 5.2).

We have already established the complete structure, including anomeric configurations, of the oligosaccharide from strain 35000. Given the similarities in the LSIMS, compositional and methylation analyses data obtained for strains 35000, 233, 188 and NYC23, it appears likely that all four strains exhibit the major oligosaccharide structure previously determined for strain 35000 (see Chapter 3). The major oligosaccharide of strain 188-2 which is a pyocin variant of the wild-type strain 188 lacks the terminal lactosamine present in the wild-type structure and contains a PEA most likely located in the inner core region (Fig. 5.1) (Campagnari et al., 1994) (see also Chapter 4).

The oligosaccharide of the Kenyan strain 33921 appears to possess the same common core region (Hep_3 Kdo) seen in the above structures while the carbohydrate branch contains only three sugars, terminal GlcNAc, 4-Glc and 3-Gal whose relative positions in the chain have not been determined. This strain also lacks the terminal

Table 5.1. ***Oligosaccharide Composition Analysis***

	Composition Analysis[a](mole ratio relative to Glucose)				
Strain	Galactose	Glucose	Heptose	Heptose[b]	$GlcNH_2$
35000	2.5	1.0	2.7	0.8	1.1
NYC23	2.6	1.0	2.7	0.8	1.1
233	2.0	1.0	3.3	---[c]	0.7
188	1.5	1.0	2.0	1.1	0.8
188-2	0.8	1.0	2.8	0.1	---
33921	1.3	1.0	2.9	---	1.0

[a] Kdo was not detected in the hydrolyzed oligosaccharide fraction due to its conversion to *anhydro*Kdo forms during acetic acid hydrolysis of LOS.

[b] This second heptose has been tentatively identified as D-*glycero*-D-*manno*-heptose based on earlier data (Chapter 2), as opposed to the major core heptoses which are L-*glycero*-D-*manno*-heptoses.

[c] The unusual D-*glycero*-D-*manno*-heptose was not found in the compositional analysis even though it was clearly present in the methylation analysis data.

Table 5.2. ***Oligosaccharide Methylation Analysis***

	Methylation Analysis[a] (relative peak area)							
Strain	t-Gal	3-Gal	6-Glc	t-Hep	2-Hep	3,4-Hep	4-Hep	4-GlcNAc
35000	1.0	1.5	1.7	0.7	0.9	0.7	0.6	1.8
NYC23	1.0	0.7	1.7	0.5	0.6	0.4	0.7	1.0
233	1.0	0.3	1.7	0.5	0.5	0.2	0.6	1.0
188	1.0	0.6	1.8	0.5	0.7	0.3	0.6	1.1
188-2	1.0	---	1.5	0.3/1.3[b]	1.3	0.4	---	---
Strain	4-Glc	3-Gal	6-Glc	t-Hep	2-Hep	3,4-Hep	4-Hep	t-GlcNAc
33921	1.0	0.7	---	0.5	0.7	0.5	---	0.9

[a] Partially methylated alditol acetates are abbreviated according to their substitution pattern as follows: terminal-galactose is 1,5-di-*O*-acetyl-2,3,4,6-tetra-*O*-methylgalactitol, 3-linked galactose is 1,3,5-tri-*O*-acetyl-2,4,6-tri-*O*-methylgalactitol, etc.

[b] Two terminal heptoses were found, the ratio stated is the unusual D-*glycero*-D-*manno*-heptose to the expected terminal core L-*glycero*-D-*manno*-heptose.

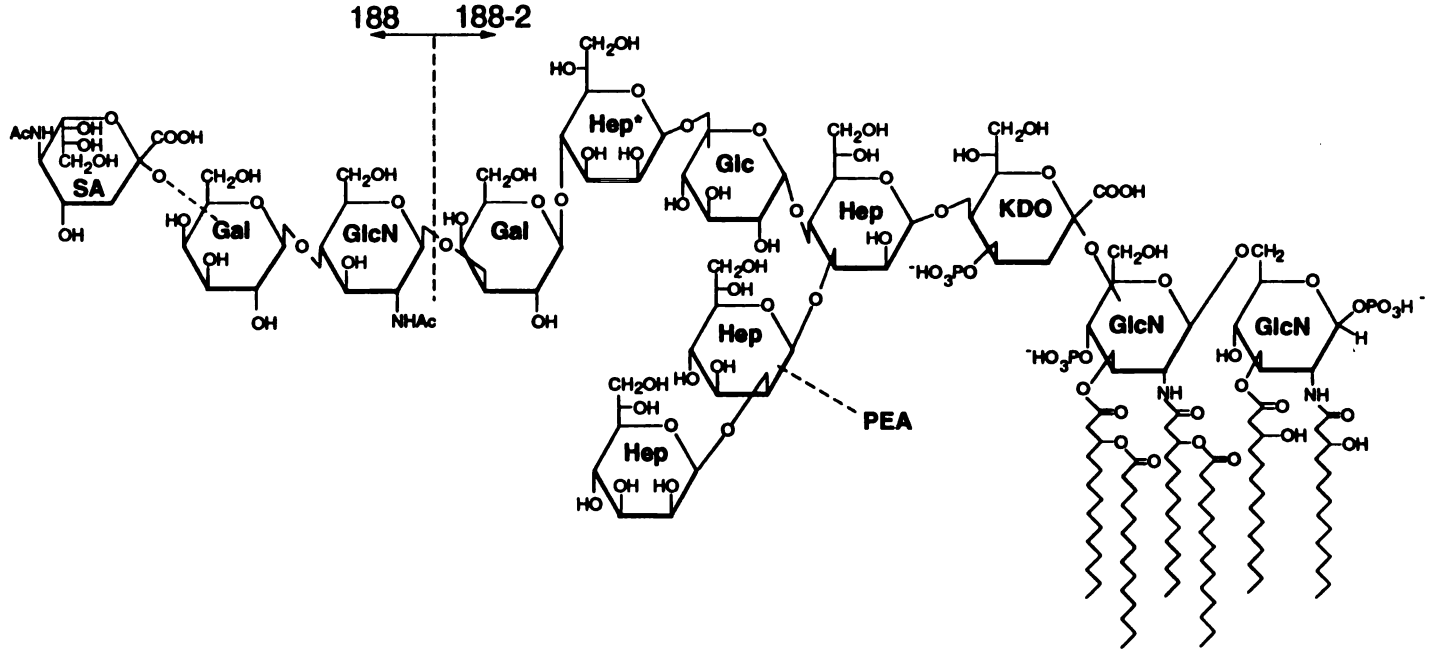

Figure 5.1. Proposed structures of LOS from *H. ducreyi* strains 188 and 188-2. Strain 188-2 lacks the terminal lactosamine evident on the wild type strain which is presumably the receptor for sialylation.

lactosamine and the 4-Hep evident in the other wild-type strains. Based on immunochemical data that show strong preferential binding to the 4C8 MAb, specific for *N. gonorrhoeae* 1291a, (personal communication from Dr. Campagnari), the terminal trisaccharide in this strain is most probably GlcNAcβ1→3Galβ1→4Glcβ1 (Fig. 5.2).

Analysis of O-deacylated LOS. SDS-PAGE analyses of the LOS from the six strains of *H. ducreyi* indicate that there are several LOS forms present in the crude LOS preparations from these strains (data not shown). After neuraminidase treatment the disappearance of some of these bands indicates that they represent sialylated analogs of the major oligosaccharides previously described. In order to determine what additional structures are present and what relationship they bear to the major oligosaccharides detected in LSIMS, a mass spectrometric study employing electrospray mass spectrometry was conducted to better assess overall LOS heterogeneity.

Fig. 5.3a shows the ESI-MS spectrum of *O*-deacylated LOS from *H. ducreyi* strain 35000 before neuraminidase treatment. The most abundant ion is the triply charged species $(M-3H)^{3-}$ at *m/z* 902.8 which corresponds to an average M_r of 2711.4 and the generic composition shown in Table 5.3. The remaining triply charged ions at *m/z* 848.6, 943.9, 970.3 1000.0 and 1041.4 represent major oligosaccharide species whose average molecular weights and structures are listed in Table 5.3. Those peaks which represent sialylated analogs are shaded. The weak peak marked with an asterisk represents the addition of lactosamine to the major species. Corresponding doubly charged ions are seen in the mass region *m/z* 1250 to 1550. Fig. 5.3b shows the mass spectrum of *O*-deacylated LOS from the same strain after neuraminidase treatment. The shaded peaks at *m/z* 1000.0, 1041.4 and 1500.3 corresponding to the sialylated analogs listed in Table 5.3 have now disappeared and the peak marked with an asterisk has increased in relative ion abundance.

Fig. 5.4a shows the ESI-MS spectrum of *O*-deacylated LOS from *H. ducreyi* strain 233 before neuraminidase treatment. The spectrum is very similar to that of Fig. 5.3a except that LOS component D is absent and the base peak is now the sialylated analog of

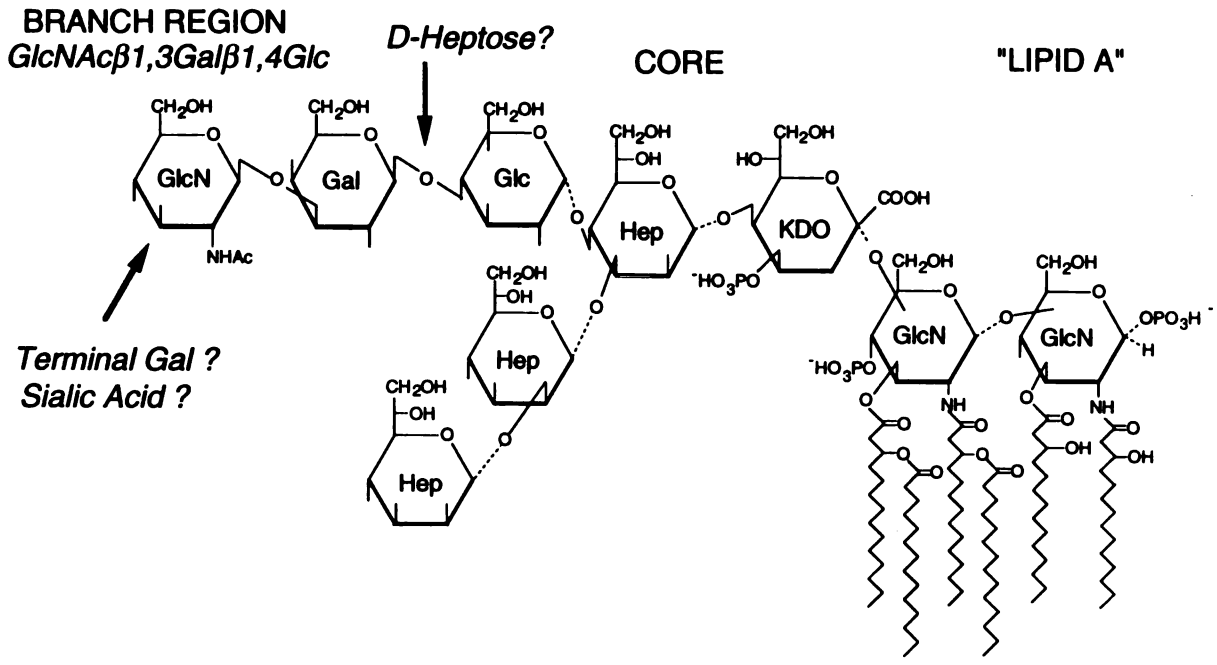

Figure 5.2. Proposed structure of LOS from *H. ducreyi* strain 33921. The structure of the branch region is based on immunochemical data that indicate strong binding to the 4C8 MAb which is specific for *N. gonorrhoeae* strain 1291_a (see text).

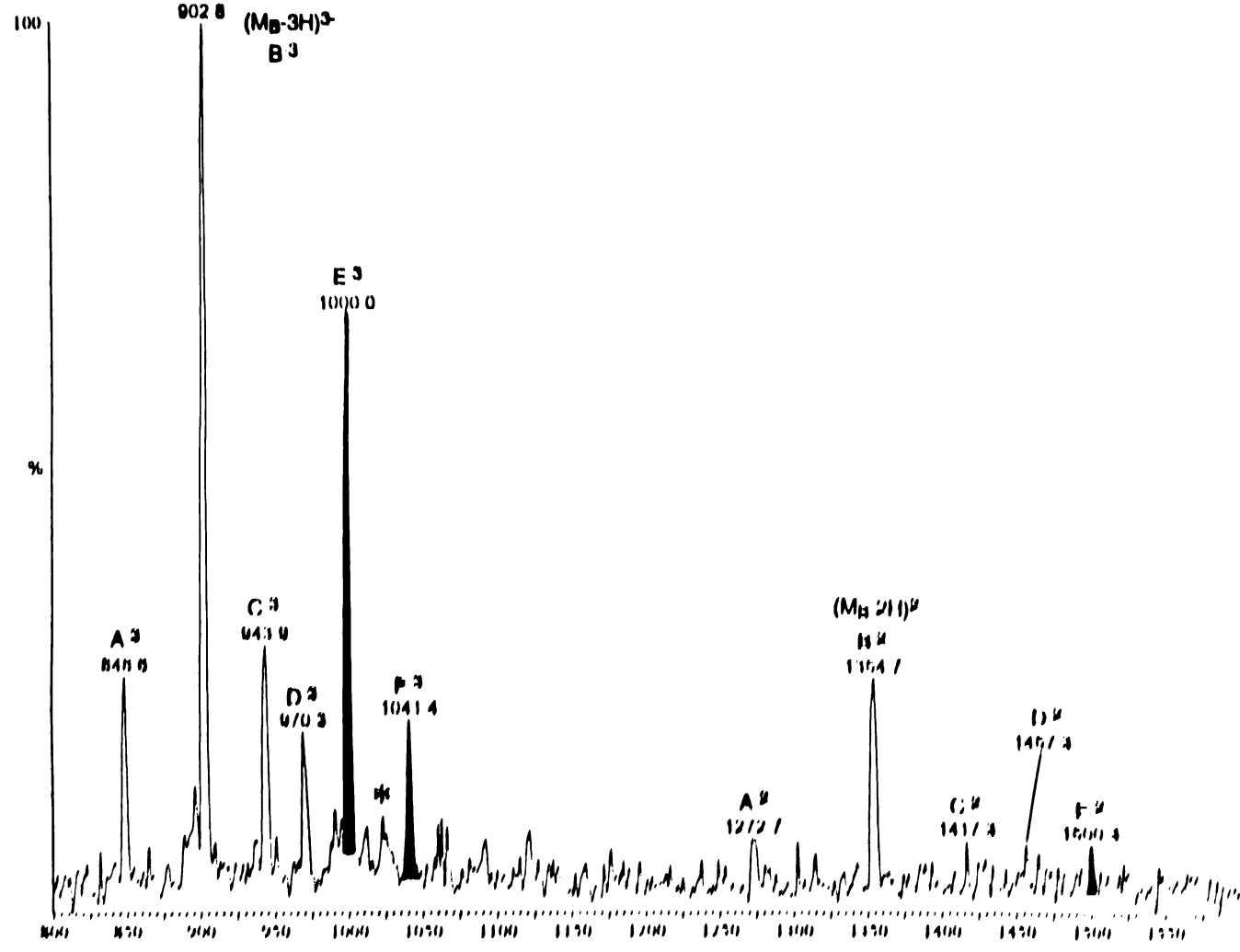

Figure 5.3. (a) Partial negative ion electrospray mass spectrum of O-desulfated LOS from *N. gonorrhoeae* strain 35000 before neuraminidase treatment. The shaded peaks represent sialylated analogues. The weak peak marked with an asterisk represents the addition of hexosamine to the major species.

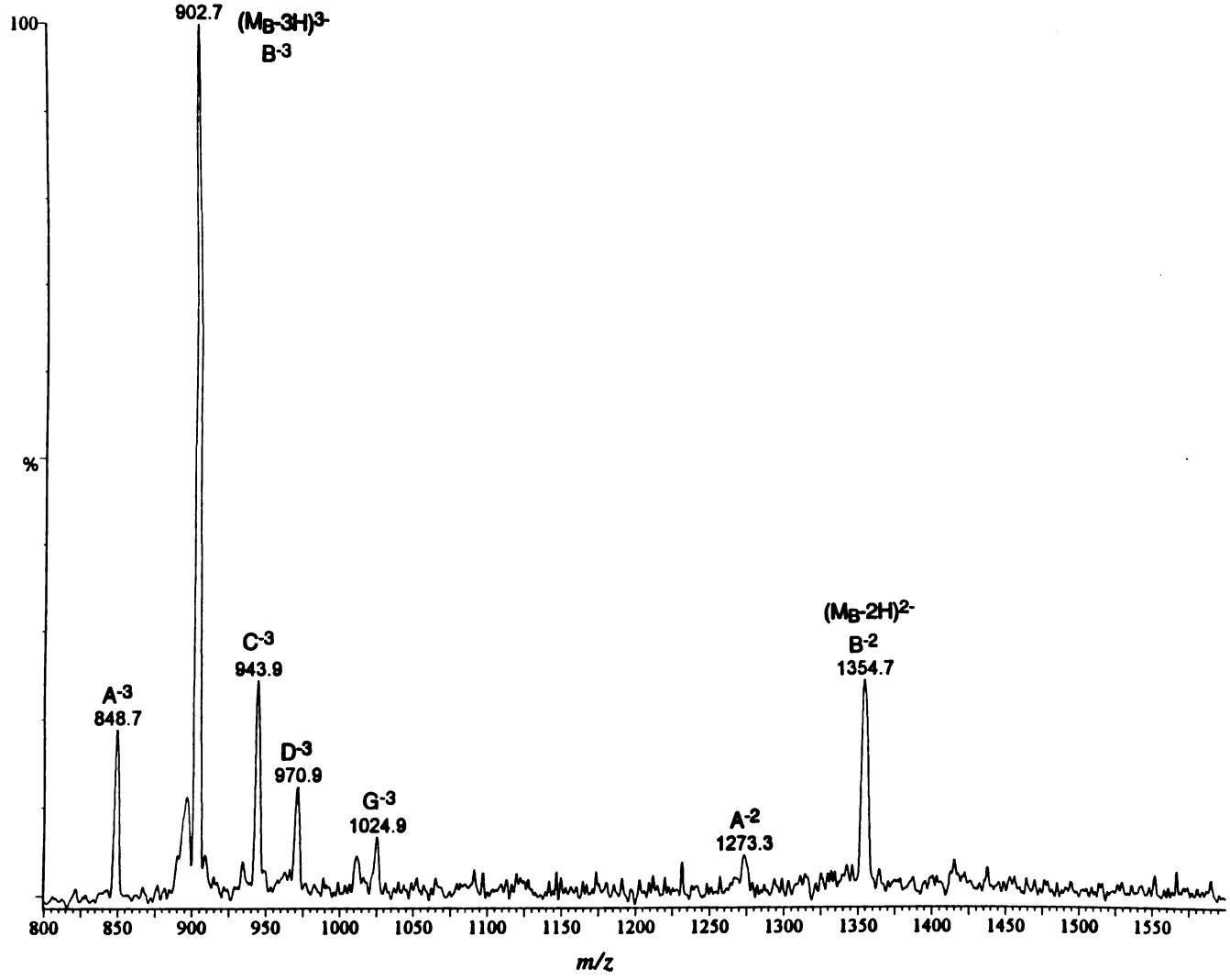

Figure 5.3. (b) Partial negative-ion electrospray mass spectrum of *O*-deacylated LOS from *H. ducreyi* strain 35000 after neuraminidase treatment.

Table 5.3. ***ESI-MS Analyses of O-deacylated LOS***[a]

M_r Observed[b]	M_r Calculated	Relative Abundance	Proposed Composition
		Haemophilus ducreyi Strain 35000	
(A) = 2548.8	2549.3	25	Hex_2 Hep_4 HexNAc Kdo(P) lipid A[c]
(B) = 2711.4	2711.5	100	Hex_3 Hep_4 HexNAc Kdo(P) lipid A
(C) = 2834.7	2834.5	27	Hex_3 Hep_4 PEA HexNAc Kdo(P) lipid A
(D) = 2913.9	2914.7	18	Hex_3 Hep_4 $HexNAc_2$ Kdo(P) lipid A
(E) = 3003.0	3002.7	66	Hex_3 Hep_4 HexNAc Neu5Ac Kdo(P) lipid A
(F) = 3127.2	3125.7	20	Hex_3 Hep_4 PEA HexNAc Neu5Ac Kdo(P) lipid A
		Haemophilus ducreyi Strain 233	
(A) = 2549.1	2549.3	24	Hex_2 Hep_4 HexNAc Kdo(P) lipid A
(B) = 2711.7	2711.5	92	Hex_3 Hep_4 HexNAc Kdo(P) lipid A
(C) = 2834.7	2834.5	41	Hex_3 Hep_4 PEA HexNAc Kdo(P) lipid A
(E) = 3003.3	3002.7	100	Hex_3 Hep_4 HexNAc Neu5Ac Kdo(P) lipid A
(F) = 3126.0	3125.7	47	Hex_3 Hep_4 PEA HexNAc Neu5Ac Kdo(P) lipid A

(continued on following page)

Table 5.3. ***ESI-MS Analyses of O-deacylated LOS*** [a] **(continued)**

M_r Observed[b]	M_r Calculated	Relative Abundance	Proposed Composition
		Haemophilus ducreyi Strain NYC23	
2342.7	2346.1	10	Hex_2 Hep_4 Kdo(P) lipid A[c]
2470.2	2469.2	9	Hex_2 Hep_4 PEA Kdo(P) lipid A
2548.2	2549.3	60	Hex_2 Hep_4 HexNAc Kdo(P) lipid A
2670.0	2672.4	44	Hex_2 Hep_4 PEA HexNAc Kdo(P) lipid A
2711.4	2711.5	58	Hex_3 Hep_4 HexNAc Kdo(P) lipid A
2835.3	2834.5	57	Hex_3 Hep_4 PEA HexNAc Kdo(P) lipid A
3001.5	3002.7	72	Hex_3 Hep_4 HexNAc Neu5Ac Kdo(P) lipid A
3125.7	3125.7	100	Hex_3 Hep_4 PEA HexNAc Neu5Ac Kdo(P) lipid A
		Haemophilus ducreyi Strain 33921	
2357.4	2357.1	72	Hex_2 Hep_3 HexNAc Kdo(P) lipid A
2480.4	2480.2	100	Hex_2 Hep_3 PEA HexNAc Kdo(P) lipid A
2602.8	2603.3	49	Hex_2 Hep_3 PEA_2 HexNAc Kdo(P) lipid A

[a] ESI-MS data for strains 188 and 188-2 are shown in Table 4.2.

[b] All molecular weights are reported as their average mass values based on the triply charged ions.

[c] After O-deacylation, the lipid A moiety is converted into diphosphoryl diacyl lipid A containing two *N*-linked β-hydroxymyristic acid chains with an average M_r of 953.0089.

the major species. Peaks representing sialylated analogs are again shaded. Fig. 5.4b shows the same spectrum after neuraminidase treatment. The shaded peaks are now missing.

The ESI-MS spectra of *O*-deacylated LOS from *H. ducreyi* strains 188 and NYC23 are similar to those of strains 35000 and 233 with the difference that the two former strains are much more heterogeneous and exhibit a greater degree of phosphorylation, as determined from their masses (Tables 4.2 and 5.3).

The ESI-MS spectrum of *O*-deacylated LOS from *H. ducreyi* strain 188-2 has a triply charged base peak at *m/z* 822.3 which corresponds to a M_r of 2469.5 and likely represents the same major structure seen in the other strains minus the terminal lactosamine with the addition of a phosphoethanolamine moiety. No sialylation of the major oligosaccharide species is evident (Campagnari et al., 1994) (see also Chapter 4).

The ESI-MS spectrum of *O*-deacylated LOS from *H. ducreyi* strain 33921 shows little similarity to the spectra obtained from the LOS of the other strains. The major ion in this spectrum is the triply charged ion seen at *m/z* 825.8 and corresponds to a species containing Hex_2 Hep_3 PEA HexNAc Kdo(P) lipid A. The peak at *m/z* 784.8 corresponds to an LOS species that is missing the PEA and the peak at *m/z* 866.6 corresponds to an LOS species containing an extra PEA. There is no evidence of an LOS species containing sialic acid in this spectrum.

Sialic Acid Content of LOS. In order to quantify the extent of sialyation of the LOS of these six strains compositional anaylses of the various LOS were performed. In these experiments, LOS samples were treated exhaustively with *Clostridium perfringens* neuraminidase and the released amount of sialic acid measured by high pH anion exchange chromatography (HPAEC) with pulsed amperometric detection. Figure 5.5 shows the HPAEC chromatogram of the LOS from *H. ducreyi* strain 35000 incubated with (a) neuraminidase and (b) heat-inactivated neuraminidase. Sialyllactose (Neu5Acα2→3Galβ1→4Glc) was used as a control and sialic acid eluted at 7.8 min. The

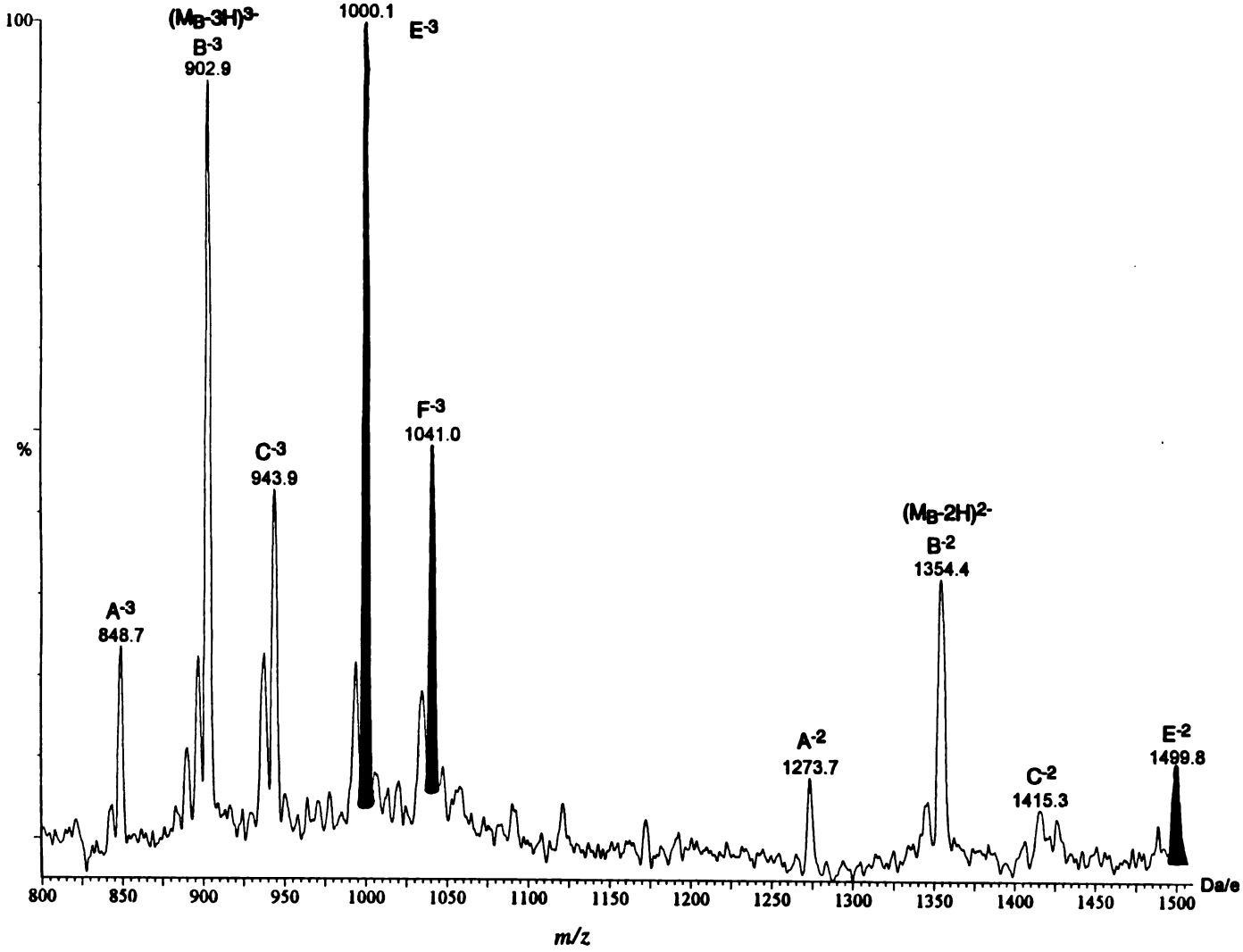

Figure 5.4. (a) Partial negative-ion electrospray mass spectrum of *O*-deacylated LOS from strain 233 before neuraminidase treatment. The shaded peaks represent sialylated analogs.

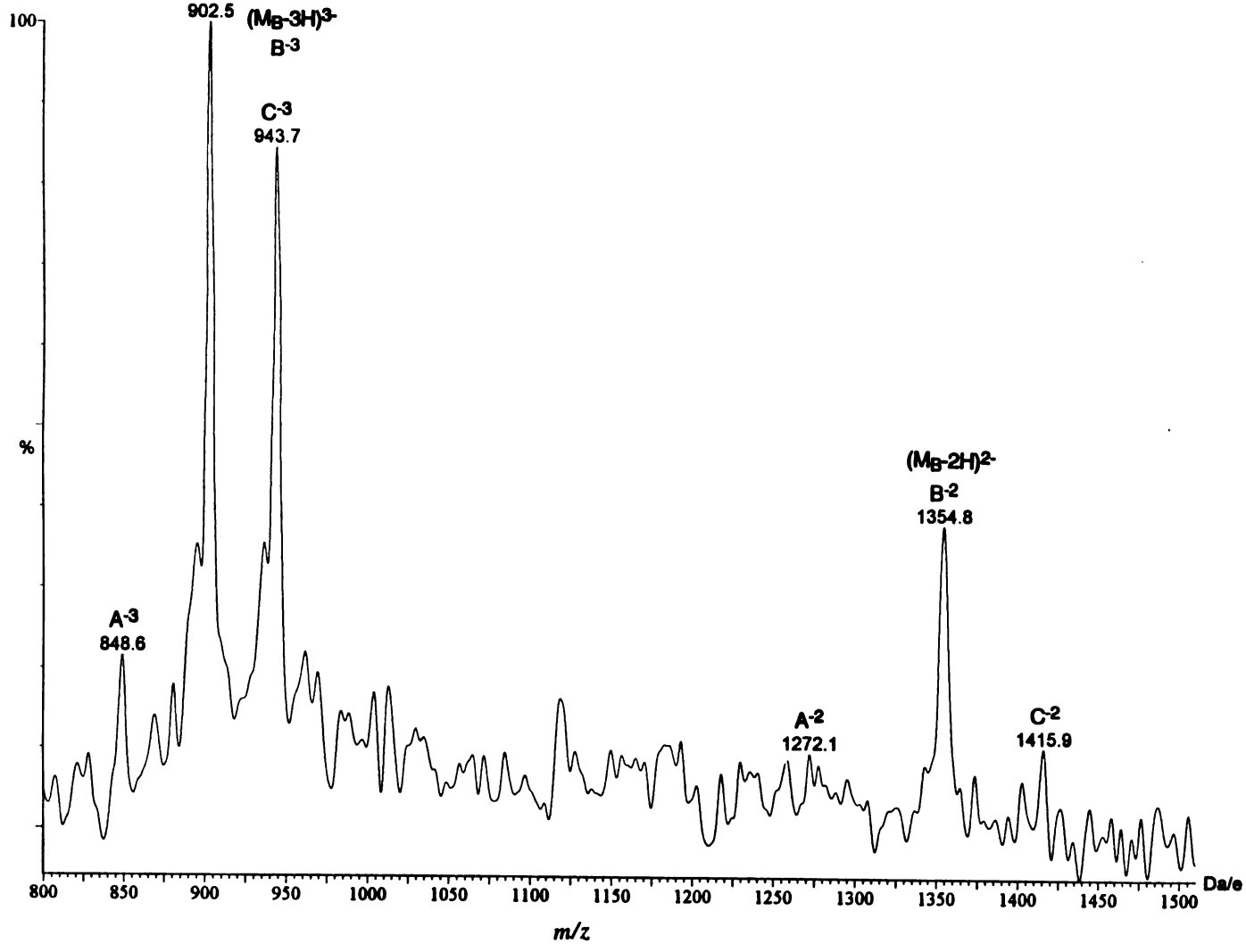

Figure 5.4. (b) Partial negative-ion electrospray mass spectrum of *O*-deacylated LOS from strain 233 after neuraminidase treatment.

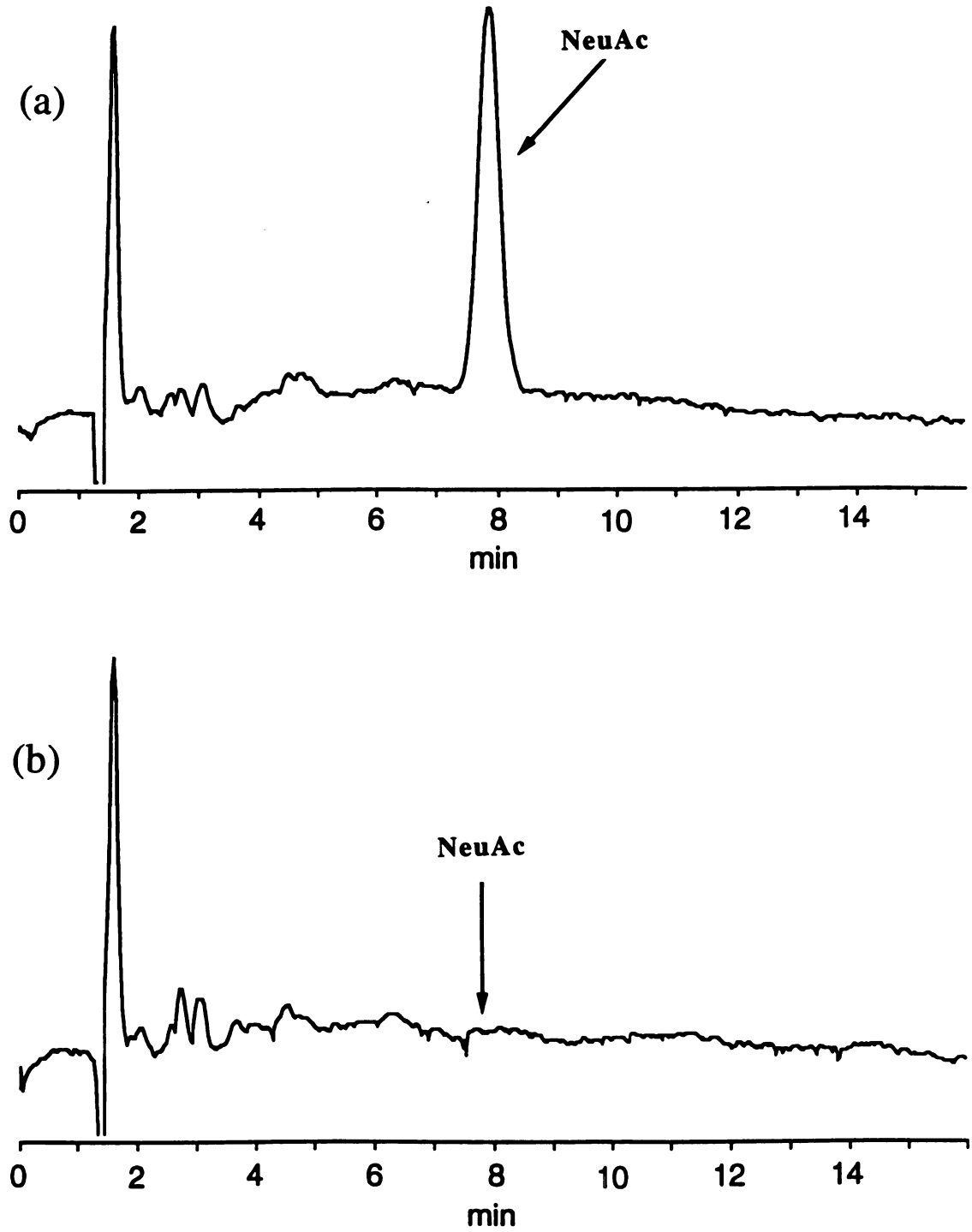

Figure 5.5. High pH anion exchange chromatogram of precipitated LOS fraction of *H. ducreyi* 35000 incubated with (a) neuraminidase and (b) heat-inactivated neuraminidase.

chromatograms of the LOS from strains 233, NYC23 and 188 looked similar to Fig. 5.6 but those of strains 188-2 and 33921 contained no peak for sialic acid. Since we are reporting the sialic acid content as a mole % of LOS, we sought to better quantify the purity of the LOS preparations by independent determination of the glucosamine content. We made the assumption that a reasonable estimate of the glucosamine content of LOS would be 3 moles of glucosamine (two from the lipid A, one from the oligosaccharide region) per mole of LOS for strains 35000, 233, NYC23, 188 and 33921 and 2 moles of glucosamine (two from the lipid A, none from the oligosaccharide region) per mole of LOS for strain 188-2. Our data (Table 5.4) showed that the sialic acid content was approximately 20 mole % for strain 35000, 97% for strain NYC 23, 54% for strain 188 and 12% for strain 233. No sialic acid could be detected in the lipooligosaccharides of strains 188-2 and 33921.

Adherence Assay. Table 5.5 shows the results of adherence assays for various strains of *H. ducreyi*. The wild-type strains 35000, 233 and 188 show the largest % bacterial adherence. Adherence for strain 33921 which lacks terminal lactosamine is greatly diminished. An *E. coli* strain and two *M. catarrhalis* strains showed no significant attachment.

Cytotoxicity Assay. Data from the cytotoxicity assays are shown in graphical form in Fig. 5.6. The LOS from *H. ducreyi* strain 188 shows the greatest cytotoxicity followed by LOS from the other wild-type strain 35000. The LOS from strain 188-2 shows virtually no cytotoxic activity and the LOS from strain 33921 becomes toxic at higher concentrations.

DISCUSSION

LSIMS, compositional analysis and methylation analysis data obtained on the oligosaccharides of strains 233, 188 and NYC23 and further analysis of their LOS by ESI-MS suggest that the major oligosaccharide structure previously determined for strain 35000 is also present in these wild-type strains. The monoclonal antibody 3F11 which recognises

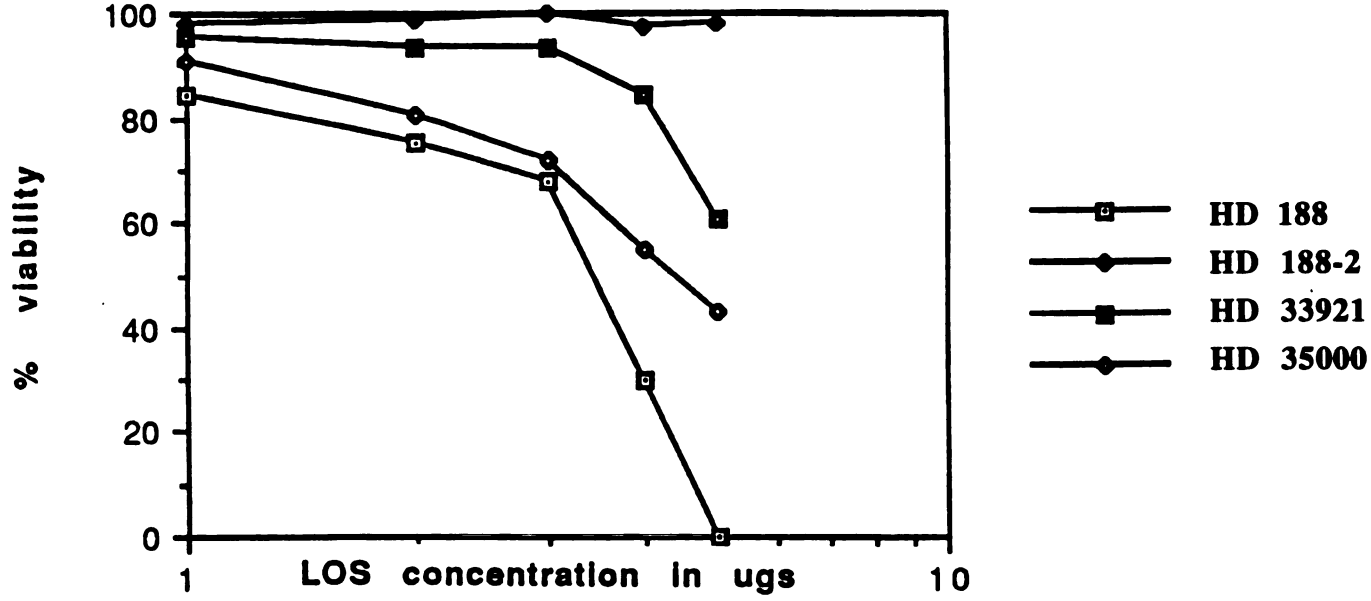

Figure 5.6. LOS cytotoxicity on keratinocytes. Each data point represents the mean of the viability from triplicate wells as measured by Trypan Blue and 3-(4,5-dimethylthiazol2-yl)-2,5-diphenyl-2H-tetrazolium bromide (Mossman, 1983). This figure is reproduced with permission from Campagnari (unpublished data).

Table 5.4. Sialic acid content of LOS from various strains of Haemophilus ducreyi

Bacterial strains	Mole % sialic acid	Sialic acid % calculated from ESI-MS data[a]
35000	20.7	34
188	54.4	30
188-2	0.0	0.0
233	12.1	48
NYC23	96.7	42
33921	0.0	0.0

[a] Calculated by taking the ratio of the sum of the heights of the sialylated peaks for the triply charged ions to the sum of the heights of the asialo peaks for the triply charged ions.

Table 5.5. % Bacterial Adherence of H. ducreyi to keratinocytes at 2 hours[a]

Bacterial strains	Experiment 1	Experiment 2	Experiment 3
H. ducreyi 35000	21.4 1.7	23.2 1.6	20.2 2.1
H. ducreyi 233	15.2 1.3	16.8 1.7	18.4 1.2
H. ducreyi 188	22.5 1.3	20.8 1.3	21.5 1.4
H. ducreyi 33921	2.4 0.8	3.2 1.2	2.2 0.6
E. coli HB 101	0.18 0.11	0.15 0.05	0.04 0.02
M. catarrhalis 48	0.04 0.02	0.08 0.04	0.04 0.03
M. catarrhalis 8184	0.11 0.06	0.06 0.02	0.07 0.04

[a] Experiments were conducted in triplicate and maximum adherence was obtained after 2 hours. An *E. coli* strain and two *M. catarrhalis* strains showed no significant attachment.

the terminal region of paragloboside (Galβ1→4GlcNAcβ1→3Galβ1→4Glcβ1–ceramide) also binds strongly to the LOS of all four wild-type strains. The variant 188-2, however, has lost the terminal LOS epitope defined by monoclonal antibody 3F11 (Campagnari et al., 1994) (see also Chapter 4). The presence of sialic acid in the LOS of all these strains, including strain 35000, suggests that terminal lactosamine may be the acceptor for sialic acid. Certainly those strains that do not contain terminal lactosamine, 188-2 and 33921, show no evidence of sialylation. It may be that lactosamine and sialyllactosamine are important terminal structures in the disease process. For example lactosamine may be required for cell adhesion (and perhaps invasion) processes. Galactose-specific lectins may exist on keratinocytes, which are probably the first cells *H. ducreyi* encounters in the host. Indeed, it has been recently demonstrated by Campagnari that adherence of the variant strain 188-2 to cultured human keratinocytes is greatly diminished compared to the wild-type strain (unpublished data). He also observed a marked decrease in the ability of strain 33921 to adhere to keratinocytes compared to other wild-type strains such as 188, 35000 and 233 (Table 5.5). It may be that sialyllactosamine is needed by the invading bacterium at a later stage for immune evasion. This would be consistent with the findings implied from studies on *N. meningitidis* and *N. gonorrhoeae* LOS, where the presence of sialic acid has been linked to the conversion from serum-sensitivity to serum resistance (Parsons et al., 1988) and to a marked decrease in susceptibility to killing by human neutrophils (Estabrook et al., 1992; Rest & Frangipane, 1992).

There is mounting evidence that sialic acid prevents the recognition of antigenic sites by components of the immune-defense system (Schauer, 1985). It may be that the bulky and negatively charged sialic acid residues together with the large and branched oligosaccharide chain cover antigenic recognition sites on the surface of the bacterial cell enabling the organism to escape the host defenses (Schauer, 1985). Although the mechanism is unknown, it appears that the negative charge of sialic acid has a great influence on the biological masking effect of this sugar, because reduction of the carboxyl

group of sialic acid to an alcohol residue drastically alters the immunological properties of bacterial antigens (Jennings et al., 1984). Table 5.4 shows the sialic acid content of the LOS from the six strains of *H. ducreyi* studied. The different levels of sialylation observed among strains is not easily rationalized. There are also large discrepancies in the amounts of sialic acid calculated from the two different methods of quantitation (see Table 5.4). There appears to be no general trend. That is to say, for strains 35000 and 233 the ESI-MS method gives higher amounts of sialic acid whereas for strains 188 and NYC23 it gives lower results. Based on the fact that ESI-MS spectra of the same LOS do not always give the same relative ion abundances, the mole % calcualtions may be more accurate. The phenomenon of phase variation, seen in *N. gonorrhoeae* and *H. influenzae* has not been observed, at least *in vitro*, in *H. ducreyi*. It may be that the level of sialylation being detected is an average value. That is to say, within the population of a given strain not all bacteria contain the same amount of sialic acid on their LOS and in the quantitation experiments an average value for the whole population is being calculated. *In vivo*, conditions may exist that select for bacteria with greater or lesser amounts of sialic acid on their LOS or some external signal in the environment may control the extent of LOS sialyation.

One would predict based on the absence of the paragloboside epitope and lack of sialylation in the oligosaccharide of strain 33921 that this strain may not prove as pathogenic as the other wild-type strains studied. Indeed, Campagnari has recently been successful in finding an assay employing cultured human keratinocytes for assessing LOS cytotoxicity and preliminary results indicate that both the pyocin variant strain 188-2 and 33921, both of which lack lactosamine and sialic acid, are considerably less toxic in this assay compared to strains 35000 and 188 (Fig. 5.6). Nevertheless intradermal inoculation of LOS from strain 33921 in rabbits caused lesions at doses similar to other *H. ducreyi* wild-type LOS. Interestingly, the oligosaccharide from strain 188-2 does not possess a lactose structure, whereas the oligosaccharide from strain 33921 has a lactose moiety

which, although not terminal, may be recognised by a family of lactose-specific lectins. Additional structural and biological studies will be needed to determine the actual roles of these LOS glycoforms in the disease mechanism of *H. ducreyi*.

CHAPTER 6.

RECENT DEVELOPMENTS IN STRATEGIES FOR LOS STRUCTURAL ANALYSIS

INTRODUCTION

Although a great deal of progress has been made in LOS structural analysis using the methods described in the previous chapters, much has yet to be accomplished to meet the needs of understanding the roles of LOS in the pathogenic and biological process. For example, one would like to be able to analyse unmodified LOS to ensure that no labile moieties that may ultimately prove to be of significant biological importance have been lost. Furthermore, one would like to ensure that no chemical degradation of LOS has taken place. It would also be useful to have more rapid mass spectrometric methods of screening LOS from a series of mutants (or wild-type strains) to determine if further investigation of their LOS structures might contribute to an understanding of structure/function.

An ongoing aim of this work has been to improve the sensitivity of mass spectrometric techniques so that analysis may be performed on smaller amounts of LOS, since very often the limiting factor in structural analysis of materials of biological origin is the quantity of sample available. This will be especially true as the structural studies are conducted on samples obtained from *in vivo* experiments. In this chapter preliminary data are presented from experiments involving recent developments in methods for analysing LOS. Hopefully, the results will show that some of the goals of sensitive LOS structural analysis are closer to being achieved. These newer, more experimental methods include matrix assisted laser desorption/ionization (MALDI) time-of-flight mass spectrometry of *O*-deacylated LOS, liquid chromatography electrospray mass spectrometry (LC/ESI-MS) of

oligosaccharides, ESI-MS of LOS directly before any chemical degradation of the molecule has taken place, and lastly, ESI-MS/MS of *O*-deacylated LOS.

Laser desorption of intact biological molecules with molecular masses in excess of ≈ 1000 Da generally requires the use of a matrix. The object of the MALDI technique is to generate large molecular ions without extensive and unspecific fragmentation (Hillenkamp & Karas, 1990). Using ^{252}Cf-plasma desorption mass spectrometry (^{252}Cf PDMS) several researchers have been successful in obtaining molecular ions for lipid A (Karibian et al., 1991) and rough LPS consisting of lipid A with up to 2 to 5 glycose moieties (Caroff et al., 1991). In the rough LPS experiments, the spectra contained ion pairs: the deprotonated molecular ions $[M-H]^-$ for the LPS species and their corresponding lipid A fragment ions. Other workers have characterized lipid A preparations using laser desorption (LD) mass spectrometry by adding KCl to the samples to promote the production of $[M+K]^+$ molecular ions (Cotter et al., 1987). Extensive fragmentation of lipid A including two-bond cleavages were observed in these spectra making interpretation difficult, if not challenging. With the laser desorption technique, fragmentation depends to a certain extent on the amount of energy deposited in the sample. It is very difficult to tune the laser wavelength to the exact energy required to desorb the molecular ion without thermal degradation. The correct choice of matrix helps to control this process by selectively absorbing some of the energy. The matrix in which the sample is dissolved is present in large excess. This serves to separate the sample molecules from one another, limiting aggregation which would prevent the formation of molecular ions as well as acting as a chromophore for absorbing energy. Using MALDI it is possible to obtain very accurate molecular weights for large biological molecules in the range of several hundred thousand daltons (Hillenkamp & Karas, 1990). In this chapter the method is used to examine *O*-deacylated LOS from *H. ducreyi* strain 35000.

In Chapter 2, the major oligosaccharide from *H. ducreyi* strain 35000 was derivatized with butyl phenylhydrazine, purified by HPLC and individual HPLC peaks run

by LSIMS. Electrospray ionization, however, is an efficient method of interfacing liquid chromatography with mass spectrometry and the effluent from the HPLC experiment can be routed into the running solvent of the electrospray mass spectrometer and analysed directly. In this chapter the BPH derivative of the major oligosaccharide from *H. ducreyi* strain 35000 was analysed in this fashion as a means for rapid on-line HPLC/ESI-MS analysis and characterization of oligosaccharides derived from LOS mixtures.

As mentioned earlier, ideally one would like to analyse the structure of the LOS molecule before any chemical degradation has taken place. Any chemical or enzymatic treatment prior to analysis could potentially remove biologically important residues or introduce artifactual heterogeneity. In this chapter unmodified LOS is solublized to the extent that it can be run directly by ESI-MS.

Lastly, up to now, ESI-MS has been used exclusively to accurately determine molecular weights and assay for oligosaccharide and LOS heterogeneity. While this is in itself a worthy end, the lack of fragmentation means that little or no information regarding molecular structure is obtained. In this chapter tandem mass spectrometry of multiply charged ions produced by ESI of *O*-deacylated LOS is investigated.

EXPERIMENTAL

MALDI/MS of O-deacylated LOS LOS was *O*-deacylated as described in Chapter 2 and prepared for mass spectrometric analysis in a matrix of 2,5-dihydroxybenzoic acid (DHB). Samples were run on a Kratos Kompact matrix-assisted laser desorption/ionization (MALDI) time-of-flight mass spectrometer (Manchester, England). Spectra were acquired in the linear mode at an acceleration voltage of 20 kV. Spectra were summed from 1 to 200 laser shots taken across the entire sample well ($\approx$ 3 mm). Oxidized insulin B-chain, $[M-H]^-$ (average mass 3494.9), and phosphokemptide, $[M-H]^-$ (average

mass 850.9), were used as external mass standards. A laser power of 55% maximum was used.

LC/ESI-MS of BPH-Oligosaccharides Butyl phenylhydrazine oligosaccharides were prepared as described in Chapter 2. A dual syringe pump (Applied Biosystems) was used to deliver the mobile phase at 50 μL/min. Microbore HPLC separation was performed on an Aquapore 300 C18 microbore column, 1.0 mm i.d. x 100 mm (Applied Biosystems). Column effluent was monitored by a variable wavelength UV detector (Applied Biosystems) equipped with a high sensitivity capillary flow cell (LC Packings) at 335 nm. The oligosaccharides were eluted with a linear gradient of 0-60% acetonitrile in 30 min. Both water (solvent A) and acetonitrile (solvent B) contained 0.05% trifluoroacetic acid. The microbore HPLC system was interfaced to a VG Biotech/Fisons Bio-Q mass spectrometer with an electrospray source by a length of fused silica capillary tubing. The column effluent was split 1:20 so that that the flow rate into the mass spectrometer was 3-5 μL/min.

ESI-MS of unmodified LOS Crude LOS were analyzed on a VG Biotech/Fisons Platform quadrupole electrospray mass spectrometer in the negative-ion mode. LOS were first dissolved in H_2O/CH_3CN/TEA (1/1/1, v/v) to make a 1 μg/μl solution and 5 μl of this solution was injected via a Rheodyne injector into a constant stream of H_2O/acetonitrile (1/1, v/v) containing 1% acetic acid running at 10 μl/min. It was important to freshly dissolve the LOS prior to the run, since degradation occurred if the sample was allowed to sit in solution. Mass calibration was carried out with an external horse heart myoglobin reference using the supplied VG/Fisons software.

ESI-MS/MS of O-deacylated LOS Tandem electrospray mass spectrometric studies of *O*-deacylated LOS were performed on a VG Biotech/Fisons Bio-Q triple quadrupole mass spectrometer. Conditions were similar to those mentioned above for ESI-MS of intact LOS. For the MS/MS experiments argon was used as the collision gas. The gas

pressure in the collision quadrupole chamber was 10^{-2} torr and the collision energy was 17V.

RESULTS

Analysis of O-deacylated LOS by MALDI/MS The negative-ion MALDI spectrum of *O*-deacylated LOS from *H. ducreyi* strain 35000 is shown in Fig. 6.1. The $[M-H]^-$ ion at *m/z* 2711.6 corresponds to the major glycoform observed earlier by ESI-MS consisting of the previously determined oligosaccharide:

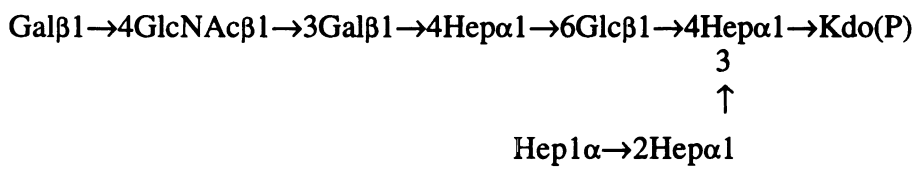

directly linked to the lipid moiety consisting of a diphosphoryl glucosamine disaccharide containing the two *N*-linked β-OH myristoyl groups. The peak at *m/z* 2548.0 represents a species containing one less hexose than the above structure, while the peaks at *m/z* 2915.5 and 3004.3 correspond to extended analogs of the structure shown above containing an additional HexNAc and sialic acid residue, respectively. Curiously, no extended analogs containing phosphoesters, which were evident in the ESI-MS spectrum of the same sample were observed in this spectrum.

LC/ESI-MS of BPH-OS The UV chromatogram of the butyl phenylhydrazine derivative of the major oligosaccharide from *H. ducreyi* strain 35000 is shown in Fig. 6.2 (a). The total ion chromatogram is shown in Fig. 6.2 (b). The UV chromatogram shows seven peaks each of which gave the same molecular ion as its base peak. The peaks represent various *anhydro*Kdo forms of the oligosaccharide which arise from β-elimination of 4-linked phosphate during acetic acid hydrolysis of the LOS. The positive-ion mass spectrum of the peak which elutes at 22.68 min is shown in Fig. 6.3. The peak at *m/z*

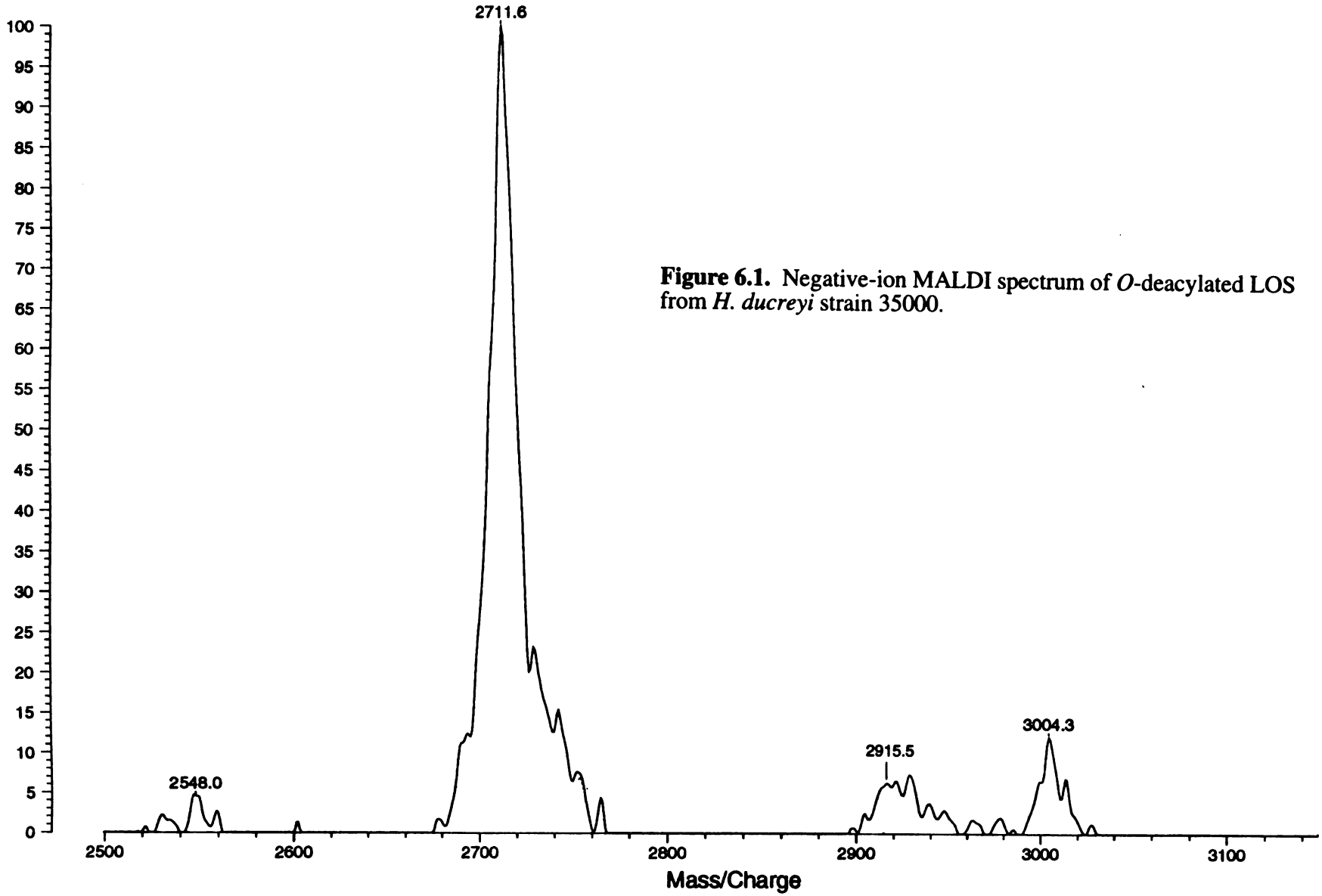

Figure 6.1. Negative-ion MALDI spectrum of *O*-deacylated LOS from *H. ducreyi* strain 35000.

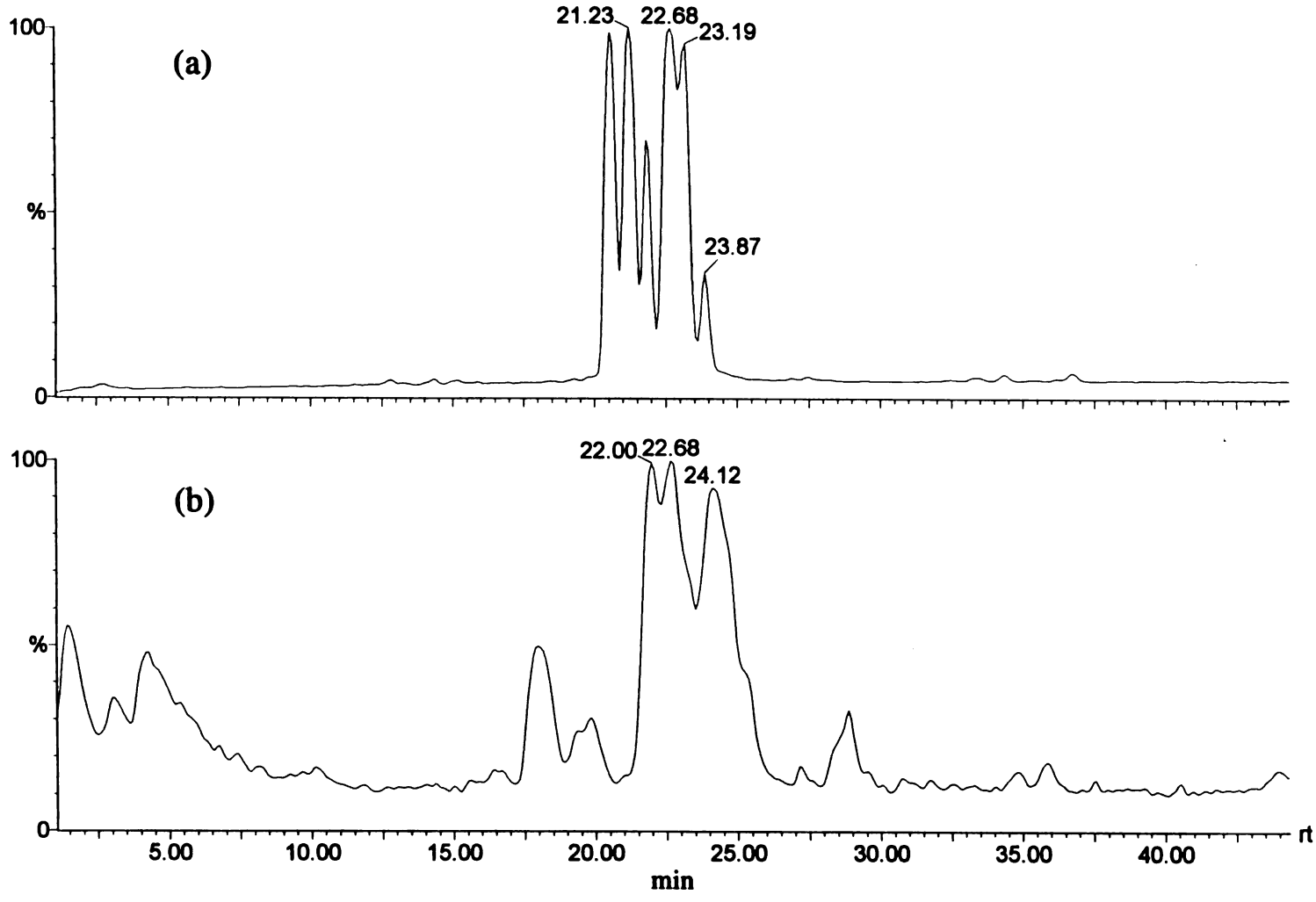

Figure 6.2. (a) UV chromatogram and (b) total ion chromatogram of the butyl phenylhydrazine derivative of the major oligosaccharide from *H. ducreyi* strain 35000.

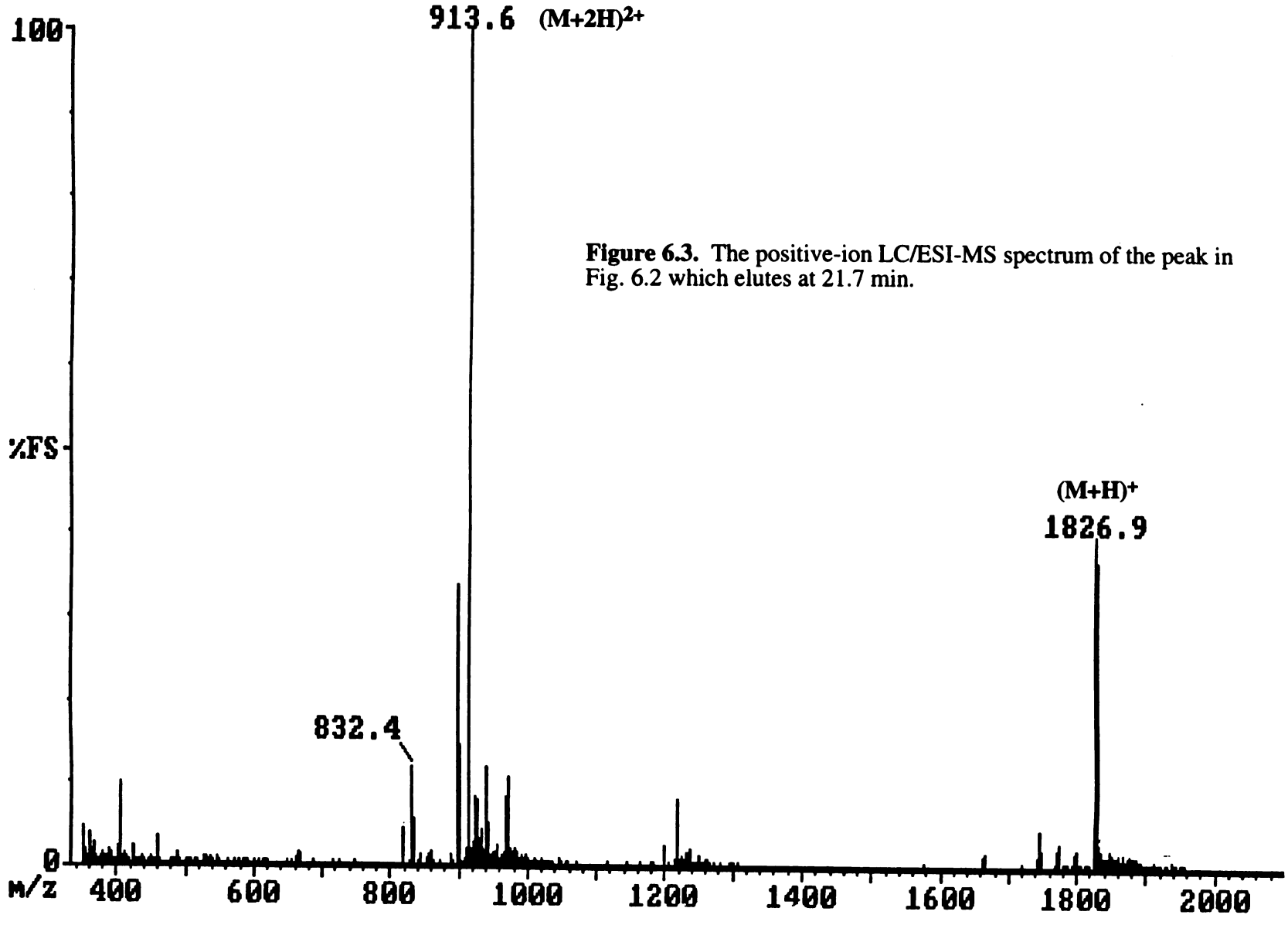

Figure 6.3. The positive-ion LC/ESI-MS spectrum of the peak in Fig. 6.2 which elutes at 21.7 min.

1826.9 is the singly charged protonated molecular ion $(M+H)^+$ for the BPH derivative of the major oligosaccharide whose structure is shown above. The peak at *m/z* 913.6 is the doubly charged ion and the peak at *m/z* 832.4 represents the loss of hexose from this oligosaccharide species.

ESI-MS Analysis of Unmodified LOS. The electrospray spectrum of the unmodified LOS from *H. ducreyi* strain 35000 is considerably more complex than its *O*-deacylated counterpart (see Fig. 5.3a) and not readily interpretable (Fig. 6.4). One possible interpretation is that two series that differ by 226 daltons, the mass of a hydroxylmyristoyl group, are present in the spectrum. The higher series shows a triply charged molecular ion $(M-3H)^{3-}$ at *m/z* 1234.7, its doubly charged counterpart at *m/z* 1852.6, as well as several extended analogs in each charge state. This triply charged molecular ion corresponds to an intact LOS species with a molecular weight of 3706.5 which is 123 Da (the mass of a PEA moiety) more than expected for the mass of the major LOS shown in Fig. 2.8. The ions at *m/z* 1275.6, 1332.0 and 1372.7 represent the addition of PEA, sialic acid, and PEA plus sialic acid, respectively, to the triply charged molecular ion. Peaks at *m/z* 1914.2, 1998.3 and 2059.7 denote the addition of PEA, sialic acid, and PEA plus sialic acid, respectively, to the doubly charged molecular ion. The lower mass series, which is a truncated analog of the higher series, representing a species with one less hydroxylmyristoyl moiety, has a triply charged molecular ion at *m/z* 1158.4 and the corresponding doubly charged ion at *m/z* 1739.3. The ions at *m/z* 1200.1 and 1800.6 signify the addition of PEA to the triply charged molecular ion and the doubly charged ion respectively. The main problem with this interpretation is that there was no evidence for an LOS species containing two PEA groups in the ESI-MS spectrum of *O*-deacylated LOS from *H. ducreyi* strain 35000. Further experiments are clearly needed to establish this structural difference.

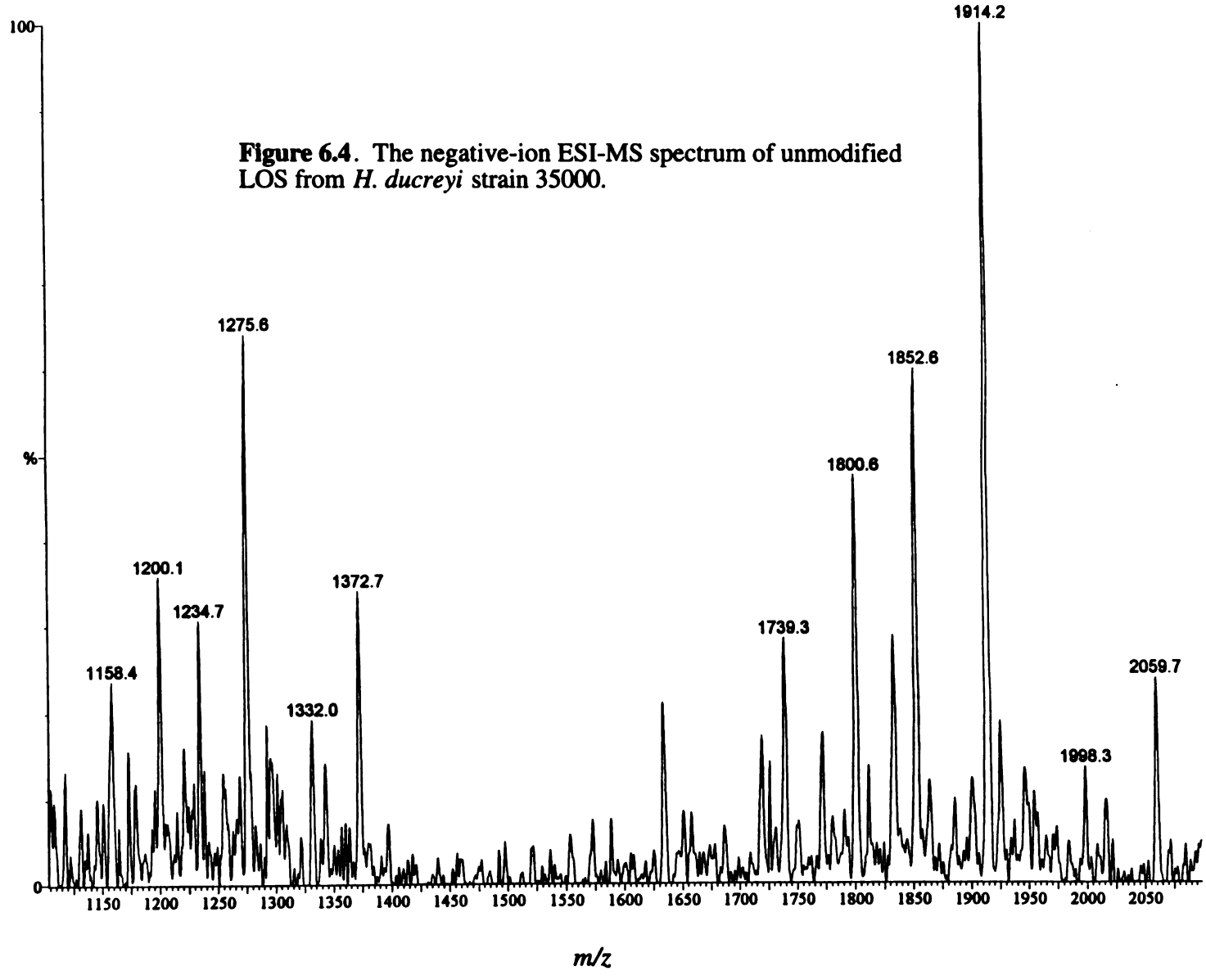

Figure 6.4. The negative-ion ESI-MS spectrum of unmodified LOS from *H. ducreyi* strain 35000.

ESI-MS/MS analysis of O-deacylated LOS The peak at *m/z* 821.4 which represents the triply charged deprotonated molecular ion $(M-3H)^{3-}$ for the *O*-deacylated LOS from *H. ducreyi* strain 188-2 (see Fig. 4.4B) was selected for low energy CID. The tandem electrospray spectrum is shown in Fig. 6.5. The fragment ions result primarily from cleavage of the labile Kdo-lipid A linkage. Besides the triply charged parent ion peak at *m/z* 821.4 there is also a triply charged peak at *m/z* 756.8 which corresponds to the loss of heptose from the parent ion. The peak at *m/z* 951.9 represents the singly charged ion $(M-H)^-$ for lipid A and its doubly charged ion is evident at *m/z* 474.3. The peak at *m/z* 1416.4 is the singly charged Y-type ion representing the loss of lipid A, H_3PO_4 and H_2O from the molecular ion. The peak at *m/z* 1372.6 represents decarboxylation of the ion at *m/z* 1416.4.

DISCUSSION

Although no new information regarding LOS glycoforms was gained from the MALDI experiment, it corroborated the heterogeneity that had been observed in ESI-MS experiments. MALDI has a greater mass range than LSIMS and together with the fact that it does not produce observable fragmentation under standard conditions, holds out hope that the method may some day be useful for examining unmodified LOS if suitable matrices can be found. In addition, the high sensitivity of the MALDI technique makes it suitable for running samples in the sub-picomole range.

The LC/ESI-MS experiment again verifies information previously obtained by separate chromatographic and mass spectrometric experiments. The major improvements accomplished by interfacing the two systems in one experiment concern the speed with which the analysis can be completed, the smaller scale on which the analysis can be performed and the larger dynamic range available in this configuration.

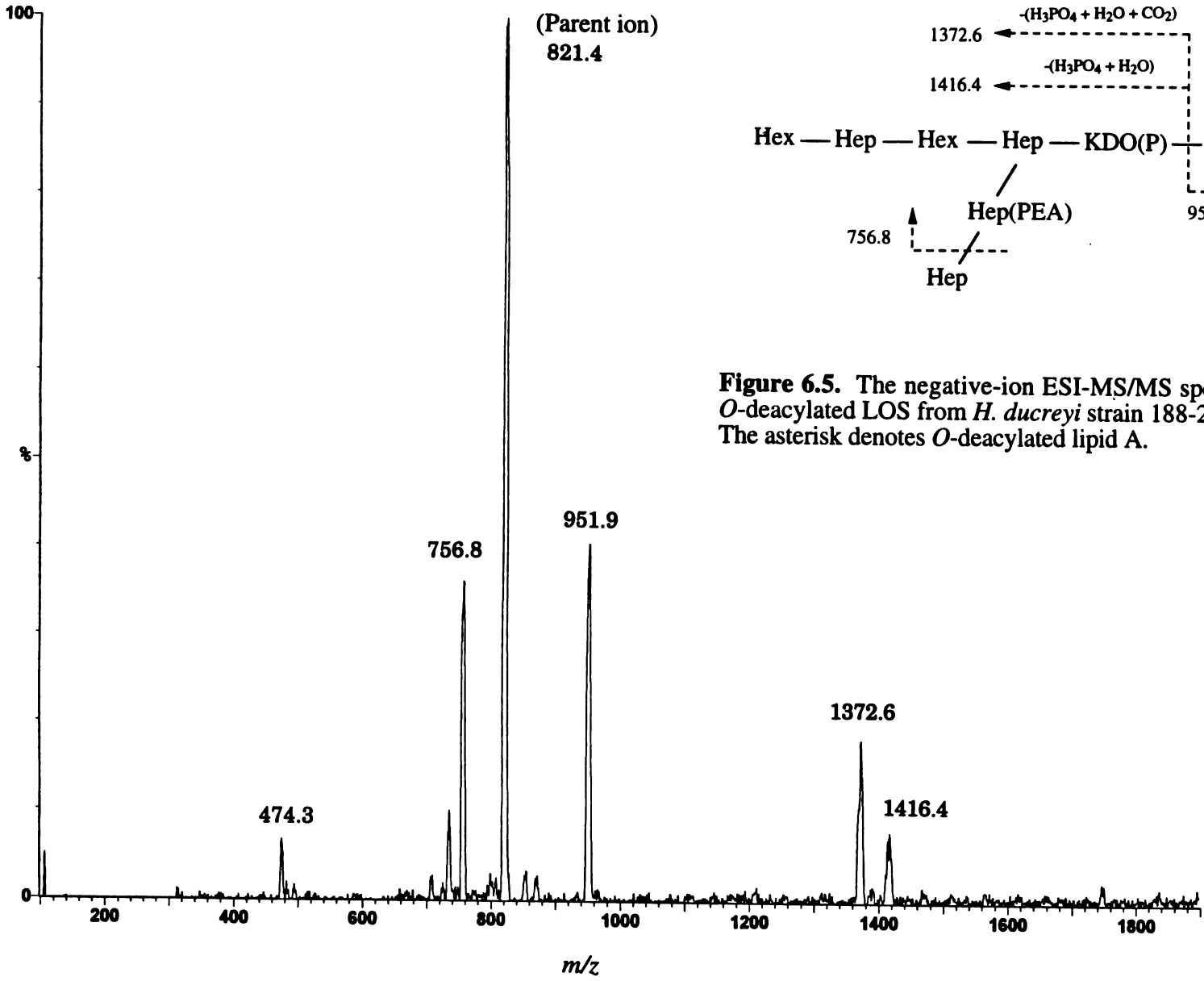

Figure 6.5. The negative-ion ESI-MS/MS spectrum of *O*-deacylated LOS from *H. ducreyi* strain 188-2. The asterisk denotes *O*-deacylated lipid A.

The traditional method of determining LOS structure has been to hydrolyse the lipid from the oligosaccharide moiety and to study each separately. This approach was possible because of the lability of the ketosidic linkage binding the lipid to the carbohydrate. Such an approach was necessary because of the difficulty in solubilizing the LOS which tends to aggregate in solution. *O*-deacylation of the LOS by mild hydrazine treatment, which renders it soluble in aqueous solution, followed by ESI-MS analysis proved to be a useful method of examining a more intact version of the molecule. However, the ideal approach of looking at the whole LOS has until now proved elusive. With the development of an effective method of solubilizing the LOS just prior to ESI-MS analysis, this obstacle has now been partially overcome. The ESI-MS spectrum of the unmodified LOS (Fig. 6.3) confirms the heterogeneity of LOS species seen in the ESI-MS spectrum of the *O*-deacylated LOS (Gibson et al., 1993). It also suggests the presence of a major LOS species containing two PEA moieties that was not observed in our previous studies. Some of the heterogeneity seen in this spectrum may be artifactual, arising from the nature of the solvent used. Clearly these are preliminary data and more efficient ways of solublizing LOS need to be explored. Perhaps milder conditions, rather than the highly basic conditions utilized in these first experiments, can be found. Furthermore, ESI-MS analyses of unmodified LOS from other strains need to be conducted so that common trends in the spectra can be examined and interpretation of the data put on a more solid footing.

The preliminary data from the tandem electrospray experiment indicate that this method gives little structural information on the oligosaccharide region and cannot be considered an alternative to tandem high energy CID LSIMS. However, the presence of the singly charged ion $(M-H)^-$ at *m/z* 951.9 for *O*-deacylated lipid A suggests that this could be used as a fast method for obtaining the molecular weight of lipid A without needing to hydrolyse in 1% acetic acid. This could save valuable time when screening different strains in order to determine if their LOS warrant further structural analysis either

by pointing to differences in the lipid A and/or oligosaccharide portion of the LOS molecules. For example, all of the strains studied to date have similar if not identical lipid A moieties once their *N*-linked fatty acid groups have been removed. That is to say the major ion in the LSIMS spectrum of the lipid A from each strain was the same although the heterogeneity differed from strain to strain. Clearly any strain whose lipid A diverged from this general pattern would be an interesting candidate for more extensive structure/function studies. Some of the advantages of the tandem electrospray method are that it permits analysis of *O*-deacylated LOS whose mass is usually outside the dynamic range of LSIMS, analysis can be done on much smaller quantities and fragmentation offers crucial structural information.

CONCLUSIONS

In this dissertation the aim of my studies has been to determine the structures of *H. ducreyi* LOS and to relate them, if possible, to their biological functions. In order to achieve this goal, the LOS from *H. ducreyi* strain 35000 was selected for in depth analysis for the following reasons. This strain had been the subject of previous biological and immunochemical studies. It was reported to be virulent in both the temperature dependent rabbit model (Purcell et al., 1991) and in the earlier rabbit model (Feiner et al., 1945; Dienst, 1948). It was also reported to contain on its LOS an epitope immunochemically similar to the terminal tetrasaccharide of paragloboside, a precursor to a major blood group antigen (Campagnari et al., 1990). The complete structure of the oligosaccharide region of this strain was determined and proved to have several interesting features, including an unusual branch heptose and an epitope, terminating in lactosamine, that mimicked structures found in human blood group antigens. The next step was to establish if these structural features were common to other strains of *H. ducreyi* and, if so, what was their biological significance. The major oligosaccharide from strain 188 turned out to be similar

to that of strain 35000. If a variant of one of these strains could be produced whose LOS lacked the terminal lactosamine, then adhesion and cytotoxicity assays on cultured human keratinocytes comparing the parent strain to the variant would yield important information concerning the biological significance of this terminal disaccharide. Strain 188-2, isolated after treatment with pyocin, was such a variant and assays showed that adherence and cytotoxicity to cultured human keratinocytes were greatly diminished in this strain. Other strains were studied and the common motif observed in the LOS of strains 35000 and 188 seemed to hold except for the Kenyan strain 33921. The Kenyan strain most likely possessed an LOS with the same oligosaccharide core structure (Hep_3 Kdo) as the other strains but had a much smaller oligosaccharide branch which lacked terminal lactosamine. Therefore, this strain's LOS provided another opportunity to test the biological importance of terminal lactosamine (and sialyllactosamine). Indeed, assays conducted on strain 33921 showed reduced adherence and cytotoxicity, corroborating the potential significant biological role of terminal lactosamine and/or sialyllactosamine. Lastly, ESI-MS showed that the oligosaccharide region of all the strains studied except strains 188-2 and 33921 contained sialic acid. It appeared that terminal lactosamine must be the acceptor for sialic acid and immunochemical studies indicated that sialic acid was important in allowing the organism to evade the host defenses.

Much work remains to be done to achieve a complete understanding of *H. ducreyi* pathogenesis. The ultimate goal is, of course, to determine the molecular basis of *H. ducreyi* pathogenesis which would then hopefully lead to more effective treatments for chancroid. Since resistance of *H. ducreyi* to most antibiotics in general use is growing at an alarming rate, a new class of antibiotics or a vaccine appears to be needed.

Based on the structure/function studies of *H. ducreyi* LOS reported in this dissertation, several approaches to designing new drugs come to mind. For example, it seems that sialylation of LOS may be necessary for *H. ducreyi* to successfully evade the host defenses and multiply. If so, to prevent the organism from adding sialic acid to its

LOS during biosynthesis of the oligosaccharide branch, one could target the sialyltransferase responsible for this step by designing inhibitors such as phosphonate analogs of the sugar nucleotide which have previously been shown to inhibit glycosyltransferases (Vaghefi et al., 1987). Alternatively, other steps prior to the sialyltransferase step could be targeted. At present, work is in progress in our laboratory to isolate the sialic acid transferase and synthase with the long-term goal of developing specific inhibitors to these enzymes.

Another possible approach would be to target the D-*glycero*-D-*manno*-heptosyltransferase which is rare in Gram-negative bacteria. An inhibitor of this enzyme would selectively prevent the addition of terminal lactosamine to the oligosaccharide chain of *H. ducreyi* LOS. Based on studies of the 188-2 variant and strain 33921, both of which lack terminal lactosamine, this disaccharide appears to be important in allowing the organism to adhere to and invade cultured human keratinocytes. The biological importance of terminal lactosamine in the LOS of *N. gonorrhoeae* has been reported (Gibson et al., 1989; John, 1990). Gonococcal strain JW31 whose LOS contains terminal lactosamine is serum-resistant whereas pyocin-resistant strains JW31R and FA5100 which lack this disaccharide are serum-sensitive.

While the most optimistic outlook for treatment of chancroid would be the design of a successful LOS vaccine, the accomplishment of this goal requires structural analysis of LOS from many different strains of *H. ducreyi*. Clearly, methods such as those described in this chapter for rapidly screening numerous LOS samples on a microscale level will be crucial to the success of these ventures. For the LOS chemist the road ahead is to adapt these new techniques as quickly and efficiently as possible to the task.

REFERENCES

Abeck, D. & Johnson, A. P. (1987). Identification of surface-exposed proteins of *Haemophilus ducreyi*. *FEMS Microbiol. Lett. 44*, 49-51.

Abeck, D., Johnson, A. P., Hartinger, A., Kollmann, M., Korting, H. C., Ballard, R. C. & Braun, F. O. (1991). Absence of extracellular enzyme activity and cytotoxicity in cell-free culture filtrates of *Haemophilus ducreyi*. *Microb. Pathog. 10*, 405-410.

Abeck, D., Johnson, A. P. & Mensing, H. (1992). Binding of *Haemophilus ducreyi* to extracellular matrix proteins. *Microb. Pathog. 13*, 81-84.

Abeck, D., Johnson, A. P., Wall, R. A. & Shah, L. (1987). *Haemophilus ducreyi* produces rough lipopolysaccharide. *FEMS Microbiol. Lett. 42*, 159-161.

Abeck, D. & Korting, H. C. (1991). Mechanisms of skin adherence, penetration and tissue necrosis production by *Haemophilus ducreyi*, the causative agent of chancroid. *Acta Derm. Venereol. Suppl. (Stockh) 174*, 1-20.

Abeygunawardana, C., Bush, C. A. & Cisar, J. O. (1990). Complete structure of the polysaccharide from *Streptococcus sanguis* J22. *Biochemistry 29*, 234-248.

Albritton, W. L. (1989). Biology of *Haemophilus ducreyi*. *Microbiol. Rev. 53*, 377-389.

Alfa, M. J., Olson, N., Degagne, P., Plummer, F., Naraara, W., Maclean, I. & Ronald, A. R. (1993). Humoral immune response of humans to lipooligosaccharide and outer membrane proteins of *Haemophilus ducreyi*. *J. Infect. Dis. 167*, 1206-1210.

Angel, A.-S. & Nilsson, B. (1990). Linkage Positions in Glycoconjugates by Periodate Oxidation and Fast Atom Bombardment Mass Spectrometry. Methods in Enzymology Vol. 193. New York, Academic Press. 587-607.

Apicella, M. A., Mandrell, R. E., Shero, M., Wilson, M. E., Griffiss, J. M., Brooks, G. F., Lammel, C., Breen, J. F. & Rice, P. A. (1990). Modification by sialic acid of *Neisseria gonorrhoeae* lipooligosaccharide epitope expression in human urethral exudates: an immunoelectron microscopic analysis. *J. Infect. Dis. 162*, 502-512.

Auzanneau, F.-I., Charon, D. & Szabó, L. (1991). Phosphorylated sugars. Part 27. Synthesis and reactions, in acid medium, of 5-*O*-substituted methyl 3-deoxy-α-D-*manno*-oct-2-ulopyranosidonic acid 4-phosphates. *J. Chem. Soc., Perkin Trans. 1* 509-517.

Basus, V. J., Billeter, M., Love, R. A., Stroud, R. M. & Kuntz, I. D. (1988). Structural Studies of α-Bungarotoxin. 1. Sequence-Specific ^{1}H NMR Resonance Assignments. *Biochemistry 27*, 2763-2771.

Batley, M., McNicholas, P. A. & Redmond, J. W. (1985). Analytical studies of lipopolysaccharide and its derivatives from *Salmonella minnesota* R595. III. Reappraisal of established methods. *Biochim. Biophys. Acta 812*, 205-216.

Bax, A. & Davis, D. G. (1985). MLEV-17-Based Two-Dimensional Homonuclear Magnetization Transfer Spectroscopy. *J. Magn. Reson. 65*, 355-360.

Bezancon, F., Griffon, V. & LeSourd, L. (1900). Culture du bacille du chancre mou. *C. R. Soc. Biol. 11*, 1048-1051.

Brade, H., Brade, L. & Rietschel, E. T. (1988). Structure-Activity Relationships of Bacterial Lipopolysaccharides (Endotoxins). *Zbl. Bakt. Hyg. 268*, 151-179.

Brentjens, R. J., Spinola, S. M. & Campagnari, A. A. (1994). *Haemophilus ducreyi* adheres to human keratinocytes. *Microb. Pathog. 16*, 243-247.

Campagnari, A., Karalus, R., Apicella, M. A., Melaugh, W., Lesse, A. J. & Gibson, B. W. (1994). Use of pyocin to select a *Haemophilus ducreyi* variant defective in lipooligosaccharide biosynthesis. *Infect. Immun. 62*, 2379-2386.

Campagnari, A. A., Spinola, S. M., Lesse, A. J., Abu Kwaik, Y., Mandrell, R. E. & Apicella, M. A. (1990). Lipooligosaccharide epitopes shared among Gram-negative non-enteric mucosal pathogens. *Microb. Pathog. 8*, 353-362.

Campagnari, A. A., Wild, L. M., Griffiths, G. E., Karalus, R. J., Wirth, M. A. & Spinola, S. M. (1991). Role of lipooligosaccharides in experimental dermal lesions caused by *Haemophilus ducreyi. Infect. Immun. 59*, 2601-2608.

Caroff, M., Deprun, C., Karibian, D. & Szabo, L. (1991). Analysis of Unmodified Endotoxin Preparations by ^{252}Cf Plasma Desorption Mass Spectrometry. *J. Biol. Chem. 266*, 18543-18549.

Check, W. (1992). International Concerns, Unusual Reports Spark AIDS Conference. *ASM News 58*, 609-612.

Clausen, H. & Hakomori, S. (1989). ABH and Related Histo-Blood Group Antigens; Immunochemical Differences in Carrier Isotypes and Their Distribution. *Vox. Sang. 56*, 1-20.

Cotter, R. J., Honovich, J., Qureshi, N. & Takayama, K. (1987). Structural determination of lipid A from gram negative bacteria using laser desorption mass spectrometry. *Biomed. Environ. Mass Spectrom. 14*, 591-598.

Dabrowski, J. (1987). Application of Two-Dimensional NMR Methods in the Structural Analysis of Oligosaccharides and Other Complex Carbohydrates. Methods in Stereochemical Analysis, Two-Dimensional NMR Spectroscopy: Applications for Chemists and Biochemists. Weinheim, West Germany, VCH Publishers, Inc. 349-386.

Dabrowski, J., Egge, H. & Dabrowski, U. (1983). Two-dimensional, ^{1}H-N.M.R. Study of Peracetylated, Reduced Derivatives of Three Oligosaccharides Isolated from Human Milk. *Carbohydr. Res. 114*, 1-10.

Deal, C. D. & Krivan, H. C. (1990). Lacto and ganglio series glycolipids are adhesion receptors for *Neisseria gonorrhoeae*. *J. Biol. Chem. 265*, 12774-12777.

Dell, A. (1987). F.A.B.-mass spectrometry of carbohydrates. *Adv. Carbohydr. Chem. Biochem. 45*, 19-72.

Dell, A., Azadi, P., Tiller, P., Thomas-Oates, J., Jennings, H. J., Beurret, M. & Michon, F. (1990). Analysis of oligosaccharide epitopes of meningococcal lipopolysaccharides by fast-atom-bombardment mass spectrometry. *Carbohydr. Res. 200*, 59-76.

Dienst, R. B. (1948). Virulence and antigenicity of *Haemophilus ducreyi*. *Am. J. Syph. Gonorrheae Vener. Dis. 32*, 289-291.

Doebber, T. W., Wu, M. S., Robbins, J. C., Choy, B. M., Chang, M. N. & Chen, T. Y. (1985). Platelet activating factor (PAF) involvement in endotoxin induced hypotension in rats. Studies with PAF-receptor antagonist kadsurenone. *Biochem. Biophys. Res. Commun. 127*, 799-808.

Domon, B. & Costello, C. E. (1988). A systematic nomenclature for carbohydrate Fragmentations in FAB-MS/MS spectra of glycoconjugates. *Glycoconjugate J. 5*, 397-409.

Ducreyi, A. (1889). Experimentelle Untersuchungen uber den Ansteckungsstoff des weichen Schankers und uber die Bubonen. *Monatsh. Prakt. Dermatol. 9*, 387-405.

Dudas, K. C. & Apicella, M. A. (1988). Selection and Immunochemical Analysis of Lipooligosaccharide Mutants of *Neisseria gonorrhoeae*. *Infect. Immun. 56*, 499-504.

Edmonds, C. G. & Smith, R. D. (1990). Electrospray Ionization Mass Spectrometry. Methods in Enzymology Vol. 193. New York, Academic Press. 412-431.

Estabrook, M. N., Christopher, N. C., Griffiss, J. M., Baker, C. J. & Mandrell, R. E. (1992). Sialylation and human neutrophil killing of group C *Neisseria meningitidis*. *J. Infect. Dis. 166*, 1079-88.

Falick, A. M., Wang, G. H. & Walls, F. C. (1986). Ion source for liquid matrix secondary ionization mass spectrometry. *Anal. Chem. 58*, 1308-1311.

Feiner, R. R., Motara, F. & Levenkron, E. (1945). Infectivity of *Haemophilus ducreyi* for the rabbit and the development of skin hypersensitivity. *Sm. J. Syph. Gonorrheae Vener. Dis. 29*, 71-79.

Fenn, J. B., Mann, M., Meng, C. K. & Wong, S. F. (1990). Electrospray ionization-principles and practice. *Mass Spectrom. Rev. 9*, 37-70.

Frangipane, J. V. & Rest, R. F. (1993). Anaerobic growth and cytidine 5'-monophosphate-*N*-acetylnueraminic acid act synergistically to induce high-level serum resistance in *Neisseri gonorrhoeae. Infect. Immun. 61*, 1657-1666.

Galanos, C., Luderitz, O., Rietschel, E. T. & Westphal, O. (1977). Newer aspects of the chemistry and biology of bacterial lipopolysaccharides with special reference to their lipid A component. International Review of Biochemistry Vol. 14. Baltimore, University Park Press. 239-335.

Gamian, A., Beurret, M., Michon, F., Brisson, J.-R. & Jennings, H. J. (1992). Structure of the L2 lipopolysaccharide core oligosaccharides of *Neisseria meningitidis. J. Biol. Chem. 267*, 922-925.

Gibson, B. W., Melaugh, W., Phillips, N. J., Apicella, M. A., Campagnari, A. A. & Griffiss, J. M. (1993). Investigation of the structural heterogeneity of lipooligosaccharides (LOS) from pathogenic *Haemophilus* and *Neisseria* species and R-type lipopolysaccharides (LPS) from *Salmonella typhimurium* by electrospray mass spectrometry. *J. Bacteriol. 175*, 2702-2712.

Gibson, B. W., Webb, J. W., Yamasaki, R., Fisher, S. J., Burlingame, A. L., Mandrell, R. E., Schneider, H. & Griffiss, J. M. (1989). Structure and heterogeneity of the oligosaccharides from the lipopolysaccharides of a pyocin-resistant *Neisseria gonorrhoeae*. *Proc. Natl. Acad. Sci. USA 86*, 17-21.

Gillece-Castro, B. L. & Burlingame, A. L. (1990). Oligosaccharide characterization with high-energy collision-induced dissociation mass spectrometry. Methods in Enzymology Vol. 193. New York, Academic Press. 689-712.

Gray, G. R. (1990). Linkage Analysis Using Reductive Cleavage Method. Methods in Enzymology Vol. 193. New York, Academic Press. 573-578.

Greenblatt, R. (1990). Chancroid could be coming to your community. *Infect. Dis. News 3*, 1-4.

Gregg, C. R., Melly, M. A., Hellerqvist, C. G., Coniglio, J. G. & McGee, Z. A. (1981). Toxic activity of purified lipopolysaccharide of *Neisseria gonorrhoeae* for human fallopian tube mucosa. *J. Infect. Dis. 143*, 432-439.

Griffiss, J. M., Schneider, H., Mandrell, R. E., Yamasaki, R., Jarvis, G. A., Kim, J. J., Gibson, B. W., Hamadeh, R. & Apicella, M. A. (1988). Lipooligosaccharides: the principal glycolipids of the neisserial outer membrane. *Rev. Infect. Dis. 10*, s287-s295.

Hakomori, S. (1964). A rapid permethylation of glycolipid and polysaccharide catalyzed by methylsulfinyl carbanion in dimethylsulfoxide. *J. Biochem. 55*, 205-208.

Hall, L. D. & Saunders, J. K. M. (1980). Complete analysis of ^{1}H NMR spectra of complex natural products using a combination of one- and two-dimensional techniques. 1-Dehydrosterone. *J. Amer. Chem. Soc. 102*, 5703-5711.

Hardy, M. R., Townsend, R. R. & Lee, Y. C. (1988). Monosaccharide Analysis of Glycoconjugates by Anion Exchange Chromatography with Pulsed Amperometric Detection. *Anal. Biochem. 170*, 54-62.

Helander, I. M., Lindner, B., Brade, H., Altmann, K., Lindberg, A. A., Rietschel, E. T. & Zähringer, U. (1988). Chemical structure of the lipopolysaccharide of *Haemophilus influenzae* strain I-69 Rd^{-}/B^{+}. Description of a novel deep-rough chemotype. *Eur. J. Biochem. 177*, 483-492.

Hellerquist, C. G. & Sweetman, B. J. (1990). Mass Spectrometry of Carbohydrates. *Biomedical Applications of Mass Spectrometry 34*, 91-143.

Hillenkamp, F. & Karas, M. (1990). Mass Spectrometry of Peptides and Proteins by Matrix-Assisted Ultraviolet Laser Desorption/Ionization. Methods in Enzymology Vol. 193. New York, Academic Press. 280-295.

Honda, S. (1984). High-Performance Liquid Chromatography of Mono- and Oligosaccharides. *Anal. Biochem. 140*, 1-13.

Ingaki, F., Kohda, D., Kodama, C. & Susuki, A. (1987). Analysis of NMR spectra of sugar chains of glycolipids by multiple relayed COSY and 2D homonuclear Hartman-Hahn spectroscopy. *FEBS Lett. 212*, 91-97.

Inzana, T. J. (1983). Electrophoretic heterogeneity and interstrain variation of the lipopolysaccharide of *Haemophilus influenzae*. *J. Infect. Dis. 148*, 492-499.

Jennings, H. J., Johnson, K. G. & Kenne, L. (1983). The structure of an R-type oligosaccharide core obtained from some lipopolysaccharides of *Neisseria meningitidis*. *Carbohydr. Res. 121*, 233-241.

Jennings, H. J., Katzenellenbogen, E., Lugowski, C., Michon, F., Roy, R. & Kasper, D. L. (1984). Structure, conformation and immunology of sialic-acid containing polysaccharides of human pathogenic bacteria. *Pure and Appl. Chem. 56*, 893-905.

John, C. M. (1990). Structural elucidation of outer membrane lipooligosaccharides from *Neisseria gonorrhoeae*. University of California at San Francisco.

John, C. M. & Gibson, B. W. (1990). Amino and Hydrazinoalkyl Benzoates for the Separation and Mass Spectrometric Analysis of Oligosaccharides from Bacterial Lipooligosaccharides. *Anal. Biochem. 187*, 8523-8527.

John, C. M., Griffiss, J. M., Apicella, M. A., Mandrell, R. E. & Gibson, B. W. (1991). The Structural Basis for Pyocin Resistance in *Neisseria gonorrhoeae* Lipooligosaccharides. *J. Biol. Chem. 266*, 19303-19311.

Johnson, A. P., Abeck, D. & Davies, H. A. (1988). The structure, pathogenicity and genetics of *Haemophilus ducreyi*. *J. Infect. 17*, 99-106.

Johnson, R. S., Her, G.-R., Grabarek, J., Hawiger, J. & Reinhold, V. N. (1990). Structural characterization of monophosphoryl lipid A homologs obtained from *Salmonella minnesota* Re595 lipopolysaccharide. *J. Biol. Chem. 265*, 8108-8116.

Johnson, R. S., Lam, Z. & Reinhold, V. N. (1990). Structural characterization of a new lipid A obtained from *C. burnetti*, the causative agent of Q fever. 38th ASMS Conference on Mass Spectrometry and Allied Topics, Tucson, Arizona, 1347-1348.

Karibian, D., Deprun, C., Szabo, L., Le Beyec, Y. & Caroff, M. (1991). ^{252}Cf-plasma desorption mass spectrometry applied to the analysis of endotoxin Lipid A preparations. *International Journal of Mass Spectrometry and Ion Processes 111*, 273-286.

Khoo, K.-H. & Dell, A. (1990). Assignment of anomeric configurations of pyranose sugars in oligosaccharides using a sensitive FAB-MS strategy. *Glycobiology 1*, 83-91.

Kibukamusoke, J. W. (1965). Venereal disease in East Africa. *Trans. R. Soc. Trop. Med. Hyg. 59*, 642-648.

Kim, J., Zhou, D., Mandrell, R. E. & Griffiss, J. M. (1992). Effect on exogenous sialylation of the lipooligosaccharides of *Neisseria gonorrhoeae* on opsonophagocytosis. *Infect. Immun. 60*, 4439-4442.

Kumar, A., Ernst, R. R. & Wuthrich, K. (1980). A two-dimensional nuclear overhauser enhancement (2d NOE) experiment for the elucidation of complete proton-proton cross-relaxation networks in biological macromolecules. *Biochem. Biophys. Res. Commun. 95*, 1-6.

Laemmli, U. K. (1970). Cleavage of structural proteins during assembly of the head of bacteriophage T4. *Nature 227*, 680-685.

Lagergård, T., M., P. & Frisk, A. (1993). Evidence of *Haemophilus ducreyi* adherence to and cytotoxin destruction of human epithelial cells. *Microb. Pathog. 14*, 417-431.

Lagergård, T. & Purven, M. (1993). Neutralizing antibodies to *Haemophilus ducreyi* cytotoxin. *Infect. Immun. 61*, 1589-1592.

Lammel, C. J., Dekker, N. P., Palefsky, J. & Brooks, G. F. (1993). In Vitro model of *H. ducreyi* adherence to and entry into eukaryotic cells of genital orgin. *J. Infect. Dis. 167*, 642-650.

Larson, G., Karlsson, H., Hansson, G. C. & Pimlott, W. (1987). Application of a simple methylation procedure for the analysis of glycosphingolipids. *Carbohydr. Res. 161*, 281-290.

Lerner, L. & Bax, A. (1987). Application of New, High-Sensitivity, ^{1}H-^{13}C-N.M.R.-Spectral Techniques to the Study of Oligosaccharides. *Carbohydr. Res. 166*, 35-46.

Lesse, A. J., Campagnari, A. A., Bittner, W. E. & Apicella, M. A. (1990). Increased Resolution of Lipopolysaccharides and Lipooligosaccharides Utilizing Tricine-Sodium-Dodecyl-Sulfate Polyacrylamide Gel Electrophoresis. *J. Immunol. Methods 126*, 109-117.

Levery, S. B. & Hakomori, S. (1987). Microscale methylation analysis of glycolipids using capillary gas chromatography-chemical ionization mass fragmentography with

selected ion monitoring. Methods in Enzymology Vol. 138. New York, Academic Press. 13-25.

Lindberg, B. (1981). Structural studies of polysaccharides. *Chem. Soc. Rev. 10*, 409-434.

Luderitz, O., Staub, A. M. & Westphal, O. (1966). Immunochemistry of O and R antigens of *Salmonella* and related *Enterobacteriaceae. Bacteriol. Revs. 30*, 192-255.

Maley, F., Trimble, R. B., Tarentino, A. L. & Plummer, T. H. (1989). Characterization of glycoproteins and their associated oligosaccharides through the use of endoglycosidases. *Anal. Biochem. 180*, 195-204.

Mandrell, R. E., Griffiss, J. M. & Macher, B. A. (1988). Lipooligosaccharides (LOS) of *Neisseria gonorrhoeae* and *Neisseria meningitidis* Have Components that are Immunochemically Similar to Precursors of Human Blood Group Antigens. Carbohydrate Sequence Specificity of the Mouse Monoclonal Antibodies that Recognize Crossreacting Antigens on LOS and Human Erythrocytes. *J. Exp. Med. 168*, 107-126.

Mandrell, R. E., Kim, J. J., John, C. M., Gibson, B. W., Sugai, J. V., Apicella, M. A., Griffiss, J. M. & Yamasaki, R. (1991). Endogenous sialylation of lipooligosaccharides of *Neisseria meningitidis. J. Bacteriol. 173*, 2823-2832.

Mandrell, R. E., Lesse, A. J., Sugai, J. V., Shero, M., Griffiss, J. M., Cole, J. A., Parsons, N. J., Smith, H., Morse, S. A. & Apicella, M. A. (1990). In vitro and in vivo modification of *Neisseria gonorrhoeae* lipooligosaccharide epitope structure by sialylation. *J. Exp. Med. 171*, 1649-1664.

Mandrell, R. E., McLaughlin, R., Abu Kwaik, Y., Lesse, A., Yamasaki, R., Gibson, B., Spinola, S. M. & Apicella, M. A. (1992). Lipooligosaccharides (LOS) of some *Haemophilus* species mimic human glycosphingolipids, and some LOS are sialylated. *Infect. Immun. 60*, 1322-1328.

Marion, D. & Wüthrich, K. (1983). Application of phase sensitive two-dimensional correlated spectroscopy (COSY) for measurements of ^{1}H-^{1}H spin-spin coupling constants in proteins. *Biochem. Biophys. Res. Commun. 113*, 967-974.

Masoud, H., Weintraub, S. T., Wang, R., Cotter, R. & Holt, S. C. (1991). Investigation of the structure of lipid A from *Actinobacillus actinomycetemcomitans* strain Y4 and the human clinical isolate PO 1021-7. *Eur. J. Biochem. 200*, 775-779.

Melaugh, W., Phillips, N. J., Campagnari, A. A., Karalus, R. & Gibson, B. W. (1992). Partial characterization of the major lipooligosaccharide from a strain of *Haemophilus ducreyi*, the causative agent of chancroid, a genital ulcer disease. *J. Biol. Chem. 267*, 13434-13439.

Michon, F., Beurret, M., Gamian, A., Brisson, J.-R. & Jennings, H. J. (1990). Structure of the L5 Lipopolysaccharide Core Oligosaccharides of *Neisseria meningitidis*. *J. Biol. Chem. 265*, 7243-7247.

Morse, S. A. (1989). Chancroid and *Haemophilus ducreyi*. *Clin. Microbiol. Rev. 2*, 137-157.

Morse, S. A., Vaughn, P., Johnson, D. & Iglewski, B. H. (1976). Inhibition of *Neisseria gonorrhoeae* by a bacteriocin from *Pseudomonas aeruginosa*. *Antimicrob. Agents Chemother. 10*, 354-362.

Mossman, T. (1983). Rapid colormetric assay for cellular growth and survival: application to proliferation and cytotoxicity assay. *J. Immunol. Methods 65*, 55-63.

Odumeru, J. A., Ronald, A. R. & Albritton, W. L. (1983). Characterization of cell proteins of *Haemophilus ducreyi* by polyacylamide gel electrophoresis. *J. Infect. Dis. 148*, 710-714.

Odumeru, J. A., Wiseman, G. M. & Ronald, A. R. (1985). Role of lipopolysaccharide and complement in susceptibility of *Haemophilus ducreyi* to human serum. *Infect. Immun. 50*, 495-499.

Odumeru, J. A., Wiseman, G. M. & Ronald, A. R. (1987). Relationship between lipopolysaccharide composition and virulence of *Haemophilus ducreyi*. *J. Med. Microbiol. 23*, 155-163.

Palmer, K. L. & Munson Jr., R. S. (1993). Identification of a hemolysin produced by *Haemophilus ducreyi* and isolation of a Tn916 transposon mutant. *Abst. Amer. Soc. Microbiol.* B-278.

Parsons, N. J., Andrade, J. R. C., Patel, P. V., Cole, J. A. & Smith, H. (1989). Sialylation of lipopolysaccharides and loss of absorption of bacterial antibody during conversion of gonococci to serum resistance by cytidine 5'-monophosphate-N-acetyl neuraminic acid. *Microb. Pathog. 7*, 63-72.

Parsons, N. J., Patel, P. V., Tan, E. L., Andrade, J. R. C., Nairn, C. A., Goldner, M., Cole, J. A. & Smith, H. (1988). Cytidine 5'-monophospho-*N*-acetylneuraminic acid and a low molecular weight factor from human blood cells induce lipopolysaccharide alteration in gonococci when conferring serum resistance to killing by huamn serum. *Microb. Pathog. 5*, 303-309.

Phillips, N. J., Apicella, M. A., Griffiss, J. M. & Gibson, B. W. (1992). Structural characterization of the cell surface lipooligosaccharides from a nontypable strain of *Haemophilus influenzae. Biochemistry 31*, 4515-4526.

Phillips, N. J., Apicella, M. A., Griffiss, J. M. & Gibson, B. W. (1993). Structural studies of the lipooligosaccharides from *Haemophilus influenzae* type b strain A2. *Biochemistry 32*, 2003-2012.

Phillips, N. J., John, C. M., Reinders, L. G., Gibson, B. W., Apicella, M. A. & Griffiss, J. M. (1990). Structural models for the cell surface lipooligosaccharides of *Neisseria gonorrhoeae* and *Haemophilus influenzae. Biomed. Environ. Mass Spectrom. 19*, 731-745.

Poulter, L. & Burlingame, A. L. (1990). Desorption Mass Spectrometry of Oligosaccharides Coupled with Hydrophobic Chromophores. Methods in Enzymology Vol. 193. New York, Academic Press. 661-689.

Purcell, B. K., Richardson, J. A., Radolf, J. D. & Hansen, E. J. (1991). A temperature-dependent rabbit model for production of dermal lesions by *Haemophilus ducreyi. J. Infect. Dis. 164*, 359-67.

Purven, M. & Lagergård, T. (1992). *Haemophilus ducreyi*, a cytotoxin-producing bacterium. *Infect. Immun. 60*, 1156-1162.

Radziejewska-Lebrecht, J. & Mayer, H. (1989). The core region of *Proteus mirabilis* R110/1959 lipopolysaccharide. *Eur. J. Biochem. 183*, 573-581.

Rance, M., Sorensen, O. W., Bodenhausen, G., Wagner, G., Ernst, R. R. & Wüthrich, K. (1983). Improved Spectral Resolution in COSY ^{1}H NMR Spectra of Proteins via Double Quantum Filtering. *Biochem. Biophys. Res. Commun. 117*, 479-485.

Redfield, A. G. & Kuntz, S. D. (1975). Quadrature fourier NMR detection: simple multiplex for dual detection and discussion. *J. Magn. Reson. 19*, 250-254.

Reitschel, E. T. (1976). Absolute configuration of 3-hydroxy fatty acids present in lipopolysaccharides from various bacterial groups. *Eur. J. Biochem. 64*, 423-428.

Rest, R. F. & Frangipane, J. V. (1992). Growth of *Neisseria gonorrhoeae* in CMP-*N*-Acetylneuraminic Acid Inhibits Nonopsonic (Opacity-Associated Outer Membrane Protein-Mediated) Interactions with Human Neutrophils. *Infect. Immun. 60*, 989-997.

Romanowska, E., Gamian, A., Lugowski, C., Romanowska, A., Dabrowski, J., Hauck, M., Opferkuch, H. J. & von der Lieth, C.-W. (1988). Structure Elucidation of the Core Regions from *Citrobacter* O4 and O36 Lipopolysaccharides by Chemical and Enzymatic Methods, Gas Chromatography/Mass Spectrometry, and NMR Spectroscopy at 500 MHz. *Biochemistry 27*, 4153-4161.

Rosam, A. C., Wallace, J. L. & Whittle, B. J. R. (1986). Potent ulcerogenic actions of platelet activating factor on the stomach. *Nature 319*, 54-56.

Schauer, R. (1985). Sialic acids and their role as biological masks. *TIBS* 357-360.

Schweda, E. K. H., Hegedus, O. E., Borrelli, S., Lindberg, A. A., Weiser, J. N., Maskell, D. J. & Moxon, E. R. (1993). Structural studies of the saccharide part of the cell envelope lipopolysaccharide from *Haemophilus influenzae* strain AH1-3 (*lic* 3 +). *Carbohydr. Res. 246*, 319-330.

Shaw, J. H. & Falkow, S. (1988). Model for invasion of human tissue culture cells by *Neisseria gonorrhoeae. Infect. Immun. 56*, 1625-1632.

Smith, H. (1977). Microbial surfaces in relation to pathogenicity. *Bact. Rev. 41*, 475-500.

Spinola, S. M., Castellazzo, A., Shero, M. & Apicella, M. A. (1990). Characterization of pili expressed by *Haemophilus ducreyi. Microb. Pathog. 9*, 417-26.

Spinola, S. M., Griffiths, G. E., Bodgan, J. & Menegus, M. A. (1992). Characterization of an 18,000-molecular-weight outer membrane protein of *Haemophilus ducreyi* that contains a conserved surface-exposed epitope. *Infect. Immun. 60*, 385-391.

Spinola, S. M., Griffiths, G. E., Shanks, K. L. & Blake, M. S. (1993). The major outer membrane protein of *Haemophilus ducreyi* is a member of the OmpA family of proteins. *Infect. Immun. 61*, 1346-1351.

Spinola, S. M., Wild, L. M., Apicella, M. A., Gaspari, A. A. & Campagnari, A. A. (1994). Experimental human infection with *Haemophilus ducreyi*. *J. Infect. Dis. 169*, 1146-1150.

Springer, T. A. & Lasky, L. A. (1991). Sticky sugars for selectins. *Nature 349*, 196-197.

States, D. J., Haberkorn, R. A. & Ruben, D. J. (1982). A Two-Dimensional Nuclear Overhauser Experiment with Pure Absorption Phase in Four Quadrants. *J. Magn. Reson. 48*, 286-292.

Sullivan, M. (1940). Chancroid. *Am. J. Syph. Gonorrheae Vener. Dis. 24*, 482-521.

Takayama, K., Qureshi, N., Hyver, K., Honovich, J., Cotter, R. J., Mascagni, P. & Schneider, H. (1986). Characterization of a structural series of lipid A obtained from the lipopolysaccharides of *Neisseria gonorrhoeae*. *J. Biol. Chem. 261*, 10624-10631.

Takayama, K., Qureshi, N., Mascagni, P., Nashed, M. A., Anderson, L. & Raetz, C. R. H. (1988). Fatty acyl derivatives of glucosamine 1-phosphate in *Escherchia coli* and their relation to lipid A. *J. Biol. Chem. 258*, 7379-7385.

Tan, E. L., Patel, P. V., Parsons, N. J., Martin, P. M. V. & Smith, H. (1986). Lipopolysaccharide alteration is associated with induced resistance of *Neisseria gonorrhoeae* to killing by human serum. *J. Gen. Microbiol. 132*, 1407-1413.

Taylor, D. N., Echeverria, P., Hanchalay, S., Pitarangsi, L., Slootman, L. & Piot, P. (1985). Antimicrobial susceptibility and characterization of outer membrane proteins of *Haemophilus ducreyi* isolated in Thailand. *J. Clin. Microbiol. 21*, 442-444.

Totten, P. A., Morton, W. R., Knitter, G. H., Clark, A. M., Kiviat, N. B. & Stamm, W. E. (1994). A Primate Model for Chancroid. *J. Infect. Dis. 169*, 1284-1290.

Townsend, R. R., Hardy, M. R., Hindsgaul, O. & Lee, Y. C. (1988). High-performance anion-exchange chromatography of oligosaccharides using pelicular resins and pulsed amperometric detection. *Anal. Biochem. 174*, 459-470.

Trees, D. L., Arko, R. J. & Morse, S. A. (1991). Mouse subcutaneous chamber model for in vivo growth of *Haemophilus ducreyi. Microb. Pathog. 11*, 387-390.

Tsai, C. M. & Frasch, C. E. (1982). A sensitive silver stain for detecting lipopolysaccharides in polyacrylamide gels. *Anal. Biochem. 119*, 115-119.

Tuffrey, M., Alexander, F., Ballard, R. C. & Taylor, R. D. (1990). Characterization of skin lesions in mice following intradermal inoculation of *Haemophilus ducreyi. J. Exp. Pathol. (Oxford) 71*, 233-244.

Vaghefi, M. M., Bernaccki, R. J., Dalley, N. K., Wilson, B. E. & Robins, R. K. (1987). Synthesis of glycopyranosylphosphonate analogues of certain natural nucleoside diphosphate sugars as potential inhibitors of glycosyltransferases. *J. Med. Chem. 30*, 1383-1391.

Walls, F. C., Baldwin, M. A., Falick, A. M., Gibson, B. W., Kaur, S., Maltby, D. A., Gillece-Castro, B. L., Medzihradszky, K. F., Evans, S. & Burlingame, A. L. (1990). Experience with multichannel array detection in tandem mass spectrometric characterization

of biopolymers at the picomole level. Biological Mass Spectrometry. Amsterdam, Elsevier. 197-216.

Webb, J. W., Jiang, K., Gillece-Castro, B. L., Tarentino, A. L., Plummer, T. H., Byrd, J. C., Fisher, S. J. & Burlingame, A. L. (1988). Structural characterization of intact, branched oligosaccharides by high performance liquid chromatography and liquid secondary ion mass spectrometry. *Anal. Biochem. 169*, 337-349.

Weisner, P., Brown, S., Kraus, S. & Perine, P. (1983). Perspectives in sexually transmitted diseases. New York, McGraw-Hill. 219-234.

Westphal, O. & Jahn, K. (1965). Bacterial lipopolysaccharides: extraction with phenol-water and further applications of the procedure. Methods in Carbohydrate Chemistry. New York, Academic Press. 83-91.

Wetzler, L. M., Barry, K., Blake, M. S. & Gotschlich, E. C. (1992). Gonococcal lipooligosaccharide sialylation prevents complement-dependent killing by immune sera. *Infect. Immun. 60*, 39-43.

Yamasaki, R., Bacon, B. E., Nasholds, W., Schneider, H. & Griffiss, J. M. (1991). Structural determination of oligosaccharides derived from lipooligosaccharide of *Neisseria gonorrhoeae* F62 by chemical, enzymatic, and two-dimensional NMR methods. *Biochemistry 30*, 10566-10575.

Yamasaki, R., Griffiss, J. M., Quinn, K. P. & Mandrell, R. E. (1993). Neuraminic acid is α2→3 linked in the lipooligosaccharide of *Neisseria meningitidis* serogroup B strain 6275. *J. Bacteriol. 175*, 4565-4568.

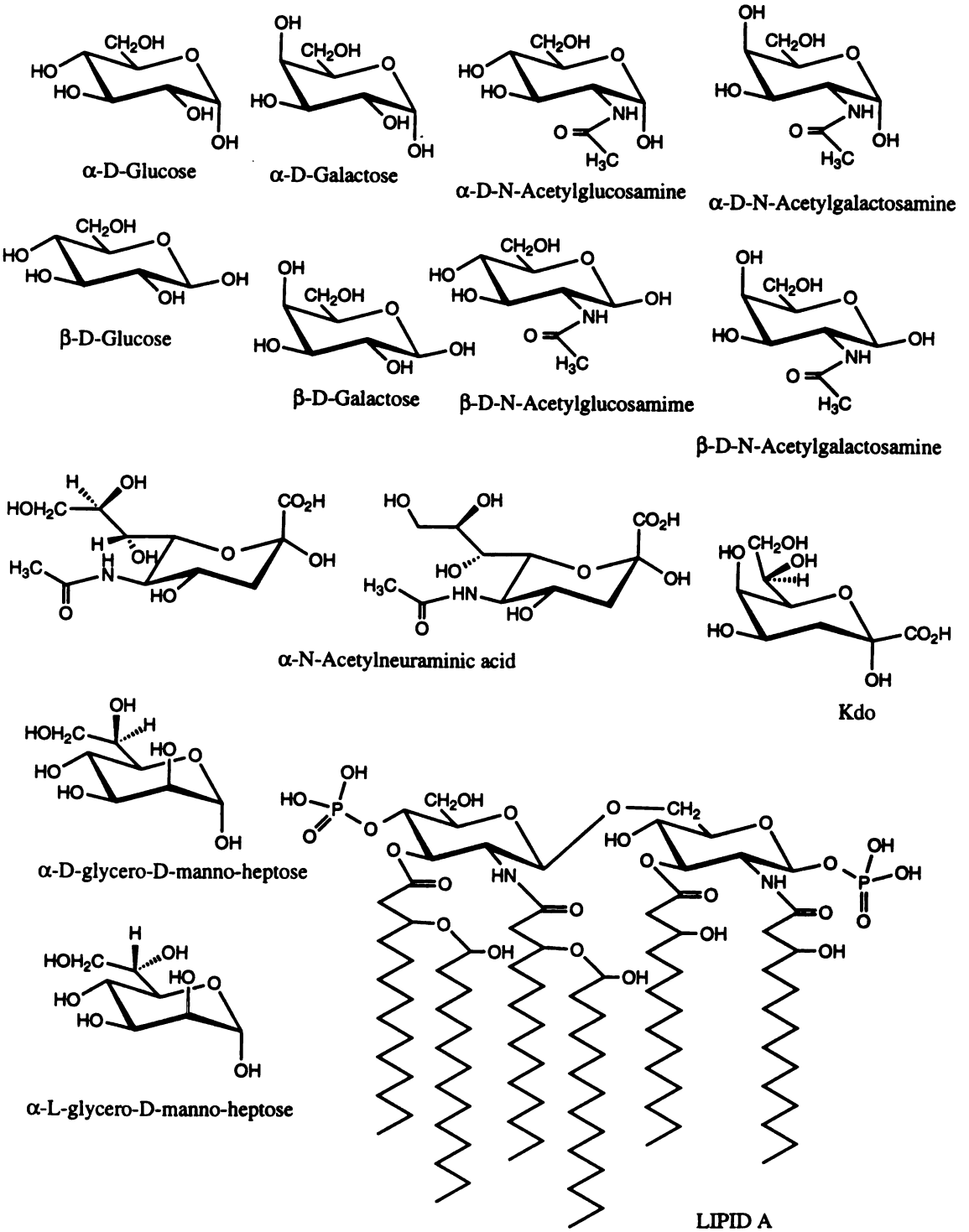

Figure 1. Structures of bacterial LOS components

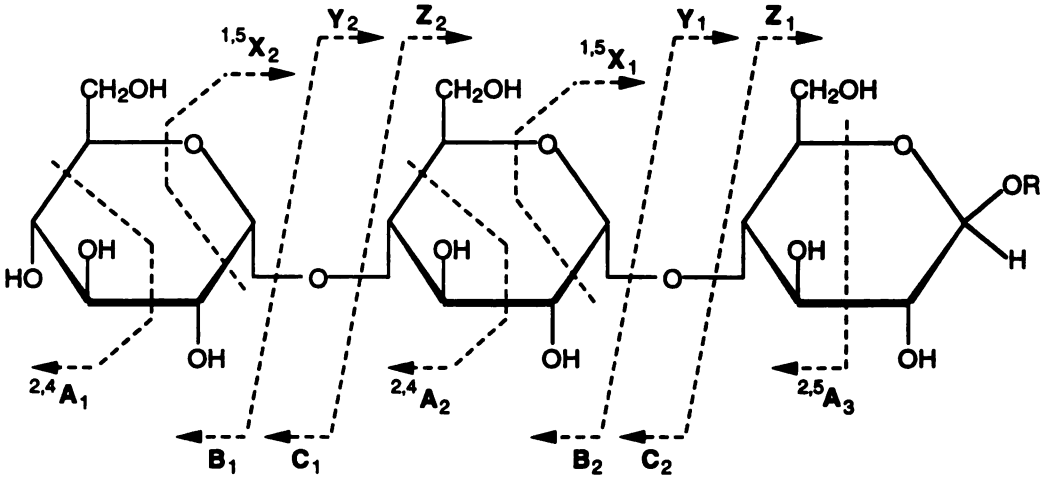

Figure 2. Mass spectrometric fragmentation types and nomenclature for carbohydrates adapted from Domon and Costello (1988). Most fragmentation processes involve the transfer of protons. For example, in the negative-ion mode deprotonation may occur on a hydroxyl group adjacent to the glycosidic bond. The resulting oxyanion can form an epoxide breaking the glycosidic bond in the process. The expelled fragment retains the glycosidic oxygen forming a C ion. Often during this process a proton is transferred from a hydroxyl group on the epoxide yielding a Z ion.

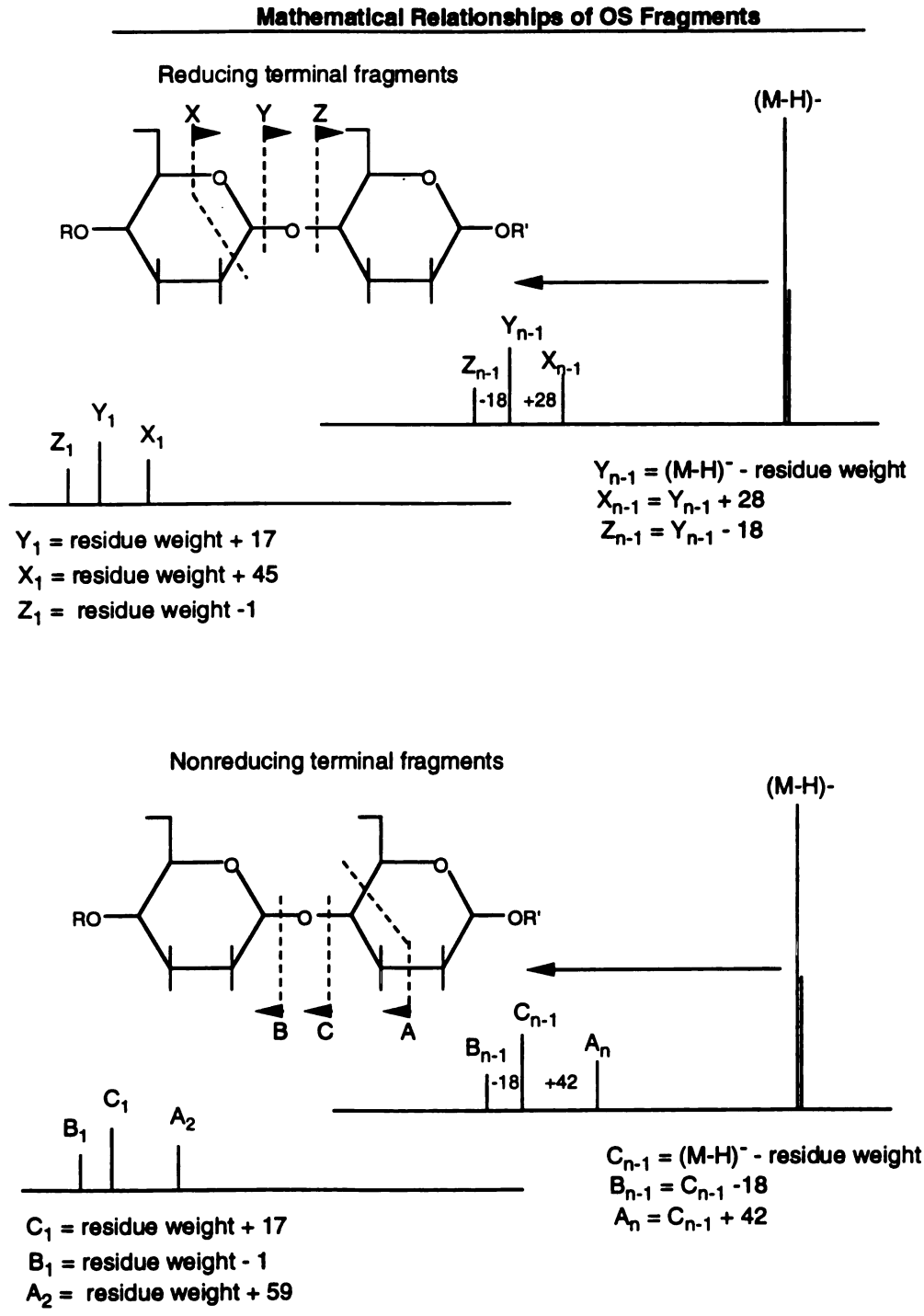

Figure 3. Mathematical relationship among oligosaccharide fragments observed in mass spectrometry.

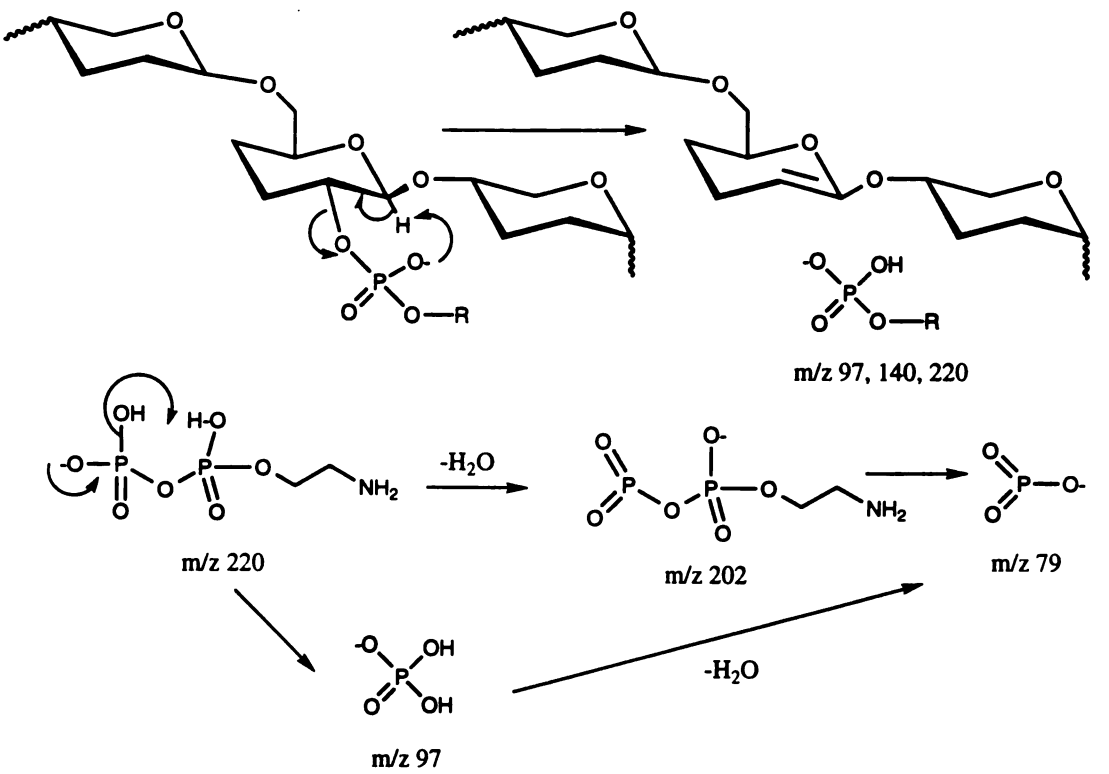

Figure 4. Fragmentation pattern of phosphate esters observed in high energy CID tandem mass spectrometry.

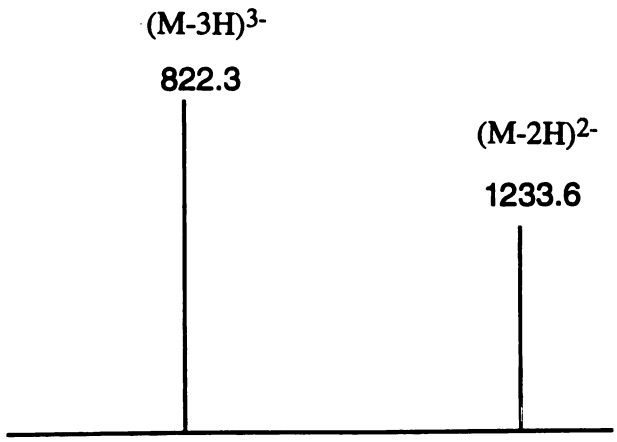

Figure 5. Method for calculating charge state and molecular weight from two adjacent peaks in an electrospray spectrum that differ by one charge. This example is based on the ESI-MS spectrum of *H. ducreyi* strain 188-2 shown in Figure 4.4B.

Let n_1 = charge on ion at *m/z* 822.3 Let n_2 = charge on ion at *m/z* 1233.6

Let m_1 = mass of 822.3 ion Let m_2 = mass of 1233.6 ion

Let M = molecular weight $m_2 > m_1$ and $n_1 > n_2$

If $n_2 = n_1 - 1$, then since this is a negative-ion spectrum $n_2 = (m_1 + 1)/(m_2 - m_1)$

$M = n_2(m_2 + 1)$ $m_1 = (M + n_1)/n_1$ and $m_2 = (M + n_2)/n_2$

Therefore $n_2 = (822.3 + 1)/(1233.6 - 822.3) = 2.00$

and $M = 2(1233.6 + 1) = 2469.2$

LOS Oligosaccharide Table

Sugar	M_r	In Chain: Nominal	Exact	Average
Hexose	**180** 180.06339 $C_6H_{12}O_6$	**162** $C_6H_{10}O_5$	**162**.052823	**162**.1424
Heptose	**210** 210.073955 $C_7H_{14}O_7$	**192** $C_7H_{12}O_6$	**192**.06339	**192**.1687
HexNAc	**221** $C_8H_{15}O_6N_1$	**203** $C_8H_{13}O_5N_1$	**203**.079372	**203**.1950
KDO	**238** $C_8H_{14}O_8$	**220** $C_8H_{12}O_7$	**220**.058302	**220**.1791
***anhdro*KDO**	**220** $C_8H_{12}O_7$	**202** $C_8H_{10}O_6$	**202**.04774	**202**.1638
NeuAc	**309** $C_{11}H_{19}O_9N$	**291** $C_{11}H_{17}O_8N$	**291**.095416	**291**.2579
P	**98** H_3PO_4	**80** HPO_3	**79**.966269	**79**.9799
PEA	**141** $C_2H_8O_4N_1P_1$	**123** $C_2H_6O_3N_1P_1$	**123**.0084678	**123**.0483
O-DPLA	**952** $C_{40}H_{78}O_{19}N_2P_2$ (ave =**953.0089**)	**934** $C_{40}H_{76}O_{18}N_2P_2$	**934**.4567	**934**.9936
Ac	**58** $C_2H_4O_2$	**42** $C_2H_2O_1$	**42**.010565	**42**.0373
H_2O		**+18** H_2O	**18**.010565	**18**.0153

Element	exact mass	average mass
C = 12	12.00000	12.011
H = 1	1.007825	1.00794
O = 16	15.9949146	15.9994
N = 14	14.0030740	14.00674
P = 31	30.973765	30.97376

Table 1. Elemental compositions and masses of bacterial LOS components. O-DPLA represents *O*-deacylated diphosphorylated lipid A.

Table 2A

Gretta Carbos Search Output for *H. ducreyi* oligosaccharides $(M-H)^-$ at m/z 1676.5

Looking for mass **1677.5000**
Tolerence + or - 0.300000
Core(mins) set at 238.0580 1 KDO 1 H2O

Settings	min	max
Hex	0	5
Hep	0	5
HexNAc	0	5
phosphate	0	0
PEA	0	4
dehydro	0	1
NeuAc	0	0
KDO	1	0
OAc	0	0

No.	Mass	Hex	Hep	HexNAc	phosph	PEA	dehydr	NeuAc	KDO	OAc
1	1677.54	3	4	1	0	0	1	0	1	0

Table 2B

Gretta Carbos Search Output for *H. ducreyi* O-deacylated LOS, pyocin variant strain 188-2

Looking for mass 2276.8000
Tolerence + or - 2.000000
Core(mins) set at 1445.3213 1 Heptos 1 Phosph 1 O-DPLA 1 KDO 1 H_2O

Settings	min	max
Hexose	0	6
Heptose	1	4
HexNAc	0	5
Phosphate	1	2
PEA	0	2
O-DPLA	1	1
NeuAc	0	1
KDO	1	1
	0	0

No.	Mass	Hexose	Heptos	HexNAc	Phosph	PEA	O-DPLA	NeuAc	KDO	
1	2274.98	1	3	1	2	0	1	0	1	0
2	**2276.99**	**2**	**3**	**0**	**1**	**1**	**1**	**0**	**1**	**0**

Looking for mass 2307.3000
Tolerence + or - 2.000000
Core(mins) set at 1445.3213 1 Heptos 1 Phosph 1 O-DPLA 1 KDO 1 H_2O

Settings	min	max
Hexose	0	6
Heptose	1	4
HexNAc	0	5
Phosphate	1	2
PEA	0	2
O-DPLA	1	1
NeuAc	0	1
KDO	1	1
	0	0

No.	Mass	Hexose	Heptos	HexNAc	Phosph	PEA	O-DPLA	NeuAc	KDO	
1	2307.02	1	4	0	1	1	1	0	1	0
2	2306.96	2	1	0	1	2	1	1	1	0

Looking for mass 2469.5000
Tolerence + or - 2.000000
Core(mins) set at 1445.3213 1 Heptos 1 Phosph 1 O-DPLA 1 KDO 1 H_2O

Settings	min	max
Hexose	0	6
Heptose	1	4
HexNAc	0	5
Phosphate	1	2
PEA	0	2
O-DPLA	1	1
NeuAc	0	1
KDO	1	1
	0	0

(continued overleaf)

Table 2B (continued)

No.	Mass	Hexose	Heptos	HexNAc	Phosph	PEA	O-DPLA	NeuAc	KDO	
1	2469.05	0	1	2	2	2	1	1	1	0
2	2469.21	0	1	3	1	1	1	1	1	0
3	2471.12	0	4	1	1	2	1	0	1	0
4	2469.16	2	4	0	1	1	1	0	1	0
5	2469.10	3	1	0	1	2	1	1	1	0

Looking for mass 2592.0000
Tolerence + or - 2.000000
Core(mins) set at 1445.3213 1 Heptos 1 Phosph 1 O-DPLA 1 KDO 1 H_2O

Settings	min	max
Hexose	0	6
Heptose	1	4
HexNAc	0	5
Phosphate	1	2
PEA	0	2
O-DPLA	1	1
NeuAc	0	1
KDO	1	1
	0	0

No.	Mass	Hexose	Heptos	HexNAc	Phosph	PEA	O-DPLA	NeuAc	KDO	
1	2592.26	0	1	3	1	2	1	1	1	0
2	2590.19	1	4	1	2	1	1	0	1	0
3	2590.36	1	4	2	1	0	1	0	1	0
4	2590.14	2	1	1	2	2	1	1	1	0
5	2590.30	2	1	2	1	1	1	1	1	0
6	2592.21	2	4	0	1	2	1	0	1	0

Looking for mass 2712.7000
Tolerence + or - 2.000000
Core(mins) set at 1445.3213 1 Heptos 1 Phosph 1 O-DPLA 1 KDO 1 H_2O

Settings	min	max
Hexose	0	6
Heptose	1	4
HexNAc	0	5
Phosphate	1	2
PEA	0	2
O-DPLA	1	1
NeuAc	0	1
KDO	1	1
	0	0

No.	Mass	Hexose	Heptos	HexNAc	Phosph	PEA	O-DPLA	NeuAc	KDO	
1	2711.39	0	4	3	2	0	1	0	1	0
2	2711.33	1	1	3	2	1	1	1	1	0
3	2711.50	1	1	4	1	0	1	1	1	0
4	2713.24	1	4	1	2	2	1	0	1	0
5	2713.41	1	4	2	1	1	1	0	1	0
6	2713.35	2	1	2	1	2	1	1	1	0
7	2711.28	3	4	0	2	1	1	0	1	0
8	2711.45	3	4	1	1	0	1	0	1	0
9	2711.23	4	1	0	2	2	1	1	1	0
10	2711.39	4	1	1	1	1	1	1	1	0